The characterisation and manipulation of a novel subset of tumour-reactive CD4+ cytotoxic T lymphocytes in human cancer

Maria Ann Veronica Marzolini

University College London

(UCL)

Thesis submitted for the degree of Doctor of Philosophy (PhD)

Declaration

I, Maria Ann Veronica Marzolini, confirm that the work presented in this thesis is my own. Where information has been derived from other sources, I confirm that this has been indicated in the thesis.

Maria Ann Veronica Marzolini

Acknowledgements

I would like to thank my principle supervisors, Prof Karl Peggs and Dr Sergio Quezada, and the lab members of the Immune Regulation and Tumour Immunotherapy and Stem Cell Transplantation and Cellular Immunotherapy groups, for their help and supervision.

I would also like to extend my gratitude to the following collaborators: Prof Teresa Marafioti and Ayse Akarca for their assistance with the immunohistochemistry experiments; Dr Richard Jenner for his supervision of the Chromatin Immunoprecipitation experiments; Prof Amit Nathwani and his team for our collaboration with the CLL samples; Prof Kwee Yong and her team for our collaboration with the Multiple Myeloma samples; Dr Evan Newell and his laboratory for their assistance with the CyTOF experiments.

I would also like to thank Cancer Research UK for funding my research and my family and friends for their support and encouragement.

Abstract

The ability of cytotoxic CD4+ T lymphocytes (CD4+ CTLs) to exert anti-tumour effects has been demonstrated in murine models of melanoma and an increase in the number of CD4+CTLs has previously been identified in the peripheral blood of patients with Chronic Lymphocytic Leukaemia (CLL) as well as in Hepatocellular Carcinoma. The project's objective was to further characterise CD4+ CTLs in human cancer and in particular in haematological malignancies. CD4+ CTLs were identified in the peripheral blood, lymph nodes and bone marrow trephine biopsies of patients with CLL. There was a significant increase in the percentage of CD4+ CTLs in the blood of Cytomegalovirus (CMV) seropositive patients with CLL. The immunophenotype of the cells was similar to CD8+ CTLs with respect to the expression of EOMES, CD57 and loss of CD27 and CD28. CD4+ CTLs were also identified in other haematological malignancies, including in the bone marrow aspirates of patients with Multiple Myeloma and in the lymph node biopsies of patients with Non-Hodgkin and Hodgkin Lymphoma. We were able to isolate CD4+ CTLs, rapidly expand them and show that they have the ability to secrete Interferon gamma as well as Granzyme B. We also performed an extensive phenotyping of the cells with CyTOF (mass cytometry) technology. Further study is required to examine the molecular and cellular determinants of their cytotoxic activity prior to exploring the potential to manipulate them for therapeutic benefit.

Impact Statement

Haematological malignancies accounted for approximately 8.4% of all new cancers diagnosed in England between the years 2001 and 2010. Chronic lymphocytic leukaemia (CLL) is the most common form of leukaemia in adults. The research included in this thesis has the potential to clearly impact on the development of cellular immunotherapies to treat CLL and other haematological malignancies in the future. Tumours interact with the immune system and establish an equilibrium between regulatory and effector T-lymphocytes which may result in either tumour rejection or escape. Manipulating this balance towards tumour rejection is an attractive aim of cancer immunotherapy. Previously, there was a scarcity of data on the role of cytotoxic CD4+ T-cells in immunotherapies for cancer. In this thesis, the presence of cytotoxic CD4+ T cells has been demonstrated in a range of haematological malignancies and their phenotype and functional profile has been characterised. Disseminating this research in international scientific journals would contribute to the knowledgebase and understanding regarding the immune landscape in these malignancies which would aid other researchers in the pursuit of novel anti-tumour therapies.

This highlights the impact of this project in laying the foundation for further research to be performed to examine this cytotoxic subset of CD4+ T cells and to further characterise their tumour-specific properties. Ultimately, we hope that this research will allow development of anti-cancer therapies based on these immune cells so that they can then be harnessed to develop a cellular immunotherapy. This can then be used in clinical trials with the aim of improving the quality of life and survival of patients with cancer.

Table of Contents

Table of Tables

Table of Figures

Chapter 1 Cytotoxic CD4+ T lymphocytes

1.1 Introduction

Manipulating the complex interaction between the adaptive immune response and tumour cells has been the focus of cancer research for many years but it is only in the past decade that significant progress has been made in the field of cancer immunotherapy resulting in clinically effective treatments. The adaptive immune response is dependent upon the recognition of antigens by lymphocytes, resulting in an immunological response, and the development of immunological memory, providing a means of protecting the host from pathogens encountered in the future. Within the T-lymphocyte cellular subset, CD8+ T-lymphocytes have a potent cytotoxic function and, following antigen recognition and activation, mediate killing of target cells. CD8+ T cells recognise antigen: MHC Class I complexes and are effective at killing cells which have been infected with intracellular pathogens. They promote apoptosis of the target cell by releasing cytolytic granules, such as perforin and granzymes, which are contained within their cytoplasm. CD8+ cells also release cytokines such as Interferon-gamma which is known to inhibit viral replication. The activation of CD8+ T-cells, which is required for them to fulfil their cytotoxic function, relies upon supplementary help supplied by CD4+ T-lymphocytes.

CD4+ T lymphocytes play a fundamental role in the adaptive immune response and traditionally their principle function has been seen as one of a 'helper' cell, interacting with fellow immune cells by secreting cytokines to promote cell differentiation, activating cytotoxic CD8+ T lymphocytes, regulating the degree of immune response and providing secondary stimulatory signals for the activation of B lymphocytes to secrete antibodies. However, evidence to suggest that CD4+ cells had the ability to acquire a cytotoxic phenotype under *in vitro* conditions and could directly lyse target cells, without relying upon other cytotoxic immune cells, challenged this concept of a solely helper role [1]**.** This observation of cytotoxicity by CD4+ cells was initially attributed to an artefact effect of long-term *in vitro* culture of CD4+ cell lines but the physiological role was soon established in murine models where CD4-dependent MHC-Class II restricted killing was shown in an *in vivo* setting in lymphocytic choriomeningitis virus (LCMV)-infected mice [2]**.** Subsequently, CD4+ cells with a cytotoxic phenotype were identified from the peripheral blood of patients with

HIV, where they can constitute up to 50% of the CD4+ population, confirming their existence *in vivo* [3].

Cytotoxic CD4+ T lymphocytes (CD4+ CTLs) are defined by their expression of cytotoxic serine proteases termed granzymes and by the cytolytic protein, perforin, and also by their functional ability to lyse target cells. Although five different granzymes have been described in humans thus far (namely granzymes A, B, H, K and M) the subtypes most commonly associated with cytotoxic CD4+ cells are granzymes A and B. The mechanisms for CTL-mediated cytotoxicity have been broadly categorised into secretory and non-secretory pathways. Both granzyme B and perforin are stored in granules within the effector CTL's cytoplasm and enact the secretory mechanism of cytotoxicity whereby, upon activation, degranulation occurs resulting in their release by exocytosis into the local environment between the effector cell and target cell. Perforin acts by forming pores in the plasma membrane of the target cells, allowing the granzymes to enter the cell and promote apoptosis by activating the caspase cascade. The finding that perforin knock-out mice fail to clear LCMV *in vivo*, implying that perforin is required for this function, but that killing activity remained in perforin-free CTLs *in vitro* suggested another pathway involved in the cytotoxic function in CTLs [4]. The analysis of perforin-deficient and Fas-Ligand deficient mice showed impaired lytic activity towards target cells demonstrating that Fas/Fas-Ligand activity was also required for cytotoxicity. The non-secretory cytotoxic mechanism relies on ligand-interaction at the cell membrane between Fas-Ligand on the surface of CTLs and Fas-Receptor on the target CTLs triggering intracellular apoptotic pathways. The mechanism of cytotoxicity employed by cytotoxic CD4+ cells still needs to be fully defined. Cytotoxic CD4+ cells reactive to EBNA1 (latent EBV antigen) exert cytotoxic effects on lymphoblastic cell lines via a the Fas/Fas-Ligand pathway [5], whereas cytotoxic CD4+ T cells detected in Chronic Lymphocytic Leukaemia (CLL) have been reported as killing via a perforin-mediated pathway [6].

In humans, the presence of cytotoxic CD4+ cells have been described widely in viral infections, including HIV [3], Cytomegalovirus (CMV) [7], Hepatitis B and C [8] and Epstein-Barr Virus (EBV) [9]. In healthy individuals, cytotoxic CD4+ cells comprise of less than 2% of the CD4+ population in the peripheral blood [10] but this percentage is often much higher in viral infections, with reported incidences of up to 50-60% of the CD4+ population[3]. In

addition to viral infections, cytotoxic CD4+ cells have also been described in autoimmune conditions, such as rheumatoid arthritis[11]**,** Sjogren's syndrome [12] and ankylosing spondylitis [13] and also post-allogeneic transplantation, both following solid organ transplantation [14] and after haematopoietic stem cell transplantation in the setting of graft-versus-host disease [15]**.** The wide range of conditions associated with elevated cytotoxic CD4+ T cell level suggest a role in conditions where there is an imbalance or dysfunction in the immune response.

The potential for cytotoxic CD4+ cells to exert anti-tumour effects has been demonstrated in murine models of advanced melanoma, where the adoptive transfer of naïve CD4+ tumour-reactive cells into lymphopenic mice resulted in the development of Class-II restricted cytotoxic activity by these cells (including expression of Granzyme B) leading to the regression of large tumours [16]. Within the human setting, elevated levels of cytotoxic CD4+ cells have been described in patients with hepatocellular carcinoma both in the peripheral blood and in the liver lesion [8]**.** In a study of 547 patients, a significant increase in cytotoxic CD4+ levels, both liver-infiltrating and circulating, was found in early stages of HCC but declined as the disease stage progressed. There was a negative correlation between the number of regulatory T cell (Tregs) and the level of cytotoxic CD4 cells in the liver and peripheral blood with more Tregs located in the tumour and fewer cytotoxic CD4+ cells when compared with the non-tumour area. Circulating and tumour-infiltrating cytotoxic CD4s were independent predictors of overall survival after the resection of the carcinoma. As many cases of HCC are associated with chronic infection with Hepatitis B virus, the level of circulating cytotoxic CD4+ cells in the HCC patients was compared with a group of patients with Hepatitis B virus only. There was a significantly higher percentage of circulating cytotoxic CD4+ T cells in the HCC group when compared with the group with Hepatitis B only, suggesting that the increase in the HCC group was not solely due to the association with viral infection.

The ability to harness the cytotoxic potential of these CD4+ CTLs and direct it against tumour has not been fully explored and the characteristics of these cells, their role in anti-tumour immunity and the potential to manipulate them for therapeutic benefit remains unclear.

1.2 The role of CD4+ CTLs in viral infections

As described above, an increase in CD4+ CTLs was first described in detail with respect to viral infection which implied that they may possess an antiviral function. In 64 healthy donors, Appay *et al* [3] examined the presence of CD4 CTLs in the peripheral blood as characterized by the CD4+ cells' expression of Perforin. They found that a mean of 2.2% of CD4+ T cells were Perforin positive. When compared to patients with HIV, there was a significant increase in the percentage of CD4+ Perforin+ cells in those patients with HIV. This highest levels were seen in patients with chronic, untreated HIV as compared with those patients with treated HIV with low viral titres. The presence of CD4+ CTLs in the peripheral blood of patients with symptomatic, primary EBV infection (IgM positive) was also examined and there was a significant increase in the percentage of CD4+ CTLs in patients with EBV when compared to healthy controls, although at a lower level than the patients with HIV. The associated increase in CD4+ CTLs in those patients with acute, untreated viruses, when compared with healthy controls, highlighted a possible role in antiviral function. The elevation of CD4+ CTLs numbers has been associated with an array of different viruses and these are explored in more detail below.

1.2.1 Cytomegalovirus and CD4+ CTLs

Cytomegalovirus (CMV), also known as human herpes-virus 5 (HHV-5), is a member of the beta-herpesvirinae family of pathogens. The seroprevalence rate of CMV in the general population is between 50-80%, although in some high-risk subgroups it can be as high as 90% and is influenced by birthplace and age, being positively associated with lower household income and increasing age [17-19]. In the majority of immunocompetent individuals, primary CMV infection is asymptomatic although in a small minority of people a syndrome similar to infectious mononucleosis may be experienced [20]. Following primary infection, the virus has a period of latency whereby it resides in mononuclear leucocytes, evading immune surveillance and being kept suppressed by the composite immune cells of the innate and adaptive immune responses to prevent development of CMV disease [21]. The complications of CMV infection are seen acutely in patients who are severely immunocompromised when an absolute and functional deficiency in CMV-reactive T lymphocytes can lead to virus reactivation and the development of CMV disease, including pneumonitis, retinitis, colitis, encephalitis and hepatitis. Clinically severe CMV-associated

disease in immunocompromised conditions is particularly seen post-allogeneic haematopoietic stem cell transplantation (HSCT) where this opportunistic, ubiquitous virus is recognised as a major contributor to morbidity and mortality in this patient group. The importance of the recovery of a CMV-specific immune response post-allogeneic HSCT was initially identified by Reusser *et al* [22] who observed that none of the patients with a detectable CMV-specific CTL response post-transplant developed CMV pneumonitis compared with a 60% mortality rate from CMV pneumonitis in those without a detectable response. Despite the advances in antiviral therapy, which is associated with an improved outcome, CMV pneumonia post-HSCT still only has a reported overall survival of 30% at 6 months after diagnosis [23].

The characterisation of CMV-specific CD4+ T cells from patients with chronic subclinical CMV infection has previously identified that CMV-specific CD4+ cells (which are CD27 negative and express Granzymes A, B and Perforin) have the ability to degranulate in response to CMV antigens and that they exhibit CMV-epitope specific cytotoxicity, thereby demonstrating antiviral properties similar to CD8+ T cells [7]. A longitudinal study of renal transplant patients, who seroconverted from CMV negative to CMV positive, revealed that CD4+ CD28- T cells, which also expressed Granzyme B (GZB), appeared in the peripheral blood after primary CMV infection and their level continued to increase even after the CMV viral load reduced to undetectable levels. When compared to renal transplant recipients who remained CMV seronegative, this increase in CD4+CD28-GZB+ T cells was not seen. The percentage of these cells in the peripheral blood was significantly higher in both the CMV seropositive healthy controls and the CMV seropositive renal transplant recipients when compared with their CMV seronegative counterparts. This increase was independent of EBV serostatus [24]. Further study of these CD4+CD28-GZB+ cells demonstrated that they could recognize CMV-peptides in a Class-II dependent manner and exhibit cytotoxicity towards target cells which had been loaded with CMV antigens. This cytotoxic function was inhibited by the addition of HLA-DR antibody thereby confirming that this function was HLA Class-II dependent.[25]

1.2.2 Epstein-Barr Virus and CD4+ CTLs

Epstein-Barr virus (EBV), also known as human herpes virus 4 (HHV-4), is a member of the human gamma-herpesvirus family and is highly prevalent in the community, with up to 90% of the adult population demonstrating evidence of previous infection. The primary infection may manifest clinically as infectious mononucleosis but may also be asymptomatic in immunocompetent individuals. Following the primary infection, the virus enters a phase of latency whereby it resides in B lymphocytes and the oropharyngeal lymphoid tissues and is kept quiescent by the host's EBV-specific cytotoxic T lymphocytes [26]. In patients who are receiving immunosuppression, or where immune reconstitution is delayed, for example in the post-transplant setting,

EBV may reactivate from its latent phase and cause a rapid B cell proliferation, resulting in post-transplant lymphoproliferative disease (PTLD). PTLD is responsible for significant morbidity and mortality in HSCT recipients, causing a clinical sequelae of fevers, lymphadenopathy, pharyngitis but also extranodal involvement, including pulmonary complications, and symptoms which may mimic severe sepsis. Prompt diagnosis is required for rapid treatment as the doubling time of EBV has been estimated at 2-4 days [27, 28] and the introduction of PCR surveillance has allowed for the early recognition of EBV reactivation.

EBV-specific CD4+ cytotoxic T cells have been isolated from human umbilical cord blood and, after culture and expansion, demonstrated EBV-specific cytotoxicity. This cytotoxicity was not inhibited by anti-Fas ligand monoclonal antibodies, indicating that the Granzyme B/Perforin cytotoxicity pathway may be responsible as Granzyme B mRNA was detected in the CD4+ CTL population. The ability to isolate and expand EBV-specific CD4+ CTLs from umbilical cord blood has a clinically translational use as an adoptive cellular therapy to prevent or treat PTLD [29].

The exact cytotoxicity mechanism involved in the functions of CD4+CTLs in association with EBV infection has shown variable results with respect to whether they are Fas-ligand mediated or involve the Granzyme B/Perforin pathway. CD4+CTL clones specific for EBNA have shown the capacity to lyse LCLs in a MHC Class II restricted, Fas/Fas-ligand dependent

manner. In contrast, CD4+ T cells clones specific for EBV LMP1 peptides all express Perforin and Granzyme A and exhibit cytotoxicity capabilities.

1.2.3 Human Immunodeficiency Virus and CD4+ CTLs

The Human Immunodeficiency Virus (HIV) is a retrovirus which causes the acquired immunodeficiency syndrome (AIDS) and results in the depletion of CD4+ T lymphocytes, thereby rendering infected individuals severely immunosuppressed and unable to mount effective immune responses to opportunistic infections. HIV targets CD4+ T lymphocytes and enters the cell by engagement with the chemokine receptors, CCR5 and CXCR4 [30]. CD4+ T lymphocytes with a cytotoxic phenotype have been identified and examined in the peripheral blood of patients with HIV and can represent up to 50% of the CD4+ T cell population [3]. As has been previously described above, the percentage of CD4+ CTLs in the peripheral blood of patients with chronic, untreated HIV is significantly higher than in those patients with primary EBV infection.

Curiel *et al* identified the presence of CD4+ HIV-1 envelope-specific CTLs from a HIV-seropositive patient's peripheral blood without the need for *in vitro* viral antigenic stimulation [31], indicating that HIV-specific CD4+ CTLs are present *in vivo*.

HIV-specific CD4+ CTLs have been generated in the presence of vaccine candidates against HIV infection [32]. Studies performed to examine the phenotype and functionality of vaccine-induced HIV-1 specific CD4+CTLs, which express Perforin, have demonstrated that they can induce potent and rapid cytolysis of antigen-pulsed cells [33] including B-LCLs expressing the HIV-1 envelope glycoprotein [34].

An extensive analysis of the phenotypic profile of HIV-specific CD4+ CTLs from the peripheral blood of patients with chronic HIV infection has demonstrated that these cells are a distinct subtype of CD4+ cells, separate from the Th1 subclass, with a transcriptional profile that is usually seen in association with NK cells and CD8+ cytotoxic T cells, particularly with respect to the expression of Granzyme A, B, K and Perforin [35]. The HIV-specific CD4+ CTLs showed comparable cytotoxicity with a resultant reduction in viral replication when compared to CD8+ CTLs. *In vitro* experiments based upon the co-culture of CD4+ CTLs and CD8+ CTLs showed the addition of CD4+CTLs increased viral inhibition when compared to CD8+ CTLs alone, particularly in the early stages of infection, suggesting a collaborative function in controlling viral infection between these two subgroups of T lymphocytes.

1.3 The Granzyme/Perforin Cytotoxicity Pathways

Traditionally, CD4+ CTLs have been defined by their expression of cytolytic proteins including Granzyme B and Perforin, which are also expressed by CD8+ CTLs and NK cells. In humans, 5 different types of Granzymes have been identified, namely Granzymes A, B, H, K and M, whereas in mice there have been 10 Granzymes identified thus far (termed Granzyme A, B, C, D, E, F, G, K, M and N). Granzymes were first described in 1987 by Masson *et al* [36]. They are located in cytoplasmic vesicles and work in conjunction with the pore-forming protein Perforin. Perforin forms pores in the plasma membranes of target cells which allows the Granzymes to enter the cell and initiate apoptosis. A congenital deficiency in Perforin is responsible for the fatal human condition Familial Haemophagocytic Lymphohistiocytosis (FHL) which is characterised by an excessive production of cytokines and dysregulation in T cell and macrophage activation [37]. A summary of the identified human Granzymes is given below:

Granzyme A

The Granzyme A (GrA) gene cluster is located on Chromosome 5 and Granzyme A is a tryptase and functions by provoking DNA fragmentation in target cells. Its mechanism of action is different to Granzyme B and can promote cell death in the absence of caspase activation. Granzyme A is thought to enter the mitochondrial matrix and cleaves the complex I protein NDUFS3, resulting in the production of superoxide anions and subsequent DNA fragmentation [38]. Granzyme A knockout mice display an impaired clearance of ectromelia virus [39] and HSV [40], indicating a role in the antiviral immune response.

Granzyme B

Granzyme B has been the most extensively studied of the identified human Granzymes. Granzyme B activates Caspase 3, thereby instigating apoptosis, by cleaving aspartic acid residues. The GrB gene cluster is located on Chromosome 14 and, *in vivo*, Granzyme B has been shown to activate Caspase 3, 7, 8 and 10.

Functionally, it mediates rapid cytotoxicity by promoting DNA fragmentation and cell lysis. Granzyme B knockout mice demonstrate an impaired immune response with an increased

predisposition to viruses. CTLs from GZB deficient mice are unable to provoke swift DNA fragmentation and apoptosis in target cells [41, 42].

The "orphan" Granzymes H, K and M

Granzymes H, K and M have been labelled as "orphan" Granzymes in view of the relative lack of research and understanding of their function, when compared with the relatively more extensively studied Granzymes A and B. Granzyme H appears to play a role in the antiviral response against human adenovirus [43] but, as no murine homologue to Granzyme H exists, knockout mice have not been generated. Like Granzyme B, its gene cluster is located on Chromosome 14. Granzyme K's gene cluster is located on Chromosome 5, like Granzyme A, and its cytotoxic mechanism of action is not fully known. It has been reported to cleave p53, resulting in potent proapoptotic activity [44]. Granzyme M Its gene cluster is located on Chromosome 19 and it is expressed on NK cells. It is a metase and functions by cleaving substrates at methionine or leucine residues. A mouse strain deficienct for Granzyme M has been reported to show an impaired immune response to murine CMV indicating that Granzyme M may have an antiviral function [45].

1.4 The classification of CD4+ T lymphocytes

Previous studies have raised the question as to whether cytotoxic CD4+ cells are allied to one particular subset of CD4+ helper cells, or whether they are a distinct, independent subtype of CD4+ cells. As an essential component of the adaptive immune response, CD4+ T lymphocytes have traditionally been labelled as a 'helper' cells but the CD4+ T lymphocytes can be further classified into subclasses depending on their cytokine production and transcription profile.

T helper 1 cells (Th1)

Th1 cells differentiate from naïve cells under the influence of the cytokine IL-12. The transcription factors STAT1 and STAT4 are upregulated and the naïve T cells differentiates into a Th1 cell. It can secrete Interferon gamma and IL-2 cytokines and these signals help to activate macrophages and assist in the immune response to intracellular bacteria. The transcription factor T-bet has been identified as a master regulator of Th1 cells.

T helper 2 cells (Th2)

Th2 cells differentiate from naïve cells as a consequence of exposure to IL-4, IL-25 and IL-33 and also with the upregulation of the transcription factor STAT6. Th2 cells secrete the cytokines IL-4, IL-13 and IL-5 and the transcription factor GATA3 is upregulated in Th2 cells. Their function helps to activate eosinophils and mast cells and thereby help the immune system to respond to parasitic infections.

T helper 17 cells (Th17)

Th17 cells are generated from naïve CD4+ cells with the upregulation of STAT3 and due to exposure to TGF-b and IL-6. RORgT is the transcription factor that is upregulated in Th17 cells and the cells produce cytokines from the IL-17 family including IL17a and IL-17f. Th17 are thought to stimulate and promote neutrophil function thereby aiding the immune response against extracellular bacteria.

T follicular helper cells (Tfh)

Similar to Th17 cells, STAT3 is upregulated in the differentiation of naïve CD4 cells to Tfh cells. In addition, the cytokine IL-6 also serves to aid differentiation to Tfh cells. The transcription factor Bcl-6 is upregulated in Tfh cells. They secrete IL-21 and provide help to B cells with respect to isotype class switching.

Regulatory T cells (Tregs)

Regulatory T cells act to control and regulate the immune system to prevent an uncontrolled immune response which could result in autoimmune diseases. They suppress T cells responses by providing inhibitory signals to the effector CD4 cells. The transcription factor FoxP3 is associated with this cell lineage and Tregs produce the cytokines IL-10, IL-35 and TGF-b.

1.5 Checkpoints at the immunological synapse – co-inhibitory and co-stimulatory receptors

The process of T cell activation occurs at the immunological synapse, whereby T cells are stimulated by the interaction of an antigen, presented in the presence of an MHC molecule, by an antigen presenting cell. The engagement of the T-cell receptor at the immunological synapse to initiate T-cell activation also requires co-stimulatory signals which occur through the engagement of co-stimulatory receptors on the T cell's surface, for example CD28. Co-inhibitory receptors are also present and upregulated at the immunological synapse and play an important role in modulating and negatively regulating the immune response, thereby limiting the potential for the development of an uncontrolled, autoimmune response.

Recent cancer research has focused on the generation of immunomodulatory antibodies designed to manipulate the immune system's co-inhibitory or co-stimulatory receptors to augment T cell effector function and the anti-tumour response. In contrast to traditional cancer therapies, which have direct cytotoxic effects on the malignant cells, this branch of cancer immunotherapy relies on indirect methods of tumour attack by manipulating the immune response in the tumour microenvironment. This indirect method has been postulated to reset the immune memory with potentially more durable responses.

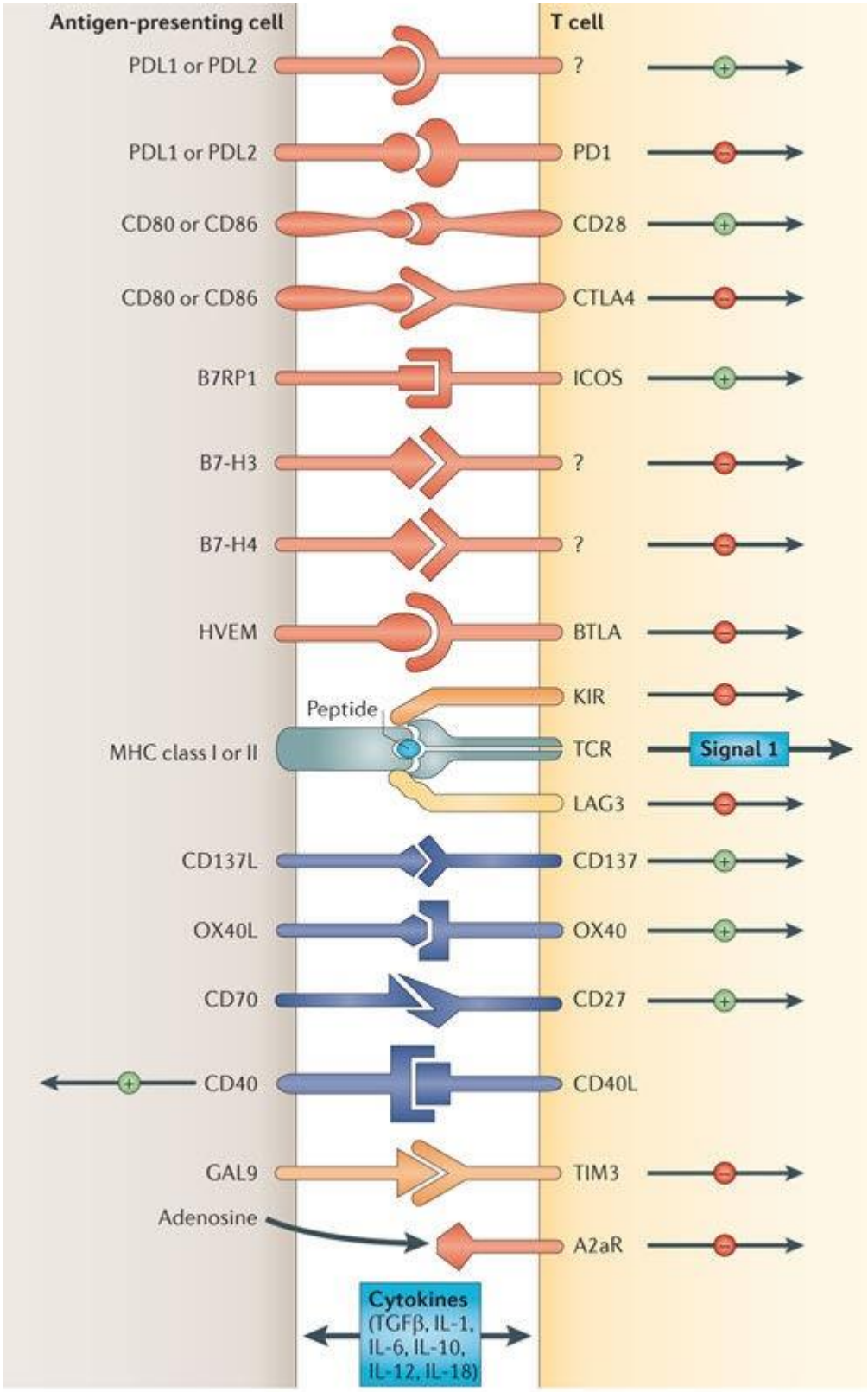

Figure 1-1: A diagram demonstrating the immunological synapse between an Antigen-presenting cell and a T-cell. The co-stimulatory and co-inhibitory receptors and their respective ligands are shown in the diagram. This image is taken from a review by Pardoll *et al* in *Nature Reviews Cancer*.

1.5.1 Cytotoxic T Lymphocyte-Associated Antigen-4 (CTLA-4)

The major breakthrough in translational cancer immunotherapy, resulting in successful Phase III clinical trials, followed the development of monoclonal antibodies against CTLA-4. CTLA-4 is a co-inhibitory receptor that is expressed on activated T lymphocytes and is constitutively expressed on regulatory T lymphocytes. It acts as an inhibitory checkpoint to restrict the magnitude and duration of the immune response (IR) generated after antigen engagement with the T cell receptor. The immune system has inherent inhibitory checkpoints to limit the degree of immune system activation, thereby preventing collateral damage of surrounding normal tissue and the sequela of autoimmunity. Both CTLA-4 and CD28, a co-stimulatory receptor, are members of the immunoglobulin (Ig) superfamily of receptors. Following the presentation of antigen by major histocompatibility complex molecules on antigen-presenting cells (APCs), the second signal for T cell activation is provided by CD28, which resides on the T cell surface, as it interacts with its respective ligands. CTLA-4's function appears to counteract that of CD28, as they share the same ligands, CD80 (B7-1), and CD86 (B7-2), which are expressed on APCs. CTLA-4 has a higher affinity for these ligands, leading to the theory that CTLA-4 may out-compete CD28 for ligand engagement, resulting in the restriction of the co-stimulatory function of CD28 [46].

The essential role played by CTLA-4 in limiting the IR and maintaining lymphocyte homeostasis was aptly demonstrated by the observations that CTLA-4 knockout mice develop fatal lymphoproliferative disorders within 3-4 weeks of birth [47, 48]. The blockade of CTLA-4 with an antagonistic antibody was postulated to increase immune stimulation by releasing the inhibitory brakes on the effector IR in the presence of tumour. Initial preclinical models confirmed this theory by showing that anti-CTLA-4 antibodies could reject tumours and also that this rejection resulted in persistent immunity when challenged for a second time with tumour cells [49]. Whilst the mechanism of action of anti-CTLA-4 antibodies is still being investigated, evidence derived from murine models has shown the blockade of CTLA-4 on both effector and regulatory T cells contributes to its anti-tumour effect. Anti- CTLA-4 antibodies act to deplete the number of regulatory T cells within tumours and the composition of the tumour microenvironment, in particular the presence of Fcγ receptor–expressing macrophages, is essential in enabling this depletion to occur [50, 51].

1.5.2 Programmed cell death protein – 1 (PD-1)

PD-1 is also a co-inhibitory member of the Ig super family of receptors. Its prime function is to restrict T cell activation and effector function in the peripheral tissues at sites of inflammation and/or infection. Its expression is induced upon activation of T cells, although it can also be expressed on B cells, natural killer cells, and monocytes. PD-1 exerts its function by interacting with its two known ligands, PD-L1 (PD-L1, also known as B7-H1 or CD274) and PD-L2 (also known as B7-DC or CD273). PD-L1 is expressed on activated T cells, B cells, and APCs, including tissue-associated macrophages. Furthermore, PD-L1 is expressed on some tumour cells allowing the tumour to circumvent T cell effector function by providing inhibitory signals to evade immune attack. PD-L1, as well as serving as PD-1's ligand, also interacts with CD80 and therefore any blocking of PD-1 does not make PD-L1 completely redundant. PD-1's second ligand, PD-L2, has a more restricted expression profile and is expressed on dendritic cells, mast cells, and macrophages.

The function of PD-1 in the maintenance of peripheral self-tolerance and the prevention of uncontrolled immune activation was established in preclinical models where it was firstly observed that PD-1 knockout mice developed autoimmune phenomenon including arthritis, glomerulonephritis, and autoimmune dilated cardiomyopathy [52, 53]. Further preclinical models demonstrated apoptosis of activated T cells when exposed to tumour-associated PD-L1 [54] and also that in vivo injection of anti-PD-L1 antibodies inhibited growth of tumours expressing PD-L1 [55]. A number of mAbs targeting PD-1 have been examined in clinical trials including Nivolumab which had shown efficacy in Hodgkin Lymphoma patients [56].

1.5.3 Inducible T-cell co-stimulator (ICOS)

Inducible T-cell co-stimulator (ICOS; CD278) is a co-stimulatory receptor that is expressed on activated T lymphocytes. It is a member of the Ig- superfamily of receptors involved in the modification of signals required for T cell activation. ICOS binds to its ligand, ICOS-L (ICOS-ligand), which is also known as B7-H2, and resides on antigen presenting cells including dendritic cells and B cells. The importance of ICOS in the activation of T cells is demonstrated by the phenotype of ICOS-deficient mice who exhibit defects in their T cell activation and proliferation functions [57]. The T cells from these mice fail to produce IL-4 when undergoing differentiation and the mice are more susceptible to autoimmune disease including encephalomyelitis. The importance of the ICOS/ICOS-L (B7-H2) interaction in

promoting T cell activation is further exemplified by the observations of mice deficient in B7-H2. B7-H2 is expressed on B cells cells and, in mice who are deficient in B7-H2, germinal centre formation is defective as ICOS is known to be expressed on germinal centre T-cells [58, 59].

1.5.4 4-1BB

4-1BB, also known as CD137, is a co-stimulatory receptor which belongs to the tumour necrosis factor superfamily of receptors. Its ligand is 4-1BBL which is expressed on antigen presenting cells. 4-1BBL deficient mice exhibit a significant reduction in CD8+ T cell effector responses, as measured by IFN-gamma secretion following peptide exposure, in the absence of 4-1BB co-stimulation when compared to wild-type mice [60]. 4-1BBL deficient mice also exhibit a reduced anti-viral immune response to influenza virus when compared with wild-type mice [61] which indicates that the 4-1BB co-stimulatory signal plays a role in antiviral effector functions. Analysis of 4-1BB ligand (4-1BBL)-deficient mice and of mice lacking both 4-1BBL and CD28 reveals a role for 4-1BBL in skin allograft rejection and in the cytotoxic T cell response to influenza virus [61].

1.5.5 OX40

OX40, also known as CD134, is a co-stimulatory receptor that belongs to the TNF-superfamily of receptors. OX40 is expressed on activated T-cells and its ligand is OX40-L which resides on antigen presenting cells. Neither OX40 nor its ligand are expressed on resting naïve T cells or antigen presenting cells but expression occurs upon activation. OX40 expression is reduced in the absence of CD28 which highlights that it is dependent upon T-cell activation to be expressed. Experiments examining mice who are deficient in OX40 have shown a reduced CD4+ T -cell proliferation in response to viral infections, indicating an important role of OX40 co-stimulation in the antiviral response [62].

1.5.6 Glucocorticoid-induced TNFR-related protein (GITR)

GITR (glucocorticoid-induced TNFR-related protein), also known as TNFRSF18, is a member of the tumour necrosis factor receptor superfamily. It is known to be constitutively

expressed on T regulatory cells and its expression is upregulated on CD4+ and CD8+ T cells following TCR engagement and T cell activation. GITR is also expressed on NK cells. Its ligand is GITR-L and this is expressed on non-lymphoid cells including APCs. Studies examining GITR -/- mice have demonstrated that engagement of the GITR receptor on effector T cells can overcome Treg suppressive effects on the effector T cells [63, 64]. This has led to the investigation of therapeutic agonist monoclonal antibodies directed towards GITR in preclinical models of cancer [65].

1.5.7 Lymphocyte activation gene 3 protein (LAG3)

Lymphocyte activation gene 3 protein (LAG3), also known as CD223, is a co-inhibitory receptor and a member of the immunoglobulin family of receptors. Its expression is upregulated on activated T cells following TCR engagement and its principle ligand is MHC Class II. LAG3 deficient mice show an increase in T cell expansion and splenomegaly after stimulation with staphylococcal enterotoxin B [66], indicating that LAG3 is instrumental in controlling and regulating T cell expansion and is a negative regulator of the immune response. It also appears to have a role in T cell exhaustion as LAG3 expression is increased on exhausted T cells [67].

1.5.8 T-cell immunoglobulin and mucin domain 3 (TIM3)

T-cell immunoglobulin and mucin domain 3 (TIM3) is a co-inhibitory receptor. It was originally described as being expressed on Th1 CD4 cells but is also expressed on CD8+ cells as well as monocytes and dendritic cells. Its ligand has been identified as Galectin-9. The interaction between TIM-3 and its ligand results in the inhibition of Th1 effector functions [68]. Like LAG3, it has also been identified as being expressed by exhausted T cells [69, 70].

1.6 Conclusion

In conclusion, cytotoxic CD4+ cells have been identified in viral infections and also some malignant conditions indicating that they may have an anti-tumour function. Although they have been identified in the peripheral blood of patients with CLL, they have never been described in the tumour microenvironment of haematological malignancies. We will

therefore investigate whether CD4+ CTLs are present in haematological malignancies and examine their phenotype and function in these conditions. By investigating their immunophenotype, we will identify whether they have any characteristics similar to other cytotoxic cells, for example NK or CD8+ cells. We will also examine whether they express the checkpoint receptors described above which could be the potential target of therapeutic interventions to augment their cytotoxic function.

The aims of the individual results chapters are as follows:

Chapter 3: The identification, characterisation and functional properties of cytotoxic CD4+ T lymphocytes in patients with Chronic Lymphocytic Leukaemia (CLL).

Samples of peripheral blood, lymph node biopsies and bone marrow trephine biopsies from patients with CLL were examined to address the following aims:

1. **To detect the presence of CD4+GZB+ cells in the peripheral blood of patients with untreated CLL.**

   This aim would identify the presence of CD4+GZB+ by flow cytometry in the peripheral blood of CLL patients and, if present, their phenotype and function could be examined.

2. **To examine the level of CD4+GZB+ cells with CMV status, age and white cell count.**

   To address whether the level of CD4+GZB+ cells was associated with an increased tumour burden (eg an increasing white cell count) or with other known viruses (eg CMV serostatus).

3. **To phenotype the cells with respect to transcription factors and cell surface markers and to compare the CD4+ and CD8+ subsets to identify any common features in the cytotoxic T cell populations.**

This aim would also allow for the identification of cell surface markers specifically associated with the cytotoxic CD4+ cells which would enable these cells to be electronically sorted and isolated for functional assays to be performed (eg ELISPOT). It would also indicate whether they shared any phenotypic features with CD8+ cells which are known to be cytotoxic.

4. **To identify the presence of cytotoxic CD4+ T lymphocytes in the tumour microenvironment of patients with CLL, specifically examining the lymph node and bone marrow microenvironments.**

   This aim would look in the tumour microenvironments where the CLL cells are known to either originate (bone marrow) or proliferate (lymph node) and to identify whether cytotoxic CD4+ cells were present in these locations.

Chapter 4: The immunophenotype of cytotoxic CD4+ T lymphocytes in CMV seropositive and CMV seronegative patients with CLL as determined by mass cytometry (CyTOF)

This chapter will look at the phenotype of the cytotoxic CD4+ T-cells in greater depth using mass cytometry (CyTOF). This will enable a detailed analysis of the similarities and differences in the phenotype of these cells between patients who are CMV seropositive and seronegative. It will also allow for the comparison of phenotype between cytotoxic CD4+ cells and CD8+ cells. The aims of the CyTOF staining and analysis of peripheral blood from patients with CLL were as follows:

1. **To identify whether mass cytometry (CyTOF) was comparable with standard flow cytometry to quantify CD4+GZB+ cells in the peripheral blood of patients with CLL.**

   Peripheral blood samples from the same patients which have been analysed by both flow cytometry and mass cytometry will be compared to establish if there is a consistency of results between the two methods.

2. **To establish if there was any difference in phenotype between the CD4+ GZB+ cells from CMV seropositive and CMV seronegative patients with CLL.**

   As described in the Introduction chapter, cytotoxic CD4+ cells have been described in association with a variety of viruses, including CMV. The mass cytometry phenotype of cytotoxic CD4+ cells from CMV seropositive and CMV seronegative patients will be compared to assess whether the cytotoxic CD4+ cells in both groups of patients share the same phenotype.

3. **To compare the phenotype of CD4+GZB+ with the phenotype of CD8+GZB+ cells in CMV seropositive and CMV seronegative patients with CLL.**

   As CD8+ cells are known to have cytotoxic functions, their phenotype will be compared with the phenotype of cytotoxic CD4+ cells. This will establish if these two cytotoxic cell types share similar phenotypic profiles.

Chapter 5: The identification and characterisation of cytotoxic CD4+ T lymphocytes in patients with Hodgkin Lymphoma, Non-Hodgkin Lymphoma and Multiple Myeloma

Although cytotoxic CD4+ cells have been described in association with viruses, and also in patients with CLL, they have never previously been described in other haematological malignancies. The purpose of this chapter is to establish if cytotoxic CD4+ cells are present in other haematological malignancies, namely lymphoma and multiple myeloma. The aims of the immunohistochemical staining of the human lymphoma-infiltrated lymph node biopsies and the bone marrow aspirates from patients with multiple myeloma were as follows:

1. **To detect whether CD4+ CTLs were present in lymphomas and multiple myeloma as they have not been previously described in these malignancies.**

   The lymph node biopsies of patients with a range of both Non-Hodgkin Lymphomas and Hodgkin Lymphoma will be examined to establish if

cytotoxic CD4 are present in this tumour microenvironment. The bone marrow aspirates of patients with untreated multiple myeloma will be examined using flow cytometry to establish if cytotoxic CD4+ cells are also present in this disease.

2. **To characterise their prevalence with respect to other components of the CD4+ compartment.**

   By using triple-colour immunohistochemistry, the lymph node biopsies of patients with lymphoma will be stained to identify the different components of the CD4+ population. This will allow the composition of the CD4+ compartment and the level of cytotoxic CD4+ cells within that compartments to be examined.

3. **To establish whether they are more prevalent in specific subtypes of lymphoma.**

   If cytotoxic CD4+ cells are identified in the lymph node biopsies of patients with lymphoma, their prevalence in the different types of lymphoma will be examined to establish if they are present in all lymphomas at the same level. If they are elevated in some types of lymphoma, when compared with reactive lymph nodes, this would guide further research into the phenotype and function of cytotoxic CD4+ cells in those lymphoma subtypes

Chapter 6: Chromatin Immunoprecipitation sequencing for low cell numbers: optimisation of techniques

This chapter will present the experiments performed to optimise the technique of Chromatin Immunoprecipitation (ChIP) sequencing for low cell numbers. The overall aim was to allow for the epigenetic determinants of cytotoxic function of the cytotoxic CD4+ cells to be examined using ChIP sequencing. The low absolute number of cytotoxic CD4+

cells isolated from the peripheral blood of patients with CLL meant that conventional, established ChIP sequencing protocols, which had been used to sequence higher cell numbers, had to be adapted and optimised. The aims of the chapter are as follows:

1. **To optimise the chromatin immunoprecipitation (ChIP) techniques for small cells numbers (eg 1 x 10^6 and 1 x 10^5 cells), in particular the optimum sonication settings required for DNA fragment generation.**

   CD4+ cells were isolated from healthy donors and experiments performed to establish if ChIP could successfully be performed on a variety of different cell numbers using different sonication settings to establish the optimum experimental protocol.

2. **The optimisation of the ChIP technique would then allow for ChIP-seq by next generation sequencing to identify the epigenetic determinants of cytotoxic CD4+ T cell function and the regulatory elements and genes that distinguish them from other CD4+ cell lineages.**

   This was the overall aim for the use of the ChIP sequencing technique on the cytotoxic CD4+ cells which had been isolated from the peripheral blood of patients with CLL.

Chapter 2 Methods

2.1 Immunohistochemistry staining of human lymphoma/CLL/reactive lymph node biopsies to detect the presence of cytotoxic CD4+ T cells

(i) Identification and acquisition of formalin-fixed, paraffin embedded lymph node biopsies

The University College London Hospitals (UCLH) Department of Histopathology's computer software, CoPath, was used to identify and locate archived human lymph node biopsies that had the formal histological diagnosis of the following diseases:

- Mantle Cell Lymphoma (MCL)
- Diffuse Large B Cell Lymphoma (DLBCL)
- Classical Hodgkin Lymphoma (CHL)
- Follicular Lymphoma (FL)
- Chronic Lymphocytic Leukaemia (CLL)
- Anaplastic Lymphoma Kinase (ALK) positive Anaplastic Large Cell Lymphoma (ALCL) and Large B Cell Lymphoma (LBCL)
- ALK negative Anaplastic Large Cell Lymphoma (ALCL) and ALK negative Peripheral T Cell Lymphoma (PTCL)

These lymphoma subtypes were chosen in part for their prevalence in the population and in part as they are all mature B cell lymphoma subtypes despite each having a distinct pathogenesis and microenvironment. As cytotoxic CD4+ cells have been found peripherally in patients with untreated CLL [71], we decided to focus on B cell malignancies and also to investigate lymph nodes infiltrated with CLL, which have not been examined previously for the presence of CD4+ CTLs. The exceptions to this are the ALCL and PTCL subtypes, which are T cell lymphomas but were chosen because Anaplastic Lymphoma Kinase (ALK) is a tumour associated antigen and potential therapeutic target of adoptive T cell therapy.

Six biopsies of each disease group were initially obtained for the B cell lymphomas and CLL. Despite attempts to locate six biopsies for ALK+/- ALCL, ALK+ LBCL and ALK-PTCL, only 1 biopsy of each of these subtypes were available with sufficient residual tissue for analysis.

The lymph node biopsies had been preserved as formalin-fixed, paraffin embedded (FFPE) blocks prior to being stored in the archive. The biopsies were cut into 2µm sections for immunohistochemical analysis. The patient characteristics and immunophenotype of the biopsies are shown in Table 16. As a control group, six lymph node biopsies with the diagnosis of "reactive lymph node" were also obtained from the Department of Histopathology archive by the same method. These biopsies were not infiltrated by a malignancy and were used as a normal control to compare with the lymphoma/CLL biopsies. The patient characteristics of the reactive lymph node biopsies are shown in Table 7. Ethical approval for their use in medical research had been obtained previously under the UCLH Department of Histopathology departmental consent process.

(ii) Location of chosen antigens for triple immunohistochemical staining

In order to identify cytotoxic CD4+ T cells in the FFPE lymph node biopsies, triple immunohistochemistry was performed. CD4, Granzyme B and FoxP3 were chose as the three antigens to detect – the combination of CD4 and Granzyme B would allow for the detection of CD4+ CTLs and the inclusion of FoxP3 would allow us to differentiate these cells from T regulatory (Treg) cells which have previously been described as occasionally expressing Granzyme B [72].

The three antigens all have distinct locations in the cells under investigation. The glycoprotein CD4, a member of the immunoglobulin superfamily of receptors, is located on the cell surface. Granzyme B is expressed by cytotoxic T lymphocytes, Natural Killer (NK) cells and NKT cells. It is stored as a granule in the cytoplasm of these cells and is released into the immunological synapse between the effector and target cell following activation and degranulation. FoxP3 (Forkhead box P3) is a transcription factor that is expressed by regulatory T cells (Tregs) (CD4+CD25+).Tregs inhibits the function of CD25- T cells, thereby controlling the amplitude of immune response. In immunohistochemical staining, FOXP3 positive staining is located in the nucleus of the cell. Therefore, all 3 antigens are located in different compartments of the cells, making visualisation with triple staining an achievable endeavour

(iii). Immunohistochemistry of the lymph node biopsies and bone marrow trephine biopsies

The lymph node biopsies were cut into 2µm sections. In collaboration with Dr. Teresa Marafioti's laboratory, triple immunohistochemical staining was performed on the biopsies for CD4 (Novocastra, Clone: 4B12), FoxP3 (Abcam, Clone 236A/EF) and Granzyme B (Novocastra, Clone 11F1). In the majority of cases, the chromogen-antibody combination was CD4 (brown), FoxP3 (red), Granzyme B (blue). In a minority of cases, a green chromogen was used to identify FoxP3, with CD4 (brown) and Granzyme B (red). Human tonsillar biopsies, previously stored as FFPE blocks, were obtained from the Department of Histopathology's archive and used as positive controls. The initial optimisation of chromogens and antibody dilutions were performed on human tonsils. During the staining process, it was determined that 1 biopsy from the MCL group and 1 biopsy from the CHL group had insufficient high quality tissue present and so these groups had only 5 biopsies included in the final data analysis. With respect to the staining of CD8, the antibody used was the Novocastra Mouse Monoclonal anti-human CD8 (Clone 4B11).

2.1.1 Protocol for single staining immunohistochemistry

The kit used for immunohistochemistry was the EnVision G/2 Doublestain system (DAB+/Permanent Red; Dako). The slides were put into a metal rank and then placed in Xylene for 10 minutes (in a fume cupboard). They are then moved to an adjacent container of Xylene for a further 10 mins. Next, they are put in 100% ethanol for 10 minutes and this step is repeated. Then they are transferred to 70% ethanol for 5 minutes, followed by 50% ethanol for 5 minutes. The slides were then washed in running tap water for 10minutes and then washed in distilled water for 5 minutes. The slides are then transferred to a microwavable container. Separately, the citrate buffer is warmed in the microwave for 10minutes (during this time, the slides remained in distilled water). The slides were then put into the citrate buffer and put in the microwave for 10 minutes. The slides and container were then removed from the microwave and put under running water for 5 minutes. The slides were placed in the humidified chamber and the Dako blocking agent was then added to the slides (200ul/slide) for 5 minutes. Excess liquid was discarded from the slides and PBS buffer was added to the slides as a washing step. The primary antibody was diluted in PBS and 200ul of the antibody was added to the slides. The slides were incubated for 30minutes in the dark in the humidified chamber. They were then washed twice with PBS for 5 minutes

each time. The excess liquid was discarded. 200ul of the secondary antibody (HRP-Polymer) was added to the slides. The slides were incubated for 30 minutes in the dark. They were then washed twice with PBS for 5 minutes each wash. DAB solution was added to the slides (200ul/slide) for 5 minutes. The slides were then washed in distilled water for 15 minutes. Haematoxylin was added to the slides for 1 minute. The slides were then washed under running water for 15 minutes. The slides were then dehydrated and mounted for analysis.

2.1.2 Triple stain immunohistochemistry

The triple stained immunohistochemistry experiments in this thesis were performed by Dr Teresa Marafioti's laboratory team using a protocol previously published [73].

(i). Location of tumour area

The triple-stained biopsy slides were reviewed with Dr Teresa Marafioti, Consultant Histopathologist, to determine the area of tumour infiltration on each biopsy. The tumour area was identified by comparing the triple-stained biopsy slide with both the original diagnostic Haematoxylin and Eosin (H+E) slide and the original diagnostic single-stained IHC slides obtained from the same biopsy block which were positive for tumour-specific markers (eg Cyclin D1 for MCL; CD30 for CHL)**.** The area, once marked upon an image of the single-tumour marker stained slide, was superimposed upon the triple-stained biopsy slide.

(ii). Scanning slides

Each of the triple stained biopsy slides were image-scanned using a Hamamatsu NanoZoomer digital slide scanner. Five layers, each of 300nm depth, were scanned at x40 resolution and saved as NanoZoomer Digital Pathology Image files for later analysis. Scanning was performed as soon as possible after triple-staining was performed to minimise the time for any chromogen degradation. The slide images were visualized using NDP.view2 (NanoZoomer Digital Pathology) software.

(iii). Counting and analysis technique

Five areas at x40 magnification were identified from the tumour area of each biopsy diagnostic of disease. For the control "reactive" lymph node biopsies, five areas at x40 magnification were chosen at random. Using Image J software, where a grid was superimposed on each area, all of the stained cells in these five areas were manually counted and allocated to one of 7 different combination groups Table 1:

Cell Type	IHC Staining Positive For:	IHC Staining Negative For:
1	CD4	FoxP3, Granzyme B
2	FoxP3	CD4, Granzyme B
3	Granzyme B	CD4, FoxP3
4	CD4, FoxP3	Granzyme B
5	CD4, Granzyme B	FoxP3
6	FoxP3, Granzyme B	CD4
7	CD4, FoxP3, Granzyme B	

Table 1: The different cell type combinations identifiable by triple immunohistochemical staining for CD4, Granzyme B and FoxP3.

The sum of the cell counting results for the five x40 sections was used as the total number of cells for each cell subgroup per biopsy slide. Statistical analysis was performed using the GraphPad Prism software programme and the analysis of variance (ANOVA) method was used for statistical analysis. Statistical significance was assumed if the P value was less than 0.05.

2.2 Flow cytometry analysis of the peripheral blood of patients with CLL to characterise the phenotype of cytotoxic CD4+ T cells

In collaboration with Professor Nathwani's laboratory, peripheral blood was obtained from patients with CLL who were attending the weekly out-patient haematology clinic at UCLH. The patients were not currently receiving CLL treatment at the time of blood sampling. Ethical approval had been obtained from the local UCL/UCLH Ethics Committee as per Prof

Nathwani's project entitled "Using insights into the biology of CLL to develop new therapies". The volume of peripheral blood available for analysis ranged from 4-20mls. The patients' clinical data was obtained from the UCLH computer database. Peripheral blood mononuclear cells (PBMCs) were isolated from the peripheral blood using FICOLL and layer separation, the cells were washed twice with complete RPMI media and counted using the MUSE® cell analyser machine. The cells were then frozen in FCS (fetal calf serum) with 10% dimethyl sulfoxide (DMSO) and stored in liquid nitrogen (see Section 2.2.1).

Initially, flow cytometry was performed on a cohort of 10 patients' peripheral blood to identify and phenotype the presence of cytotoxic CD4+ T cells. All of the patients had Binet Stage A CLL (with fewer than 3 areas of lymphadenopathy, no anaemia or thrombocytopaenia) [74]**,** had not received any treatment for their CLL. Four panels of 11 or 12 fluorochrome-conjugated antibodies were used to examine both intracellular and extracellular compartments (Table 3).

The samples were processed using the Fortessa FACS machine and flow cytometry data was analysed using the FlowJo software programme. Statistical analysis was performed using the GraphPad Prism software programme. Statistical significance was assumed if the P value was less than 0.05.

2.2.1 Ficolling whole blood to isolate PBMCs

PROCEDURE

1. Mix whole blood 1:1 with plain RPMI.
2. For each 20mls of blood-RPMI mixture, underlay the mixture with 10mls of Ficoll in a 50ml conical tube.
3. Centrifuge layered Ficoll at 750G for 20 minutes at 20^{o}C, setting centrifuge acceleration and deceleration to minimum.
4. Inspect the gradient. Spun Ficoll should show serum, buffy coat and red cell pellet layers
5. Isolate lymphocytes from Ficoll/RPMI interphase layer and add 30 ml plain RPMI

6. Spin cells at 2000 rpm or 400G for 5min at 4°C and pour off supernatant

7. Spin the buffy coat-RPMI mix at 2000 rpm for 5 minutes at 4°C, pour off supernatant

9. Re-suspend all the pellets in 30mls of complete medium and spin at 4 °C at 2000 rpm for 5 minutes

10. If cells are to be frozen: resuspend cells in 5 ml freezing media (10 % DMSO in FCS) and aliquot into cryotubes. Freeze at -80 C

Panel 1

Extracellular

Target	Fluorophore
CD4	BV711
CD8	V500
CD3	605NC
CD19	BV785
ICOS	PE-Cy7
Viability Dye	APC-Cy7

Intracellular

Target	Fluorophore
FoxP3	AF700
Eomes	APC
Ki67	FITC (BD)
CTLA4	PE
Granzyme B	V450

Panel 2

Extracellular

Target	Fluorophore
CD4	Q655
CD8	v500
CD3	605NC
CD19	BV785
Viability	APC-Cy7
CD28	FITC
CD27	AF700
CD57	PE

Intracellular

Target	Fluorophore
Tbet	BV711
Granzyme B	V450
EOMES	APC

Panel 3

Extracellular

Target	Fluorophore
CD5	FITC
CD4	BV711
CD8	v500
CD3	605NC
CD19	BV785
Viability	APC-Cy7
PD-1	Q655
PD-L1	PE-Cy7
Tim3	PE
VISTA	Biotin
Streptavidin	PerCP-Cy5.5

Intracellular

Target	Fluorophore
Granzyme B	V450
Eomes	APC

Panel 4

Extracellular

Target	Fluorophore
CD5	FITC
CD4	BV711
CD8	v500
CD3	605NC
CD19	BV785
Viability	APC-Cy7
CD137	AF700
OX40	PE-Cy7
CD40L	PE

Intracellular

Target	Fluorophore
Granzyme B	V450
Eomes	APC

Table 2: The four panels of fluorochrome-conjugated anti-human antibodies used to characterise the peripheral blood samples from patients with CLL.

Anti-human antibody	Fluorophore	Qty/sample	Company	Catalogue Number	Clone
CD4	BV711	1 ul	BioLegend	317440	OKT4
CD8	V500	1 ul	BD Biosciences	651617	RPA-T8
CD3	605NC	1 ul	eBioscience	83-0037-42	OKT3
CD19	BV785	3 ul	BioLegend	302240	HIB19
ICOS	PE-Cy7	0.25 ul	BioLegend	313519	C398.4A
Viability Dye	APC-Cy7	1 in 1000	eBioscience	65-0865-14	N/A
FoxP3	AF700	1 ul	eBioscience	56-4776-41	PCH101
Eomes	APC	1 ul	eBioscience	51-4877-41	WD1928
Ki67	FITC (BD)	5 ul	BD Pharmingen	556026	B56
CTLA4	PE	5 ul	eBioscience	12-1528	eBio20A
Granzyme B	V450	1 ul	BD Biosciences	561151	GB11
CD4	Q655	1 in 20	Biolegend	317435	OKT4
CD28	FITC	5 ul	eBioscience	11-0289-41	CD28.2
CD27	AF700	5 ul	eBioscience	56-0279-42	O323
CD57	PE	5 ul	eBioscience	12-0577-42	TB01
Tbet	BV711	1 in 20	BioLegend	644819	4B10
CD5	FITC	5 ul	eBioscience	11-0058-42	L17F12
PD-1	Q655	5 ul	eBioscience	86-2799-41	J105
PD-L1	PE-Cy7	1 in 200	BD Biosciences	558017	MIH1
Tim3	PE	5 ul	eBioscience	12-3109-42	F38-2E2
Streptavidin	APC	1 ul	Biolegend	405207	N/A
CD137	AF700	1 in 200	Biolegend	309816	4B4-1
OX40	PE-Cy7	20 ul	Biolegend	350012	ACT35
CD40L	PE	5 ul	eBioscience	12-1548-42	24-31
Granzyme A	FITC	5 ul	Cambridge Bioscience	507204	CB9
Lag3	Biotin	2.5 ul	R+D systems	BAF2319	N/A
ThPOK	PE	5 ul	BD Bioscience	565730	6/hcKrox
RORγt	PE	5 ul	BD Bioscience	563081	Q21-559
Runx3	APC	10 ul	R+D systems	IC3765A	527327
GATA-3	PerCP-Cy5.5	5 ul	eBioscience	46.9966-42	TWAJ
IFN gamma	PE	5 ul	eBioscience	12-7319-82	4S.B3
Perforin	v500	5 ul	Biolegend	308120	dG9

Table 3: The fluorophore-conjugated anti-human antibodies used for flow cytometry experiments.

2.3 FACS staining protocol for flow cytometry

- Use a 96-well round- bottom plate. Transfer 200ul of the cell suspensions into the wells.
- Centrifuge the plate at 2000 rpm for 2 minutes at 4^{o}C. Discard the supernatant and resuspend the pellets in 50ul of the extracellular mastermix of antibodies.
- Incubate for 30minutes, on ice, in the dark
- Wash 2 and a half times with FACS buffer. (each wash involves adding 200ul of FACS buffer to each well, centrifuging at 2000 rpm for 2 minutes at 4^{o}C and discarding the supernatant).
- Resuspend in 100ul of PermFix solution from the FoxP3 buffer kit (this is made 1:4 of FoxPerm concentrate in diluent).
- Incubate for 30 minutes, on ice, in the dark.
- Wash 2 and a half times with Fox buffer
- Resuspend in 50ul of the intracellular antibody mastermix.
- Incubate for 30 minutes, on ice, in the dark.
- Wash 2 and a half times with Fox buffer
- Resuspend in 150ul of FACS buffer and transfer to bullet tubes for analysis on the Fortessa machine.

<u>Superblock – made up in PBS</u>

- 5% mouse serum
- 5% rat serum
- 2% FBS
- 0.1% sodium azide

<u>FACS buffer</u>

- 500mls of PBS
- 2% fetal calf serum (FCS)
- 2mmol EDTA

<u>Fox buffer</u>

- 1:10 of Fox buffer from the FOXP3 buffer kit (eBioscience; cat. #: 00-5523-00) in dH_2O.

Complete RPMI

- 500mls RPMI
- 50mls FCS
- 5mls of L-glutamic acid
- 5mls Penicillin-Strep
- 500ul mercaptuethanol

Number of Patients	Type of sample	Experiment	Aim of experiment
6 patients (Not on treatment)	Lymph node biopsy	Triple immunohistochemistry staining for CD4, Granzyme B (GZB) and FoxP3.	To establish if cytotoxic CD4+ cells (CD4+GZB+) were present in the lymph node tumour microenvironment of patients with CLL and compared to reactive lymph node biopsies.
90 patients (Not on treatment)	Peripheral blood	Flow cytometry staining for CD4, Granzyme B and CD57.	To identify the percentage of CD4+GZB+ cells in the peripheral blood of patients with CLL and to compare it to their age, CMV serostatus and white cell count.
- 45/90 had samples taken at 2 different time points. - 18/90 had samples taken at 3 different time points.	Peripheral blood	Flow cytometry staining for CD4, Granzyme B and CD57.	To identify the percentage of CD4+GZB+ cells in the peripheral blood of patients with CLL and to establish if the levels changed over time in these untreated patients.
A subgroup of 10 patients from the 90 patients (not on treatment)	Peripheral blood	Extended flow cytometry staining examining co-inhibitory and co-stimulatory receptors and transcription factors.	To perform an in-depth, extended phenotype analysis of cytotoxic CD4+ cells in the peripheral blood of patients with CLL.
A subgroup of 10 patients from the 90 patients (not on treatment)	Lymph node biopsies and bone marrow trephine biopsies	Triple immunohistochemistry staining for CD4, CD8 and Granzyme B (GZB).	To compare the levels of CD4+GZB+ and CD8+GZB+ cells in paired lymph node and bone marrow trephine biopsies from the same patients with untreated CLL and to examine if there is a difference in these two tumour microenvironment locations.
A subgroup of 14 patients (7 CMV seropositive, 7 CMV seronegative) from the 90 patients (not on treatment).	Peripheral blood	Mass cytometry (CyTOF) analysis	To compare the extended phenotype of CD4+GZB+ cells in those patients who are CMV seropositive with those patients who are CMV seronegative.
1 patient (CMV seropositive) from the group of 90 patients (not on treatment)	Peripheral blood	Electronic cell sorting of CD4+CD57+, CD4+CD57-, CD8+CD57+ and CD8+CD57-.	The electronically sorted cells were expanded in culture and used to perform functional experiments, namely a cytotoxicity assay and ELISPOT assays examining Interferon gamma and Garnzyme B secretion in the context of stimulation with CMV peptide. Autologous B-cells were used as antigen-presenting cells.

Table 4: The different samples collected from patients with CLL and the experiments performed on the samples.

2.4 Flow Cytometry of Multiple Myeloma Bone Marrow Aspirate samples

In collaboration with Prof Kwee Yong's laboratory, we had access to bone marrow aspirate samples from patients with newly diagnosed Multiple Myeloma. Ethical approval had been given for the use of these samples for research. The bone marrow aspirate samples were processed according to the protocol listed below:

The resultant cells were then stained for flow cytometry according to the Flow Cytometry protocol listed above and the results analysed on the Fortessa Flow Cytometry machine.

2.4.1 Protocol for isolating mononuclear cells from bone marrow aspirates:

- A cell strainer was placed over a 50ml Falcon tube
- The cell strainer was pre-wet with HBSS buffer.
- The bone marrow aspirate was poured onto the cell strainer and the plunger of a 5ml syringe was used to crush the particles against the strainer.
- The strainer was rinsed with additional HBSS.
- The bone marrow aspirate sample tube was also washed with HBSS and this was added to the cell strainer.
- The total volume in the Falcon tube (containing bone marrow aspirate and HBSS should be 20mls).
- The bone marrow aspirate/HBSS solution was then underlayed with 10mls of FICOLL and centrifuged at 750G for 20mins at 20^{o}C.
- The mononuclear cells were isolated from the interphase layer and 20mls of HBSS was added.
- The cells were centrifuged at 2000 rpm or 400G for 5min at 4^{o}C and the supernatant was discarded.
- The cells were resuspended in 10mls of complete RPMI and centrifuged at 4 ^{o}C at 2000 rpm for 5 minutes.
- The supernatant was discarded and the cells were resuspended in FACS buffer for FACS staining.

2.5 Chromatin Immunoprecipitation techniques

2.5.1 Cross-Linking Cells

Venesection of healthy subject to obtain 20mls of peripheral blood. Using the protocol above, the blood was ficolled to obtain PBMCs. The resultant cells were counted using the MUSE® cell analyser machine. MACS buffer was made using 500mls of PBS, 2.5g BSA and 2 mM EDTA. A CD4+ negative cell selection was performed using the LS MACS columns (cat. # 130-042-401), the MACS magnet and Miltenyi Biotec CD4+ T cell isolation kit (human) (cat. # 130-096-533). The resultant negatively selected CD4+ cells were tested for purity by flow cytometry.

For the cross-linking of the cells, 10mls of 11% formaldehyde solution was made using:

- 11% formaldehyde
- 0.1M NaCL
- 1mM EDTA
- 0.5mM EGTA
- 50mM Hepes
- dd H20

1/10th volume of the 11% formaldehyde solution was added to the cells and the solution was swirled.

The cells were left at room temperature for 20 minutes.

Then 1/20th volume of 2.5M glycine was added to the cells to stop the reaction and the solution was mixed.

The cells were then centrifuged at 1300rpm for 10 minutes at 4^{o}C.

The supernatant was poured off and the pellet was resuspended in 1ml of PBS.

The tubes were centrifuged at 1500rpm at 4^{o}C for 10 minutes.

The supernatant was poured off and the pellet was resuspended in 1ml of PBS.

The tubes were again centrifuged at 1500rpm at 4^{o}C for 10 minutes.

The supernatant was poured off,

The tubes with the pellets of cells were flash-frozen in liquid nitrogen for 15 seconds and then transferred to the -80 °C freezer.

2.5.2 Cell Lysis and Sonication test

The Bioruptor Pico water bath machine was turned on and allowed to cool down to a temperature of 4 °C for 30 minutes.

Young lysis buffer 3 was made (use 100ul of lysis buffer for up to 1 x 10^6 cells)

- 10mM Tris Ph8
- 100mM NaCl
- 1mM edta
- 0.5mM EGTA
- 0.1% sodium deoxycholate
- 0.5% N-lauryl sarcosine
- dH2O

Complete protease inhibitor (Roche; 11873580001) was made by dissolving 1 tablet into 2mls of dd H20. This was added to the lysis buffer.

100ul of the lysis buffer/compete protease inhibitor mix was added to the pellet of cross-linked cells and lysis was allowed to occur for 15 minutes on ice.

100ul of the cell lysate was transferred to the 1.5ml Bioruptor Microtubes with caps on.

The samples were then sonicated in the Bioruptor Pico water bath for varying lengths of cycles, depending on the conditions being tested.

To the 100ul of sonicated sample, 35ul of TE and 15ul of 10% Triton X-100 were added and the samples were mixed well. 150ul of elution buffer was added to the sample and mixed gently.

The samples was centrifuged at 13.000 rpm for 10 minutes at 4 °C and the supernatants were taken to a new tube.

6ul of RNaseA (10ug/ul) was added and the sample was incubated at 37 °C for 1 hour.

3ul of Proteinase K was added and the cross-links were reversed at 65 °C for 1 hour.

An equal volume of phenol:chloroform:isoamyl alcohol was added to the sample. The phases were separated using phase-lock heavy tubes.

The tubes were first centrifuged at 13000rpm for 1 minute to pellet the gel. Then the phenol:DNA mix was added to the tubes and centrifuged at 13,000 rpm for 5 minutes.

The aqueous phase above the gel was transferred to a new tube.

1.5ul of glycogen, 5M of NaCL and 2 volumes of ethanol were added to the sample. The sample was precipitated overnight at -20 °C.

The samples were then centrifuged at 13,000rpm for 20 minutes at 4 °C. The supernatant was removed and the pellet was washed with 500ul of -20 °C 75% ethanol. The pellet was vortexed and the sample centrifuged for 10 minutes again. The supernatant was removed. The pellet was air-dried at room temperature for 5 minutes. The sample was then resuspended in 30ul of dH2O and the DNA concentration was determined using the Nanodrop or Qubit fluorometer.

2.5.3 Agarose Gel Electrophoresis

A 2% agarose gel electrophoresis was performed. 100mls of TAE and 2g of agarose were prepared to set with 2.5ul of SYBR-safe added to the mix. 3ul of loading dye was added to each sample. 6ul of the ladder was added to the end well of the gel. Each sample was made up to a volume of 15ul to add to each well. The gel was run at 130v for 30 minutes and then analysed.

2.5.4 The Agilent Bioanalyser machine

The Agilent Bioanalyser machine was used to detect the sonication efficiency by using the DNA High-sensitivity chip.

2.6 Chromatin Immunoprecipitation (Jenner Lab protocol)

A. Bind antibody to beads.

- For 50ml PBS/BSA, weigh 0.25g of BSA (Sigma A7906) into a 50ml Falcon tube. Add 5ml 10x PBS and 45ml ddH_2O. Vortex and shake to dissolve BSA. Filter through 0.22uM syringe filter into a new 50ml tube. Place on ice.
- Add 100µl Dynal protein G magnetic beads to 900µl cold PBS/BSA in 1.5ml eppendorf tube.
- Collect the beads by spinning at 3000 rpm for 3 minutes at 4^{o}C. Remove liquid.
- Resuspend beads in 1ml cold PBS/BSA and collect the beads with the magnet.
- Leaving tubes in magnet rack, remove liquid with aspirator.
- Take out magnet and resuspend beads in 1ml cold PBS/BSA.
- Collect beads with magnet again, aspirate and resuspend beads in 250µl PBS/BSA.
- Add 10-20 µg of antibody and incubate for around 6-8hrs on rotating platform (9 rpm) in cold room.

B. Cell lysis and sonication

See protocol above

- For small cell numbers (< 1 million cells), use Axygen maximum recovery tips as well as maximum recovery 1.7ml microtubes.

C. Checking sonication

- Take 10% of lysate and freeze the rest.
- **See protocol above**

For <1 million cells, purify DNA with Zymo DNA affinity columns.

Elute in as small a volume that the columns alllow. Qubit the samples and calculate from the input sample the total amount of chromatin in your sample.

Run 10-20ul of the chromatin on the Bioanalyser Agilent high-sensitivity chip. At least 50% of the chromatin should be between 300bp and 1kb.

D. Chromatin immunoprecipitation

- If frozen, thaw lysates on ice. Add lysis buffer 3 + Complete up to 450ul per IP. Add Triton X-100 (10%) to a final volume of 10% and gently mix. Spin down insoluble material at 13,000rpm, 20 mins, 4^{o}C. Ideally use lysate equivalent to 130ug or more of DNA per ChIP (minimum 100ug DNA).

- Save 2% of lysate for input (whole cell extract (WCE)) and store at -20^{o}C.

- After 4-8 hours of antibody incubation, pull out antibody-bound beads with the magnet.

- Wash beads three times with PBS/BSA, using the magnet each time to pull beads out of solution.

- Resuspend beads in 20ul PBS/BSA.

- Add bead solution to sonicated cell lysate and immunoprecipitate on rotator at 9rpm overnight in cold room (~16 hours).

E. Wash IPs, elute and reverse crosslinks

- Requires Young wash buffer, TE+50mM NaCl and Elution solution. These can be made beforehand and stored at 4°C (wash buffer and TE+NaCl) or RT (elution solution).

- Take off lysate/bead mix and transfer 1ml to eppendorf tube in rack with magnet.

- Allow beads to bind then aspirate supernatant. Add more lysate/bead mix and repeat until all beads have been transferred.

- Remove magnet and add 1ml wash buffer. Invert magnet rack 6 times. Reverse tube orientation (so beads will be pulled to opposite wall of tube) and reintroduce magnet to capture beads.

- Repeat wash 6 times.

- Wash once with TE+50mM NaCl. Aspirate liquid and spin down 3000rpm, 5 min, 4°C.

- Remove remaining liquid and place on ice. Resuspend beads in 100ul elution buffer and incubate at 65°C for 1 hour. Vortex every 10 minutes.

- At same time, thaw WCE sample and add elution buffer up to 200ul.

- Spin down beads 13,000rpm, 1 minute, room temp. Take off supernatant into new tube and place back at 65°C for 6-7 hours. Freeze beads (which still have some DNA and protein associated with them) at -80°C.

- Save 10ul of IP eluates and half of WCE eluates at -80°C. Add 110ul of TE to remaining 90ul of IP eluate and 100ul of TE to the remaining 100ul of WCE. Freeze at-20°C.

F. RNaseA and ProteaseK treatment.

- Thaw IP and WCE tubes.

- Add 4ul of RNaseA (10ug/ul, 25x stock) to IPs and WCEs (so final concentration is 0.2µg/µl). Incubate 37°C 2 hours.

- Add 2ul of proteinase K (stock is 50x) to IPs and WCE (so final concentration is 0.2µg/µl). Incubate 55°C 2 hours.

- Add equal volume phenol:chloroform:isoamyl alcohol (25:24:1) (Fluka). Make sure is neutral pH (NOT acid phenol) and that it is the current bottle.

- Separate phases with phase-lock heavy tubes. First spin tubes 13,000rpm for 1 minute to pellet gel then add phenol:DNA mix and spin again 13,000rpm for 5 minutes.

- Transfer aqueous phase above gel to new tube. Add 1.5ul glycogen (or glycoblue), 5M NaCl (stock is 25x) and ethanol (2 volumes). Precipitate overnight at -20°C.

- Next day, spin down DNA 13,000rpm, 20 mins, 4°C. Remove supernatant and wash pellet with 500ul -20°C 75-80% ethanol. Briefly vortex pellet.

- Spin again for 10 mins and remove supernatant. Spin briefly again and remove remaining liquid with pipette.

- Air dry pellet for 5 minutes on bench. Resuspend pellet in 60ul 10mM Tris pH8. Nanodrop or use Qubit to quantitate the DNA in the samples.

G. Q-PCR to test for enrichment

- Use 0.5ul or 1ul of IP sample per well. Dilute WCEs to a concentration similar to the IPs (so 10-20ng/ul). If you have multiple WCEs, dilute them by the same ratio rather than to the same concentration to preserve differences in chromatin amount between samples.

- Quantify IPs relative to a dilution series of WCE DNA (eg. 100ng, 25ng, 5ng, 1ng, 0.2ng, 0.04ng).

2.7 Electronic cell-sorting of CD4+CD57+ cells

The PBMCs were thawed and resuspended in complete RPMI. They were centrifuged at 1500rpm for 5 minutes at 5°C, the supernatant was discarded and the pellets were resuspended in MACS buffer. CD19 microbeads (Miltenyi Biotec) were added to the sample and the B-cells were magnetically removed from the samples to enrich the CD3+ population. The remaining CD19 negative cells were stained with fluorophore-conjugated antibodies for CD4, CD8 and CD57. They were then electronically cell-sorted into CD4+CD57+, CD4+CD57- CD8+CD57+ and CD8+CD57- populations using the FACS Aria machine.

2.8 Rapid Expansion Protocol (REP) for T-cells

Following the electronic cell-sorting of the CD4+CD57+ cells from the peripheral blood of patients with CLL, the cells were expanded using this rapid expansion protocol.

Feeder cells:

3 buffy coats (from 3 healthy donors) are collected separately and washed in 2 x 10mls RPMI1640.

Resuspended in 1ml RPMI1640 and irradiate at 30Gy.

Cells are washed with 2 x 10ml RPMI1640.

The 3 buffy coats are mixed in 5ml X-VIVO/5% HuS and counted.

Adjust with X-VIVO/5% HuS (Human serum) to reach 2 x 10^7 cells/5ml.

Leave in incubator at 37^{o}C for 1-2 hours.

REP master mix (20ml/culture + 20ml for control flask)

2 x 10^7 feeder cells/5ml X-VIVO/5% HuS

15mls X-VIVO/5% HuS

1.2 x 10^5 u IL-2 (final concentration = 6000u/ml)

0.6ug anti-CD3 (OKT3)

0.5ml HEPES

Pre-cultured or sorted T cells, usually 10^5 – 5 x 10^6 T-cells/flask.

The REP-culture is performed in a T25 flask.

After 5 days, refresh 10ml media with new X-VIVO/5% HuS + IL-2 6000u/ml.

Thereafter, refresh media (10ml) twice per week. When T-cell start expanding, increase volume gradually with media containing IL-2 6000u/ml.

2.9 CyTOF – cytometry by time of flight

The CyTOF experiments for staining (cytometry by time of flight) were performed by Dr Evan Newell's laboratory using their published protocol [75]. The samples used were PBMCs from the peripheral blood of patients with CLL.

The data was gated on CD3+ T cells, then the samples were downsampled to equalise the cell numbers for each patient and tSNE was performed to summarise all the types of T cells. FlowJo software was used to analyse the raw FACS files. Two panels were used, an extracellular and intracellular/cytokine panel. These panels are detailed in the main results chapter. The cells used for the intracellular panel had been activated with PMA and Ionomycin prior to staining, whereas the cells used for the extracellular panel had not been stimulated.

The data was analysed using the GraphPad Prism Statistical software and the heat maps were also generated using this programme.

2.10 Enzyme-Linked ImmunoSpot (ELISPOT) protocol for Interferon Gamma Detection

The Human Interferon-Gamma ELISPOT^{PLUS} plates (Mabtech; 3420-4APT-2) were used for this experiment.

2.10.1 The negative selection of B-CLL cells to use as antigen presenting cells in the assay

The frozen CLL PBMC vials were thawed and transferred into a 15ml Falcon tube. 8mls of RPMI was added to the tube and it was centrifuged at 1500rpm at 5^{o}C for 5 minutes. The supernatant was aspirated and discarded. The pellet was resuspended in 5mls of RPMI and the cells were counted using the MUSE® cell analyser machine. A negative B-CLL selection was then performed using the Human B-CLL Cell Isolation Kit (Miltenyi Biotec; 130-103-466) and magnetic columns. The resultant B-CLL were resuspended in complete RPMI to make a concentration of 500,000 cells in 100ul.

2.10.2 The expanded CD4+ cells from patients with CLL

The expanded CD4+ were resuspended in complete RPMI media and added to the wells of the ELISPOT plate in the conditions described below.

There was a 5:1 ratio of APCs cells to CD4+ cells in each well (total well volume = 200ul)

Condition	Number of CD4+ cells (either CD57+ or CD57-)	Number of B-CLL cells (APCs)
1	50,000	250,000
2	10,000	50,000
3	5,000	25,000
4	2,500	12,500

Table 5: The 4 different conditions examined in the Elispot experiments.

Each of the conditions had the addition of either CMV peptivator IE-1 (Miltenyi Biotec; 130-093-493) or CMV peptivator pp65 (Miltenyi Biotec; 130-093-438).

The negative controls were the same conditions as above but without the addition of the CMV peptide.

The positive control was 250,000 PBMCs (in 200ul of complete RPMI medium) from a healthy donor, cultured with anti-CD3 (supplied with the ELISPOT kit) at a dilution of 1:1000.

2.10.3 Preparation of the Elispot plate

The Elispot plate was prepared as per the MabTech instructions. In brief, the plate was washed 4 times with sterile PBS (200ul per well). The plate was conditioned with complete RPMI (200ul/well) for 30 minutes at room temperature. The medium was removed and then the cell suspensions (of B-CLL and CD4+ cells with or without CMV peptide depending on the experimental condition) were added to the wells. The plate was wrapped in aluminium foil and placed in the incubator at 37^{o}C for 48 hours.

After 48 hours, the plate is emptied and washed 5 times with PBS (200ul/well). The ALP detection antibody (7-BP-ALP) is diluted at 1:200 in in filtered PBS + 0.5% FCS. 100ul is added to each well and the plate is incubated for 2 hours at room temperature.

The BCIP/NBT-Plus substrate solution is filtered and 100ul of substrate is added to each well. The ELIPOST is then developed until spots occurred. Then wash in tap water to stop the substrate reaction.

Leave the plate to dry and then analyse the plate by counting spots using the ELSIPOT plate reader (AID EliSpot/FluoroSpot Reader Systems; EliSpot Software Version 7.x)

2.11 ELISPOT protocol for Granzyme B Detection

The same experimental procedure was used for Granzyme B detection as described above except that the plates used were the Human Granzyme B ELISPOT^{PLUS} plates (Mabtech; 3485-4APW-2). The detection antibody used was GB11-biotin which was diluted to 1ug/ml in PBS + 0.5% FCS. 100ul was added to each well and incubated for 2 hours at room temperature. The plate was washed 5 times with PBS and Streptavidin-ALP at a dilution of 1:1000 in

PBS+0.5% FCS was added to each well (100ul/well) and incubated for 1 hour at room temperature. The same BCIP/NBT-Plus substrate solution was filtered and 100ul added to each well. The plate was developed until the spots appeared and then the reaction was stopped by washing with tap water. After a period of drying, the plate was analysed using the same EliSPOT reader as for the Interferon-Gamma EliSPOT plate described above.

2.12 Cytotoxicity assay with expanded CD4 cells

The cytotoxicity assay was performed in 96 well round-bottomed plates. Autologous B-CLL cells were negatively selected using the magnetic beads described in the ElipSPOT protocol above. These cells were then CFSE labelled as per the CFSE labelled protocol detailed below. The cells were then counted and made up to 10,000 cells in 100ul of complete RPMI media and transferred to the plate wells. These cells were the target cells. The effector cells were the expanded CD4+CD57+, CD4+CD57-, CD8+CD57+, CD8+CD57- cells. The effector cells were added at 20:1, 10:1, 5:1, 2:1 and 1:1 effector:target ratios. The total volume in each well was 200ul. The cells were then incubated at 37^{o}C for 24 and 48 hours. The negative control were target cells alone with no effector cells. The experiment was performed in triplicates.

Counting beads were added to the samples prior to analysis on the Fortessa flow cytometry machine to allow for numeric comparisons between samples.

2.12.1 CFSE staining

Reagents:

- HBSS + BSA 0.1% solution at 37 C
- CFSE solution: CellTrace CFSE Cell Proliferation Kit Life Technologies C34554). Dilute 1 vial of CFSE with 20uL DMSO (provided in the Cell Proliferation kit). Leave at room temperature.

Method:

- Resuspend cells up to 2 x 10^7 cells/mL in 1mL of warm HBSS + BSA 0.1%.
- Resuspend CFSE in 1mL of warm HBSS + BSA 0.1%. The volume depends on the desired final CFSE concentration
    - For 10uM add 4 uL

- Mix 1mL of cell suspension with 1 mL of CFSE solution
- Incubate at 37 C for 10 minutes
- Quench the reaction by adding 5 volumes of cold RPMI medium and incubate 5 mins on ice.
- Centrifuge 1400rpm for 10mins
- Wash the pellet 4X with cold HBSS

Chapter 3 The identification, characterisation and functional properties of cytotoxic CD4+ T lymphocytes in patients with Chronic Lymphocytic Leukaemia (CLL)

3.1 Introduction

Chronic Lymphocytic Leukaemia (CLL) is a clonal B-cell lymphoproliferative disorder characterised by the presence of >5 x 10^9/l circulating clonal B cells (typically CD5+, CD23+, FMC7-, weak expression of surface Ig) which have persisted for greater than 3 months [76]. It has a median age of presentation of 72 years and there is a recognised familial predisposition identified in 5-10% of patients with CLL [77]. Presenting symptoms and signs may include lymphadenopathy, B symptoms, cytopenias accompanying bone marrow infiltration, autoimmune haemolytic anaemia and an increased susceptibility to infections. Both the Rai clinical staging system [78] and the Binet staging system [79] have been used as prognostic scores in CLL. Progression to a high grade lymphoma ("Richter's transformation") may occur in patients with CLL and is associated with a poor prognosis [80]. There have been major breakthroughs in CLL management in recent years with the advent of targeted therapies such as Ibrutinib (a BTK-inhibitor), Idelalisib (a PI3K delta inhibitor), and Venetoclax (a BCL-2 inhibitor) [81]. Whilst targeting the B-cell receptor signalling pathways, the new therapies also have an effect on the T cell populations in the tumour microenvironment. For example, Ibrutinib affects the tumour microenvironment by reducing the overall number of T cells, in particular the number of Th17 subclass of CD4+ cells [82].

CLL often causes a clinically significant immunodeficiency which results in an increased acquisition of infections. Hypogammaglobulinaemia, which is well recognised in this condition, may require treatment with immunoglobulin infusions. There is also a recognised dysfunction in T cell function in patients with CLL. An impairment in the immune synapse formation between the T-cell and antigen-presenting cells in patients with CLL has been described and *in vitro* treatment with the immunomodulatory drug Lenalidomide reverses this impairment in synapse formation [83]. There is a known expansion in both the CD4+ and CD8+ T cell compartments in CLL. CD8+ T cells from patients with CLL retain the capacity to produce cytokines despite expression of surface markers which have often been linked to T cell exhaustion [84]. Furthermore, cytotoxic CD4+ T cells (expressing perforin) have previously been described in the peripheral blood of these patients where they can constitute up to 60% of the total CD4+ population [85].

3.2 Aims

The aims of this chapter were as follows:

1. To detect the presence of CD4+GZB+ cells in the peripheral blood of patients with untreated CLL.
2. To examine the level of CD4+GZB+ cells with CMV status, age and white cell count.
3. To phenotype the cells with respect to transcription factors and cell surface markers and to compare the CD4+ and CD8+ subsets to identify any common features in the cytotoxic T cell populations.
4. To identify the presence of cytotoxic CD4+ T lymphocytes in the tumour microenvironment of patients with CLL.

3.3 The identification of CD4+ Granzyme B+ cells in lymph node biopsies from patients with CLL when compared to reactive lymph nodes

To establish whether CD4+GZB+ cells were present in the tumour microenvironment of patients with CLL, formulin-fixed, paraffin embedded (FFPE) lymph node biopsies infiltrated with CLL from 6 patients were obtained from the Department of Histopathology, UCLH. As a normal control, 6 FFPE lymph node biopsies with the histological diagnosis of "reactive lymph node" were also obtained. In collaboration with Prof Marafioti's laboratory, the lymph node biopsy slides underwent triple immunohistochemistry to stain for CD4, Granzyme B and FoxP3. Each of the triple stained biopsy slides were image-scanned using a Hamamatsu NanoZoomer digital slide scanner. The slide images were visualized using NDP.view2 (NanoZoomer Digital Pathology) software.

Five areas at x40 magnification were identified from the tumour area of each biopsy diagnostic of disease. For the control "reactive" lymph node biopsies, five areas at x40 magnification were chosen at random. Using Image J software, where a grid was superimposed on each area, all of the stained cells in these five areas were manually counted and allocated to one of 7 different combination groups (Figure 3-1).

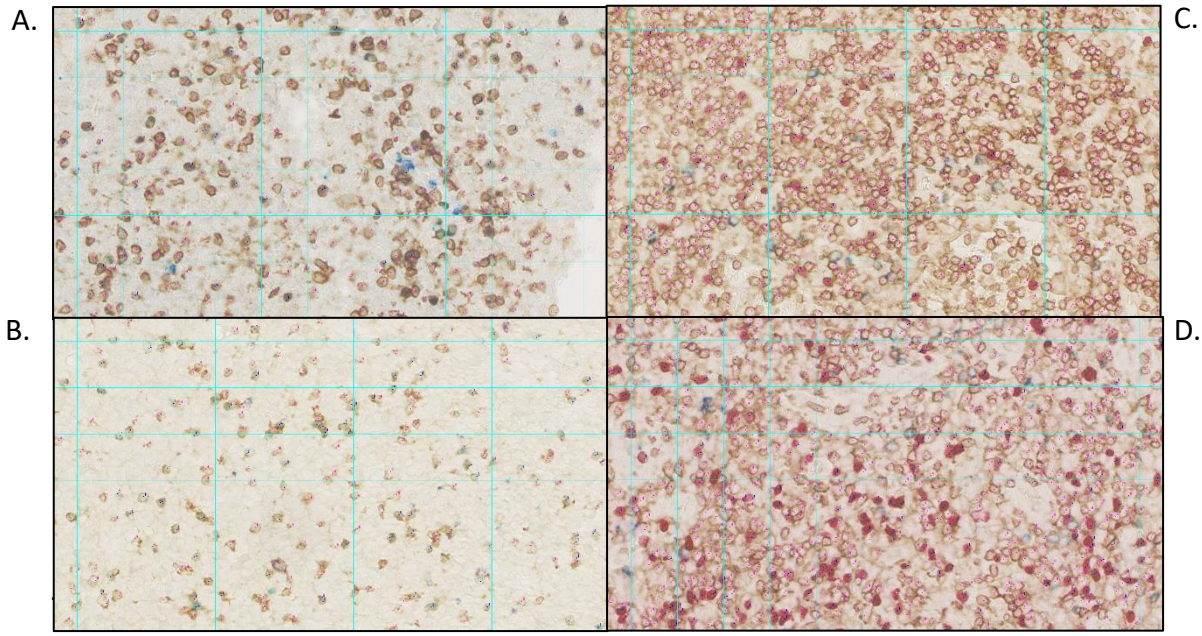

Figure 3-1: The cell-counting technique for triple-colour immunohistochemistry. Figure 3.1A and 3.1B are lymph node biopsies at x40 magnification with a histological diagnosis of Chronic Lymphocytic Leukaemia (CLL). Figures 3.1C and 3.1D are lymph node biopsies at x40 magnification with a histological diagnosis of reactive lymphadenopathy. Using ImageJ software, a grid has been superimposed upon the images and each cell has been counted and marked with a corresponding number depending upon the cell type that it represents. The number of each cell type counted is recorded in the ImageJ programme and collated for data analysis. Figure 3.1A, 3.1C and 3.ID: CD4 (brown), FoxP3 (red) and Granzyme B (blue). Figure 3.1B: CD4 (brown), FoxP3 (green), Granzyme B (red).

CD4 = Brown
FoxP3 = Red
Granzyme B = Blue

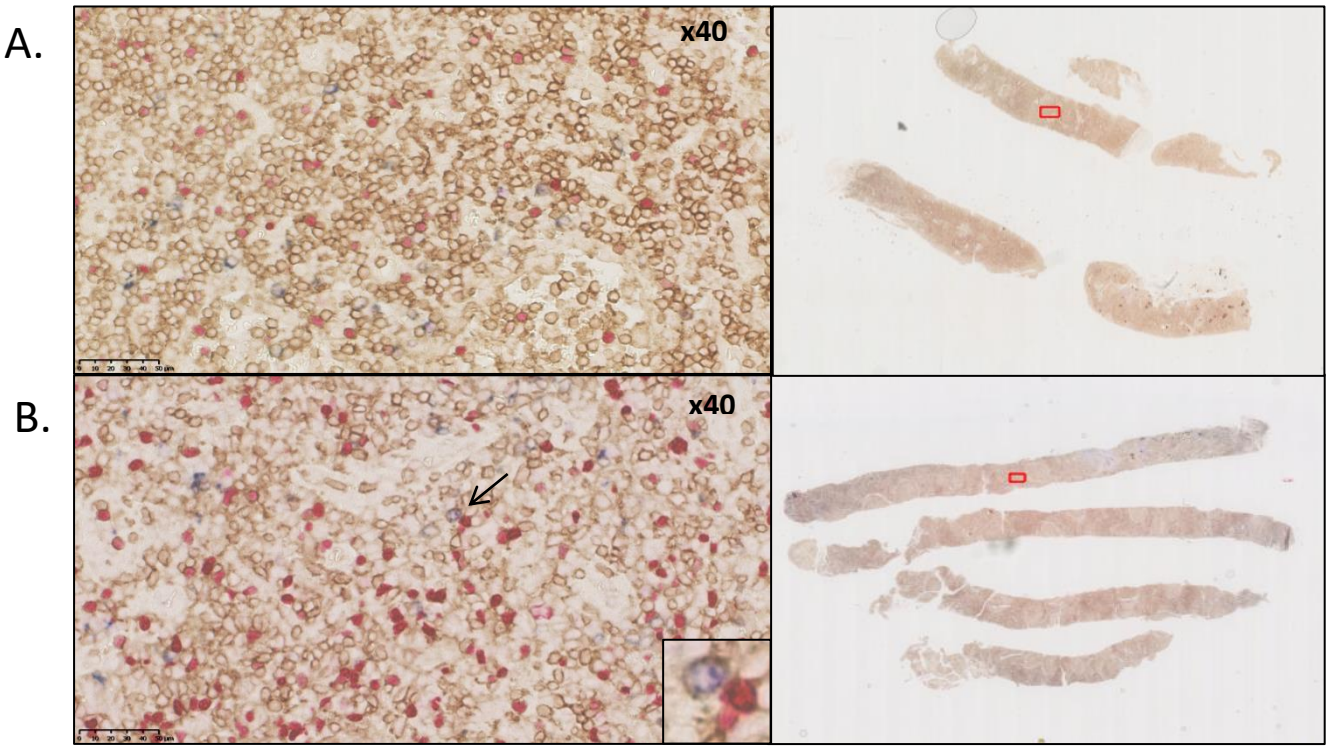

Figure 3-2: Two examples of lymph node core biopsies which have the histological diagnosis of a "reactive" lymph node. These lymph node biopsies have been stained using triple-colour immunohistochemistry for CD4 (brown), FoxP3 (red) and Granzyme B (blue). The image on the left is a x40 magnification field of the lymph node biopsy. This x40 magnification field corresponds to the red box located in the image of the lymph node core biopsy in the image on the right. In Figure 3.2B, the arrow corresponds to the site of the magnified image in the box in the right-hand corner. This shows a CD4+GZB+ (Brown and Blue) cell.

The clinical characteristics of the patients with CLL whose biopsies were studied are shown in Table 6. The clinical characteristics of the patients with a diagnosis of "reactive lymph node" whose biopsies were studied are shown in Table 7.

Case	Histological Diagnosis	Age at time of biopsy (Years)	Sex	Immunophenotype	Proliferative index (Ki67)	CMV serological status (IgG)
1	Chronic Lymphocytic Leukaemia	51	F	CD20, CD5, CD23.	<5%	Negative
2	Chronic Lymphocytic Leukaemia	57	M	CD20, CD5, CD23.	Not specified	Negative
3	Chronic Lymphocytic Leukaemia	65	M	CD20, CD19, CD5, CD23.	25%	Positive
4	Chronic Lymphocytic Leukaemia	51	M	CD20, CD5, CD23, bcl-2	Not specified	Positive
5	Chronic Lymphocytic Leukaemia	84	M	CD20, CD5, CD23, CD79a	Not specified	Unknown
6	Chronic Lymphocytic Leukaemia	69	M	CD20, CD5, CD23.	Not specified	Unknown

Table 6: The patient characteristics, histological diagnosis and immunophenotype of the 6 lymph node biopsies infiltrated with Chronic Lymphocytic Leukaemia (CLL) which underwent triple-colour immunohistochemistry. M = Male, F = Female.

Case	Histological Diagnosis	Age at time of biopsy (Years)	Sex	Clinical indication for biopsy	CMV serological status (IgG)
1	Reactive lymphadenopathy	65	F	Cervical Lymphadenopathy	Unknown
2	Reactive lymphadenopathy	11	M	Cervical Lymphadenopathy	Unknown
3	Reactive lymphadenopathy	45	F	Inguinal lymphadenopathy	Unknown
4	Reactive lymphadenopathy	69	F	Weight loss and Lymphadenopathy	Unknown
5	Reactive lymphadenopathy	35	M	Lymphadenopathy	Negative
6	Reactive lymphadenopathy	32	M	Cervical Lymphadenopathy	Positive

Table 7: The patient characteristics, histological diagnosis and clinical indication of the 6 lymph node biopsies with a histological diagnosis of "reactive lymphadenopathy" which underwent triple-colour immunohistochemistry. M = Male, F = Female

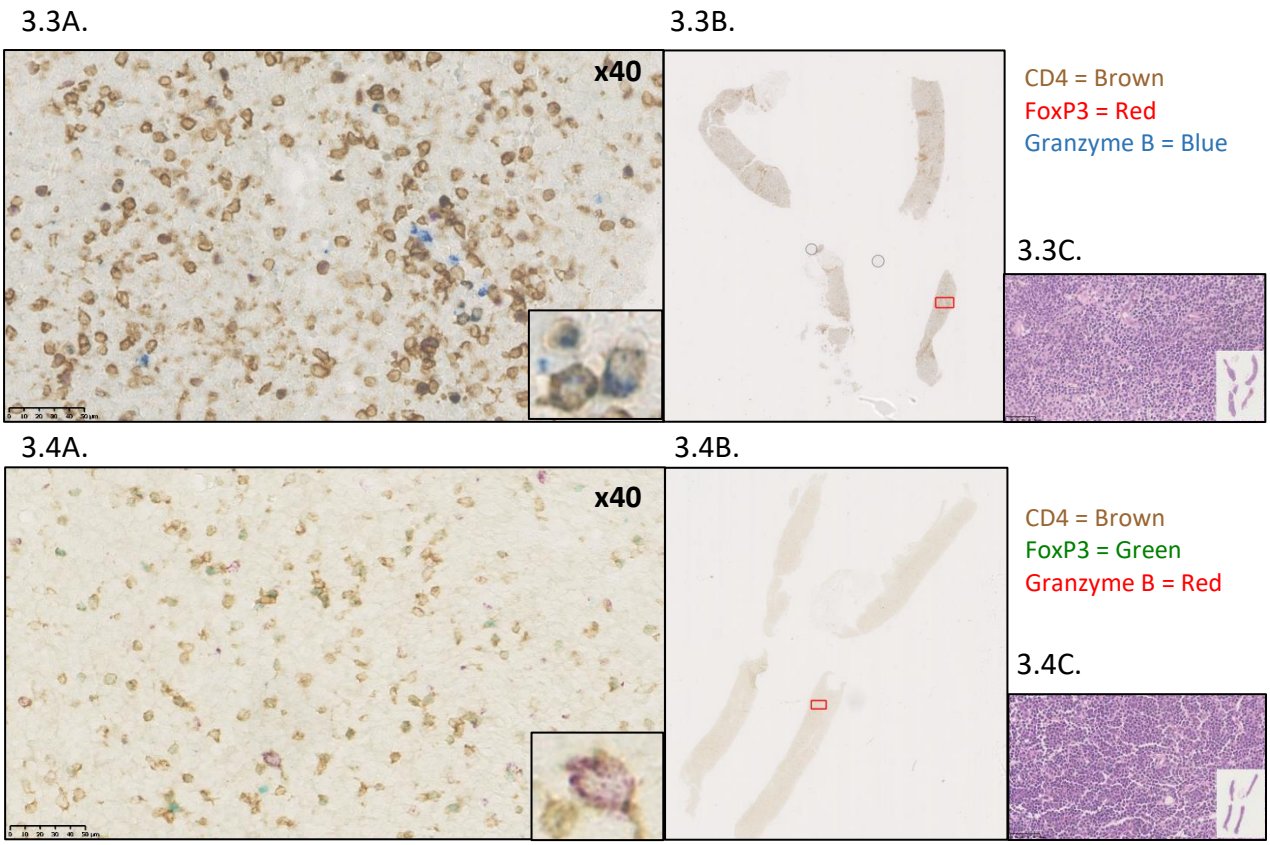

Figure 3-3: A lymph node core biopsy with a histological diagnosis of Chronic Lymphocytic Leukaemia which has been stained for CD4 (brown), FoxP3 (red) and Granzyme B (blue). Figure 3.3A shows a x40 magnification field of the lymph node biopsy. This x40 magnification field corresponds to the red box located in the image of the lymph node core biopsy in Figure 3.3B. Figure 3.3C shows a x40 magnification from the Haematoxylin and Eosin (H+E) staining of the lymph node core biopsy.

Figure 3-4: A lymph node core biopsy with a histological diagnosis of Chronic Lymphocytic Leukaemia which has been stained for CD4 (brown), FoxP3 (green) and Granzyme B (red). Figure 3.4A shows a x40 magnification field of the lymph node biopsy. This x40 magnification field corresponds to the red box located in the image of the lymph node core biopsy in Figure 3.4B. Figure 3.4C shows a x40 magnification from the Haematoxylin and Eosin (H+E) staining of the lymph node core biopsy. The magnified images in the boxes in the right-hand bottom corner of Figure 3.3A show CD4+GZB+ cells.

3.3.1 Results: CD4+ populations

(1) CD4+Granzyme B+ population

The CD4+GZB+ cells reflect the cytotoxic CD4+ cell population. There is a trend towards a higher absolute number of CD4+GZB+ in the CLL lymph nodes when compared to the reactive lymph nodes (Figure 3.5D). The percentage of CD4+GZB+ cells out of the total stained cells is significantly higher in the CLL lymph nodes when compared with the reactive lymph nodes (Figure 3.6D; P= 0.0043). When considering the composition of the CD4+ compartment only, the percentage of CD4+GZB+ out of the total CD4+ cells is significantly higher in the CLL lymph nodes (Figure 3.7B; P=0.0043).

(2) CD4+FOXP3+ population

The CD4+FOXP3+ population reflects the T regulatory (Tregs) cells present in the lymph node biopsies. There is a significant increase in the absolute number of CD4+FOXP3+ cells present in the reactive lymph node biopsies when compared to the CLL lymph node biopsies (Figure 3.5E; P=0.0087). However, as a percentage of the total stained cells, there was no significant difference between the reactive lymph nodes and CLL lymph nodes (Figure 3.6E). There was also no significant difference in the percentage of CD4+FOXP3+ cells out of the total CD4+ population between the two lymph node groups (Figure 3.7C).

(3) CD4+ (Granzyme B-, FOXP3-) population

The CD4+ population (single stain positive) include those CD4+ cells that are not T regulatory cells (as they are FoxP3 negative) and are not cytotoxic cells (as they are Granzyme B negative). There is a significant decrease in the absolute number of CD4+ cells in the CLL lymph nodes when compared to the reactive lymph nodes (Figure 3.5A; P=0.0043). However, there is no significant difference in the percentage of CD4+ cells out of the total stained cells or out of the total CD4+ cells between the CLL and reactive lymph nodes (Figures 3.6A and 3.7A).

(4) CD4+Granzyme B+ FOXP3+ population

The CD4+Granzyme B+ FOXP3+ cells represent the T regulatory cells that also express Granzyme B. The absolute number of these cells was low in both the reactive and CLL lymph nodes (Figure 3.5G). The percentage of CD4+GZB+FOXP3+ cells out of the total stained cells and total CD4+ population was low at less than 1%. There was no significant difference in the percentages between the CLL and reactive lymph nodes (Figure 3.6G and 3.7D). Therefore, the majority of Tregs in these lymph node biopsies did not express Granzyme B

3.3.2 Results: Granzyme B+ populations

The Granzyme B+ cell populations, as well as including cytotoxic CD4+ cells (as discussed above), also include other cytotoxic lymphocytes, namely CD8+ lymphocytes, NK (Natural Killer) and NKT cells.

(1) Granzyme B+ (CD4- FOXP3-) population

There was a significant decrease in the absolute number of Granzyme B positive (CD4-FOXP3-) cells in the CLL lymph nodes when compared to the reactive lymph nodes (Figure 3.5C; P=0.0260). However, there was no significant difference in the percentage of GZB+ cells of the total stained cells when the CLL and reactive lymph nodes were compared (Figure 3.6C).

(2) Granzyme B+ FOXP3+ (CD4-) population

The overall absolute number of GZB+FOXP3+ cells was very low (less than 15 cells) in each lymph node biopsy (Figure 3.5F). There was no significant difference in the absolute number or percentage of stained cells between the reactive and CLL lymph node biopsies (Figure 3.5F and 6F).

3.3.3 Results: FOXP3+ (CD4- Granzyme B-) population

This population was low in both absolute numbers and percentage of total stained cells (Figure 3.5B and Figure 3.6B). Although there was a trend towards an increase in percentage of FOXP3+ cells as a total of all stained cells in the CLL lymph node biopsies, the overall

percentages were small and this was not statistically significant (Figure 3.6B). There was no statistical significance difference in the absolute number of FOXP3+ cells between the two lymph node groups (Figure 3.5B).

3.4 Summary of Immunohistochemistry Results

The comparison between the CLL lymph nodes and reactive lymph nodes identifies that cytotoxic CD4+GZB+ cells are present in the CLL lymph node tumour microenvironment. There is a significant increase in the percentage of cytotoxic CD4+GZB+ out of both the total stained cells and the CD4+ population in the CLL lymph nodes when compared to the reactive lymph nodes. The significant decrease in the absolute numbers of CD4+ (FOXP3-GZB-), GZB+ (CD4-FOXP3-) and CD4+FOXP3+ (GZB-) cells in the CLL lymph nodes, when compared to the reactive lymph nodes, is likely to be related to the abnormal CLL B-lymphocytes infiltrative populations in the lymph nodes decreasing the absolute numbers of other cell types. This is reinforced by there being no statistically significant difference in the percentages of these cell types when calculated as a percentage of total stained cells and CD4+ populations.

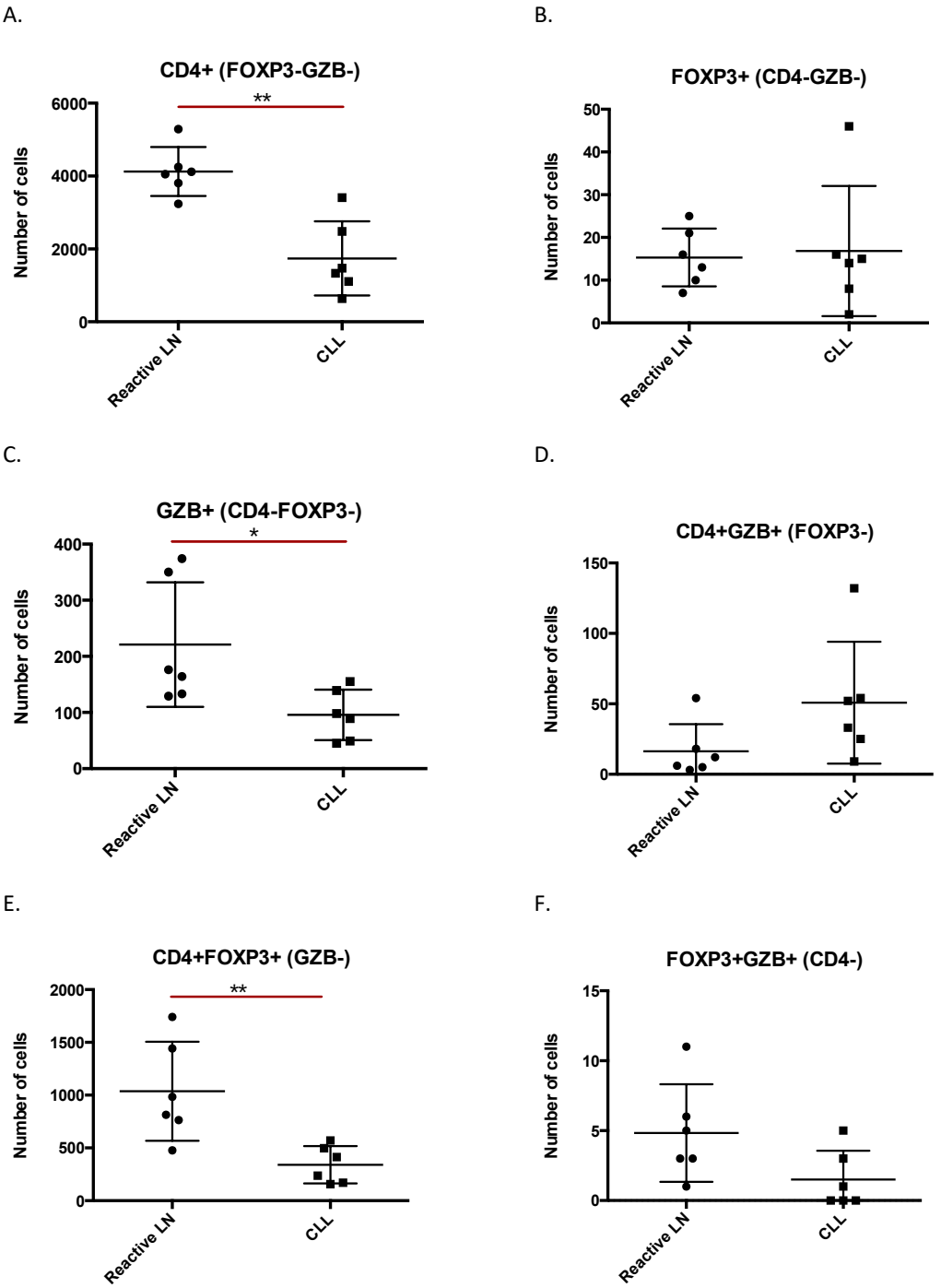

Figure 3-5: The absolute number of cells counted in the CLL and reactive lymph node biopsies which have been triple IHC stained for CD4, FoxP3 and Granzyme B. Figures 3.5A-G show the results for each positive staining outcome. Figures 3.5A-C show those cells that are positive for single markers (CD4+, FOXP3+ or GZB+). Figures 3.5D-F show those cells that are positive for double markers (CD4+GZB+, CD4+FOXP3+, FOXP3+GZB+) and Figure 3.5g shows the triple positive cells (CD4+FOXP3+GZB+). Figure 3.5A shows that there is a significant increase in the absolute number of CD4+ (FOXP3-GZB-) cells in reactive LNs when compared to CLL LNs (P=0.0043). Figure 3.5C shows a significant increase in the absolute number of GZB+ (CD4-FOXP3-) cells in the reactive LNs when compared with the CLL LNs (P=0.0260). Figure 3.5E shows a significant increase in the absolute number of CD4+FOXP3+ (GZB-) cells in reactive LNs when compared to CLL LNs (P=0.0087). There is no significant difference in the absolute numbers of FOXP3+ (CD4-GZB-), CD4+GZB+ (FOXP3-), FOXP3+GZB+ (CD4-) or CD4+FOXP3+GZB+ in reactive LNs and CLL LNs (Figures 3.5B, 3.5D, 3.5F and 3.5G). The Mann-Whitney U test was used for statistical analysis.

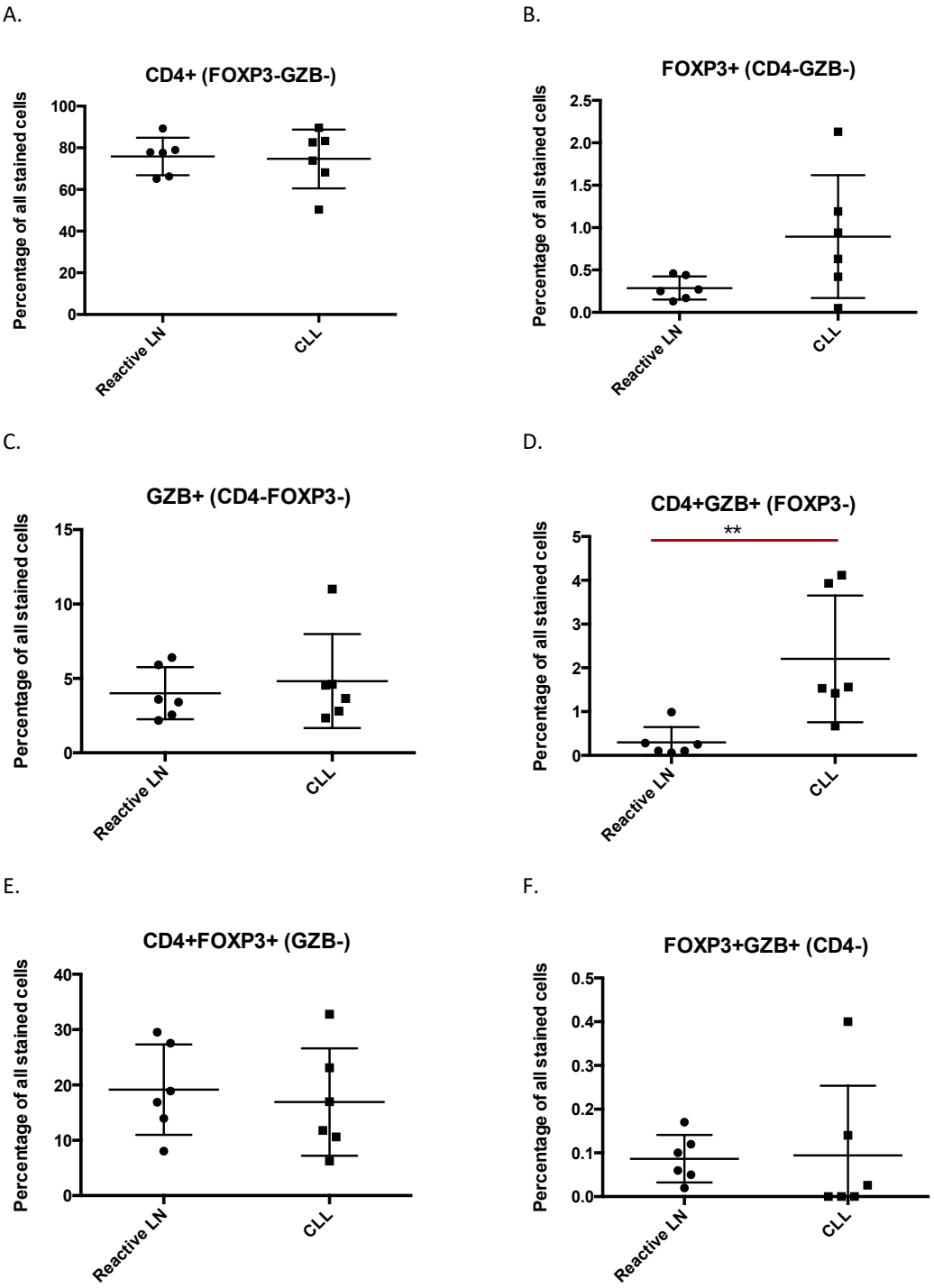

Figure 3-6: The percentage number of each cell type out of the total stained cells in the human lymph node biopsies following IHC staining for Granzyme B, CD4 and FOXP3. Figures 3.6A-G show the results for each positive staining outcome. Figures 3.6A-C show those cells that are positive for single markers (CD4+, FOXP3+ or GZB+). Figures 3.6D-F show those cells that are positive for double markers (CD4+GZB+, CD4+FOXP3+, FOXP3+GZB+) and Figure 3.6G shows the triple positive cells (CD4+FOXP3+GZB+). Figure 3.GA shows that the percentage of CD4+ (FOXP3-GZB-) cells out of the total stained cells was consistently high (approx. 60-90%) but there was no significant difference in the percentage of CD4+ (FOXP3-GZB-) cells between reactive and CLL LNs. Figure 3.6D shows a significant increase in the percentage of CD4+GZB+ (FOXP3-) cells (out of the total stained cells) in the CLL LNs when compared to the reactive LNs (P=0.0043). There was no significant difference in the percentage of other cell types out of the total stained cells (Figures 3.6A-C, 3.6E-G) when compared between reactive LNs and CLL LNs. The Mann-Whitney U test was used for statistical analysis.

A.

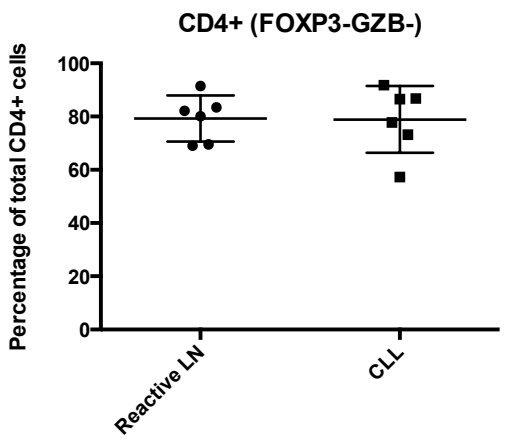

B.

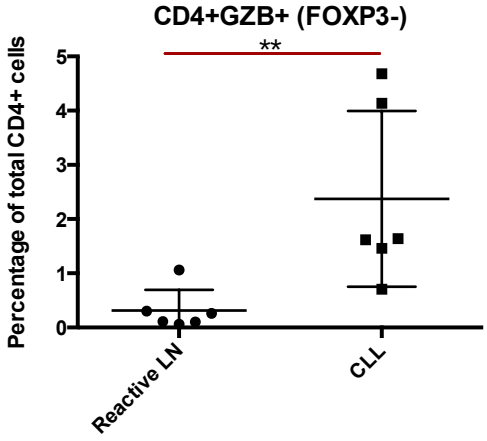

C.

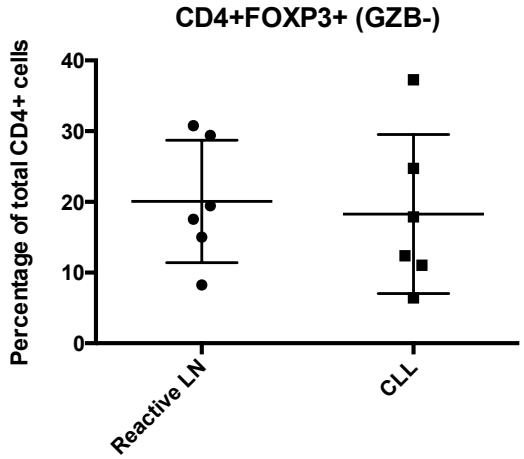

D.

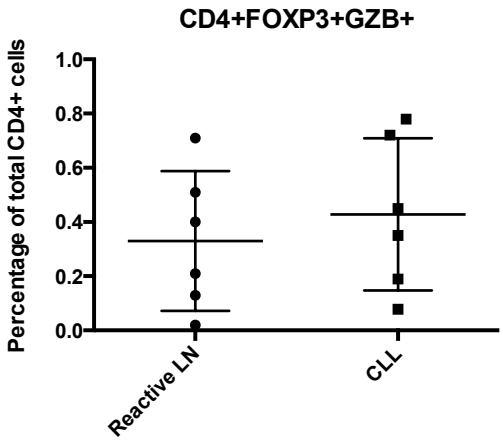

Figure 3-7: The percentage of stained cells out of the total CD4+ cells in the human lymph node biopsies following triple IHC staining for CD4+, Granzyme B and FOXP3. Figures 3.7A-D show the results for each positive staining outcome. Figure 3.7A shows the percentage of cells that are positive for CD4+ only (FOXP3-GZB-). Figures 3.7B-C show the percentage of cells that are positive for double markers (CD4+GZB+ or CD4+FOXP3+) and Figure 3.7D shows the percentage of triple positive cells (CD4+FOXP3+GZB+). The majority of cells in the CD4+ T cell compartments are CD4+ (FOXP3-, GZB-) (Figure 3.7A) for both the reactive LN and CLL LNs. There is a statistically significant increase in the percentage of CD4+GZB+ (FOXP3-) cells (of the total CD4+ cells) in the CLL LNs when compared with the reactive LNs (P=0.0043; Figure 3.7B). There is no significant difference in the percentage of either CD4+FOXP3+ (GZB-) cells or CD4+FOXP3+GZB+ cells between the reactive LNs and CLL LNs (Figures 3.7C-D). *CLL – Chronic Lymphocytic Leukaemia; GZB = Granzyme B, LN = Lymph Node.*

Patient	1	2	3	4	5	6	7	8	9	10
Age (years)	65	66	47	57	68	59	47	54	71	70
Sex (Male/Female)	M	M	M	M	M	M	M	F	M	M
White Blood Cell Count (WBC) (x 10^9/L)	42.6	25.89	16.27	48.04	27.26	69.61	22.45	13.45	19.77	15.45
Lymphocyte Count (x 10^9/L)	39.96	18.12	10.8	42.76	20.45	61.95	13.02	9.76	13.4	9.33
CMV serostatus	Positive	Positive	Positive	Negative	Negative	Positive	Positive	Positive	Negative	Positive

Table 8: The patient characteristics of the 10 patients with CLL who were all Binet Stage A and not on treatment for CLL. Their peripheral blood was tested by Flow Cytometry for the extended immunophenotype panels. M = Male, F = Female.

3.5 Flow cytometry analysis of the peripheral blood of patients with CLL to characterise the phenotype of cytotoxic CD4+ T cells

In collaboration with Professor Nathwani's laboratory, peripheral blood was obtained from patients with CLL who were attending the weekly out-patient haematology clinic at UCLH. Initially, flow cytometry was performed on a cohort of 10 patients' peripheral blood to identify and phenotype the presence of cytotoxic CD4+ T cells. All of the patients had Binet Stage A CLL (with fewer than 3 areas of lymphadenopathy, no anaemia or thrombocytopenia) [79] and had not received any treatment for their CLL. The clinical details of the 10 patients who had an extended phenotype analysis are shown in Table 8. Over a 3-year duration, 90 patients with CLL who were not receiving treatment had blood samples collected and analysed for the presence of cytotoxic CD4+ cells. The clinical details of those patients are shown in Table 9.

3.5.1 The presence of CD4+GZB+ cells in the peripheral blood of patients with CLL

CD4+ Granzyme B+ cells were detected in the peripheral blood of patients with CLL by flow cytometry (Figure 3-8). Whilst healthy controls have less than 2% of their CD4+ population expressing a cytotoxic phenotype [10], in the CLL population, this was elevated to up to 82% in some cases with a median percentage of 7.83% (range: 0.14 – 82.06%) in the cohort of 90 CLL patients.

Characteristic	Number
Number of Patients	90
Median age (years)	67 (41-90)
Female/Male	29/61
Median White Blood Cell Count (x 10^9/l)	30.02 (3.56 – 369.94)
Median Haemoglobin (g/dL)	13.4 (6.8 – 16.5)
Median Platelets (x 10^9/l)	170 (8 – 334)
Median Neutrophil Count (x 10^9/l)	4.37 (1.01 – 24.04)
Median Lymphocyte Count (x 10^9/l)	25.13 (0.41 – 336.65)
CMV status - Seropositive - Seronegative - Unknown	 48 21 21
Current CLL Treatment:	None
Previous CLL Treatment: Yes No	 14 76

Table 9: Table of patient characteristics of all CLL patients with CD4+GZB+ counts.

3.5.2 Percentage of CD4+Granzyme B+ cells and association with CMV serological status

The CMV serological status was known in 69 patients: 21 were CMV seronegative and 48 were CMV seropositive. There is a significant increase in the percentage of CD4+ cells that express Granzyme B in the peripheral blood of patients with CLL in those patients who are CMV seropositive when compared with those who are CMV seronegative (P<0.0001) (Figure 3-8A). Both groups have a higher than average percentage when compared to healthy controls in the literature [71]**.** The median percentage of CD4+GZB+ cells in CMV positive patients was 10.62% (range: 0.929-82.06%) and in CMV negative patients was 3.06% (range: 0.60 – 18.8%). There was no documented evidence of CMV-related clinical disease in any of the patients included in this report.

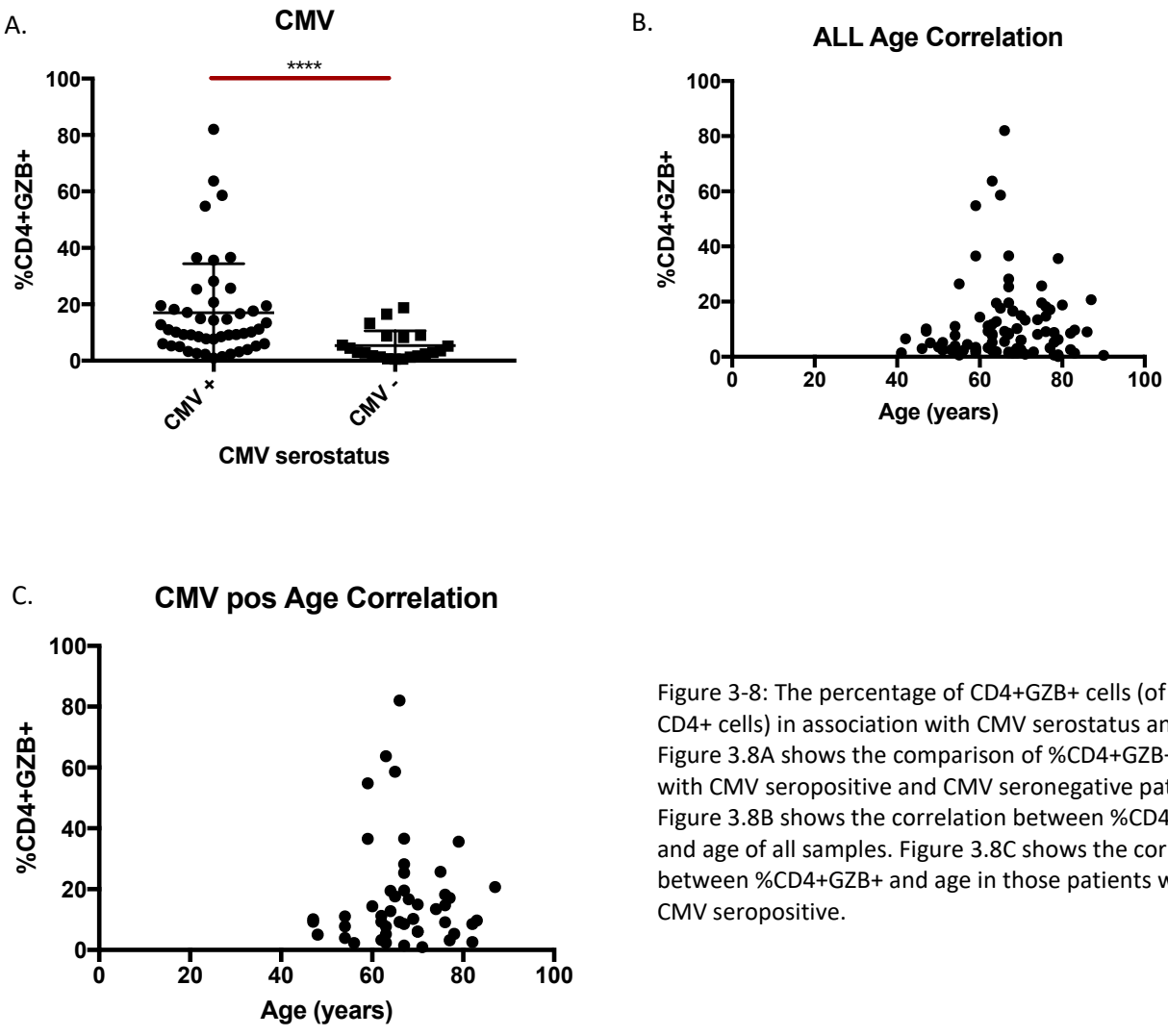

Figure 3-8: The percentage of CD4+GZB+ cells (of total CD4+ cells) in association with CMV serostatus and age. Figure 3.8A shows the comparison of %CD4+GZB+ cells with CMV seropositive and CMV seronegative patients. Figure 3.8B shows the correlation between %CD4+GZB+ and age of all samples. Figure 3.8C shows the correlation between %CD4+GZB+ and age in those patients who are CMV seropositive.

3.5.3 Percentage of CD4+Granzyme B+ cells and comparison with total white cell count

In crude terms, the white cell count (WBC) level could be seen as a marker of disease burden in CLL as an increasing WBC can be interpreted as a sign of disease progression. The percentage of CD4+GZB+ cells was compared with the total white cell count (Figure 3-9). Initially the comparison was made with all samples analysed from the 90 patients. This did not show a correlation between the level of CD4+GZB+ cells and the total white cell count of the patient [Pearson R value: -0.04078 (95% CI: -0.2481 to 0.1701)]. In view of the previously demonstrated association of CMV serostatus and CD4+GZB+ level, a comparison was made between the CD4+GZB+ level and total white cell count in those patients who were CMV seropositive only. This did not show a correlation between CD4+GZB+ level and total white cell count [Pearson R value: -0.1361 (95% CI: -0.4074 to 0.1572)] (Figure 3-9).

3.5.4 Percentage of CD4+Granzyme B+ cells and comparison with the lymphocyte count

The total white cell count would include non-lymphoid cells including neutrophils, basophils and eosinophils. Therefore, the total lymphocyte count was compared to the CD4+GZB+ level as the majority of the lymphocyte count would be expected to include the neoplastic B-CLL cells. Figure 3-9 C shows the comparison of the lymphocyte count with CD4+GZB+ for all 90 patients. There was no correlation between CD4+GZB+ level and lymphocyte count in this group of patients [Pearson R value: -0.03845 (95% CI: -0.2459 to 0.1724]. Figure 3-9 D shows the comparison of the lymphocyte count with CD4+GZB+ for the CMV seropositive patients only. There was no correlation between CD4+GZB+ level and lymphocyte count in the CMV seropositive group of patients [Pearson R value: -0.1302 (95% CI: -0.4023 to 0.163)].

3.5.5 Percentage of CD4+Granzyme B+ cells and comparison with age

The percentage of CD4+GZB+ cells in the peripheral blood was compared with the age of the patients with CLL. Previous research has found an increase in the percentage of cytotoxic CD4+cells in the older population (10). When examining the level of CD4+GZB+ in all 90 patients with CLL, no correlation was found with the patients' age (Figure 3-8B) [Pearson r value: 0.0373 (95% CI: -0.1723 to 0.2437)]

When examining the subgroup of patients who were CMV seropositive, there was also no correlation demonstrated between the patients' age and the level of CD4+GZB+ cells (Figure 3-8C) [Pearson r value: -0.0066 (95% CI: -0.2902 to 0.278)].

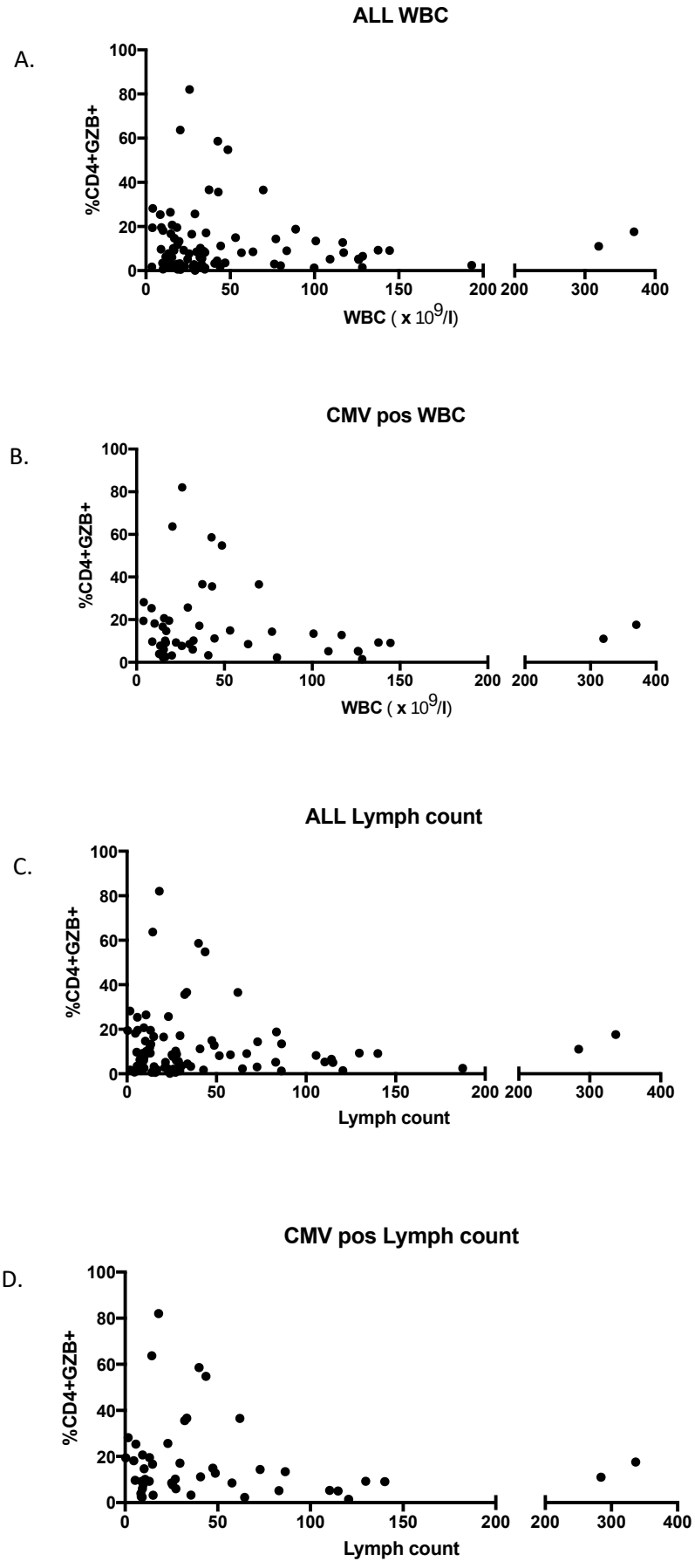

Figure 3-9: The percentage of CD4+GZB+ cells (of total CD4+ cells) in association with total white cell count and total lymphocyte count. Figure 3-9A shows the comparison of %CD4+GZB+ cells with the total white cell count for all samples. Figure 3-9B shows the comparison of %CD4+GZB+ cells with total white cell count for only CMV seropositive samples. Figure 3-9C shows the comparison of %CD4+GZB+ cells with total lymphocyte count for all samples. Figure 3-9D shows the comparison of %CD4+GZB+ cells with total lymphocyte count for only CMV seropositive samples.

3.5.6 Phenotype of CD4+GZB+ cells

An extended phenotype analysis of the CD4+GZB+ cells identified in the peripheral blood of 10 patients with CLL was performed using flow cytometry (Figure 3-11). This phenotype was compared to CD8+GZB+ cells to identify any similarities in the phenotype between these two types of CTL. Although the CD4+CTLs comprised up to approximately 80% of the CD4+ population in some patients, the median percentage of CD4+ cells expressing Granzyme B was 11.30% (range 0.6404 – 81.89%) whereas the median percentage of CD8+ cells expressing Granzyme B was 68.82% (range 51.92-89.14%). The CD8+ population expressed Granzyme B at a significantly higher level than the CD4+ population (P=0.0007) (Figure 3-10).

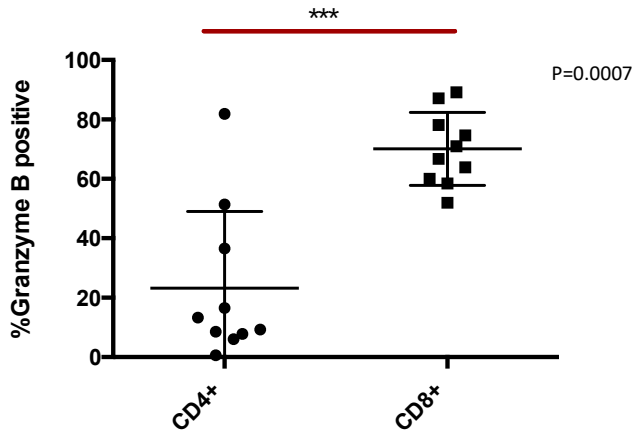

Figure 3-10: The percentage of CD4+ cells and CD8+ cells that are Granzyme B positive in the peripheral blood of patients with CLL.

Regarding the expression of co-inhibitory receptors, PD-1 is expressed in the majority of CD4+GZB+ cells (median: 66.4%; range: 11.2-92%). PD-1 (Programmed cell death protein-1) is a co-inhibitory member of the Ig superfamily of receptors. Its prime function is to restrict T-cell activation and effector function in the peripheral tissues at sites of inflammation and/or infection. Cytotoxic T-lymphocyte-associated protein 4 (CTLA-4), a member of the immunoglobulin superfamily of receptors and a co-inhibitory receptor expressed on activated T cells and constitutively expressed on Tregs, is not expressed on the majority of CD4+GZB+ cells. Two additional co-inhibitory receptors, LAG3 and TIM3, are also not expressed on the majority of CD4+GZB+ cells (Figure 3-11).

With respect to the co-stimulatory receptors, Inducible T-cell co-stimulator (ICOS; CD278) is a co-stimulatory receptor that is expressed on activated T lymphocytes. It is not expressed on CD4+GZB+ cells. 41BB, OX40, CD40L and GITR are also not expressed on the majority of CD4+GZB+ cells. Another member of the immunoglobulin superfamily of receptors, CD28,

which acts as a co-stimulatory receptor to provide a secondary signal for T cell activation following antigen presentation, has a low level expression in CD4+GZB+ cells (median expression: 27.2%; range: 0.7 – 74.1%). Likewise, the majority of CD4+GZB+ cells do not express CD27, a member of the TNF receptor superfamily (Figure 3-11). CD27 is expressed on naïve T lymphocytes and its expressed is upregulated upon TCR stimulation. The loss of CD27 implies that the T lymphocyte has been exposed to antigen.

With respect to the transcription factors analysed, FoxP3 was not expressed on the CD4+CTLs thereby distinguishing them from the Treg subset of CD4+ cells. Eomes and Tbet were highly expressed in CD4+GZB+ cells (Eomes median expression: 72.8%, range: 22.8-95.1%; Tbet median expression: 89.7%, range: 76.1 – 93.6%). As discussed previously, both Eomes and Tbet have been strongly implicated in the development of cytotoxicity in CD8+ cells. Ki67, a marker of proliferation, is also low in the CD4+GZB+ subsets (Figure 3-11). Interestingly, the majority of CD4+GZB+ cells express CD57 (HNK-1), a glycan carbohydrate epitope which is also expressed on NK cells and adhesion molecules of neural cells [86]**.**

3.5.7 Phenotype of CD4+GZB- cells

The CD4+GZB- cell subset will contain those CD4+ cells that are effector CD4+ cells which are not cytotoxic and also includes the T regulatory subset. Regarding the co-inhibitory receptors, as in the CD4+GZB+ subset, there is low expression of CTLA-4 and LAG3 (median: 29.3%; range: 12.1-34.7%) in the minority of cells. PD-1 has a median expression of 46.9% (range: 35.8 – 74.0%).

With respect to the co-stimulatory receptor expression, there is a low expression of 41BB, CD40L and ICOS which is similar to the CD4+GZB+ subset. The expression of OX40 is higher than in the CD4+GZB+ cells. In contrast to the CD4+GZB+ cells, the majority of CD4+GZB- cells express CD28 (median: 97.8%; range: 84.8 – 99.4%). In addition, the majority of CD4+GZB- cells express CD27 (median: 80.9%; range: 46.9 – 86.4%), unlike the Granzyme B positive cells.

In contrast to the CD4+GZB+ cells, the majority of CD4+GZB- cells do not express CD57. There is a low expression of the proliferation marker Ki67. The transcription factor profile shows that the majority of CD4+GZB- cells do not express EOMES, unlike the Granzyme B + CD4+ cells, and the majority of CD4+GZB- cells do express Tbet (median: 56.9%; range: 40.8 – 62.4%).

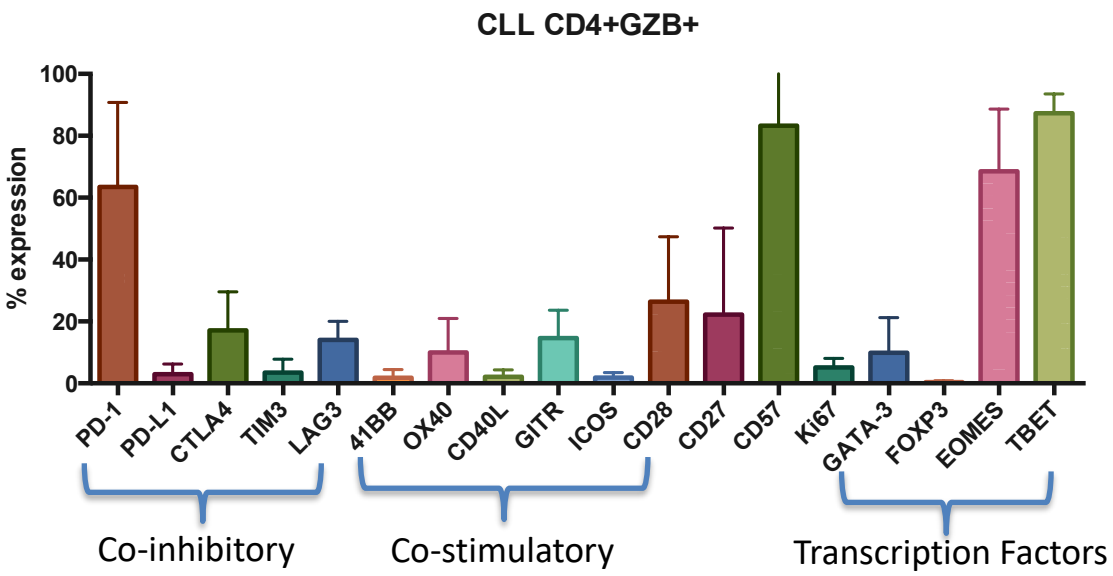

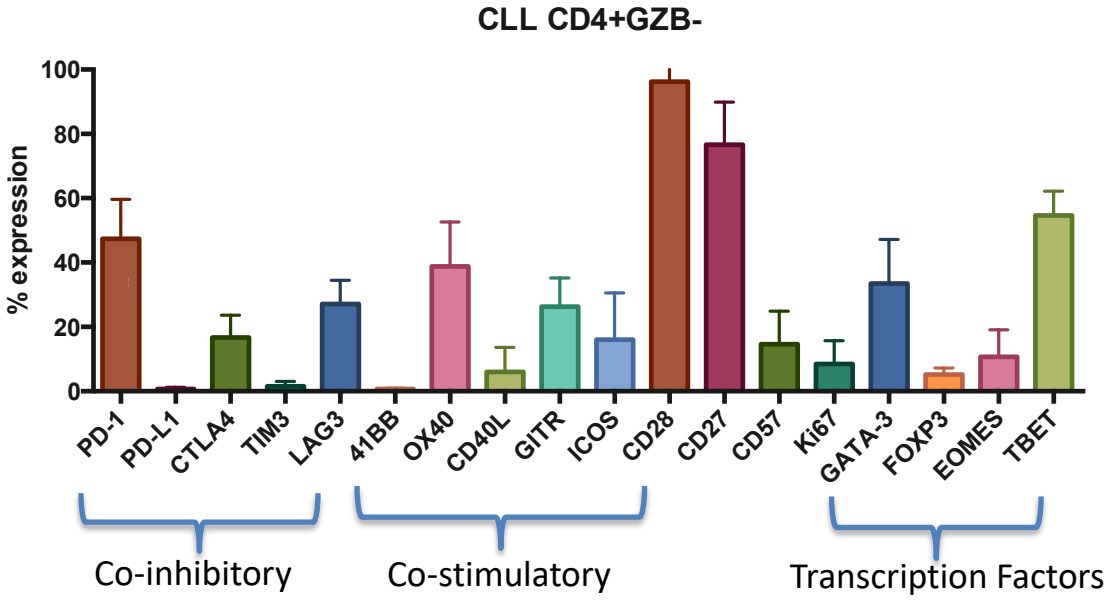

Figure 3-11: The immunophenotype of the CD4+GZB+ and CD4+GZB- cells from the peripheral blood of 10 patients with CLL.

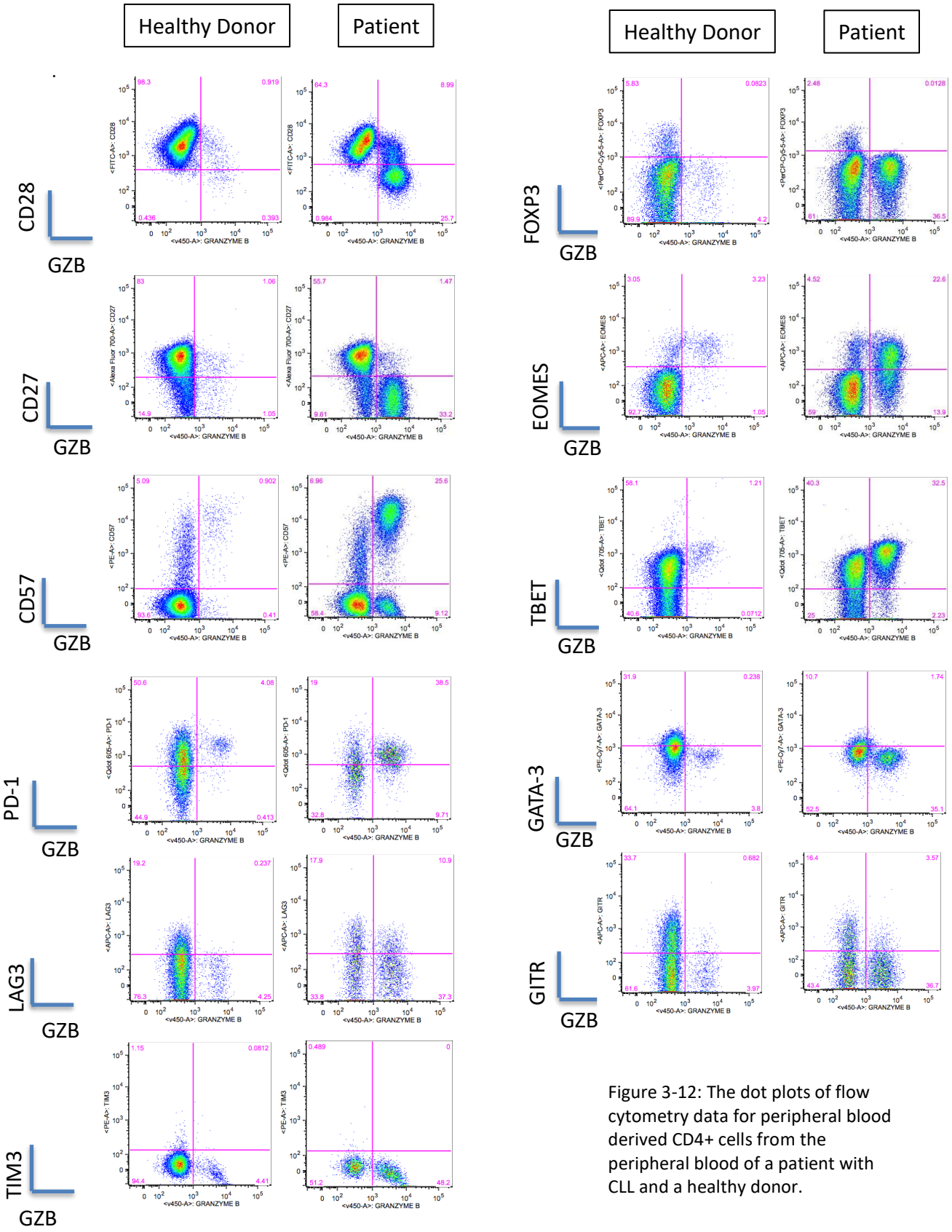

Figure 3-12: The dot plots of flow cytometry data for peripheral blood derived CD4+ cells from the peripheral blood of a patient with CLL and a healthy donor.

CD4+ cells

3.5.8 Phenotype of CD8+GZB+ cells

The phenotype of the CD8+GZB+ cells appears more similar to the CD4+GZB+ cells than the CD4+GZB- cells. Similar to the CD4+GZB+ cells, PD-1 is the only co-inhibitory receptor that is expressed on the majority of CD8+GZB+ cells (Figure 3-13).

Regarding the co-stimulatory receptors, there is a low expression of all of the markers examined. CD8+GZB+ cells also have a low expression of CD28 and CD27, similar to the CD4+GZB+ cells. Furthermore, CD57 is expressed on the majority of CD8+GZB+ cells (median: 90.3%; range: 70.0 – 98.2%). Ki67, the proliferation marker, is also low on the CD8+GZB+ cells. With respect to the transcription factors, the majority of CD8+GZB+ cells do not express GATA-3 and FOXP3, whereas the majority do express EOMES (median: 87.0%; range: 76.9 – 90.9%) and Tbet (median: 75.3%; range: 61.3 – 82.9%).

3.5.9 Phenotype of CD8+GZB- cells

The CD8+GZB- cells comprise the minority percentage of CD8+ cells. Their phenotype is similar to the CD4+GZB- cells with respect to the high expression of CD28 (median: 85.4%; range: 59.9 – 93.1%) and CD27 (median: 84.0%; range: 32.7 – 94.1%) in the majority of cells and a low expression of CD57 (median: 32.0%; range: 10.7 – 61.3%) (in contrast to the Granzyme B+ subsets of CD4+ and CD8+ cells). The majority of CD8+GZB- cells do not express the other co-stimulatory receptors and co-inhibitory receptors, except PD-1 which is expressed in approximately half of the CD8+GZB- cells (median: 51.7%; range: 37.6 – 91.3%). Similar to the CD8+GZB+ cells, the majority of CD8+GZB- cells express EOMES although in contrast, the majority do not express TBET (median 26.2%; range: 15.6 – 35.0%). Ki67 has a low expression on this subset of CD8+ cells (Figure 3-13).

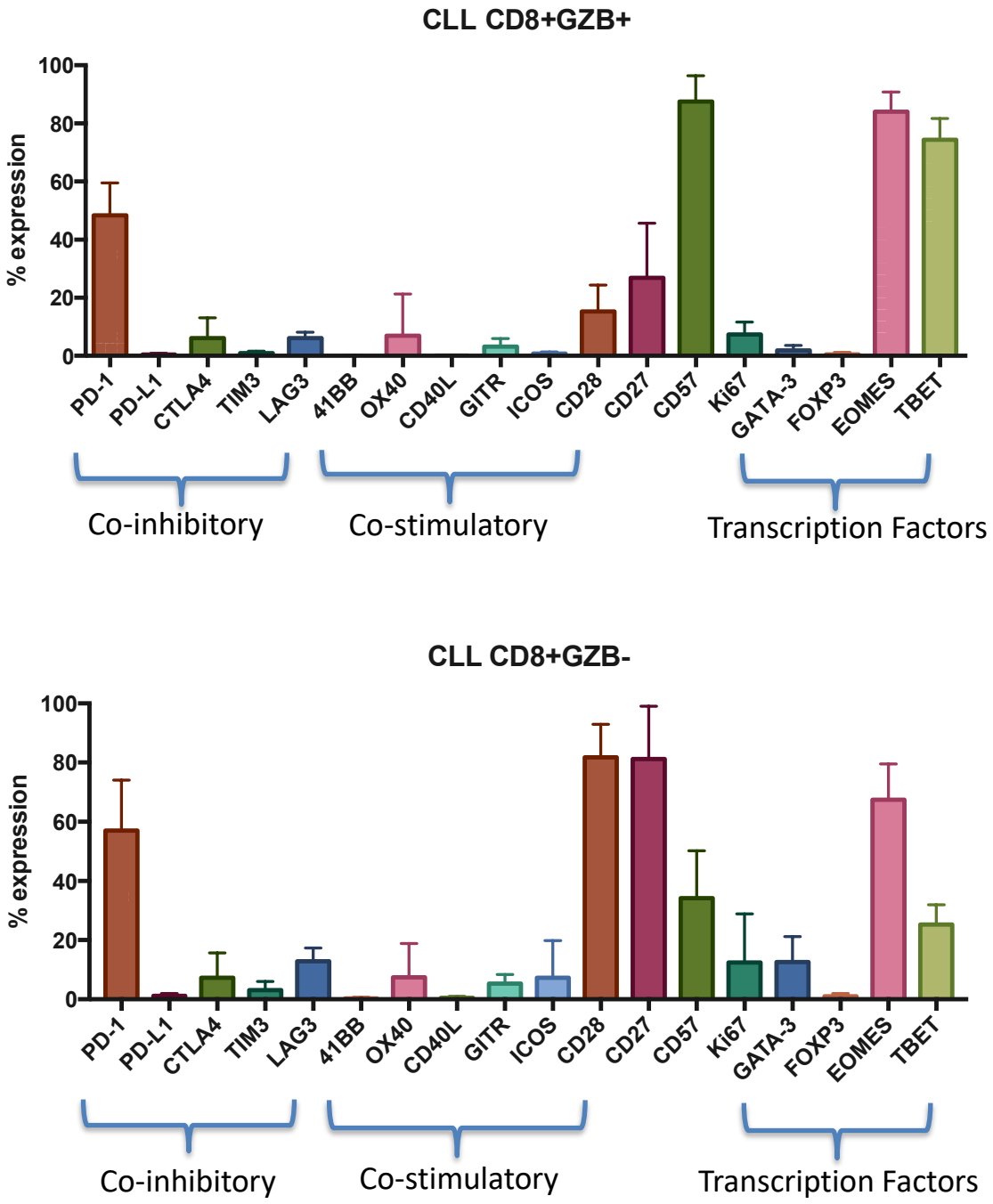

Figure 3-13: The immunophenotype of the CD8+GZB+ and CD8+GZB- cells from the peripheral blood of 10 patients with CLL.

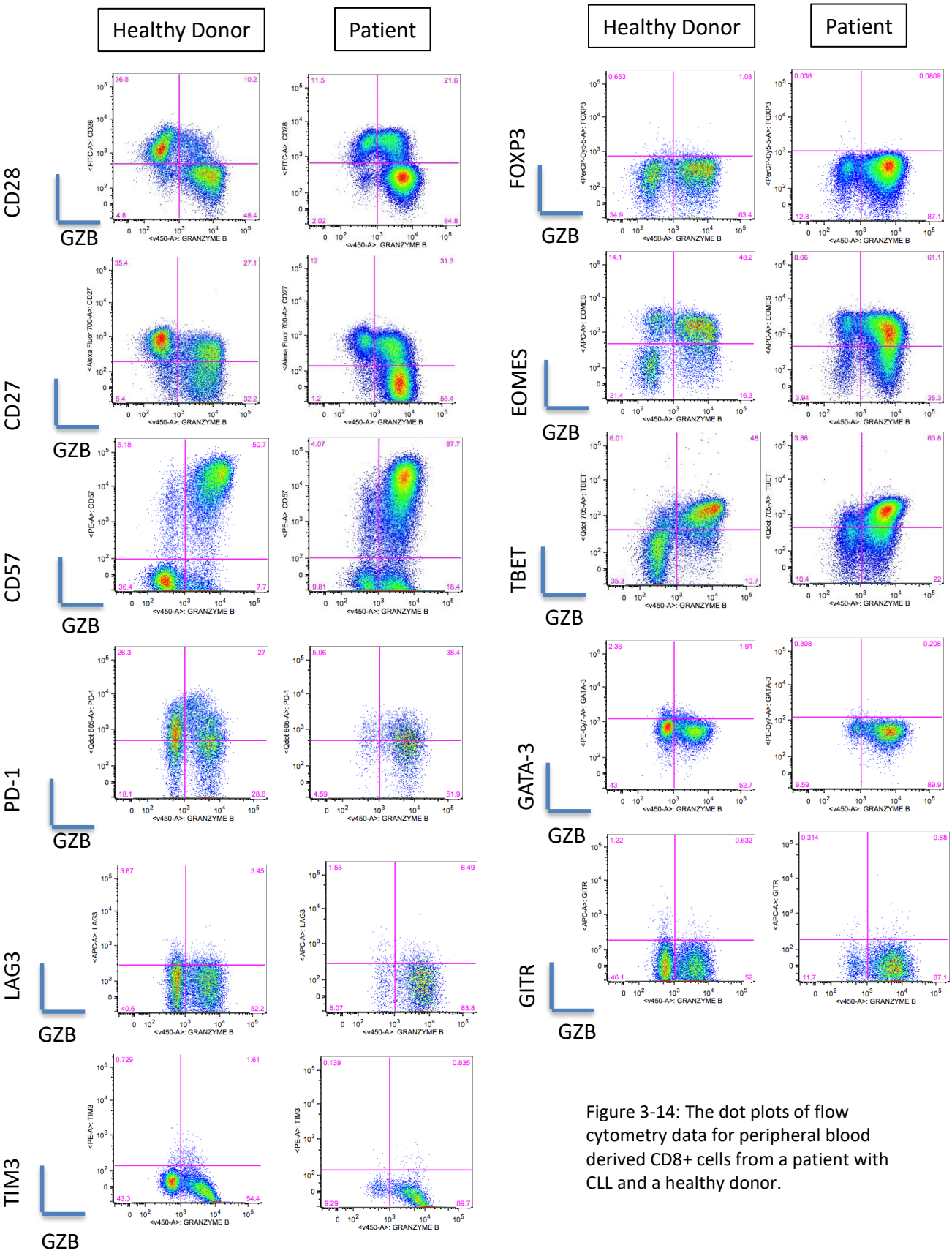

Figure 3-14: The dot plots of flow cytometry data for peripheral blood derived CD8+ cells from a patient with CLL and a healthy donor.

3.5.10 Comparison of CD4+GZB+ cells and CD8+GZB+ cells

In summary, the CD4+GZB+ subset's phenotype most closely resembles the CD8+GZB+ cell subset with a high expression of CD57, low expression of the CD28 and CD27 cell surface receptors, a high expression of the transcription factors EOMES and TBET (which have been implicated in the determination of cytotoxicity) and the higher expression of PD-1 when compared to the Granzyme B negative subsets. There was no significant difference in the percentage expression of PD-1, CD28, CD27 or CD57 between the CD4+GZB+ and CD8+GZB+ cells (Figure 3-15).

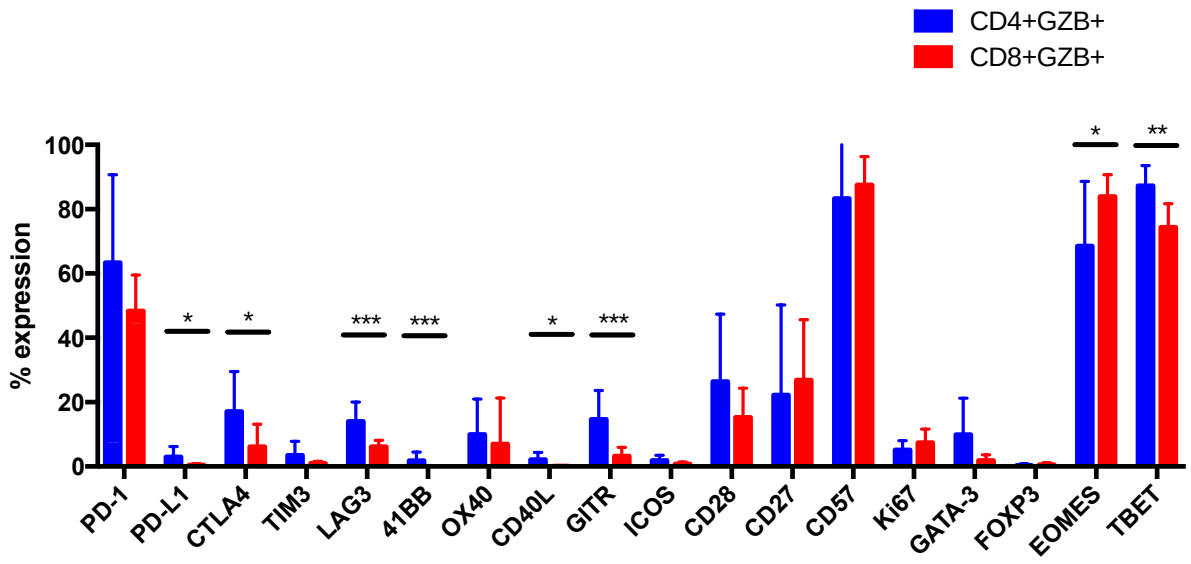

Figure 3-15: The comparison of the CD4+GZB+ and CD8+GZB+ phenotype in the peripheral blood of 10 patients with CLL. A significant difference in level of expression between the CD4+GZB+ and CD8+GZB+ cells were seen in the following markers: PDL1: P=0.0433; CTLA-4: P=0.0147; LAG3: P=0.0003; 41BB: P=0.0007; CD40L: P=0.0184; GITR: P=0.0002; EOMES: P=0.0232; TBET: P=0.0015. The Mann Whitney U test was used for statistical analysis.

3.5.11 The comparison of peripheral blood immunophenotyping in samples which have been processed immediately and those samples which have been frozen at -80°C and then thawed.

The peripheral blood from patients with CLL were obtained on a weekly basis. We decided to check whether freezing the cells affected their phenotype when compared with cells which were stained "fresh" (without freezing). Figure 3-16 and Figure 3-17 show the results of the comparison between fresh and frozen phenotype analysis for CD4+ and CD8+ cells from a patient with CLL and a healthy donor. The results show that the percentage difference in expression of markers between frozen and fresh CD4+ samples was consistently less than 5% for the majority of antigens examined.

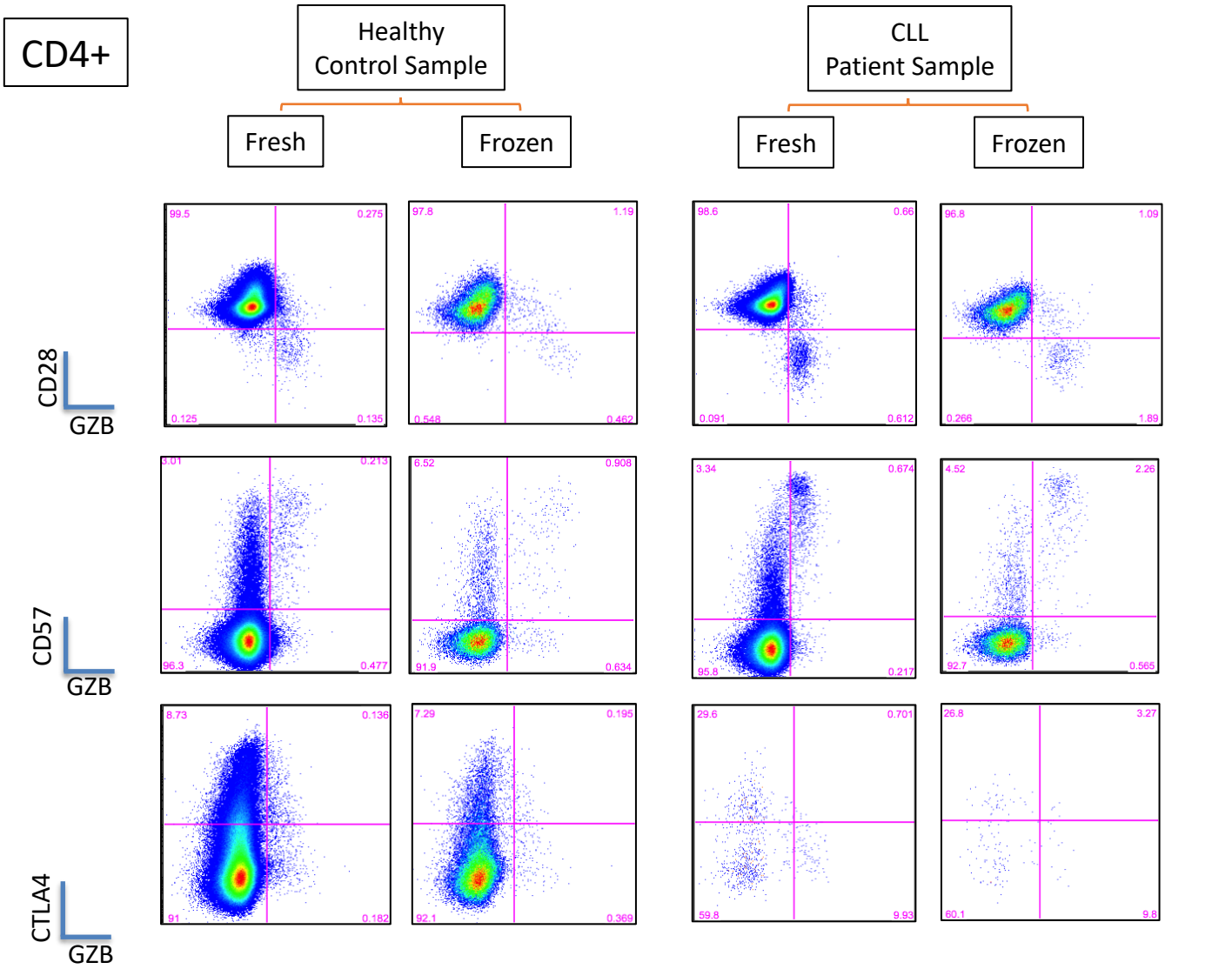

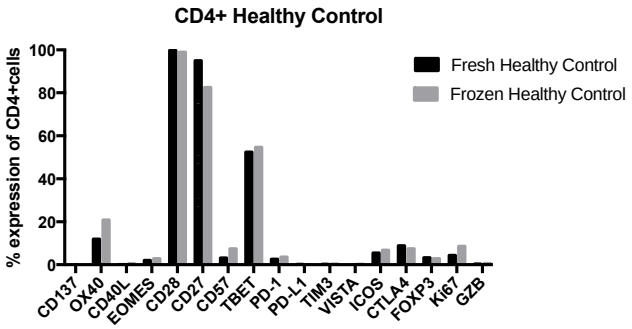

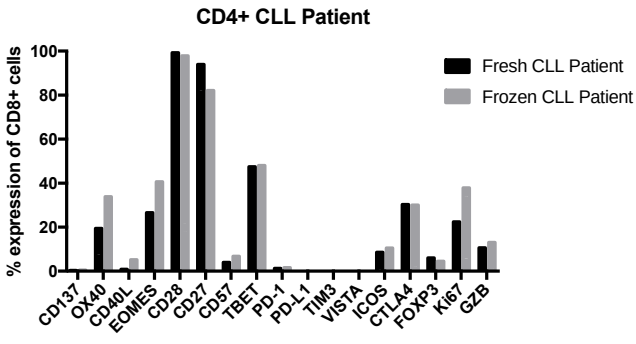

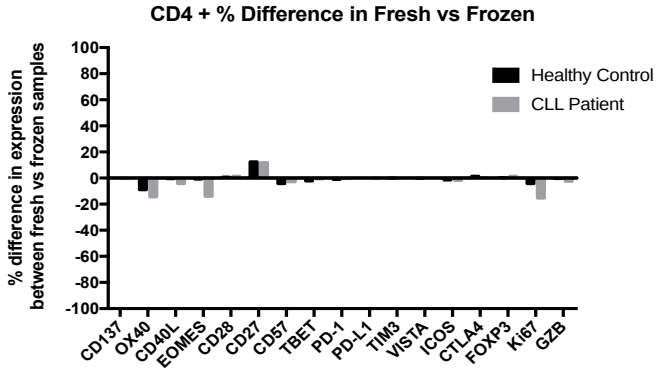

Figure 3-16: Comparison of the CD4+ phenotype of peripheral blood samples from a healthy control and a patient with CLL. The samples were either stained "fresh" or 24 hours after being "frozen" at -80°C.

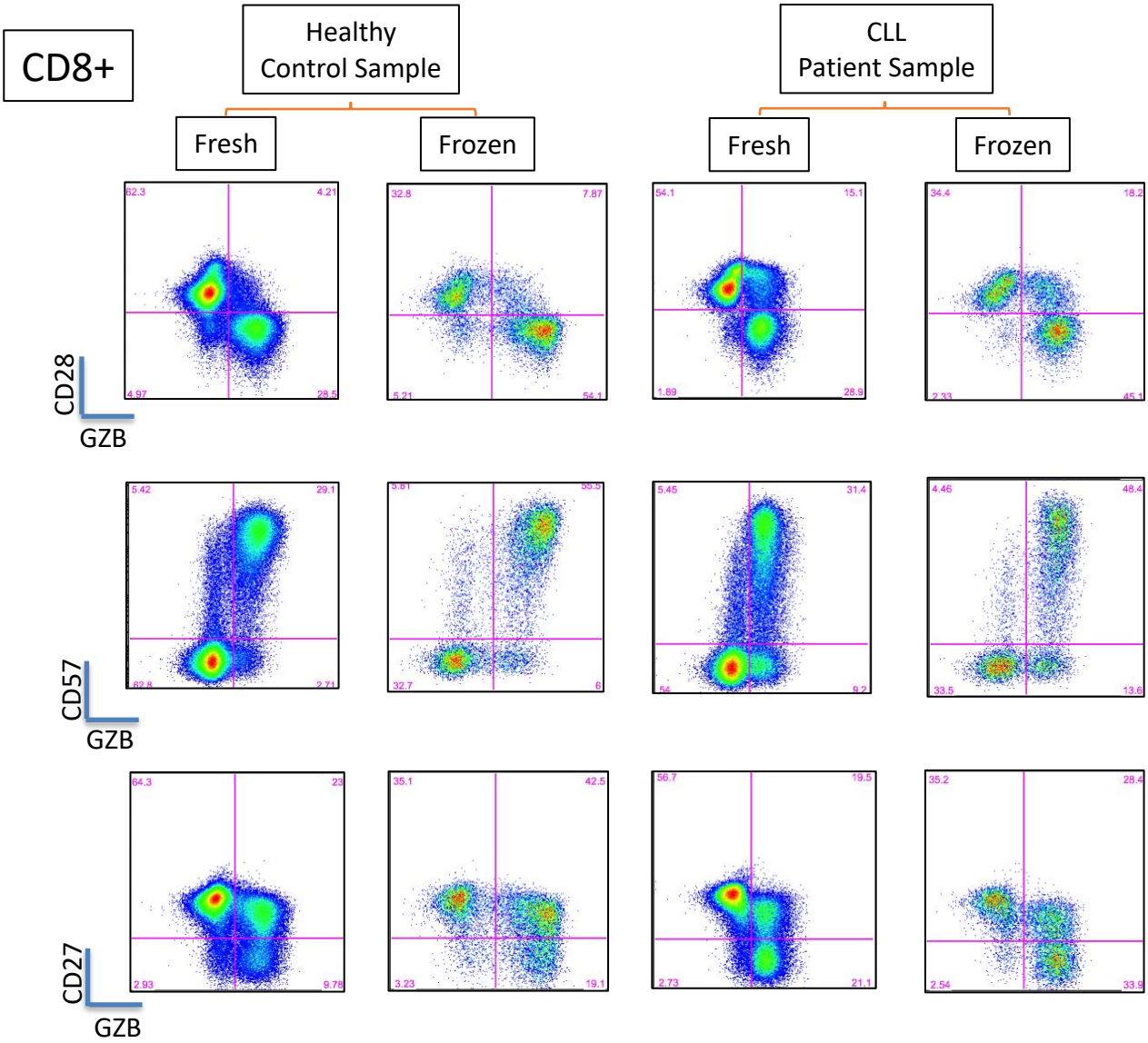

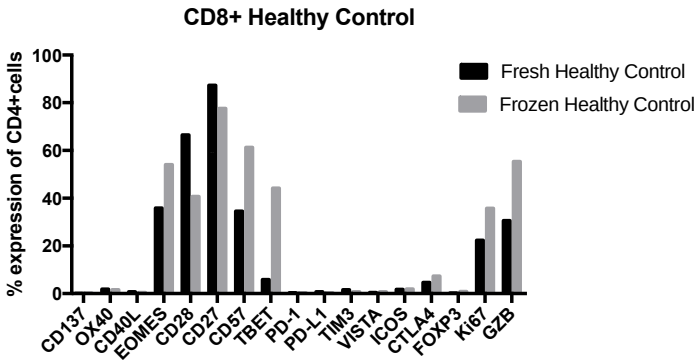

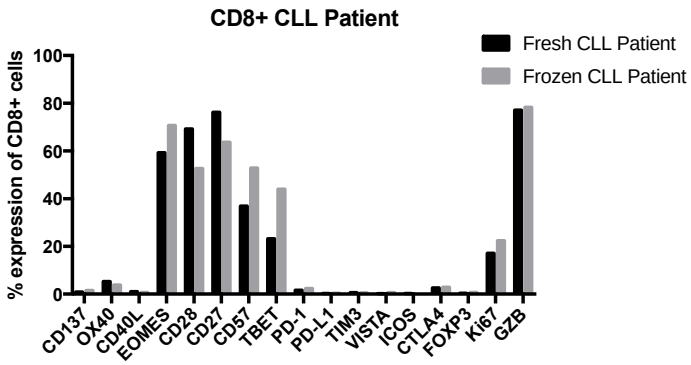

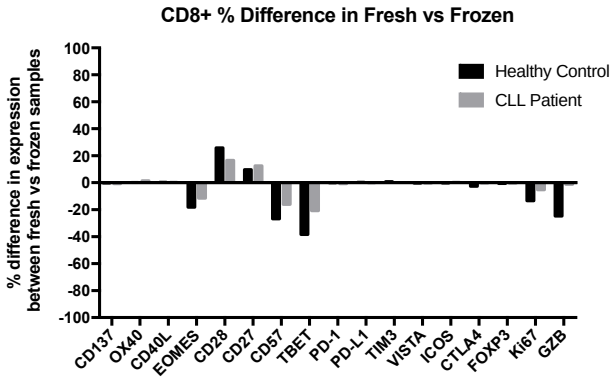

Figure 3-17: Comparison of the CD8+ phenotype of peripheral blood samples from a healthy control and a patient with CLL. The samples were either stained "fresh" or 24 hours after being "frozen" at -80°C.

3.5.12 The level of CD4+GZB+ cells in the peripheral blood of patients with CLL over time

Forty-five patients had peripheral blood collected at 2 different time points and the level of CD4+GZB+ cells were assessed in both samples. A comparison was made between the percentage of CD4+GZB+ (of total CD4+ cells) in both samples to examine whether the CD4+GZB+ level remained stable over time. Figure 3-18A shows the CD4+GZB+ values for each of the paired samples. Figure 3-18B shows the difference in percentage CD4+GZB+ levels between the two samples for each patient. Figure 3-18C shows the median and range for the difference in percentage CD4+GZB+ levels. As can be seen in Figure 3-18C, the median difference in CD4+GZB+ values between the 2 samples for this group of patients was 0.19% (range: -25.00% to 46.11%). The median time between the two samples was 189 days (range: 7 – 735 days).

Eighteen patients had peripheral blood collected at 3 different time points. Figure 3-18D shows the CD4+GZB+ values for the paired samples at the 3 time points.

Figure 3-18E shows the median and range for the percentage difference in CD4+GZB+ level between the 1st and 2nd samples, the 1st and 3rd samples and the 2nd and 3rd samples. The median difference in CD4+GZB+ percentage between the 1st and 2nd samples was 2.67% (range: -5.44 to 46.11%). The median difference in CD4+GZB+ percentage between the 1st and 3rd sample was 3.89% (range: -26.1% to 49.39%) and the median difference between the 2nd and 3rd sample was 0.2% (range: -41.8 to 17.54%). The median time between the second and third blood samples was 178.5 days (range: 28-427 days). These results demonstrate that for the majority of the patients studied and who remained off treatment, the percentage CD4+GZB+ in the peripheral blood remains stable over time.

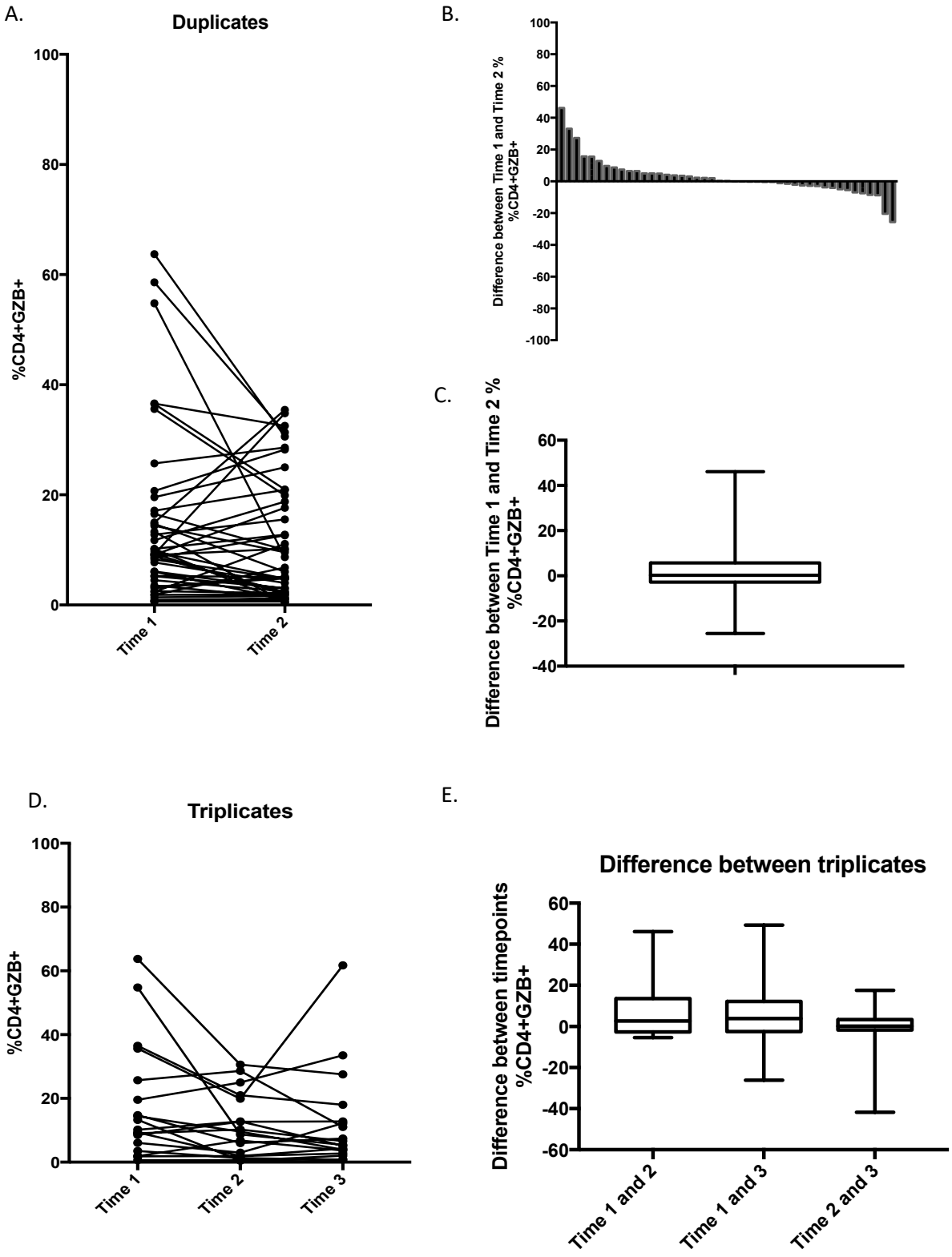

Figure 3-18: The comparison of CD4+GZB+ levels in the peripheral blood of patients with CLL over time. Figure A shows the percentage of CD4+GZB+ cells (of total CD4+ cells) in those patients who had 2 peripheral blood samples analysed at different time points. Figure B shows the percentage difference in CD4+GZB+ levels between the two time points. Figure C shows the median and range of the difference in CD4+GZB+ levels at the two time points. Figure D shows the percentage of CD4+GZB+ cells (of total CD4+ cells) in those patients who had 3 peripheral blood samples analysed at different time points. Figure E shows the median and range of the difference in CD4+GZB+ levels at the three difference time points.

3.5.13 The expression of Perforin and Granzyme A on CD4+ and CD8+ cells in the peripheral blood of patients with CLL

The cytotoxic CD4+ cells in this project were defined by their expression of the serine protease Granzyme B. The CD4+GZB+ cells were examined by flow cytometry to detect whether they also expressed the cytolytic proteins Perforin and Granzyme A (GZA). As Figure 3-19 shows, the majority of CD4+GZB+ cells expressed Perforin and Granzyme A. There was a significant increase in the expression of Perforin on CD4+GZB+ cells when compared with CD4+GZB- cells (P = 0.0001). There was no significant difference in the level of expression between CD4+GZB+ and CD8+GZB+ cells. There was a significant increase in Perforin expression on CD8+GZB+ cells when compared with CD8+GZB- cells (P=0.0038) and there was also a significant increase in Perforin expression on CD8+GZB+ cells when compared with CD4+GZB- cells (P = <0.0001). Figure 3.23 also shows that the majority of CD4+GZB+ cells expressed Granzyme A and that there was a significant increase in expression of GZA on CD4+GZB+ cells when compared with CD4+GZB- cells and CD8+GZB- cells. The majority of CD8+GZB+ cells expressed Granzyme A and this expression was significantly increased on CD8+GZB+ cells when compared with CD8+GZB- cells and CD4+GZB- cells. This data confirms that cytotoxic CD4+ cells in the peripheral blood of patients with CLL, which express Granzyme B, also express the cytolytic protein Perforin and the serine protease Granzyme A. This expression is also shared with the cytotoxic CD8+GZB+ cells.

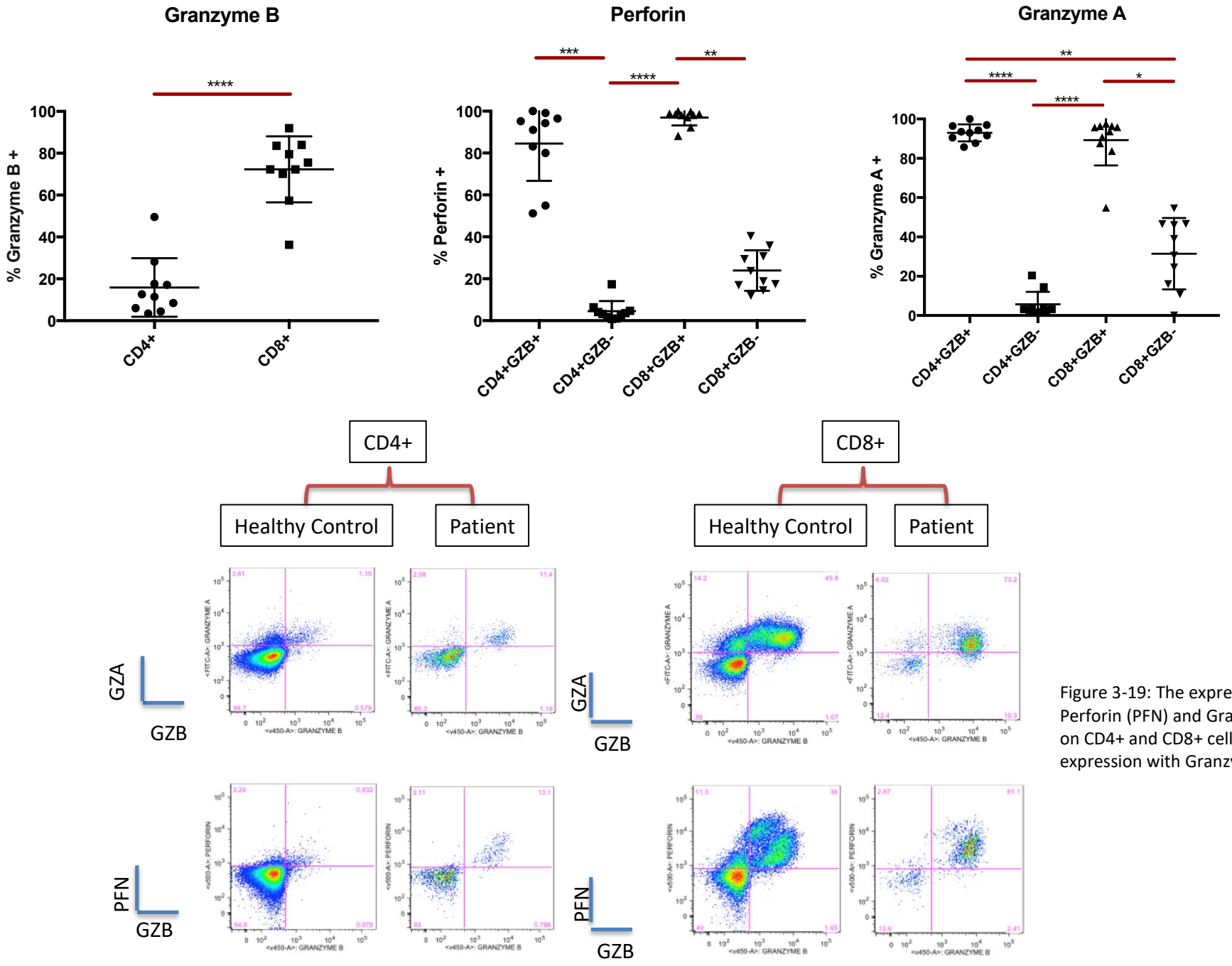

Figure 3-19: The expression of Perforin (PFN) and Granzyme A (GZA) on CD4+ and CD8+ cells and their co-expression with Granzyme B (GZB).

3.5.14 Summary of CLL flow cytometry results

Cytotoxic CD4+ cells are present in the peripheral blood of patients with untreated CLL and there is a statistically significant increase in the percentage of CD4+ cells expressing GZB in patients who are CMV seropositive. The phenotype of CD4+GZB+ cells is very similar to CD8+GZB+ cells, both expressing the transcription factors EOMES and Tbet, a high expression of CD57, low expression of CD28 and CD27 (suggesting antigen exposure) and are negative for FoxP3 and CTLA-4, markers which are closely associated with Treg cells.

3.6 The presence of CD4+GZB+ in the different tumour microenvironment compartments in patients with CLL – comparison of lymph node and bone marrow trephine biopsies

It has been previously shown in this chapter that CD4+GZB+ cells are present in the lymph node biopsies of patients with CLL and that the level of CD4+GZB+ cells is increased in comparison with reactive lymph nodes. It has also been shown that CD4+GZB+ cells are present in the peripheral blood of patients with CLL. The tumour microenvironment in CLL is known to provide survival signals to B-CLL cells [87], thereby promoting their proliferation and persistence. Therefore, we decided to examine the presence of CD4+GZB+ cells in the major CLL tumour microenvironments of CLL in the form of lymph node and bone marrow biopsies and to compare their composition with CD8+ cells between the two sites. This was achieved by triple-colour immunohistochemistry for CD4, CD8 and GZB. The lymph node and bone marrow trephine biopsies were paired samples from 10 patients with CLL who were not currently receiving therapy for CLL.

3.6.1 The comparison of CD4+GZB+ and CD8+GZB+ cells in lymph nodes and bone marrow trephine biopsies

When examining the absolute numbers of cells, it should be noted that the lymph node biopsies studied were often larger, and more cellular than the bone marrow trephine biopsies examined. Therefore, as can be seen in Figure 3-20, the absolute number of CD4+ (CD8-, GZB-) (P=0.0007), CD8+ (CD4-GZB-) (P=0.0068) and CD4+CD8+ (GZB-) (P=0.0040) cells was significantly higher in the lymph node biopsies when compared with the bone marrow

trephine biopsies. There was no significant difference in the absolute number of GZB+ (CD4-CD8-), CD4+GZB+, CD8+GZB+ and CD4+CD8+GZB+ cells between the lymph node and bone marrow trephine biopsies.

(1) The composition of the CD4+ cells

The majority of cells in the total CD4+ compartment were CD4+ (CD8-GZB-) in both the lymph node and bone marrow trephine biopsies (Figure 3-20). There was a significant increase in CD4+ (CD8-GZB-) cells in the lymph node biopsies when compared with the bone marrow trephine biopsies. Conversely, there was a significant increase in percentage of CD4+GZB+ cells (of total CD4+ cells) in the bone marrow trephine biopsies when compared with the lymph node biopsies. The CD4+CD8+ (GZB-) and CD4+CD8+GZB+ cells were very small components of the total CD4+ cells (<5% of total CD4+ cells) and there was no difference in the percentage level between the lymph node and bone marrow biopsies.

(2) The composition of the CD8+ cells

The majority of the total CD8+ cells were CD8+ (CD4-GZB-) in both the lymph node and bone marrow biopsies and there was no significant difference in the levels between the two locations. The next major component of the total CD8+ cells were the CD8+GZB+ (CD4-) cells and there was also no significant difference in their level between the lymph node and bone marrow biopsies. Both the CD4+CD8+ (GZB-) and CD4+CD8+GZB+ cells were present at very low levels (<5% of total CD8+ cells) although there was a significant increase in CD4+CD8+ (GZB-) cells in the lymph node biopsies when compared with the bone marrow trephine biopsies (P=0.0040).

(3) The composition of the GZB+ cells

The majority of the total GZB+ cells were the CD8+GZB+ (CD4-) cells. As previously mentioned, there was no significant difference in their levels between the lymph node and bone marrow biopsies. The next major component were the CD4+GZB+ (CD8-) cells, which were significantly increased in the bone marrow biopsies when compared with the lymph node biopsies (P=0.0068). The GZB+ (CD4-CD8-) cells, which will include the NK cell population, showed no significant difference in percentage of total GZB+ cells when the two

biopsy sites were compared. There was also no difference in the level of CD4+CD8+GZB+ cells, which were present at very low levels only.

3.6.2 Summary of comparison between lymph node and bone marrow biopsies

These results demonstrate for the first time that CD4+GZB+ cells have been identified and described in the bone marrow microenvironment in patients with CLL. The identification of their presence in both of the major tumour microenvironments in CLL, at sites where B-CLL cells undergo extensive proliferation and survival advantage, indicates the need for further characterisation of their role in this environment. If these cells had been absent at these sites, then it would have potentially served to lessen the likelihood of an anti-tumour function. Their significant increase in the bone marrow, when compared with the lymph node biopsies, is discussed further in Chapter 7. Further characterisation of CD4+GZB+ cells in the CLL tumour microenvironment is warranted, particularly with respect to their phenotype in the different tumour sites.

A.

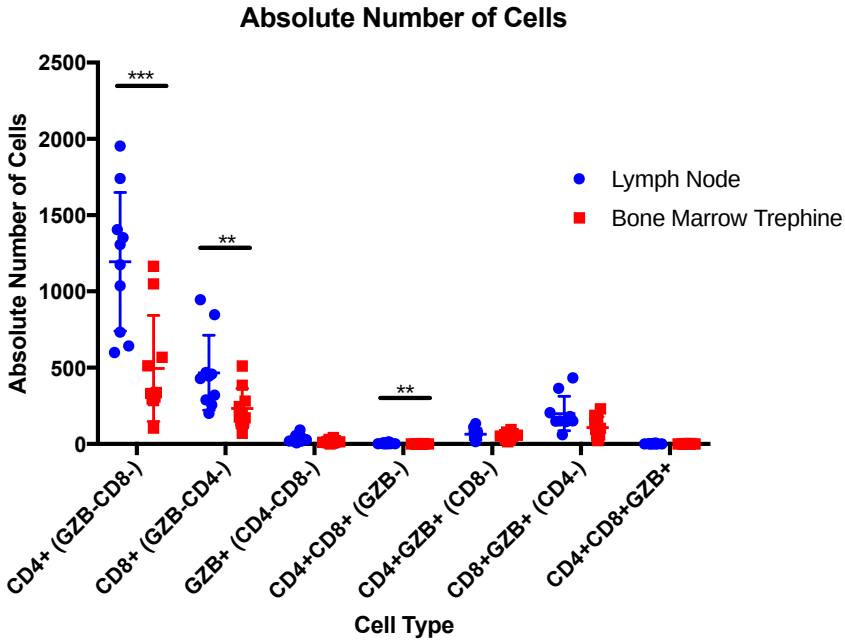

B.

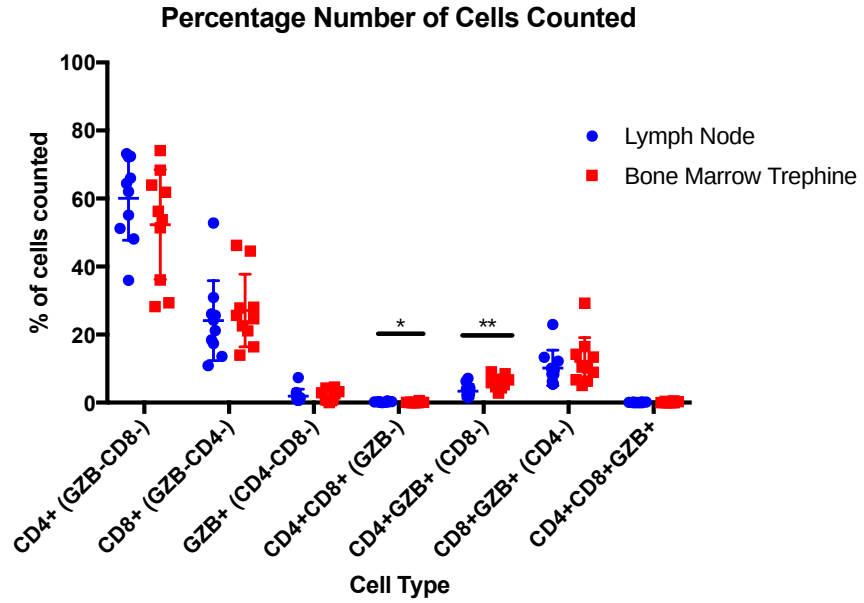

C.

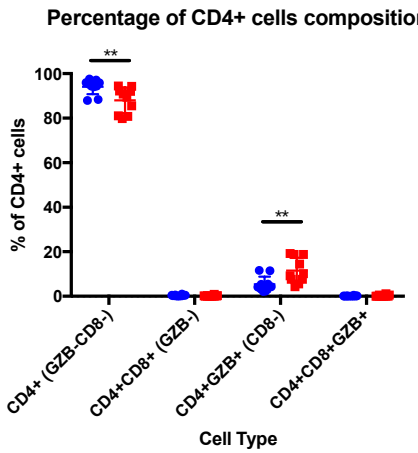

D.

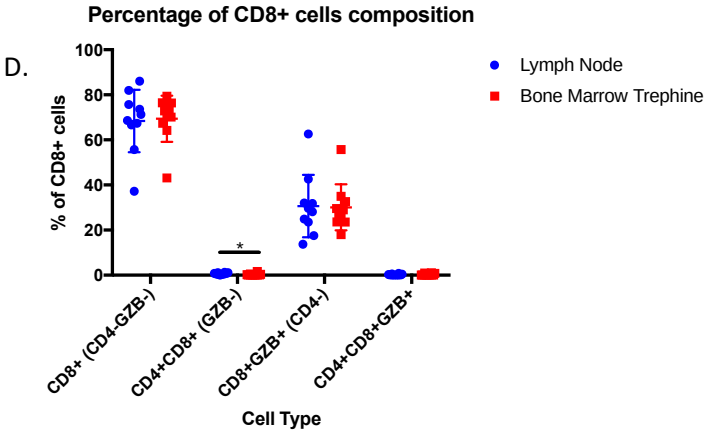

E.

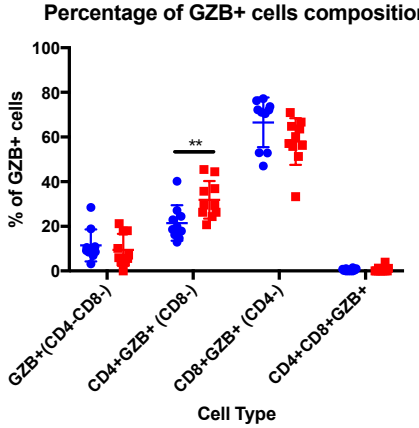

Figure 3-20: The comparison of cell populations in lymph node and bone marrow trephine biopsies in patients with CLL. The biopsies were stained for CD4, CD8 and Granzyme B using triple colour immunohistochemistry.

CD8/CD4/GZB Lymph Node

CD8 = Red, CD4 = Brown, Granzyme B = Blue

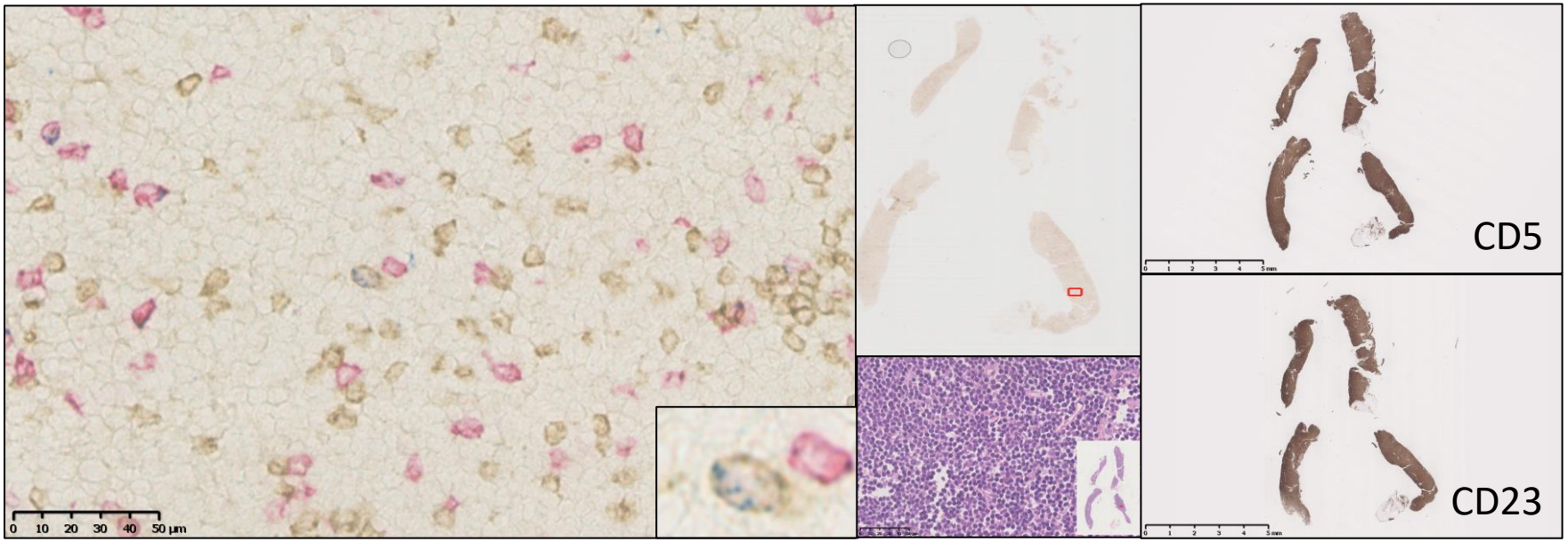

Bone Marrow Trephine Biopsy

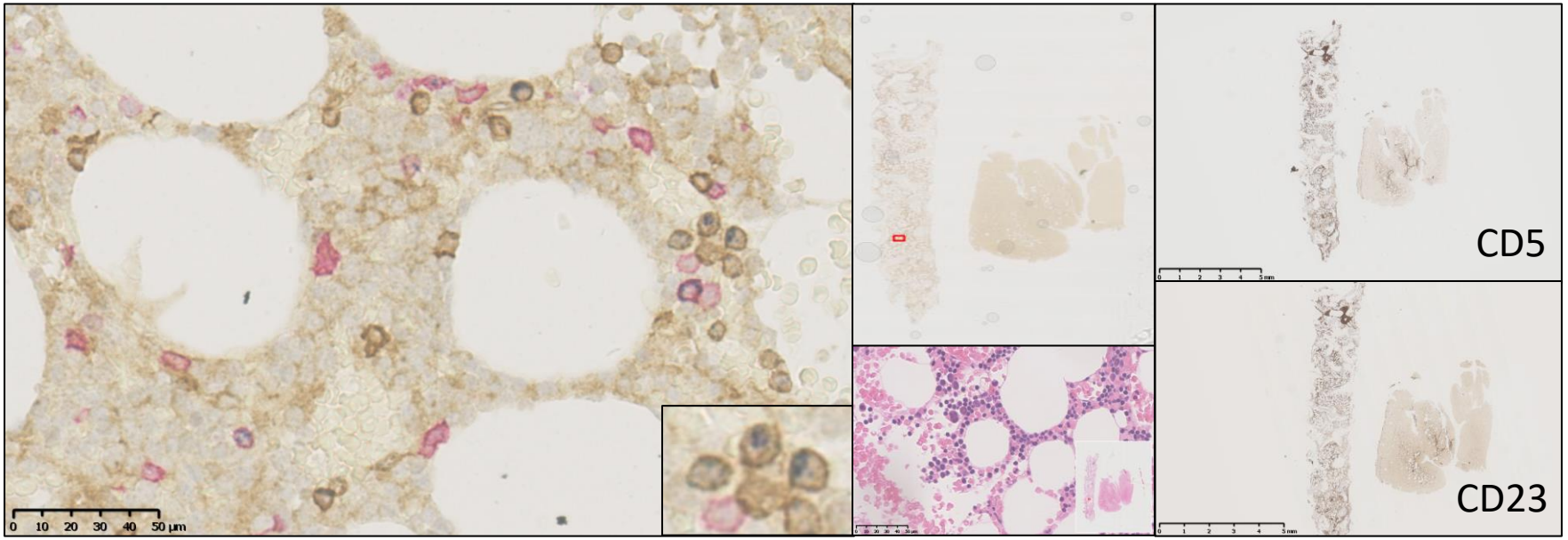

Figure 3-21: The triple colour immunohistochemistry stained lymph node and bone marrow trephine biopsy from the same patient with CLL. The three stains were CD8 (red), CD4 (brown) and Granzyme B (Blue). The H+E slide and single stained slides for CD23 and CD5 are also shown.

CD8/CD4/GZB

Lymph Node

CD8 = Red, CD4 = Brown, Granzyme B = Blue

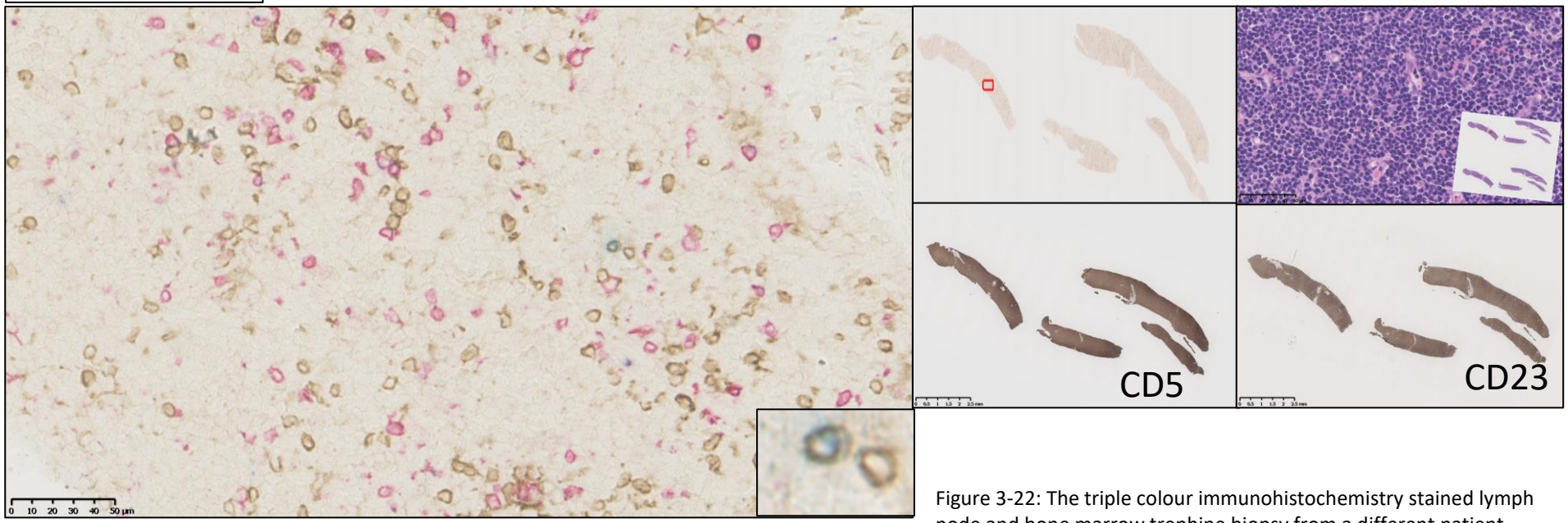

Figure 3-22: The triple colour immunohistochemistry stained lymph node and bone marrow trephine biopsy from a different patient with CLL. The three stains were CD8 (red), CD4 (brown) and Granzyme B (blue). The H+E slide and single stained slides for CD23 and CD5 are also shown.

Bone Marrow Trephine Biopsy

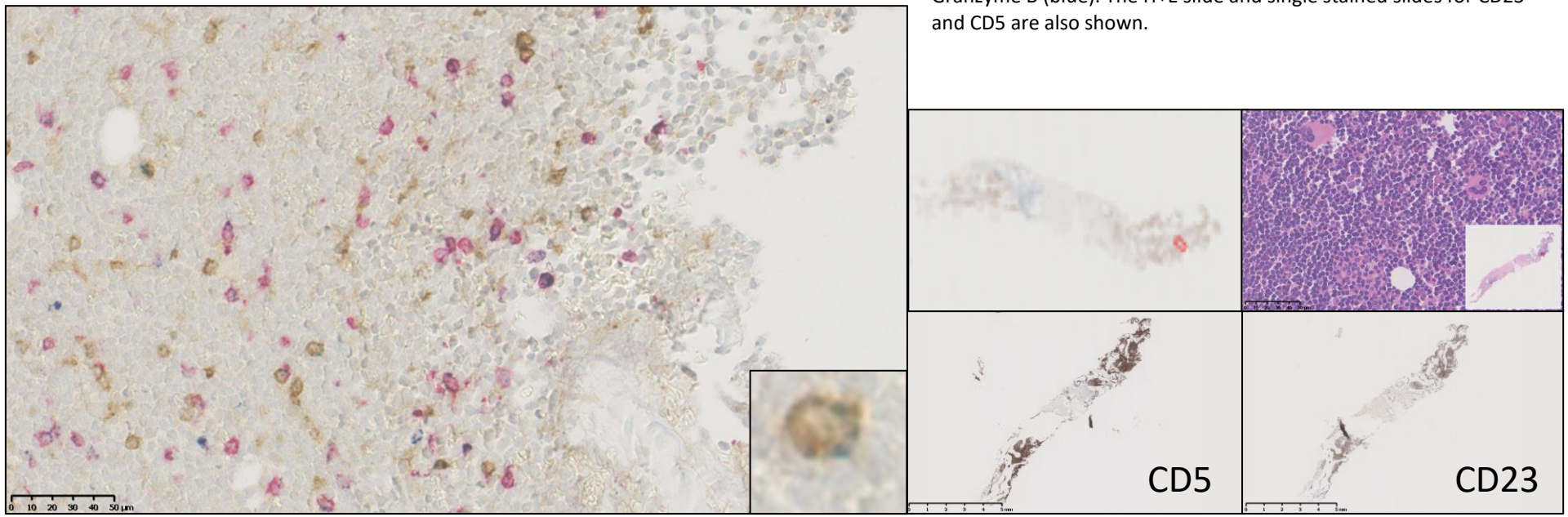

CD8/CD4/GZB

Lymph Node

CD8 = Red, CD4 = Brown, Granzyme B = Blue

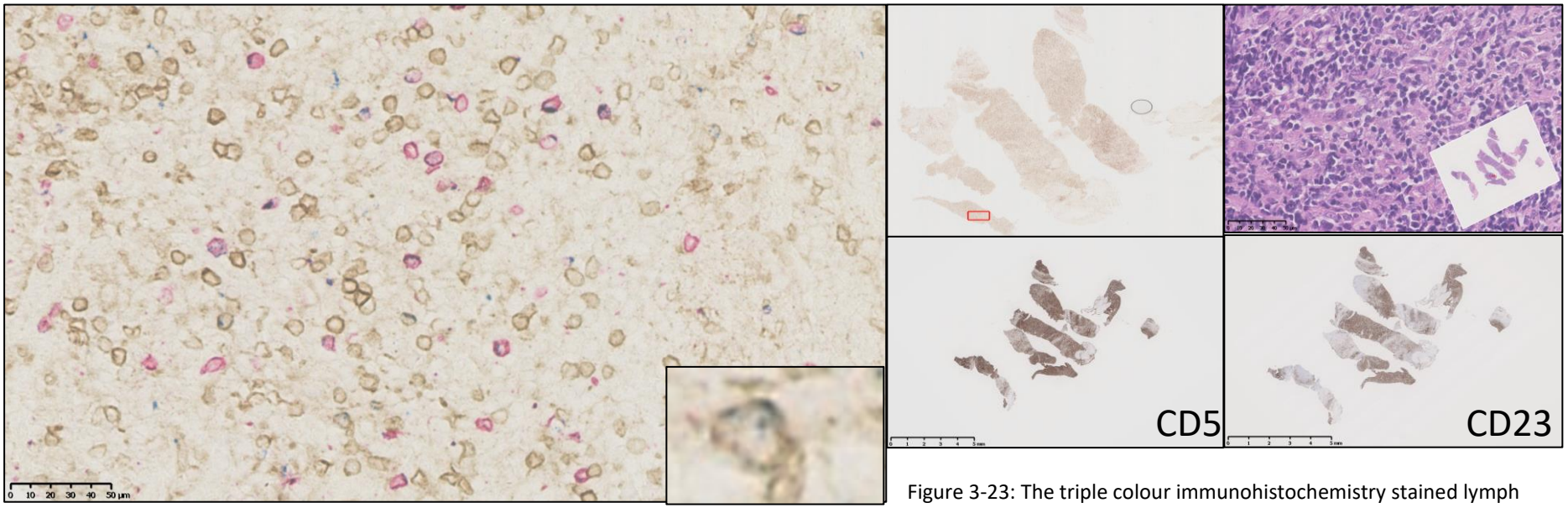

Figure 3-23: The triple colour immunohistochemistry stained lymph node and bone marrow trephine biopsies from a different patient with CLL. The three stains were CD8 (red), CD4 (brown) and Granzyme B (blue). The H+E slide and single stained slides for CD23 and CD5 are also shown.

Bone Marrow Trephine Biopsy

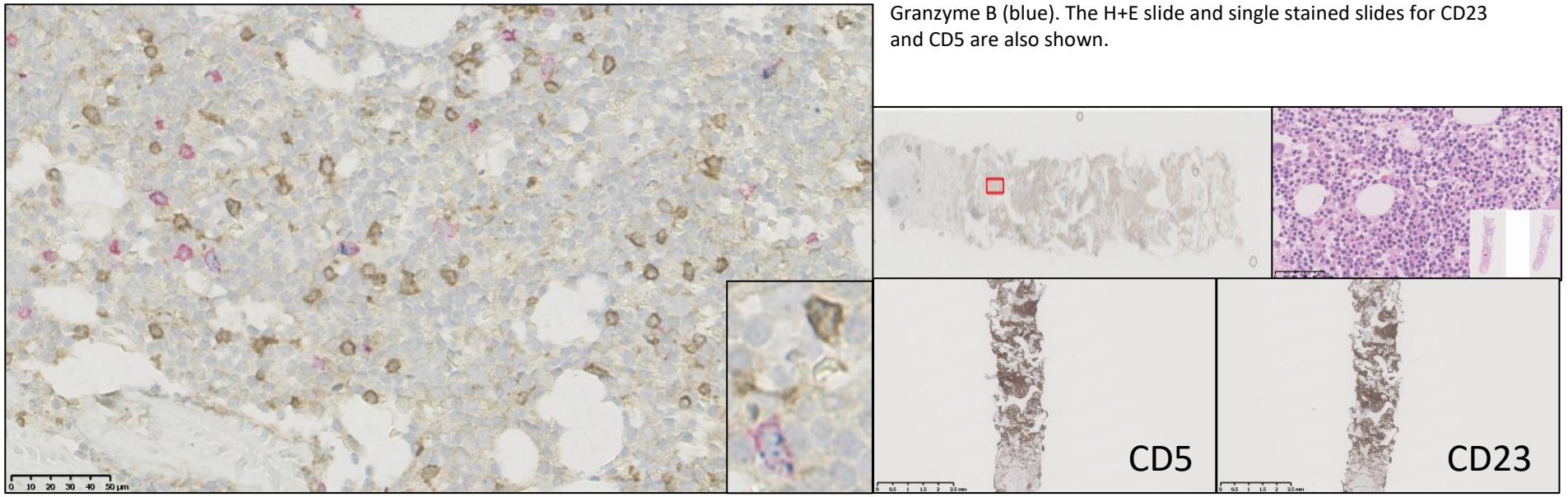

Tonsil Control

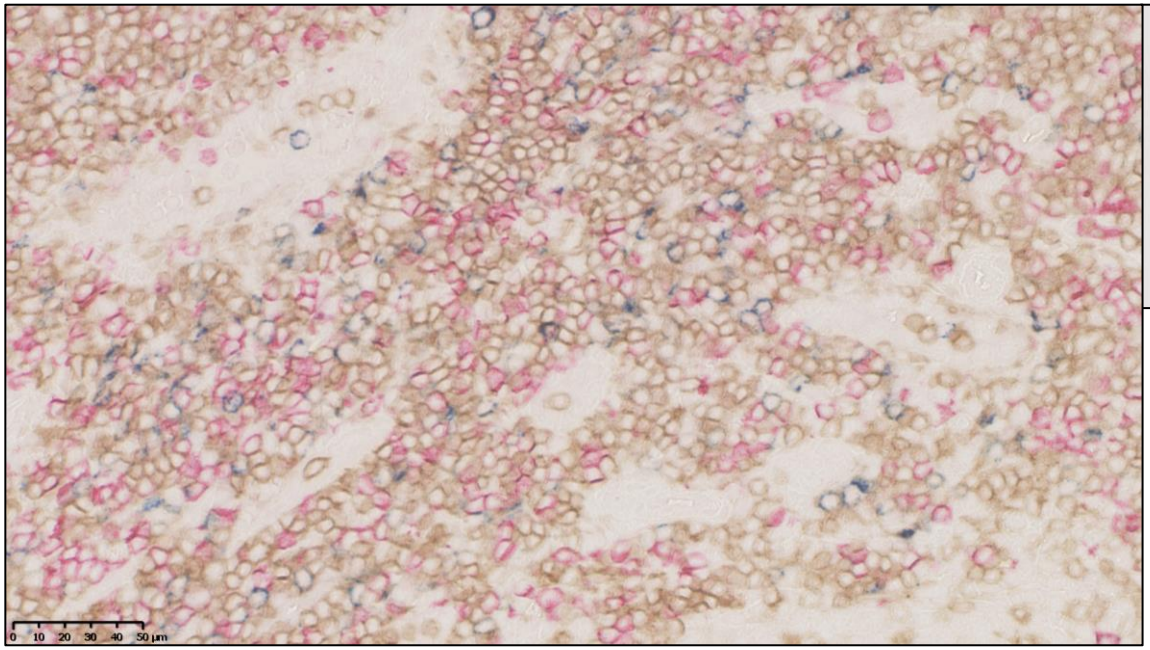

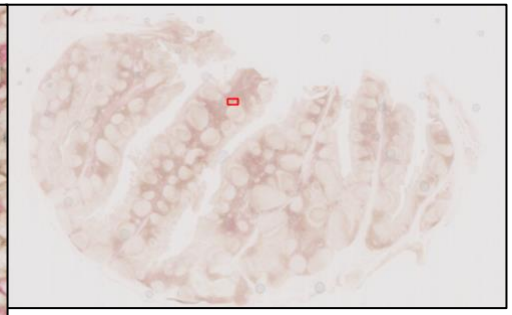

CD8 = Red
CD4 = Brown
Granzyme B = Blue

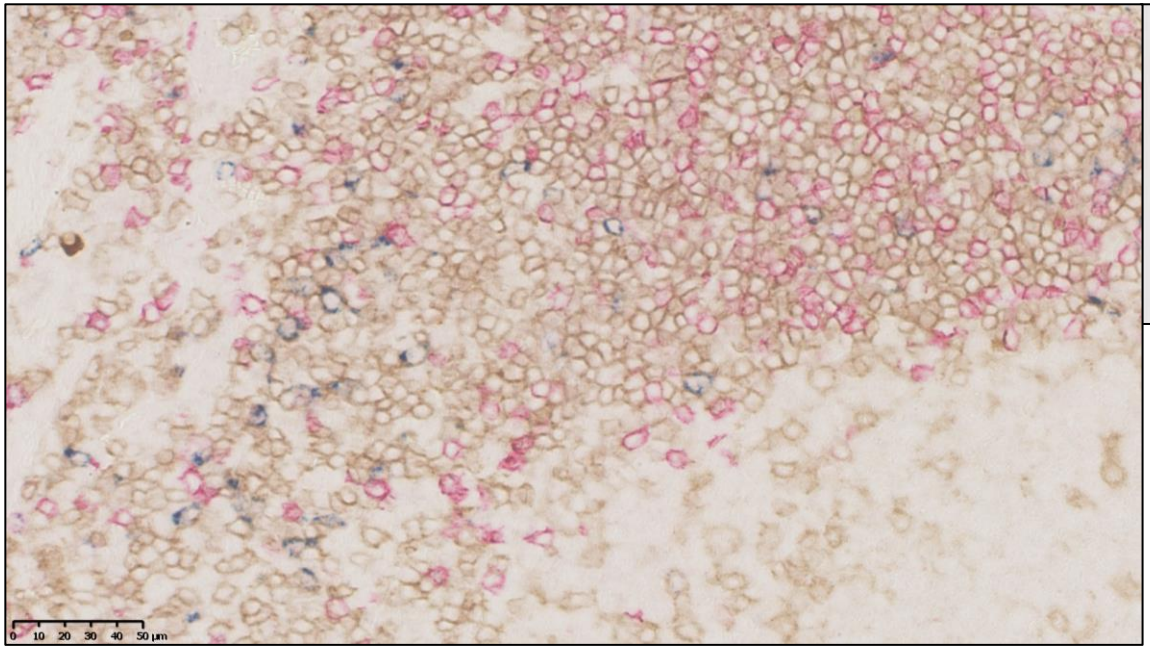

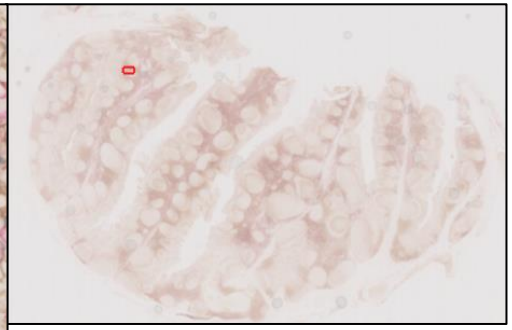

CD8 = Red
CD4 = Brown
Granzyme B = Blue

Figure 3-24: The tonsil controls for triple immunohistochemistry with CD8 (red), CD4 (brown) and Granzyme B (blue).

3.7 Expansion of CD4+CTLs from the peripheral blood of patients with CLL

Within the project proposal, the largest volume of peripheral blood obtained from a patient with CLL was 20mls. This resulted in only a small yield of CD4+CTLs which were insufficient in number for direct *in vitro* experimental assays. To counter this problem of low cell numbers, we electronically sorted the CD4+CTLs from the peripheral blood samples and used the rapid cell expansion protocol (section 2.8) to expand the cells *in vitro*, thereby increasing cell numbers and enabling assays to be performed. The previously mentioned association of CD57 expression with GZB expression on CD4+ cells enabled us to electronically sort the cells as CD4+CD57+, CD4+CD57-, CD8+CD57+ CD8+CD57- subgroups prior to rapid cell expansion by cell culturing techniques.

In an attempt to maximise the yield of CD4+GZB+ cells, the samples used for cell sorting were from patients who were CMV seropositive. The electronic cell sorting gating strategy is shown in Figure 3-25A. After cell-sorting, a purity check for each cell type was performed to check for any contamination of the samples. This is shown in Figure 3-25B.

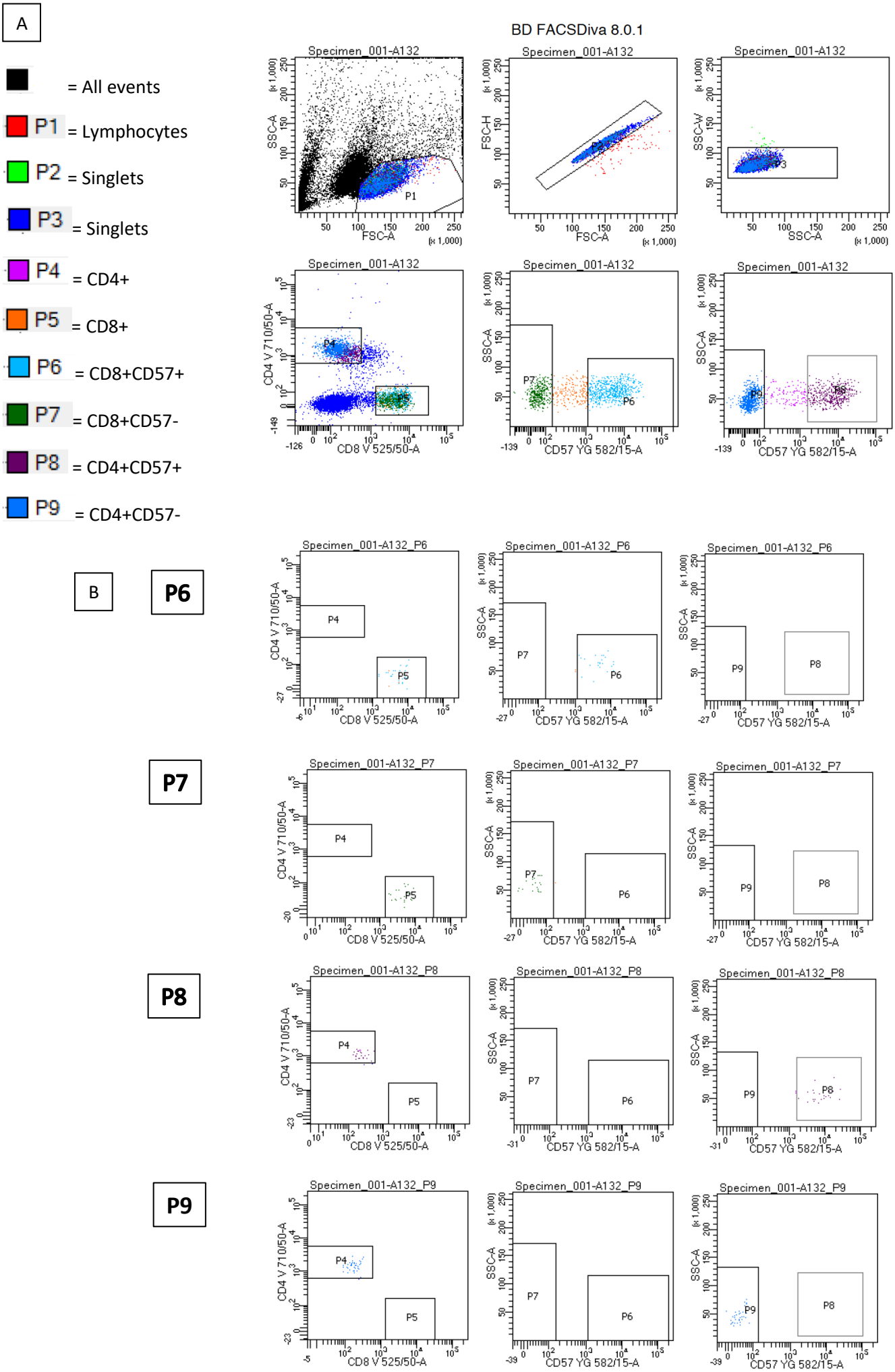

Figure 3-25: The gating strategy (A) and purity check (B) for the electronically cell-sorted CD4+CD57+ (P8), CD4+CD57- (P9), CD8+CD57+ (P6) and CD8+CD57- (P7) cells.

3.7.1 The detection of Interferon Gamma secretion by ELISPOT

The successful expansion of CD4+CD57+ cells allowed for their utilisation in functional assays, including ELISPOT studies. The aim was to detect whether the isolated and expanded CD4+CD57+ cells were CMV-reactive and produced Interferon gamma in the context of CMV-peptide (in this case both pp65 and IE-1 peptide mixes were examined) and autologous B-CLL cells, which were used as antigen-presenting cells. CD4+CD57- cells were also examined in the same experiment. Peripheral blood mononuclear cells from a healthy donor were stimulated with anti-CD3 as a positive control. CD4+ cells in the presence of B-CLL cells but without the addition of CMV peptide were used as negative controls. The expanded cells had been rested for 7 days prior to the experiments being performed. The T cells:APC ratio was 5:1 and different quantities of CD4+ cells were examined in triplicates (50,000; 10,000; 5000 and 2500 cells). The ELISPOT assay plate was kept at 37oC for 48 hours. Figure 3-27 shows the results of the experiment. Irrespective of the presence or absence of CMV peptide, Interferon gamma was produced by the CD4+CD57+and the CD4+CD57- cells, with the highest number of reactive cells seen in the wells with the highest number of CD4+ cells (50,000) (Figure 3-27).

3.7.2 The detection of Granzyme B secretion by ELISPOT

Concurrently, the same assay described above was performed with an ELISPOT to detect Granzyme B secretion from CD4+CD57+ cells in the context of CMV-peptides (pp65 and IE-1). As above, the positive control was a healthy donor's PBMCs stimulated with anti-CD3. The negative control was the assay without the addition of peptide. It would be expected that upon stimulation with CMV-peptide, the CD4+CD57+ cells would secrete Granzyme B. Figure 3-26, however, shows that the maximum Granzyme B secretion was seen in the absence of both peptides, a result that was unexpected. It does confirm, though, that CD4+CD57+ cells are capable of secreting Granzyme B.

The assay requires further optimisation, particularly in the context of the Interferon gamma ELISPOT results which showed Interferon Gamma secretion without the requirement for CMV-antigen presence.

3.7.3 The cytotoxicity of CD4+CD57+ cells in the presence of B-CLL cells

Using the expanded cells, cytotoxicity assays were performed to examine the cytotoxic potential of these expanded cells in the presence of autologous B-CLL cells. The effector cells were CD4+CD57+, CD4+CD57-, CD8+CD57+ and CD8+CD57- cells which had been isolated and expanded, as described above, from the peripheral blood of a patient with CLL. The target cells were negatively selected autologous B-CLL cells which had been CFSE-labelled. Effector:target ratios of 20:1, 10:1, 5:1, 2:1 and 1:1 were examined. The experiment was performed at 24 and 48 hour time-points. The results are seen in Figure 3-28. At both 24 and 48 hours, CD4+CD57+ cells had greater cytotoxic ability than CD4+CD57- cells with the greatest cytotoxicity seen at an effector:target ratio of 20:1.

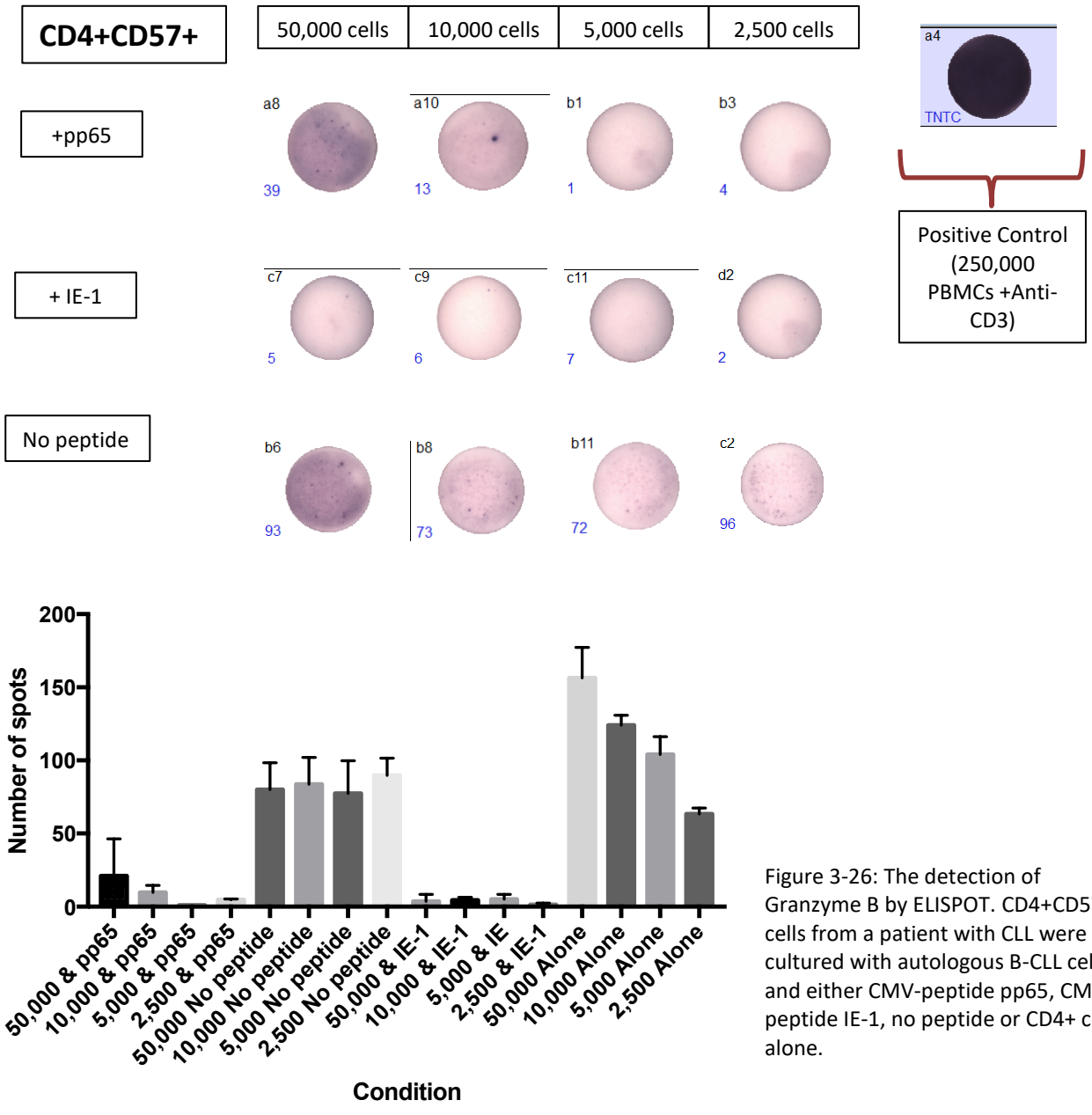

Figure 3-26: The detection of Granzyme B by ELISPOT. CD4+CD57+ cells from a patient with CLL were co-cultured with autologous B-CLL cells and either CMV-peptide pp65, CMV-peptide IE-1, no peptide or CD4+ cells alone.

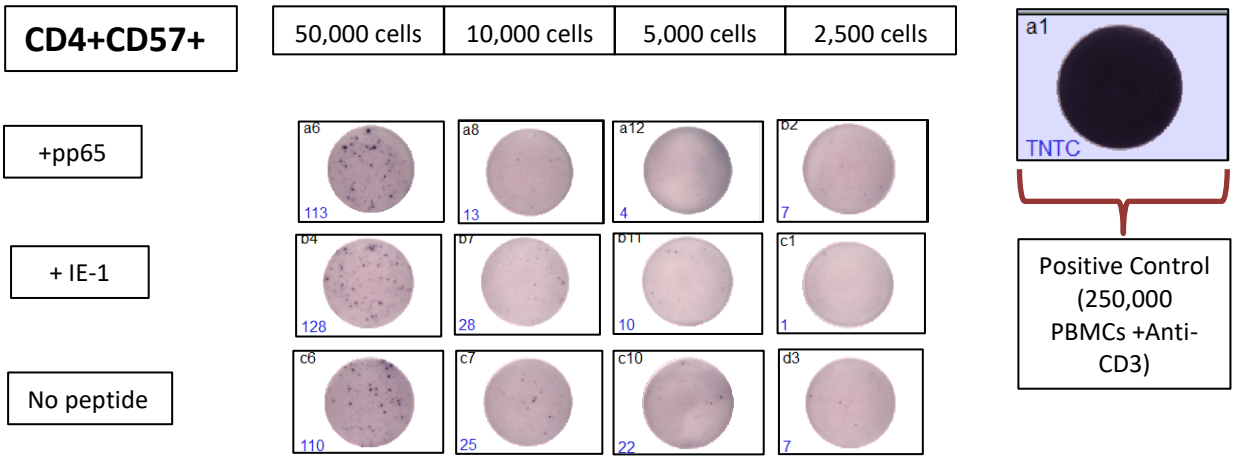

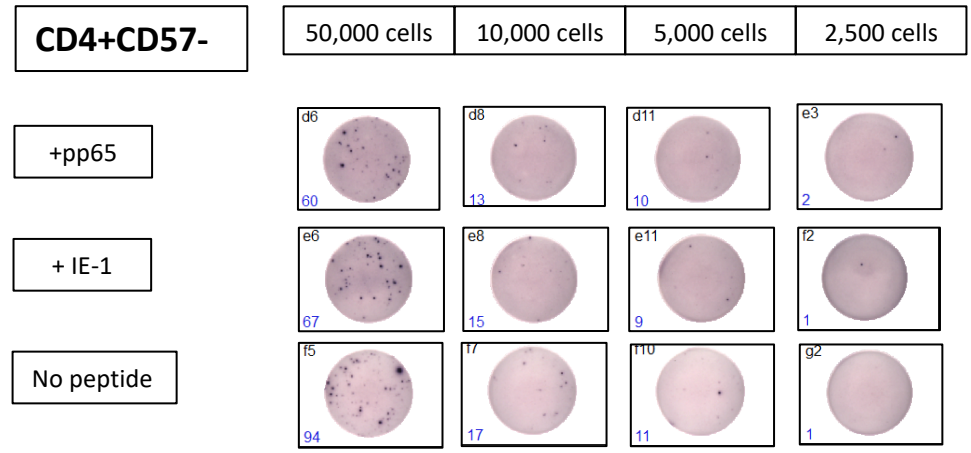

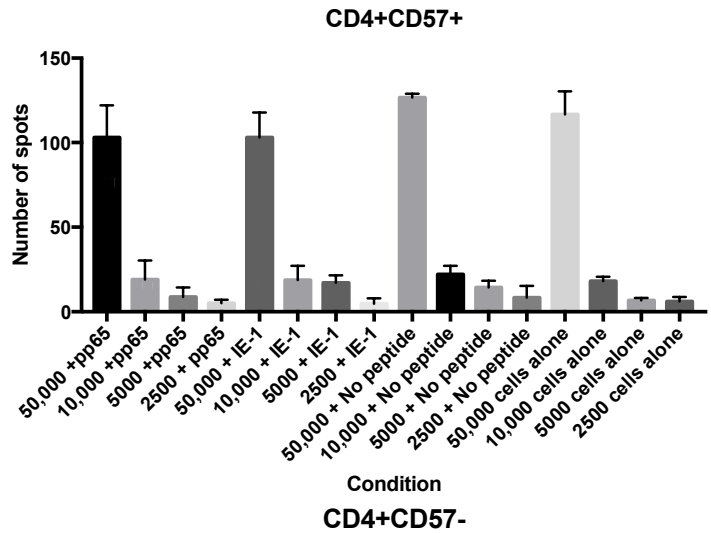

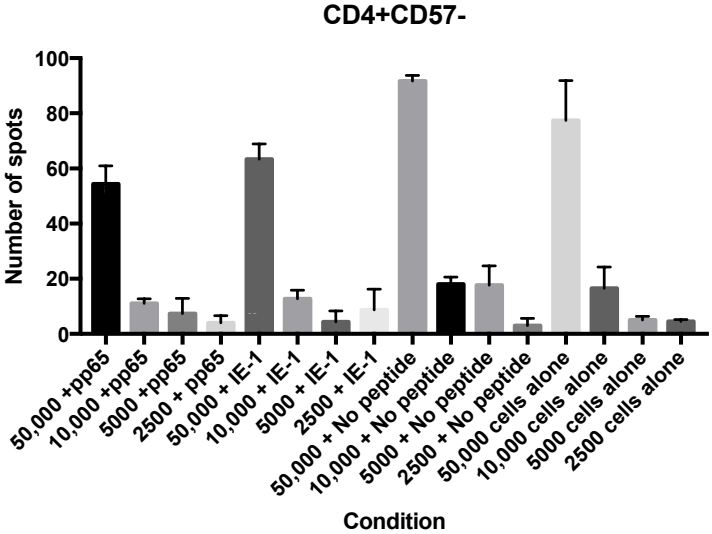

Figure 3-27: The detection of Interferon Gamma by ELISPOT. CD4+CD57+ and CD4+CD57- cells from a patient with CLL were co-cultured with autologous B-CLL cells and either CMV-peptide pp65, CMV-peptide IE-1, no peptide or CD4+ cells alone.

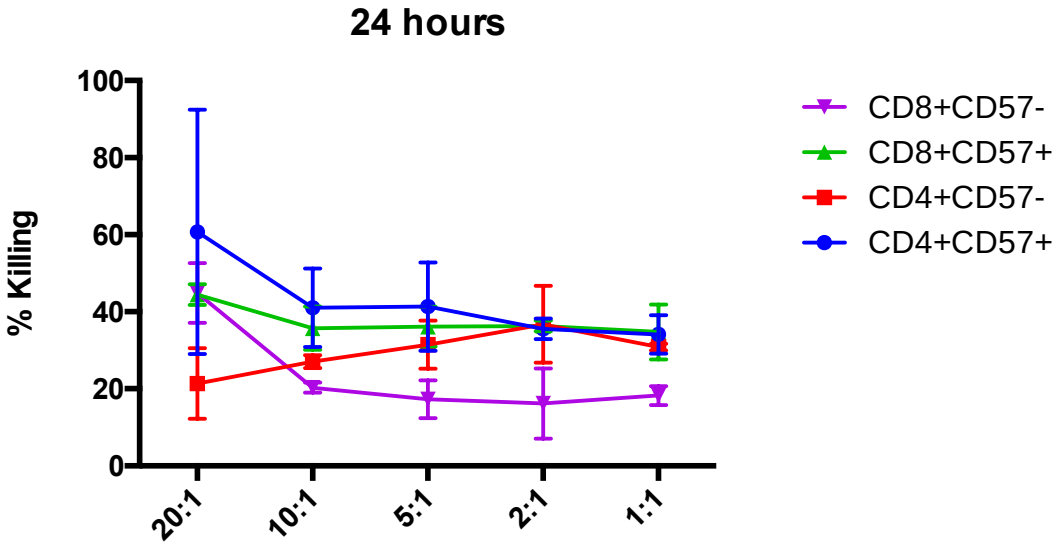

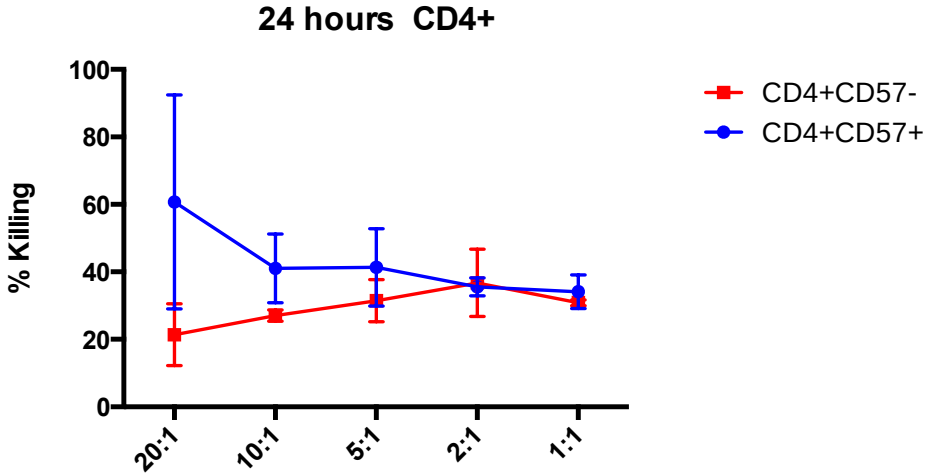

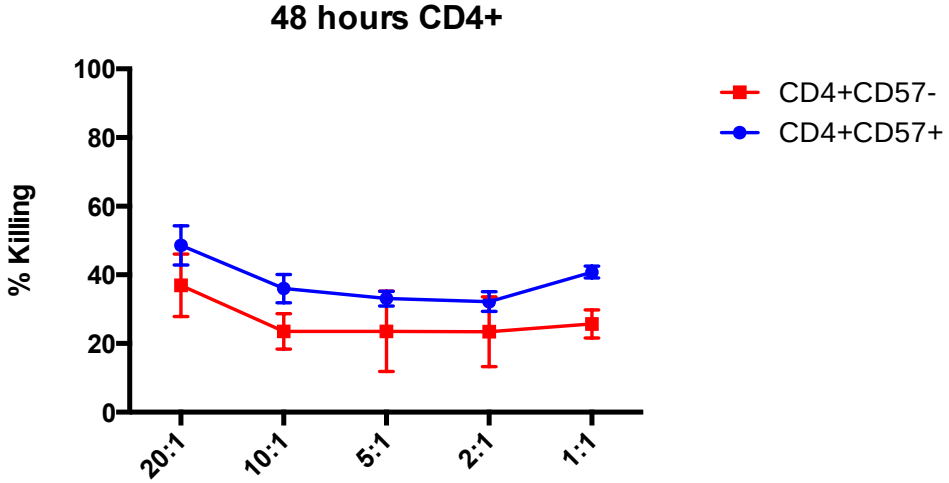

Figure 3-28: Cytotoxicity assays using CD4+CD57+. CD4+CD57-, CD8+CD57+ and CD8+CD57- cells as effector cells and autologous B-CLL cells as targets. Effector:target ratios of 20:1, 10:1, 5:1. 2:1 and 1:1 were examined. The assay was performed for the time-points of 24 hours and 48 hours.

3.8 Discussion

This chapter has described the presence and characteristics of CD4+CTLs, as defined by their expression of Granzyme B, in the context of Chronic Lymphocytic Leukaemia. In the lymph nodes of patients with CLL, CD4+GZB+ cells are significantly increased when compared with reactive lymph nodes. They are present in the peripheral blood of patients with CLL and can constitute up to 60% of CD4+ cells.

The percentage of CD4+ CTLs is significantly increased in those patients who are CMV seropositive when compared with those who are CMV seronegative. This would support the hypothesis that the CD4+ CTLs may have an antiviral function and represent an expanded CMV-specific CD4+ population. This also concurs with the previously described data on CD4+Perforin+ cells in the peripheral blood of patients with CLL [85]. The lack of a correlation of CD4+CTL level with total white cell count and lymphocyte count may reflect the uniform nature of the patient group who all had clinically stable CLL which was not requiring treatment. It would be useful to perform a longitudinal study of patients who are stable but who progress over time and require treatment. If CD4+CTLs retain an anti-tumour function, it may be expected that their level would increase in response to progressive disease. Unlike previous research examining CD4+Perforin+ cells [88], we did not find a correlation between the level of CD4+GZB+ cells and the patient's age.

The phenotype of the CD4+GZB+ cells in the peripheral blood of patients with CLL shows a remarkable similarity with CD8+GZB+ cells, particularly in the expression of CD57, CD27 and CD28. The CD4+GZB+ cells share a phenotype that is unlike the CD4+ helper cellular subsets, suggesting that this is a distinct CD4+ subset in its own right. The identification of CD57+ as a surface marker of CD4+GZB+ cells was valuable in allowing for their electronic cell-sorting and use in *in vitro* assays. It is also valuable for the isolation of the cells without the need to permeabilise the cells, which would need to be performed if the cells were identified by their intracellular expression of Granzyme B. The ability to isolate cells without permeabilisation is necessary when performed next generation sequencing studies.

CD57 is also expressed on CD8+ CTLs and the cytotoxic NK cells. In patients with HIV, HIV-specific CD4+ CTLs are also identifiable by their expression of CD57 [35]. As CD57+ is associated with

cytotoxic cells, we also examined the expression of other cytolytic markers on CD4+GZB+ CTLs and showed that Perforin and Granzyme A were also highly expressed, suggesting an accessory role in the cytotoxic function of these cells. The majority of CD4+GZB+ cells expressed the co-inhibitory receptor PD-1. In view of their low proliferation rate and expression of CD57, which is sometimes seen in terminally differentiated cells, some researchers have suggested that CD4+CTLs are in an exhausted state as a result of chronic antigen stimulation [10]. The ability to expand and stimulate the cells and their production of cytokines in response to stimulation would suggest that these cells are not exhausted. It should also be noted that the additional co-inhibitory receptors LAG-3 and TIM-3, which have increased expression in exhausted T cells [89], were not expressed by the CD4+ CTLs.

In studying the tumour microenvironment of lymph node biopsies infiltrated with CLL, a comparison needed to be made with a normal control which would ideally have been a lymph node biopsy from a 'normal', healthy donor. This was not available, however, as lymph node biopsies are only routinely performed on symptomatic patients and not healthy individuals. Other researchers have tried to address this issue by obtaining lymph node biopsies from patients undergoing other surgical procedures, for example, patients having cardiac surgery where some of the lymph nodes may be removed during the operation. As this was not available to us, we used lymph node biopsies which had a histological diagnosis of "reactive lymph node" as our surrogate normal control. The indication for the biopsy being performed in these patients was usually to investigate lymphadenopathy and so it could not be said that these patients were "normal" or asymptomatic per se. However, as none of these patients had a diagnosis of malignancy or active detectable viral infection, they were used as our normal controls.

The identification of CD4+ CTLs in the bone marrow and lymph nodes of patients with CLL has confirmed that they are present in the tumour microenvironment which is essential if they have an anti-tumour function. Further studies to characterize their phenotype in the tumour microenvironment, either through immunohistochemistry of histological biopsies or the acquisition of fresh tumour samples for flow cytometry, should be performed and a comparison made with their phenotype in the peripheral blood.

Despite 7 days of resting without cytokine supplementation, the expanded CD4+ cells were still able to secrete Interferon gamma, even in the absence of CMV-peptide antigenic presentation. These results suggest that the cells remain highly activated following the rapid expansion protocol and their secretion of Interferon gamma is non-specific and not in response to the presentation of CMV peptide by APCs. The rapid expansion protocol involves the addition of high doses of IL-2 at regular intervals. IL-2 has been implicated in the production of both Granzyme B and Perforin in cytotoxic CD8+ cells during *in vitro* culture [90]. This raises the possibility that the addition of high concentrations of IL-2 has resulted in non-specific, enhanced expression of Granzyme B. This may then result in non-specific cytotoxic activity. The immunohistochemistry and flow cytometry experiments, whilst confirming the presence of Granzyme B in CD4+ cells, have only examined Granzyme B in its intracellular location. In contrast, the ELISPOT experiments do confirm that CD4+CD57+cells are able to secrete Granzyme B into the extracellular environment.

A further limitation of the ELISPOT assay was the unknown HLA type of the patient whose peripheral blood was used as the source of CD4+CD57+ cells. Therefore, the CMV-peptide that the patient's CMV-specific T cells would recognize was unknown. To maximise the chance of generating a CMV-specific response, both the CMV-pp65 and CMV-IE-1 peptides were including in the study. In the context of these results, it is apparent that further optimisation of the functional assays needs to be performed. The use of cell expansion techniques that do not involve high-concentrations of IL-2 may help to eliminate the influence of this cytokine on Granzyme B production and experiments to identify the optimum length of cell resting time, prior to functional assays, should also be performed.

Chapter 4 The immunophenotype of cytotoxic CD4+ T lymphocytes in CMV seropositive and CMV seronegative patients with CLL as determined by mass cytometry (CyTOF)

4.1 Introduction

The striking similarities in the phenotype between the CD4+Granzyme B (GZB)+ cells and CD8+GZB+ cells in the peripheral blood of patients with Chronic Lymphocytic Leukaemia (CLL) [shown in Chapter 3] suggest that these two subtypes may be more closely related than originally appreciated. The similarities may be related to their cytotoxic function or may be related to a common reactivity towards a specific antigen. The possibility that these cells are Cytomegalovirus (CMV)-reactive has been raised previously [91] and the increased percentage of CD4+GZB+ cells in the peripheral circulation of those patients who are CMV seropositive would serve to support this hypothesis.

Historically, T lymphocyte dysfunction in patients with CLL has been thought to contribute to the overall immunodeficient state in the disease. CMV-specific CD8+ T cells from patients with CLL, however, have been shown to still retain their capacity to produce cytokines following stimulation and have preserved cytotoxicity function in the presence of targets which had been loaded with CMV-peptides [92, 93]. The percentage of CMV-specific CD4+ cells are expanded, as a total of the CD4+ population, in patients with CLL, especially in those receiving chemotherapy [94]. This expansion of CMV-specific T cells may serve to contribute to the relative lack of CMV-related diseases reported in patients with CLL and the lack of association of CMV seropositivity with clinical outcome in this patient group [95].

The association of the CMV status and cytotoxic CD4+ level does not, however, explain the presence or median percentage of CD4+GZB+ cells in CMV seronegative patients being 3.06% (range: 0.60 – 18.8%), above the normal range in healthy individuals. Therefore, we decided to undertake a comparison of the phenotype of CD4+GZB+ cells in CMV seronegative and CMV seropositive patients with CLL by using CyTOF (mass cytometry) which allowed us to compare an extended phenotype analysis of these two patient groups.

4.2 Principles of CyTOF

The ability to perform single-cell immunophenotypic analysis by fluorescence-based flow cytometry has revolutionised both the diagnosis of pathological conditions, particularly haematological malignancies [96], and also the understanding of basic immunology. The technique's assistance in the identification of new immunological cellular subsets has allowed for greater understanding of the complexities of the immune system. Furthermore, as has been demonstrated in Chapter 3, fluorescence based flow-cytometry can be used for cell-sorting to isolate specific cell subsets for functional experiments. There are, however, limitations with the technique of flow cytometry. The number of parameters that can be examined is limited by the number of lasers available in a particular flow cytometry machine and there are often only a maximum of 12-14 parameters per panel. There is a risk of auto-fluorescence interfering with the data output and a need for extensive compensation techniques to limit any fluorescent spectral overlap which may affect the data quality.

Mass cytometry, also known as CyTOF (cytometry by time-of-flight), is a relatively new method of single-cell phenotype examination which enables the acquisition and analysis of multiple parameters. It is based upon the combined principles of flow cytometry and mass spectrometry. Antibodies to specific cellular antigens are labelled with metal isotopes rather than fluorophores. The metal isotopes that are employed are often from the Lanthanide family of metals (atomic numbers 57-71, for example including Lanthanum, Cerium and Praseodymium) (Table 12). These metals are seldom seen in human biology, thereby limiting any potential overlap of antigen identification. In view of the number of isotopes available, CyTOF panels can routinely include 40 parameters, allowing for in depth single-cell immunophenotyping [75, 97, 98].

The samples under examination are "barcoded", which consists of the samples being tagged with different metal isotopes, allowing them to be stained together and then each sample's data being identified and isolated during the analysis stage. This eliminates the possibility of a large variation between samples due to variations in different experiments. The Palladium family of isotopes are often used in barcoding, including in our experiments. Cisplatin is used for the live-dead stain as it enables Platinum to bind to any dead cells that are present in the sample, allowing for their identification and elimination from the final data analysis. During the CyTOF process, the cells which have been stained with metal-conjugated antibodies enter the cell introduction system where they are vaporized in a high temperature chamber to produce an ionized cloud.

The disadvantages of mass cytometry include the inability to sort cells, the relative expense related to acquiring the metal isotopes and the generation of a large volume of data which often requires complex data analysis.

The CyTOF data shown in this chapter was acquired in collaboration with Dr Evan Newell's laboratory. Two panels were used to analyse the peripheral blood samples. The first panel, entitled "extracellular", (Table 10) focused predominantly on extracellular markers although it did include some intracellular markers, including Granzyme A and B. The second panel, entitled "intracellular" (Table 11) focused more on cytokines and the cells analysed were initially re-stimulated prior to staining [99]. This is in contrast to the extracellular panel where the cells were not re-stimulated.

4.3 Aims:

The aims of the CyTOF staining and analysis of PBMCs from patients with CLL were as follows:

1. To identify whether mass cytometry (CyTOF) was comparable with standard flow cytometry to quantify CD4+GZB+ cells in the peripheral blood of patients with CLL.

2. To establish if there was any difference in phenotype between the CD4+GZB+ cells from CMV seropositive and CMV seronegative patients with CLL.

3. To compare the phenotype of CD4+GZB+ with the phenotype of CD8+GZB+ cells in CMV seropositive and CMV seronegative patients with CLL.

4.4 Extracellular Panel

Y89Di: CD45	Sm154Di: CD49a
Pd102Di: BC	Gd155Di: Foxp3
Rh103Di: BC	Gd156Di: CCR7
Pd104Di: BC	Gd157Di: CD27
Pd105Di: BC	Gd158Di: CD56
Pd106Di: BC	Tb159Di: ICOS
Pd108Di: BC	Gd160Di: PD-1
Pd110Di: BC	Dy161Di: Vd1
Cd112Di: CD14	Dy162Di: CD161
Cd113Di: BC	Dy163Di: CXCR3
Cd114Di: CD14	Dy164Di: CCR9
In115Di: CD57	Ho165Di: CD38
La139Di: gdTCR	Er166Di: CXCR5
Ce140Di: CD3	Er167Di: CD49d
Pr141Di: HLA-DR	Er168Di: CCR2
Nd142Di: CLA	Tm169Di: CD25
Nd143Di: Va7_2	Yb170Di: CCR6
Nd144Di: Granzyme_B	Yb171Di: Intb7
Nd145Di: CD62L	Yb172Di: CD45RA
Nd146Di: CD8	Yb173Di: CD19
Pm147Di: CD45RO	Yb174Di: CX3CR1
Nd148Di: Vd2	Lu175Di: CCR5
Sm149Di: CD4	Yb176Di: CD127
Sm150Di: CD103	Ir191Di: DNA
Eu151Di: CCR4	Ir193Di: DNA
Sm152Di: Ki67	Pt195Di: Cisplatin
Eu153Di: Granzyme_A	Bi209Di: CD16

Table 10: The extracellular panel of metal-tagged antibodies used in the CyTOF experiments. BC = barcoding.

4.5 Intracellular Panel

Y89Di: CD45	Sm154Di: CCR7
Pd102Di: BC	Gd155Di: Granzyme_A
Rh103Di: BC	Gd156Di: Vd2
Pd104Di: BC	Gd157Di: CD38
Pd105Di: BC	Gd158Di: CD56
Pd106Di: BC	Tb159Di: Intb7
Pd108Di: BC	Gd160Di: PD-1
Pd110Di: BC	Dy161Di: CCR9
Cd112Di: CD14	Dy162Di: CTLA-4
Cd113Di: BC	Dy163Di: CD40L
Cd114Di: CD14	Dy164Di: Vd1
In115Di: CD57	Ho165Di: Va7.2
La139Di: gdTCR	Er166Di: CXCR5
Ce140Di: CD3	Er167Di: CD161
Pr141Di: HLA-DR	Er168Di: CCR2
Nd142Di: TNFa	Tm169Di: IL-4
Nd143Di: IFNg	Yb170Di: IL-10
Nd144Di: Granzyme_B	Yb171Di: CCR6
Nd145Di: IL-8	Yb172Di: GM-CSF
Nd146Di: CD8	Yb173Di: CCR4
Pm147Di: CD45RA	Yb174Di: IL-22
Nd148Di: CD19	Lu175Di: CX3CR1
Sm149Di: CD4	Yb176Di: IL-17A
Sm150Di: CD103	Ir191Di: DNA
Eu151Di: IL-2	Ir193Di: DNA
Sm152Di: CD25	Pt195Di: Cisplatin
Eu153Di: CD107a	Bi209Di: CD16

Table 11: The intracellular panel of metal-tagged antibodies used in the CyTOF experiments. BC = barcoding.

Chemical Symbol	Metal	Chemical Symbol	Metal
Y	Yttrium	Gd	Gadolinium
Rh	Rhodium	Tb	Terbium
Pd	Palladium	Dy	Dysprosium
Cd	Cadmium	Ho	Holmium
In	Indium	Er	Erbium
La	Lanthanum	Tm	Thulium
Ce	Cerium	Yb	Ytterbium
Pr	Praseodymium	Lu	Lutetium
Nd	Neodymium	Ir	Iridium
Pm	Promethium	Pt	Platinum
Eu	Europium	Bi	Bismuth
Sm	Samarium		

Table 12: The key of metals that were conjugated to antibodies in the CyTOF experiments.

4.6 Patient Characteristics of Samples Analysed

The peripheral blood mononuclear cells (PBMCs) from 14 patients with CLL were analysed using the two CyTOF panels listed above (Table 10 and Table 11). Seven of the patients were CMV seropositive and 7 patients were CMV seronegative. The median age of the patients was 68 years of age (range 46-87 years). None of the patients were currently receiving treatment for CLL. Thirteen of the 14 patients had never received treatment for their CLL. One patient had previously received therapy with Rituximab and Chlorambucil 5 years prior to their PBMCs being collected and they had not received any CLL-directed therapy in the intervening 5-year period. The patient characteristics are shown in Table 14. The median white cell count was 30.69 x 10^9/L (range 10.21 – 141.3 x 10^9/L) with a medium lymphocyte count of 24.36 x 10^9/L (range 4.66 – 130 x 10^9/L) and a median neutrophil count of 4.68 x 10^9/L (range 1.89-7.07 x 10^9/L). The medium haemoglobin level was 14.6g/L (range 11.5-16.5g/L) with a medium platelet count of 169 x 10^9/L (range 61 – 334 x 10^9/L). There was no significant difference between the CMV seronegative and seropositive groups with respect to their age, white cell count, lymphocyte count, neutrophil count, platelet count and haemoglobin level (Table 13). There was a significant difference between the percentage of CD4+GZB+ cells as determined by flow cytometry (P = 0.0006) (Figure 4-1) with a significant increase in those patients who were CMV seropositive. This is consistent with the data previously shown in Chapter 3.

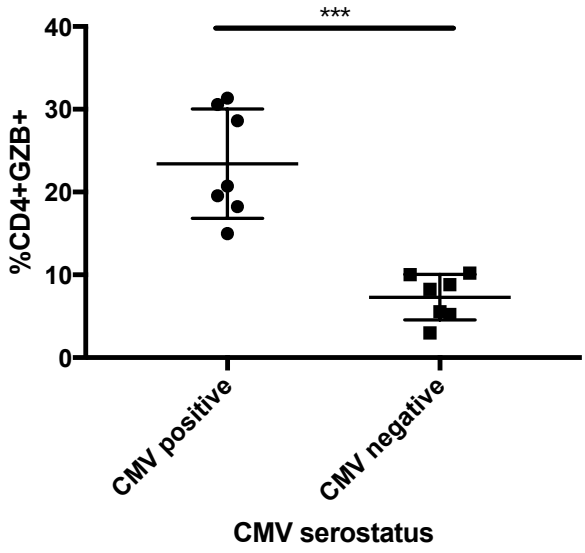

Figure 4-1: The percentage of CD4+GZB+ cells of the total CD4+ cells in the 14 patients with CLL as measured by flow cytometry. There is a significant increase in the percentage in those patients who are CMV seropositive (P=0.0006).

	CMV seropositive patients	CMV seronegative patients	P value (two-tailed)
Median white cell count (x 10^9/L)	21.33 (10.21-51.21)	34.3 (18.68 – 141.36)	0.2593
Median lymphocyte count (x 10^9/L)	14.87 (4.66-48.75)	27.78 (6.04 – 130)	0.3176
Median haemoglobin level (g/L)	150 (115 – 165)	141 (119 – 161)	0.7104
Median Neutrophil count (x 10^9/L)	4.88 (1.89-5.8)	3.53 (2.67 – 7.07)	0.8048
Median Platelet count (x 10^9/L)	172 (61-230)	149 (83 – 334)	0.972
Median Age (years)	70 (65-87)	66 (46-86)	0.3636
Median %CD4+GZB+ (as determined by flow cytometry)	20.7 (14.98 – 31.36)	8.26 (2.98 – 10.23)	0.0006*

Table 13: The patient characteristics of the 14 patients with CLL whose PBMC samples were examined by CyTOF as divided by CMV seropositive or seronegative status. The Mann Whitney U test was used to compare the two groups. *= statistically significant difference.

Sample	Age (years)	Treatment	White Cell Count ($x 10^9/L$)	Neutrophils ($x 10^9/L$)	Lymphocytes ($x 10^9/L$)	Haemoglobin (g/L)	Platelets ($x 10^9/L$)	CMV serostatus	% CD4+ GZB+ count (of CD4s)
1	78	Previously Rituximab and Chlorambucil - completed in Jan 2010	34.3	5.49	27.78	119	149	Negative	8.81
2	76	None	10.21	4.88	4.66	143	172	Positive	18.248
3	46	None	18.68	2.91	6.038	156	176	Negative	2.98
4	51	None	24.71	2.67	21.5	140	83	Negative	5.22
5	86	None	141.36	7.07	130	130	149	Negative	10.23
6	65	None	51.21	1.89	48.75	125	175	Positive	31.355
7	87	None	15.61	5.42	9.41	115	166	Positive	20.7
8	63	None	35.07	5.12	27.21	141	223	Negative	8.26

Sample	Age (years)	Treatment	White Cell Count (x 10^9/L)	Neutrophils (x 10^9/L)	Lymphocytes (x 10^9/L)	Haemoglobin (g/L)	Platelets (x 10^9/L)	CMV serostatus	CD4+ GB+ count (of CD4s)
9	66	None	33.34	3.53	28.84	161	334	Negative	5.546
10	67	None	18.46	4.47	13.14	165	138	Positive	19.56
11	64	None	21.33	5.08	14.87	150	230	Positive	30.588
12	70	None	53.21	4.26	47.36	152	61	Positive	14.98
13	76	None	28.04	5.8	20.97	160	203	Positive	28.602
14	69	None	48.49	3.15	37.19	149	119	Negative	10.022

Table 14: The patient characteristics of each of the 14 patients with CLL whose blood was analysed in the CyTOF experiments.

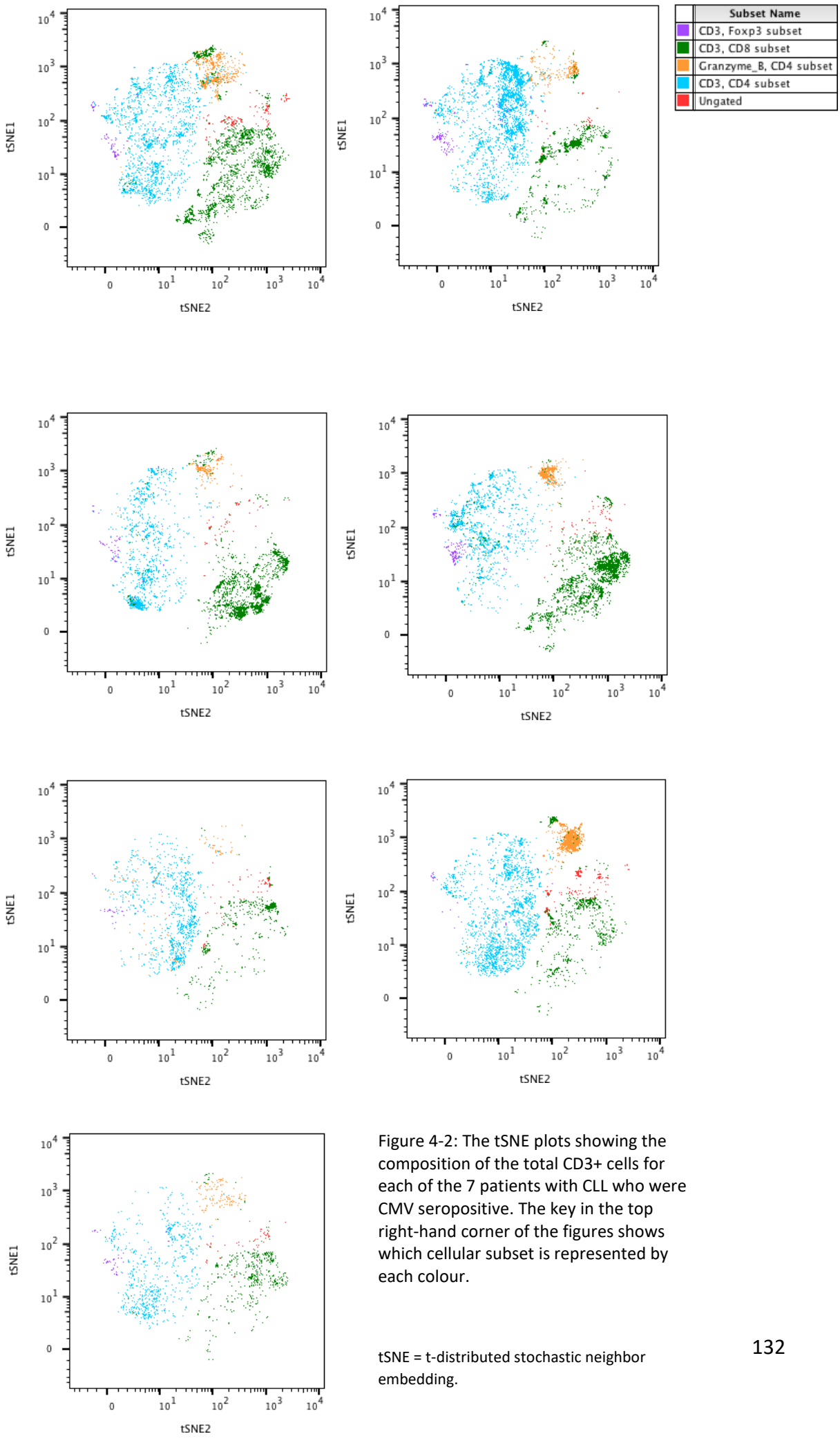

Figure 4-2: The tSNE plots showing the composition of the total CD3+ cells for each of the 7 patients with CLL who were CMV seropositive. The key in the top right-hand corner of the figures shows which cellular subset is represented by each colour.

tSNE = t-distributed stochastic neighbor embedding.

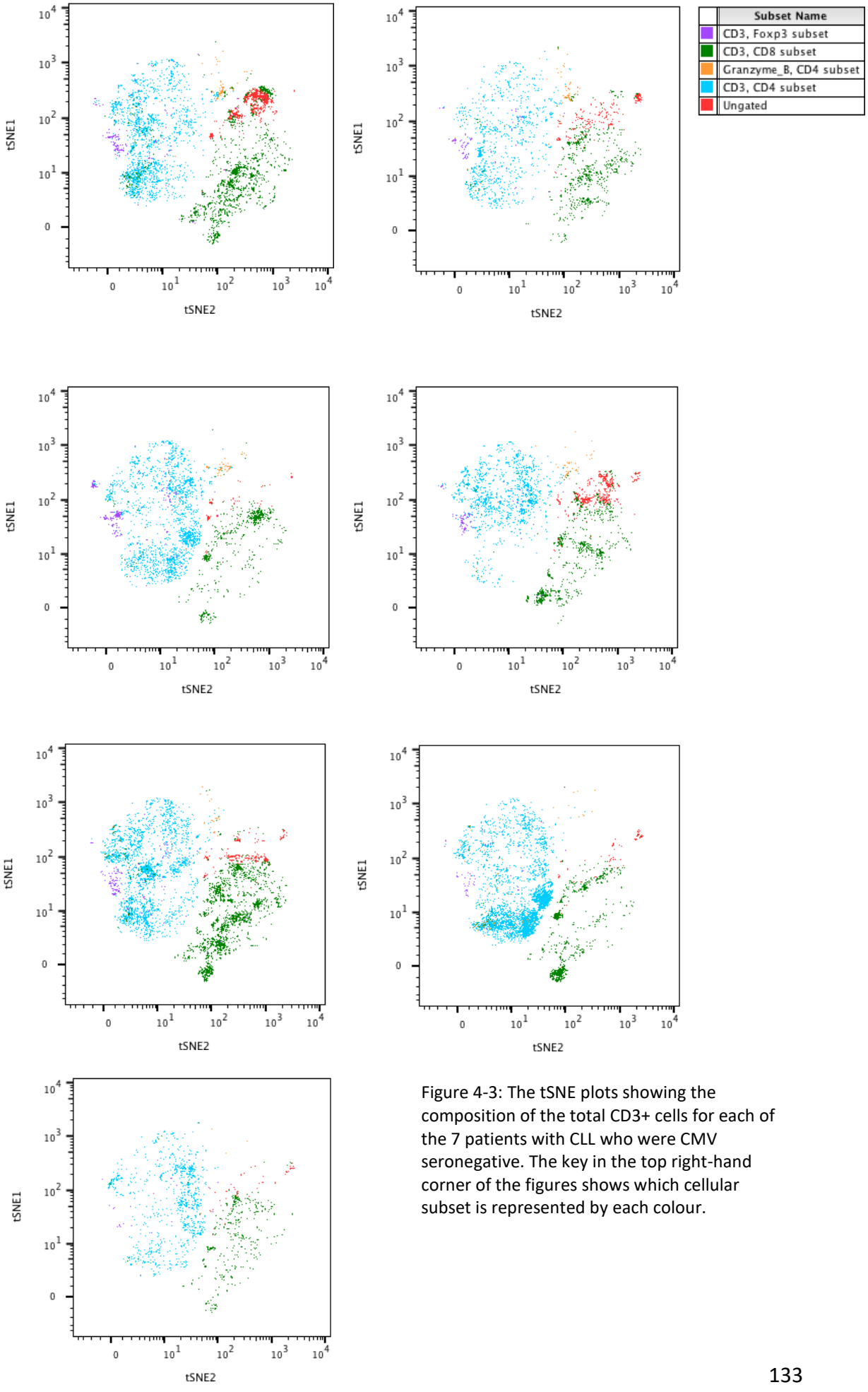

Figure 4-3: The tSNE plots showing the composition of the total CD3+ cells for each of the 7 patients with CLL who were CMV seronegative. The key in the top right-hand corner of the figures shows which cellular subset is represented by each colour.

A.

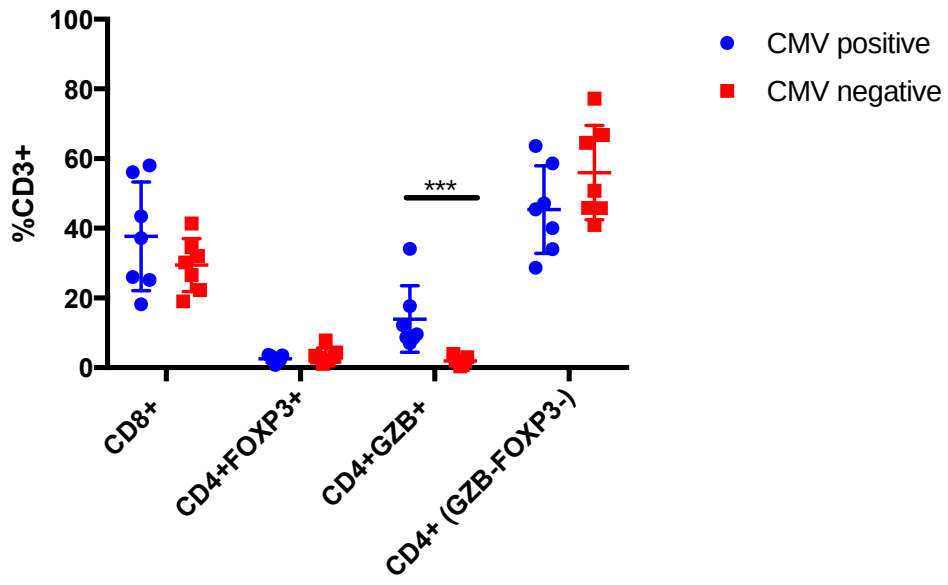

B.

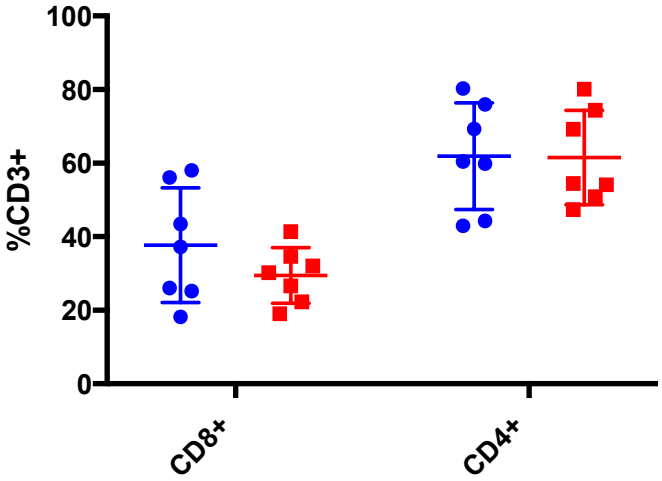

C.

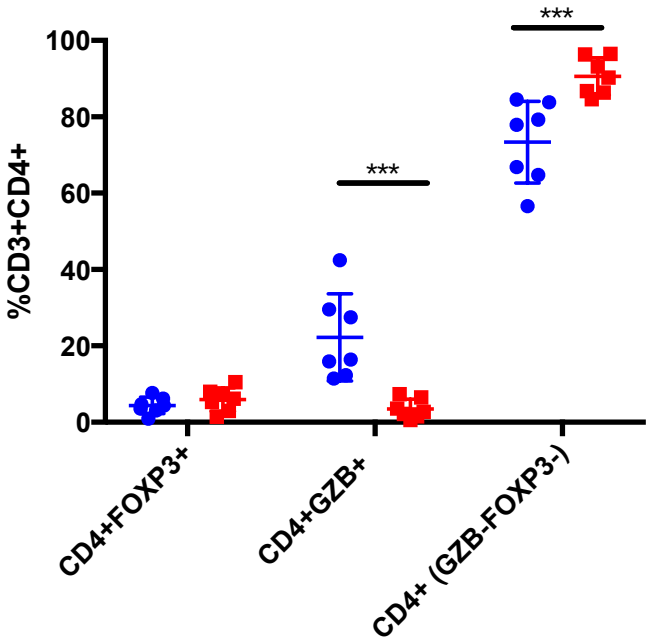

Figure 4-4: A-C: The composition of the total CD3+ cells in the 14 patients with CLL who have been subdivided into CMV serostatus, as determined by CyTOF analysis. Figure 4.4A shows the percentage of CD8+, CD4+FOXP3+, CD4+GZB+ and CD4+ (GZB-,FOXP3-) as a percentage of total CD3+ cells. Figure 4.4B shows the percentage of CD8+ and CD4+ cells of the total CD3+ cells. Figure 4.4C shows the composition of the total CD3+CD4+ cells for the 14 patients.

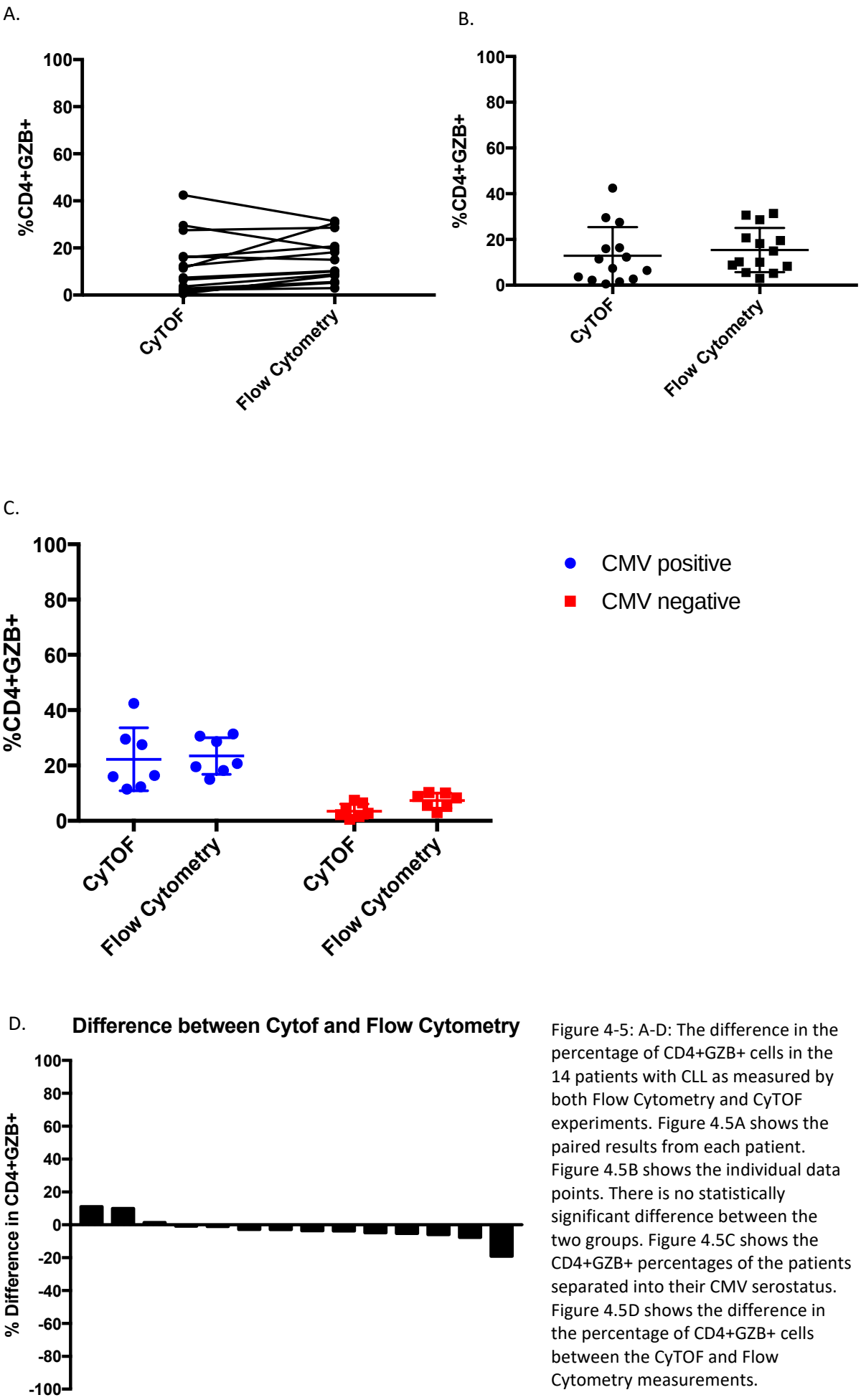

Figure 4-5: A-D: The difference in the percentage of CD4+GZB+ cells in the 14 patients with CLL as measured by both Flow Cytometry and CyTOF experiments. Figure 4.5A shows the paired results from each patient. Figure 4.5B shows the individual data points. There is no statistically significant difference between the two groups. Figure 4.5C shows the CD4+GZB+ percentages of the patients separated into their CMV serostatus. Figure 4.5D shows the difference in the percentage of CD4+GZB+ cells between the CyTOF and Flow Cytometry measurements.

4.7 CD3+ cell subsets

The CyTOF data analysed in this chapter was focused specifically on the CD3+ cellular subsets in the 14 patients with CLL. The tSNE maps of the subgroup composition of the total CD3+ cells for CMV seropositive and CMV seronegative patients show that the largest subgroup of CD3+ cells were those that were CD4 positive (Figure 4-2 and Figure 4-3). When examining the composition of different subgroups of CD3+ cells, Figure 4-4A demonstrates that the percentage of CD4+GZB+ cells as a percentage of total CD3+ cells was significantly higher in those patients who were CMV seropositive than in those who were CMV seronegative (P=0.0006). There was no statistically significant difference between the percentage of Tregs (CD4+FOXP3+), CD8+ cells or CD4+ (GZB-, FOXP3-) cells as a percentage of total CD3+ cells between the CMV seropositive and seronegative patients (Figure 4-4A). There was also no statistically significant difference in the level of total CD3+CD4+ cells and CD3+CD8+ cells as a percentage of total CD3+ cells between the CMV seronegative and CMV seropositive patients (Figure 4-4B).

4.7.1 CD4+ T lymphocyte subsets

The composition of the CD3+CD4+ compartment showed that, as a percentage of the total CD3+CD4+ cells, there was a significant increase in CD4+GZB+ cells in those patients who were CMV seropositive (P=0.0006) (Figure 4-4C). There was also a significant increase in the CD4+ (GZB-FOXP3-) cells in those patients who were CMV seronegative when compared to the CMV seropositive patients (P=0.0006). There was no significant difference in the percentage of CD4+FOXP3+ cells between those patients who were CMV seropositive or seronegative.

4.7.2 CD4+GZB+ cells: Comparison between Flow Cytometry and Mass Cytometry (CyTOF) quantification

The PBMCs samples had initially been analysed using Flow Cytometry with a limited panel which has been described in Chapter 2. The data obtained from the samples using both Flow Cytometry and CyTOF analysis were assessed to see if the two techniques were comparable. There was no statistically significant difference in the percentage of CD4+GZB+ cells using both techniques in either the CMV seropositive or seronegative patients (Figure 4-5). The median

difference in CD4+GZB+ percentage between the CyTOF and Flow Cytometry techniques was -3.23% (Range -19.1 – 11.1%) (Figure 4-5). This demonstrates that the two techniques are comparable when examining the measurement of CD4+GZB+ cells in the peripheral blood.

4.8 Extracellular panel: CD4+GZB+ phenotype

The percentage level of expression for each of the phenotypic markers assessed in the extracellular CyTOF panel on the CD4+GZB+ cells from all 14 patients is shown in a heat-map in Figure 4-6. The heat map represents the scale of expression levels from 0% (green) to 100% (red). The majority of the phenotypic markers' expression levels did not significantly differ between CMV seropositive and seronegative patients except PD-1, CD27, Intb7 and CD161. As expected, the CD4+GZB+ cells did not express CD14, CD19, gdTCR, HLA-DR, Va7_2, Vd2, CD103 or CD16. The majority of the CD4+GZB+ cells did not express Ki67 or ICOS and this supports the previous flow cytometry data presented in Chapter 3. The majority of CD4+GZB+ cells did express CD57 with a median percentage expression of 89.0% (range: 18.1 – 98.9%) and also Granzyme A with a median percentage expression of 74.9% (range: 13.2 – 90.8%). They are also positive for CD49d (median: 88.7%; range: 52.5 – 97.5%), CX3CR1 (median: 76.0%; range: 12.2 – 89.4%) and CD45RO (median: 66.9%; range: 18.2 – 100%). Approximately a third of CD4+GZB+ cells expressed CD45RA (median: 32.8%; range: 9.96 – 86.5%).

The majority of CD4+GZB+ cells did not express the following chemokine receptors: CCR2 (median: 1.48%; range: 0 – 19.9%), CCR4 (median: 5.49%; range: 1.60 – 34.5%), CCR6 (median: 5.37%; range: 1.42 – 19.9%), CCR7 (median: 5.73%; range: 1.34-76.3%), CCR9 (median: 4.91%; range: 1.78-19.9%).

4.8.1 The difference in phenotype of CD4+GZB+ cells between CMV seropositive and CMV seronegative patients.

For the majority of phenotypic markers examined in the extracellular panel, there was no statistically significant difference in their percentage expression on CD4+GZB+ cells between the CMV seropositive and CMV seronegative patients. However, there was a statistically significant difference in the following phenotypic markers:

1. PD-1

The percentage of PD-1 (programmed cell death protein-1) expression in CD4+GZB+ cells was significantly increased in those patients who were CMV seronegative when compared with patients who were CMV seropositive (P=0.0262) (Figure 4-7A). PD-1 is a co-inhibitory receptor of the immunoglobulin superfamily of cell-surface receptors. In the CMV seronegative patients, the median percentage expression of PD-1 was 82.5% (range: 30.4 – 68.6%) compared with a median percentage expression of 57.9% (range: 18.1 – 88.2%) in the CMV seropositive group of patients.

2. CD27

CD27 is a member of the tumour necrosis factor receptor superfamily. The percentage of CD27 expression in CD4+GZB+ cells was significantly increased in those patients who were CMV seronegative when compared with those patients who were CMV seropositive (P=0.0041) (Figure 4-7B). In the CMV seronegative patient group, the median percentage expression of CD27 was 66.8% (range: 39.6 – 83.9%) compared with a median percentage expression of 8.3% (range: 3.3 – 64.8%) in the CMV seropositive group of patients.

3. Intb7

The percentage of Intb7 expression in CD4+GZB+ cells was significantly increased in those patients who were CMV seronegative when compared with those patients who were CMV seropositive (P=0.0023) (Figure 4-7D). In the CMV seronegative patient group, the median percentage expression of Intb7 was 35.3% (range: 12.9 – 60.4%) compared with a median percentage expression of 4.6% (range: 1.6 – 15.9%) in the CMV seropositive group of patients.

4. CD161

CD161, also known as NK1.1, is a member of the C-type lectin family which is expressed on Natural Killer (NK cells) and also some T cells. The percentage of CD161 expression on CD4+GZB+ cells was significantly increased in the CMV seropositive group of patients when compared with the CMV seronegative patient group (P=0.0379) (Figure 4-7E), although the

overall expression percentage remained low. The median percentage of expression of CD161 on CD4+GZB+ cells in the CMV seropositive group was 22.1% (range: 1.2-65.8 %) compared with a median percentage expression of 11.6% (range: 0-18.8%) in the CMV seronegative group of patients.

5. CD127

CD127 functions as the IL-7 receptor on T lymphocytes. Although not statistically significant, there was a trend to an increase in the percentage of CD127 expression on CD4+GZB+ cells in the CMV seropositive patients when compared to the CMV seronegative group of patients (P= 0.0513) (Figure 4-7D). The median percentage expression was 31.5% (range: 13.3 – 48.1%) in the CMV seropositive group of patients compared with a median percentage expression of 5.9% (range: 0-62.2%) in the CMV seronegative group.

Extracellular panel: CD4+GZB+ phenotype

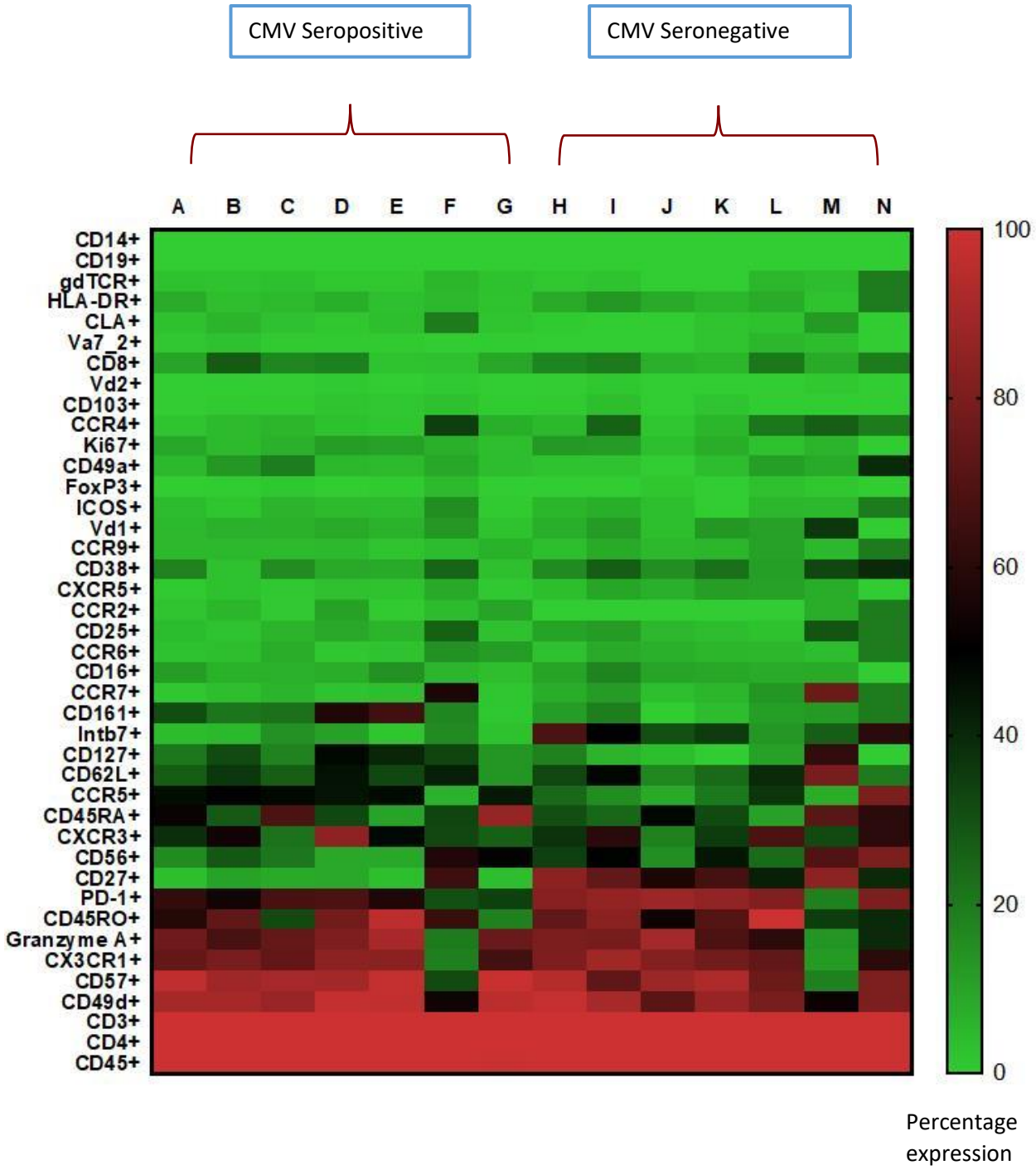

Figure 4-6: The heat map analysis of CyTOF expression data for the CD4+GZB+ subset of cells (extracellular panel). Each column represents a different patient's sample and these have been divided into CMV seropositive and CMV seronegative groups of patients. Each row represents the cell expression data for each particular marker (as listed in the left hand column).

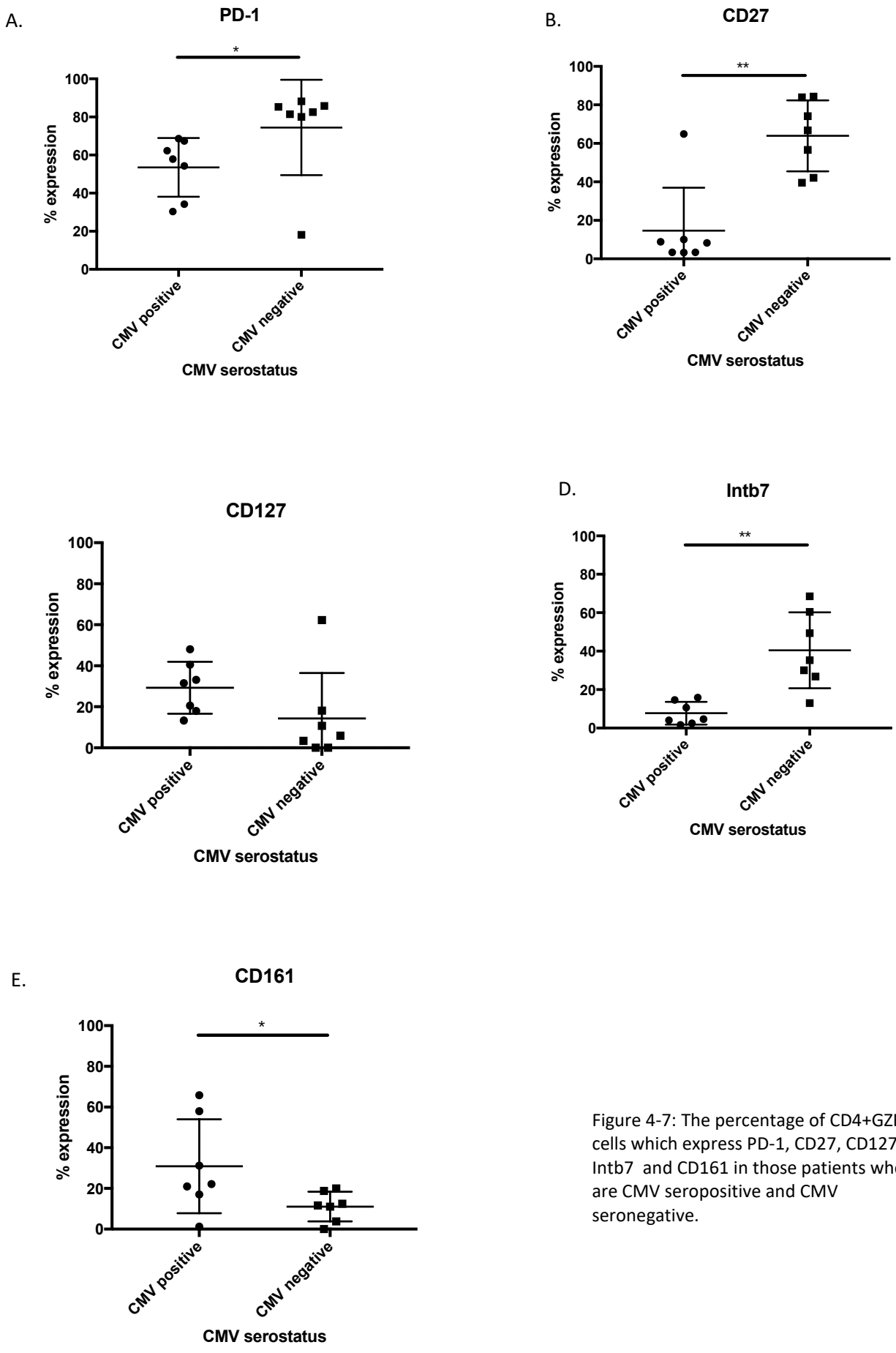

Figure 4-7: The percentage of CD4+GZB+ cells which express PD-1, CD27, CD127, Intb7 and CD161 in those patients who are CMV seropositive and CMV seronegative.

4.9 Extracellular panel: CD8+GZB+ phenotype

The percentage level of expression for each of the phenotypic markers assessed in the extracellular CyTOF panel on the CD8+GZB+ cells from all 14 patients is shown in a heat-map in Figure 4-8. The only phenotypic marker which showed a significant difference between those patients who were CMV seropositive and those patients who were CMV seronegative was CD27. All other markers' expression levels did not differ significantly between the two CMV serostatus groups. The CD8+GZB+ cells did not express CD14, CD19, gdTCR, Va7_2, Vd2, Vd1 and CD103. Similar to the CD4+GZB+ subset, their proliferation index, as measured by Ki67, was low. As expected, FoxP3 was not expressed.

The CD8+GZB+ did express CD57 (median percentage expression: 88.1%; range: 50.2 – 96.6%), CX3CR1 (median: 78.4%; range: 55.7 – 91.2%), Granzyme A (median: 84.4%; range: 65.1 – 94.9%) and CD49d (median: 91.1%; range: 66.9 – 97.8%). In contrast to the CD4+GZB+ cells, the majority of CD8+GZB+ cells expressed CD45RA (median: 68.8%; range: 40.5 – 93.1%).

The majority of CD8+GZB+ did not express the following chemokine receptors: CCR2 (median percentage expression: 1.4%; range: 0 – 4.5%), CCR6 (median 4.5%; range: 1.7 – 11.3%), CCR7 (median: 4.5%; range: 2.0 – 17.7%), CCR9 (median: 6.1%; range: 1.8 – 9.9%).

4.10 The difference in phenotype of CD8+GZB+ cells between CMV seropositive and CMV seronegative patients.

The only phenotypic marker which showed a significant difference in expression levels between the CMV seropositive and seronegative groups was CD27. The level of CD27 expression was significantly higher in those patients who were CMV seronegative when compared with those patients who were CMV seropositive (Figure 4-9A) (P=0.007). The median percentage of expression of CD27 in the CMV seronegative patients was 59.0% (range: 27.2 – 76.6%) compared with a median percentage of expression of 22.5% (range: 13.2 – 56.7%) in the CMV seropositive patients.

Although the majority of CD8+GZB+ cells did not express CCR4 (overall median expression of 6.3%; range: 2.1 – 23.4%), there was a trend of an increase in percentage expression of CCR4 in the CMV seronegative population when compared with the CMV seropositive group of patients (P = 0.0530). This did not, however, reach statistical significance (Figure 4-9C).

In contrast to the CD4+GZB+ cellular subset, there was no statistically significant difference in expression of PD-1, CD161 or Intb7 between the CMV seronegative and seropositive populations. The majority of CD8+GZB+ cells express PD-1 with a median percentage expression of 56% (range: 27.5 – 72.5%). The majority of CD8+GZB+ cells also express CD161 with a median percentage expression of 56.2% (range: 27.6 – 94%). A minority of CD8+GZB+ cells expressed Intb7 with a median expression level of 27.7% (range: 10.0 – 56.6%).

Extracellular panel: CD8+GZB+ phenotype

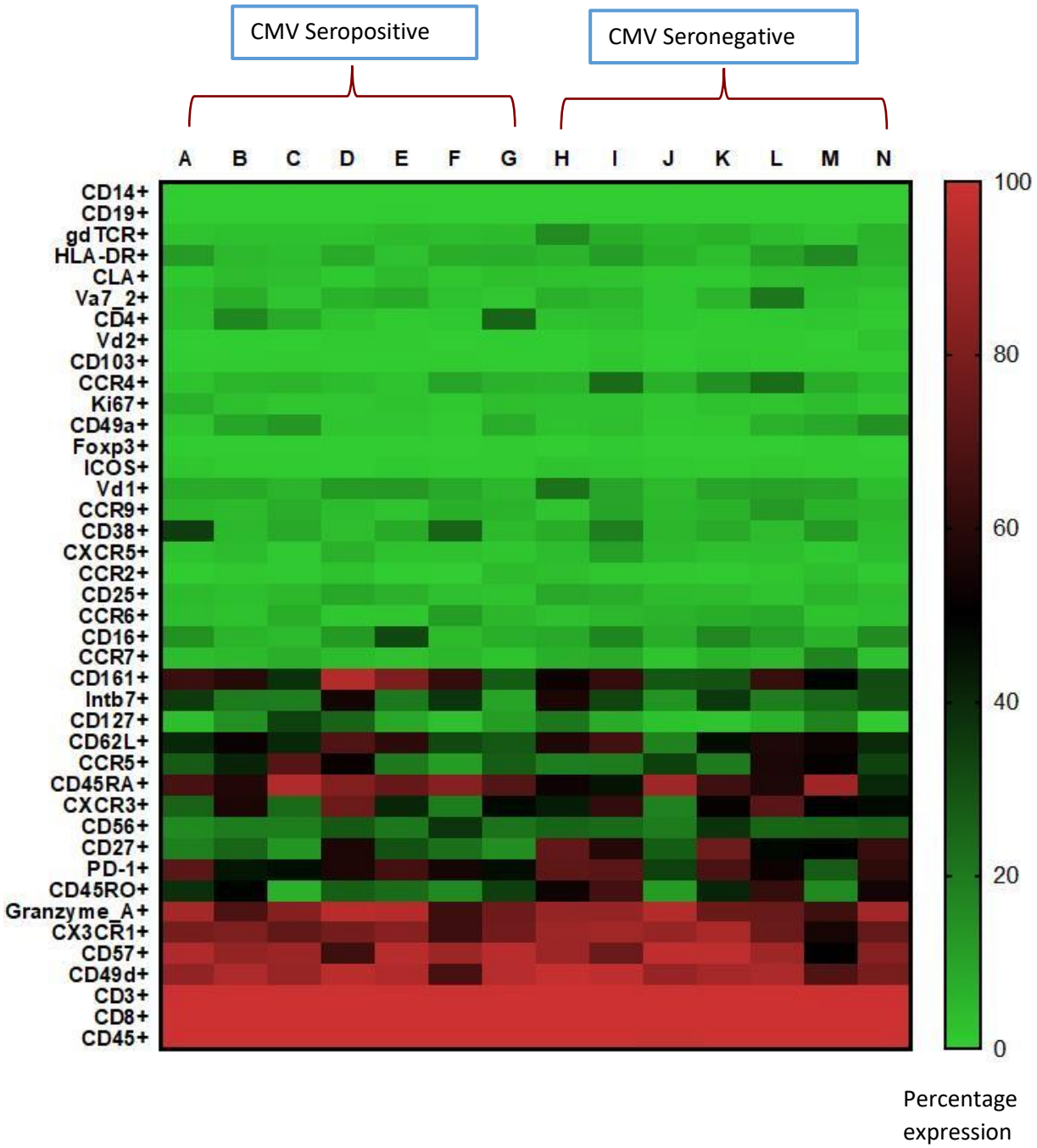

Figure 4-8: The heat map analysis of CyTOF expression data for the CD8+GZB+ subset of cells (extracellular panel). Each column represents a different patient's sample and these have been divided into CMV seropositive and CMV seronegative groups of patients. Each row represents the cell expression data for each particular marker (as listed in the left hand column).

A.

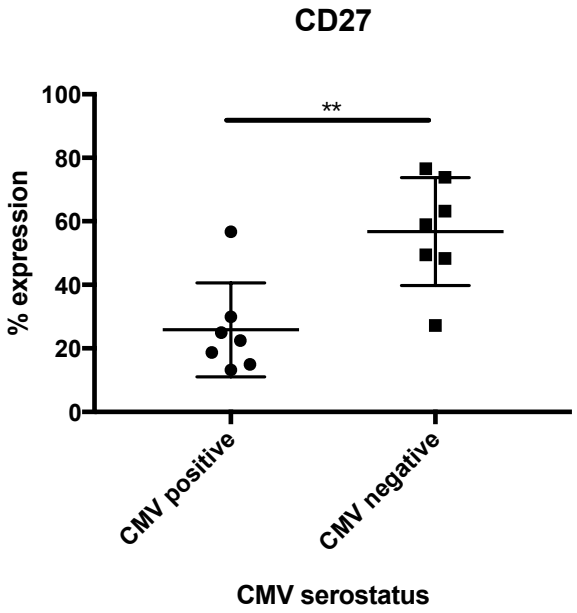

B.

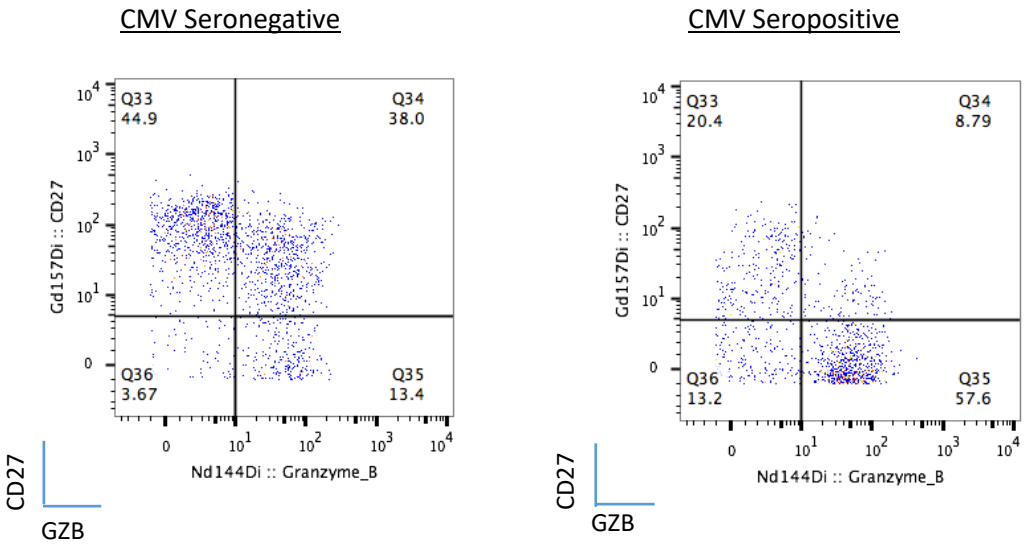

C.

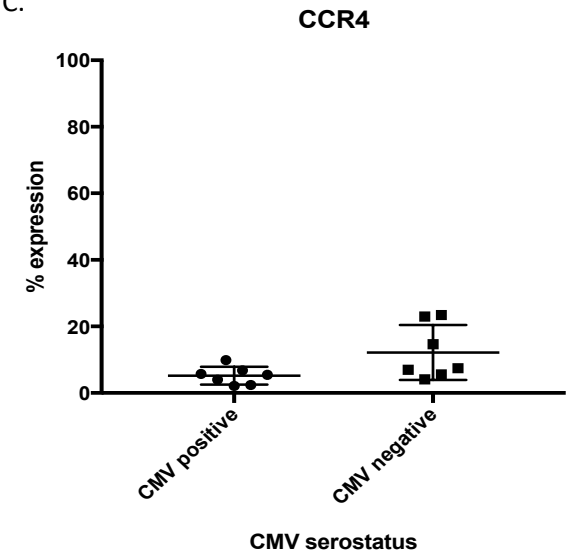

Figure 4-9 A-C: The difference in expression levels of CD27 and CCR4 on CD8+GZB+ cells in CMV seropositive and CMV seronegative patients.

4.11 The comparison between CD4+GZB+ and CD8+GZB+ phenotypes as determined by the extracellular CyTOF panel

The phenotypes of the CD4+GZB+ and CD8+GZB+ cell subsets share many similarities. The majority of both groups of cytotoxic cells express CD57 (Figure 4-10H), Granzyme A (Figure 4-10G), CX3CR1 and CD49d. There was no significant difference in the expression of Granzyme A (P=0.0556), CD57 (P=0.8388), CX3CR1 (P=0.3287) and CD49d (P=0.7006) between the CD4+GZB+ and CD8+GZB+ cells. Whilst both CD57 and Granzyme A expression was shown in Chapter 3, CX3CR1 and CD49d had not been previously studied. Both groups are negative for Ki67, signifying a low proliferation index, which supports previously published data regarding T cells in the peripheral blood of patients with CLL [100].

Regarding cytokine receptors, both groups of cytotoxic cells do not express the majority of cytokine receptors that were examined (namely CCR2, CCR6, CCR7, CCR9).

With respect to immune checkpoint receptors, the majority of CD4+GZB+ and CD8+GZB+ cells did not express ICOS, although in the minority of cells that did express ICOS, there was a significant increase in expression in the CD4+GZB+ subset when compared with the CD8+GZB+ cellular subset (P= 0.0005) (Figure 4-10E). There was no significant difference in expression of PD-1 between the CD4+GZB+ and CD8+GZB+ cells (Figure 4-10F). Although there was a significant difference in expression of PD-1 on CD4+GZB+ cells depending on CMV serostatus, there was no significant difference in PD-1 expression between the CMV seropositive and CMV seronegative patients in the CD8+GZB+ cell subsets.

The expression of CD45RO was significantly higher in the CD4+GZB+ subset when compared with the CD8+GZB+ subset of cells (P=0.0042) (Figure 4-10A) whereas, conversely, the CD45RA expression was significantly higher in the CD8+GZB+ cells when compared with the CD4+GZB+ (P=0.0030) (Figure 4-10B). The expression of CD62L was significantly higher in the CD8+GZB+ cells than in the CD4+GZB+ cells (P= 0.0241) where the CD8+GZB+ has a median expression of 49.4% (range: 17.9 – 69.1%). The expression of CD161 was significantly higher in the CD8+GZB+ cells when compared with CD4+GZB+ cells (P=0.0002), although it should be noted

that, within the CD4+GZB+ cellular subgroup, there was a significant difference in expression between those patients who were CMV seropositive and those who were CMV seronegative.

A.

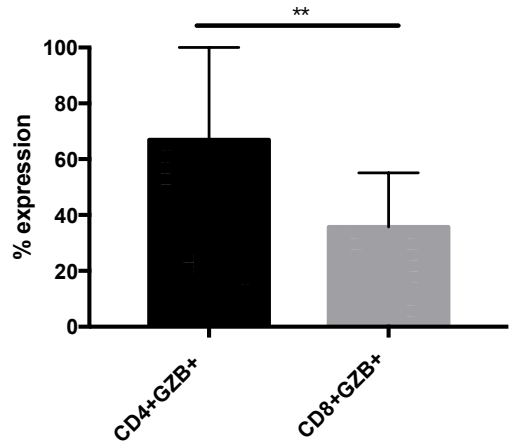
CD45RO
**
% expression
100
80
60
40
20
0
CD4+GZB+
CD8+GZB+

B.

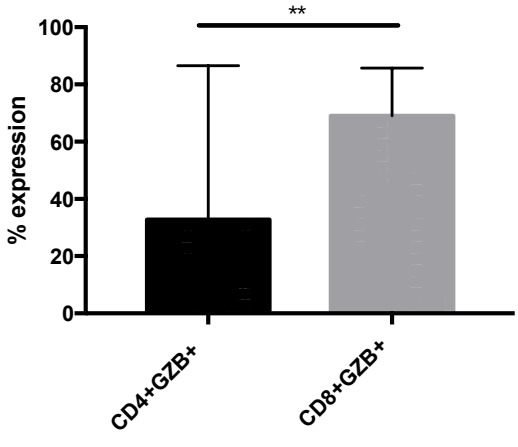
CD45RA
**
% expression
100
80
60
40
20
0
CD4+GZB+
CD8+GZB+

C.

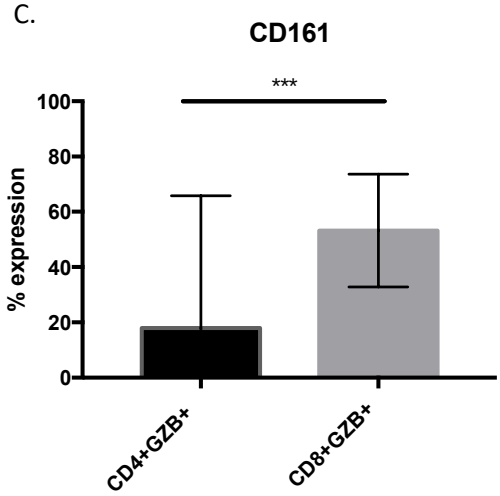
CD161
***
% expression
100
80
60
40
20
0
CD4+GZB+
CD8+GZB+

D.

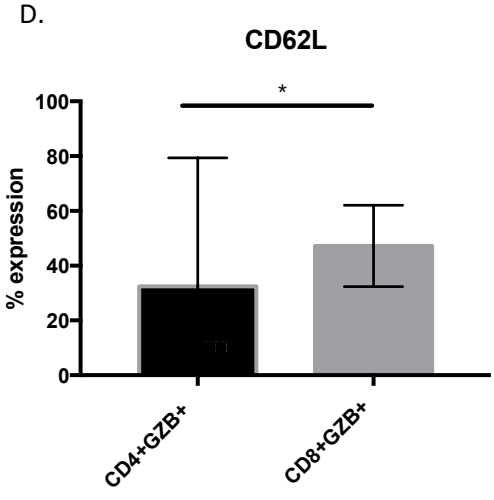
CD62L
*
% expression
100
80
60
40
20
0
CD4+GZB+
CD8+GZB+

E.

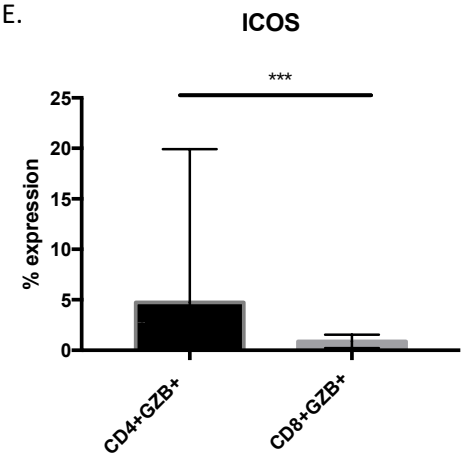
ICOS
***
% expression
25
20
15
10
5
0
CD4+GZB+
CD8+GZB+

F.

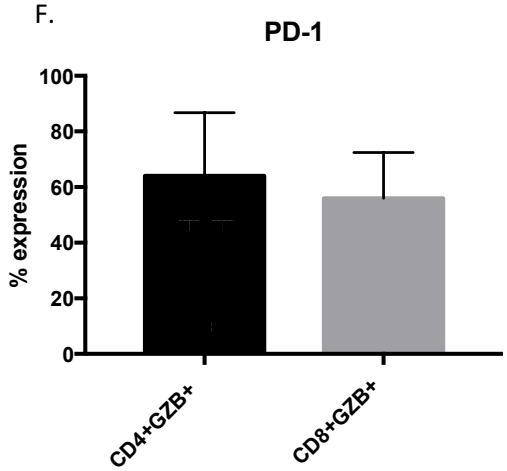
PD-1
% expression
100
80
60
40
20
0
CD4+GZB+
CD8+GZB+

G.

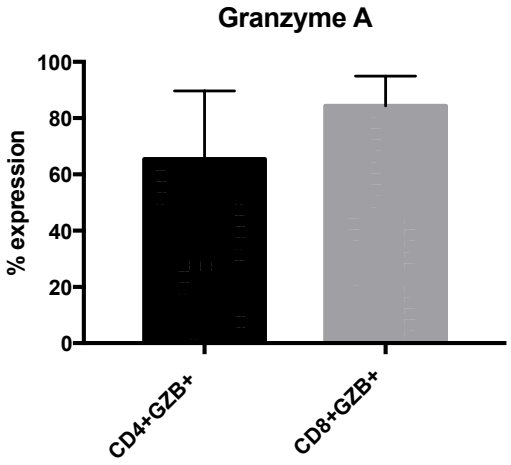

H.

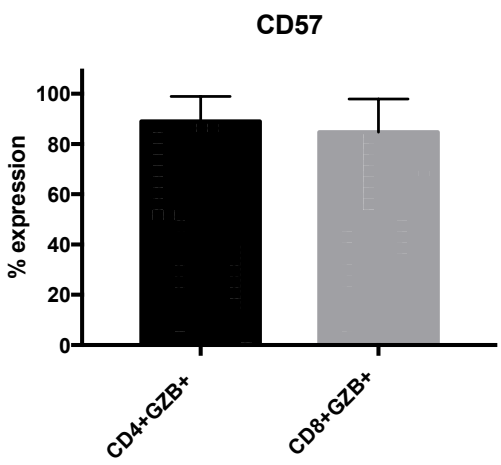

Figure 4-10: A-H: The difference in percentage expression for particular phenotypic markers between CD4+GZB+ and CD8+GZB+ cellular subsets as determined by the CyTOF extracellular panel. The phenotypic markers shown are CD45RO (Figure A), CD45RA (Figure B), CD161 (Figure C), CD62L (Figure D), ICOS (Figure E), PD-1 (Figure F), Granzyme A (Figure G) and CD57 (Figure H). There was a significant difference in percentage expression of CD45RO (P=0.0042), CD45RA (P=0.0030), CD161 (P=0.0002), CD62L (P=0.0241), ICOS (P=0.0005) and Va7_2 (P=0.0003) between the CD4+GZB+ and CD8+GZB+ cellular subsets. The bar charts represent the median levels of percentage expression with the range. The Mann Whitney U test was used to assess for statistical differences.

Intracellular panel: CD4+GZB+ phenotype

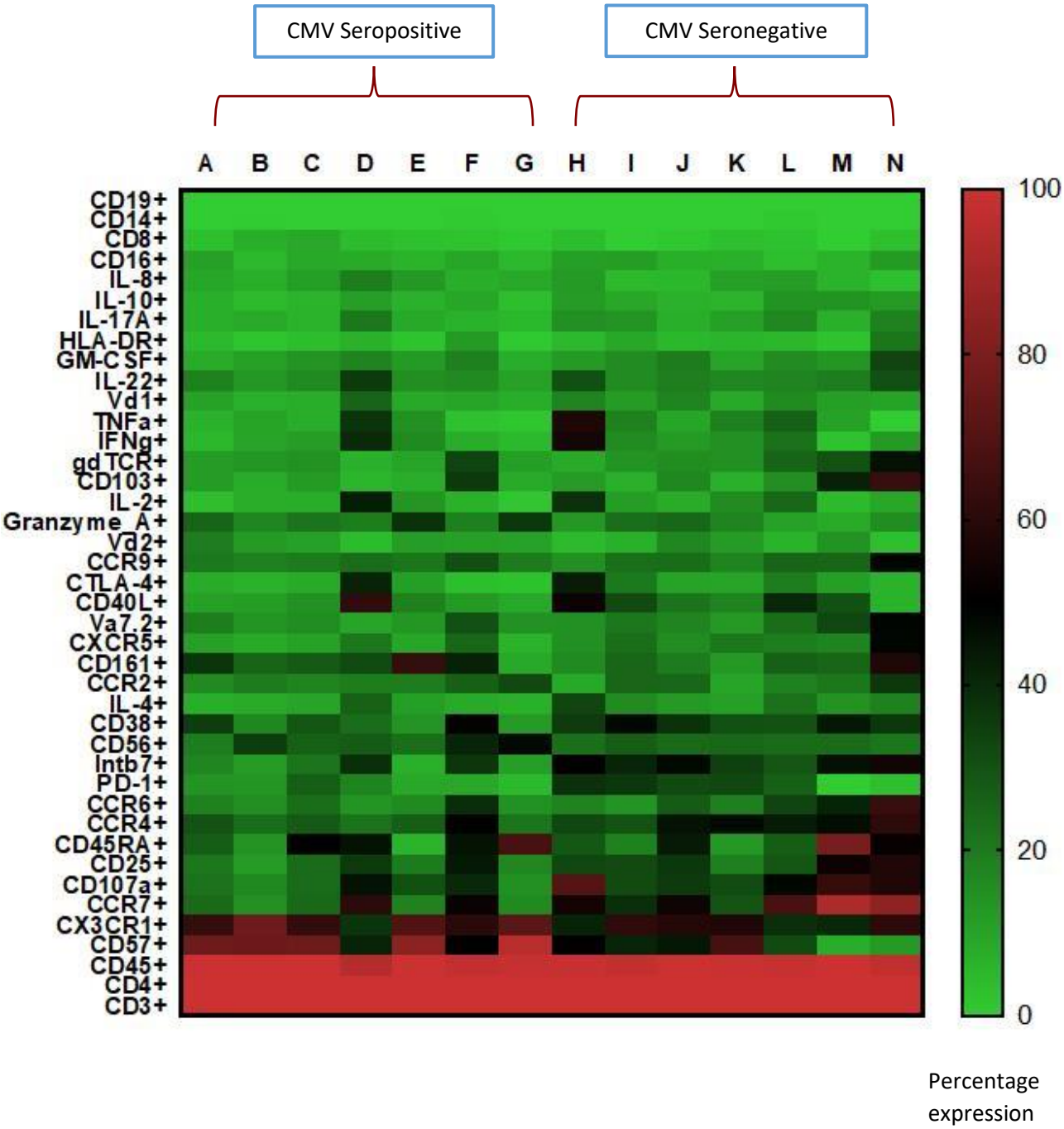

Figure 4-11: The heat map analysis of CyTOF expression data for CD4+GZB+ subset of cells (intracellular panel). Each column represents a different patient's sample and these have been divided into CMV seropositive and CMV seronegative groups of patients. Each row represents the cell expression data for each particular marker (as listed in the left hand column).

4.12 Intracellular panel: CD4+GZB+ phenotype

Unlike the extracellular panel, the cells used in the intracellular panel had been re-stimulated prior to staining to assess for cytokine production. The CD4+GZB+ cells predominantly expressed CX3CR1 (median expression: 98.7%; range: 94.6 – 100%) and also CD57 (median: 50%; range: 7.6 – 95.3%), although to a lower level than the unstimulated cells (Figure 4-11).

Granzyme A expression was decreased following re-stimulation with a median expression of 18.9% (range: 8.4 – 37.7%). The majority of CD4+GZB+ cells were negative for the co-inhibitory receptors including CTLA-4 (median: 10.0%; range: 2.5 – 42.9%) and PD-1 (median: 15.6%; range: 0 – 37.9%). CD40L is also not expressed by the majority of CD4+GZB+ (median: 17.9%; range: 6.0 – 61.6%) which is in concordance with the CLL flow cytometry data shown in Chapter 3.

CD4+GZB+ cells have not previously been designated to one particular subgroup of CD4+ cells. Interferon-gamma (IFNg) and IL-2, whose production is associated with the Th1 subset of CD4+ cells, were only expressed by a minority of CD4+GZB+ cells (IFNg median expression: 12.1%, range: 2.1- 55.3%; IL-2 median expression: 8.6%, range: 1.4 – 42.5%). IL-4, whose production is associated with the Th2 subset of CD4+ cells, was also not expressed by the majority of CD4+GZB+ cells (median expression: 11.7%, range: 6.9 – 32.9%). GM-CSF which is produced by Th1 and some Th2 cells was also not expressed by the majority of CD4+GZB+ cells (median: 13.4%; range: 7.6 – 33.2%). The Th17 subset of T helper cells is identified by the production of the IL-17 family of cytokines and also, the majority of CD4+GZB+ did not express IL-17A (median: 8.5%; range: 5.1 – 20.5%).

4.12.1 The difference in phenotype of CD4+GZB+ cells between CMV seropositive and CMV seronegative patients.

The majority of phenotypic markers examined in the intracellular panel did not show a statistically significant difference between the patients who were CMV seropositive and CMV seronegative. The phenotypic markers that did show a significant difference in expression on CD4+GZB+ between the CMV seronegative and CMV seropositive cells are listed below:

CCR7

Whereas in the unstimulated cells CCR7 was not expressed, the expression of CCR7 on CD4+GZB+ cells after re-stimulation was significantly increased in the patients who were CMV seronegative (P=0.0175) (Figure 4-12A). The median expression of CCR7 on the CD4+GZB+ cells from CMV seronegative patients was 54.6% (range: 29.4-92.4%) compared with a median expression of 24.0% (range: 14.4-60.2%) in those patients who were CMV seropositive.

CD57

Unlike the unstimulated extracellular panel results, upon re-stimulation on the intracellular panel, the expression of CD57 on CD4+GZB+ was significantly decreased in the CMV seronegative population when compared with the CMV seropositive group of patients (P=0.0111) (Figure 4-12E). The median expression of CD57 in the CMV seropositive group was 76.5% (range: 41.1-95.3%) compared with a median expression level of 40.9% (range: 7.6-66.7%) in the CMV seronegative patients.

CD107A

CD107a, which is known to be expressed on activated T cells, was significantly increased on the CD4+GZB+ from the CMV seronegative patients when compared with the CD4+GZB+ cells from the CMV seropositive patients (P = 0.0175) (Figure 4-12F). The median expression of CD107A on CD4+GZB+ from the CMV seronegative patients was 48.3% (range: 31.8-70.8%) compared with a median expression of 23.8% (range: 14.6-45.2%) from the CMV seropositive group of patients.

CCR4

The expression of CCR4 on CD4+GZB+ cells was significantly increased in the CMV seronegative group of patients when compared with those who were CMV seropositive (P=0.0262) (Figure 4-12D). The median expression level was 44.9% (range: 29.5-60.6%) on the CD4+GZB+ cells from the CMV seronegative patients and 26.9% (range: 21.1-49.2%) in the cells from CMV seropositive patients.

Intb7

In the extracellular, unstimulated panel, the expression level of Intb7 on CD4+GZB+ cells was significantly increased in the CMV seronegative group. This significant difference was also shown on the intracellular panel (P=0.0070) (Figure 4-12C) where the median expression level of Intb7 on CD4+GZB+ in the CMV seronegative group was 45.8% (range: 28.9-54.4%).

IL-4

There was a significant increase in the expression of IL-4 in those patients who were CMV seronegative when compared with the group who were CMV seropositive (P= 0.0262) (Figure 4-12B). Despite the significant difference in expression level between the CMV seropositive and CMV seronegative patients, the majority of CD4+GZB+ cells from both groups of patients did not express IL-4. There was a median expression level of 15.9% (range: 10.8 – 32.9%) in the CMV seronegative patients compared with a median expression level of 8.5% (range: 6.9-26%) in the CMV seropositive patients.

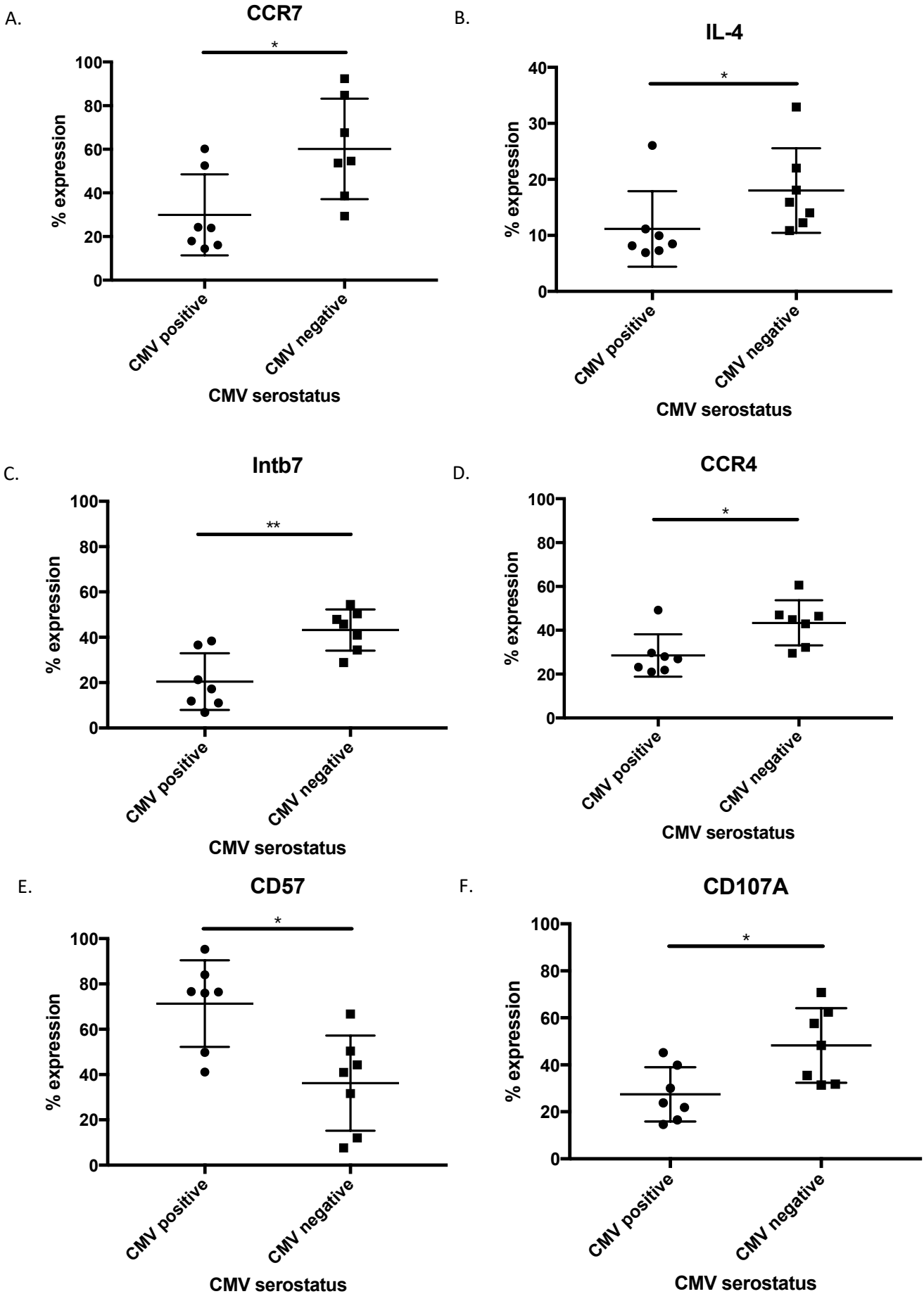

Figure 4-12: A-F: The difference in percentage expression of CCR7, IL-4, Intb7, CCR4, CD57 and CD107A on CD4+GZB+ cells between CMV seropositive and CMV seronegative patients.

Intracellular panel: CD8+GZB+ phenotype

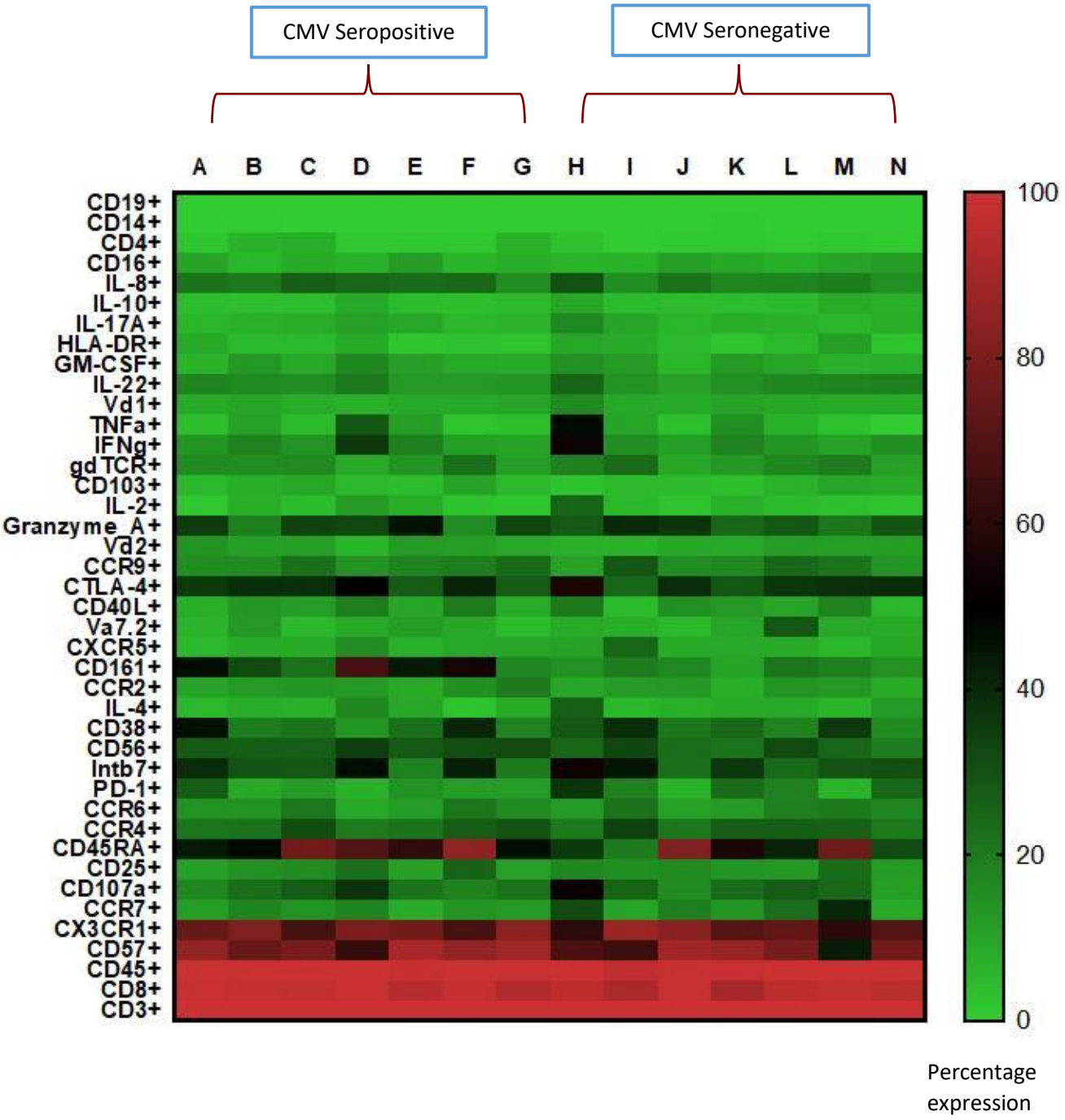

Figure 4-13: The heat map analysis of CyTOF expression data for the CD8+GZB+ subset of cells (intracellular panel). Each column represents a different patient's sample and these have been divided into CMV seropositive and CMV seronegative groups of patients. Each row represents the cell expression data for each particular marker (as listed in the left hand column).

4.13 Intracellular panel: CD8+GZB+ phenotype

The re-stimulated, intracellular panel showed that the CD8+GZB+ cells expressed CD57 (median expression: 79.2%, range: 42.8-90.8%), CX3CR1 (median expression: 74.7%, range: 60.2 – 87.6%) and CD45RA (median expression: 52.2%, range: 19.6 – 85.1%), which is in concordance with the results obtained from the extracellular, unstimulated panel. Like the CD4+GZB+ cells, there was a lower level of Granzyme A expression (median expression: 30.8%, range: 15.4 – 45.3%) on re-stimulation when compared with the unstimulated, extracellular panel (median expression: 88.1%, range: 50.2-96.6%).

Like the CD4+GZB+ cells, the majority of CD8+GZB+ did not express the co-inhibitory receptors CTLA-4 (median expression: 38.2%, range: 24.8 – 56.8%), or PD-1 (median expression:13.0%, range: 6.2-37.0%). The majority of CD8+GZB+ also did not express CD40L (median expression: 12.1%, range: 5.3 – 20.2%).

The cytokines examined also showed that the majority of CD8+GZB+ cells did not express IL-2 (median expression:4.2%, range: 1.4 – 25.2%), IFNg (median expression: 14.4%, range: 10.1-52.7%), IL-4 (median expression: 7.9%, range: 2.3-26.8%), IL-17A (median expression: 7.1%, range: 5.3 – 10.8%) and GM-CSF (median expression: 9.2%, range: 5.5-16.7%). The majority of CD8+GZB+ also did not express IL-8, IL-10 or IL-22.

4.13.1 The difference in phenotype of CD8+GZB+ cells between CMV seropositive and CMV seronegative patients.

The majority of phenotypic markers examined on the CD8+GZB+ cells using the re-stimulated intracellular panel showed no significant difference in expression between the CMV seropositive and CMV seronegative groups of patients. The only phenotypic marker that showed a significant difference in expression level was CD161, which was significantly increased in the CMV seropositive patients when compared with the CMV seronegative patients (P=0.0041) (Figure 4-14). The median expression level was 43.5% (range: 16.6-67.6%) in the CMV seropositive patients compared with a median expression level of 16.4% (range: 10.2-21.1%) in the CMV seronegative patients.

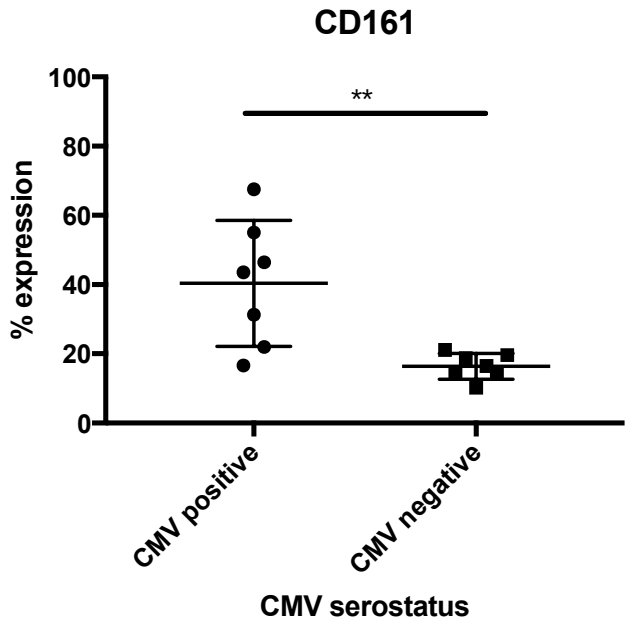

Figure 4-14: The percentage expression of CD161 on CD8+GZB+ cells in the CMV seropositive and CMV seronegative patients.

4.13.2 The comparison between CD4+GZB+ and CD8+GZB+ phenotypes as determined by the intracellular CyTOF panel

As previously shown in the extracellular, unstimulated panel, the majority of CD4+GZB+ and CD8+GZB+ cells also expressed CX3CR1 and CD57 on testing with the re-stimulated intracellular panel. There were differences in the degree of expression between the CD4+GZB+ and CD8+GZB+ cells. The majority of CD4+GZB+ and CD8+ GZB+ cells expressed CX3CR1 but there was a significant increase in expression on the CD8+GZB+ cells when compared with the CD4+GZB+ cells (P = 0.0005) (Figure 4-15A). Furthermore, the majority of CD4+GZB+ and CD8+GZB+ cells expressed CD57 but CD8+GZB+ expressed a significantly higher level of CD57 than the CD4+GZB+ cells (P = 0.0106) (Figure 4-15C). In concordance with the extracellular panel, the level of CD45RA was significantly increased in the CD8+GZB+ cells when compared with the CD4+GZB+ cells (P = 0.0395) (Figure 4-15B).

The expression of the serine protease Granzyme A on the extracellular panel was expressed by the majority of CD4+GZB+ (median: 74.9%) and CD8+GZB+ cells (median: 84.4%). On re-stimulation, however, the median percentage of expression for both cellular subsets was lower (CD4+GZB+ median: 18.9% vs CD8+GZB+ median: 30.8%,) and there was a significant increase in the expression in the CD8+GZB+ cells when compared with the CD4+GZB+ cells (P=0.0079) (Figure 4-15D).

Although the majority of CD4+GZB+ and CD8+GZB+ cells did not express CTLA-4, the minority of cells that did express CTLA-4 was significantly higher in the CD8+GZB+ cells when compared with the CD4+GZB+ cells (P=0.0003) (Figure 4-15E).

A.

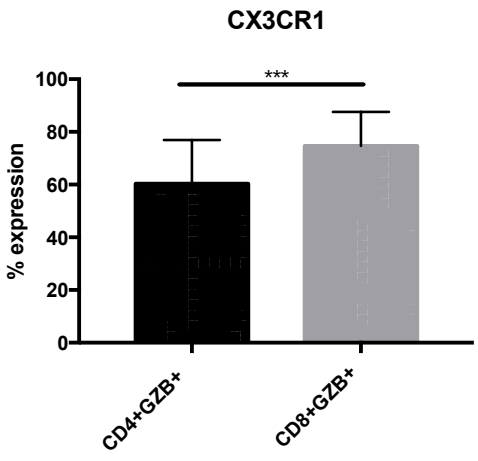

B.

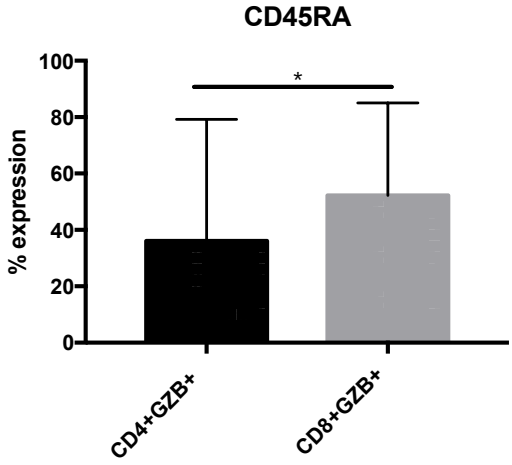

C.

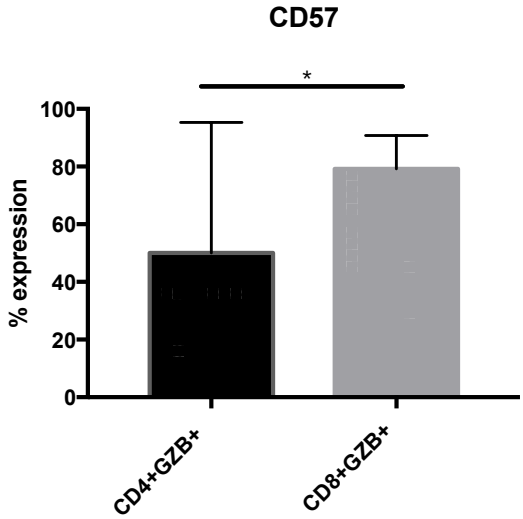

D.

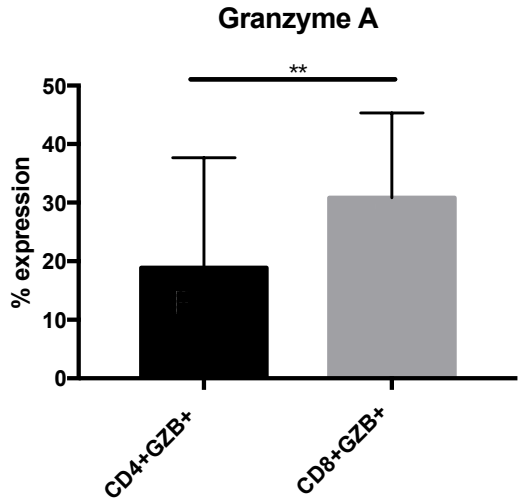

E.

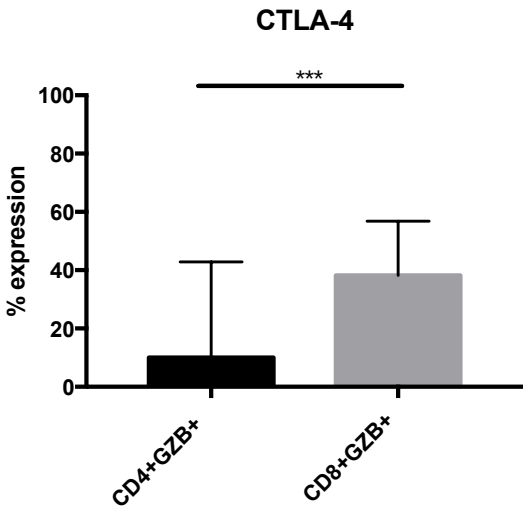

Figure 4-15: The percentage expression of phenotypic markers on CD4+GZB+ and CD8+GZB+ where there was a significant difference in expression level between the two cellular subsets.

4.14 Discussion

The data presented in this chapter has demonstrated that the techniques of flow cytometry and CyTOF produce comparable results when assessing the levels of CD4+GZB+ in the peripheral blood of patients with CLL.

The extracellular, unstimulated CyTOF panel results show that the CD4+GZB+ cells exhibit a phenotype that shares many similarities with the CD8+GZB+ cells. Both subsets express high levels of CD57 as well as the serine protease Granzyme A. CX3CR1 (a chemokine receptor for CX3CL1) regulates leucocyte migration and cell adhesion and is expressed on NK cells and activated T cells [101]. It is highly expressed on both CD4+GZB+ and CD8+GZB+ cells. The expression, on Granzyme B-expressing CD4+ and CD8+ cells, of phenotypic markers that are usually associated with NK cells may reflect their common cytotoxic function. The significantly increased expression of CD161, also known as NK1.1 [102], on the CMV seropositive patients' CD4+GZB+ cells, when compared with the CMV seronegative group, may be associated with their antigen experience and development of cytotoxic function in association with exposure to CMV. [102]

The significantly decreased expression of CD27 in the CMV seropositive groups in both the CD4+GZB+ and CD8+GZB+ cellular subsets is reflective of the antigen experience of these cells. A key difference between the CD4+GZB+ and CD8+GZB+ cells was the expression of CD45RA and CD45RO. The expression of CD45RO was significantly higher in the CD4+GZB+ subset when compared with the CD8+GZB+ subset of cells. Conversely, the expression of CD45RA was significantly higher in the CD8+GZB+ cells. CD45RA expression is typically associated with naïve T cells and, upon antigen experience, T cells typically gain CD45RO and lose expression of CD45RA. This difference suggests that the CD4+GZB+ cells may be more antigen experienced than the CD8+GZB+ cells.

Following re-stimulation, the CD4+GZB+ cells retain CX3CR1 and CD57 expression, although the overall level of CD57 expression is less, which parallels the data shown in Chapter 3. This decrease in CD57 expression was more marked in the CMV seronegative patients.

The significantly higher expression of PD-1 on CD4+GZB+ cells from the CMV seronegative patients, when compared with those who were CMV seropositive, is perhaps a surprising result. Previous research groups have hypothesised that cytotoxic CD4+ cells have been subjected to chronic antigenic stimulation, in this case to CMV antigens, which may consequently lead to T cell exhaustion. T cell exhaustion is characterised by the upregulation of co-inhibitory receptors including PD-1 [89]. The decrease in PD-1 expression suggests that the CMV seropositive CD4+GZB+ are not exhausted and may retain effector functions. There is a further decrease in PD-1 expression on the CD4+GZB+ cells following re-stimulation, which also adds weight to the proposal that they may not be exhausted.

The analysis of the composition of CD4+ cells in the patients showed a significant increase in the percentage of CD4+GZB+ in CMV seropositive patients with an associated significant decrease in CD4+ (GZB-FOXP3-) cells. There was no difference in the percentage of CD4+FOXP3+ cells (of the total CD4+ cells) between the CMV seropositive and CMV seronegative groups. The CD4+ (GZB-FOXP3-) cells will include naïve CD4+cells, and this reciprocal difference in percentages is likely to reflect the differentiation of naïve CD4+ cells into CD4+GZB+ cells.

In conclusion, this chapter demonstrates that CD4+GZB+ and CD8+GZB+ cells from patients with CLL share many common phenotypic markers which are reflective of their shared cytotoxic function. There are few phenotypic differences between the CMV seronegative and CMV seropositive groups of each cellular subsets but these differences are likely to represent the degree of antigenic exposure and stimulation related to CMV. This study was performed on 14 patients and further studies should include a larger cohort of patients which would allow a correlation with clinical outcome to be undertaken. Further phenotypic analyses by CyTOF of the peripheral blood of CMV seropositive and seronegative healthy individuals, who do not have CLL, would provide valuable information on the phenotype of these cells in controls who do not have the known immunodeficiency that is associated with CLL.

Chapter 5 The identification and characterisation of cytotoxic CD4+ T lymphocytes in patients with Hodgkin Lymphoma, Non-Hodgkin Lymphoma and Multiple Myeloma

5.1 Introduction

Following the characterisation of cytotoxic CD4+ T lymphocytes in Chronic Lymphocytic Leukaemia (CLL), a mature B-lymphocyte lymphoproliferative disorder, we decided to extend our investigation to focus on examining their presence in the tumour microenvironment of other haematological malignancies, specifically in the lymph nodes of mature B-cell Lymphoma subtypes (as well as Anaplastic Large Cell Lymphoma, a T cell neoplasm) and the bone marrow aspirate samples of patients with newly-diagnosed Multiple Myeloma. Cytotoxic CD4+ T lymphocytes have not previously been described in the tumour microenvironment of Lymphoma subtypes or in Multiple Myeloma. The Lymphoma subtypes that were examined included:

- Classical Hodgkin Lymphoma
- Diffuse Large B Cell Lymphoma
- Follicular Lymphoma
- Mantle Cell Lymphoma
- ALK+ and ALK- Anaplastic Large B Cell Lymphoma (ALCL)

5.2 Lymphoma Subtypes

5.2.1 Hodgkin Lymphoma

Hodgkin Lymphoma (HL) was first described by Thomas Hodgkin in 1832, following his observations that the clinical presentation and post-mortem findings of six individuals shared common abnormalities of the lymph nodes and spleen [103] It is one of the less common forms of lymphoma with an annual incidence of 2.7 per 100,000 [104]. The Reed-Sternberg cells present in Hodgkin Lymphoma are positive for CD30, CD15 and PAX5 in the majority of cases and negative for CD45 on immunophenotype analysis. The Classical Hodgkin Lymphoma (CHL) subtype comprises of 95% of all HL diagnoses. CHL is further divided into 4 histological subgroups: lymphocyte-rich CHL, nodular sclerosis CHL, mixed cellularity CHL and lymphocyte-depleted CHL [76].

Following a series of therapeutic advances over the recent decades, up to 90% of patients with early-stage disease and 70% of those with late-stage disease can expect to be cured with first-line chemotherapy. Approximately 15– 20% of patients will relapse or have primary refractory disease and for these patients, high-dose chemotherapy with autologous stem cell transplantation (ASCT) is considered to be the treatment of choice.

The disease exhibits many features of potential immunoresponsiveness. Epstein-Barr Virus (EBV) is present in up to 40%– 60% of cases of HL, where it is thought likely to play a role in its pathogenesis. Immunotherapy consisting of an infusion of EBV-specific T cells has been shown to induce responses in post-transplantation lymphoproliferative disease (PTLD), which is known to be EBV driven, [105] and the recent studies exploring the use of autologous EBV-latent membrane protein (LMP)-specific T-cells in the treatment of patients with lymphoma (including HL) have shown their ability to induce durable remissions [106]. Furthermore, HL has a distinctive tumour microenvironment as the tumour mass is only comprised of 1% of malignant cells, while the remaining population consists of an infiltration of reactive cells. The observation that these malignant cells are able to survive in an environment populated with an array of immune cells demonstrates the ability of the Reed-Sternberg cell to effectively evade or subjugate the host's immune defences. A significant population of this reactive infiltrate consists of the immunosuppressive CD4+ T regulatory (Tregs) lymphocytes and the Reed-Sternberg cell protects itself by releasing cytokines, promoting the differentiation of naïve T-cells into Tregs and also by the up-regulation of surface molecules, including Fas-ligand, which stimulates apoptosis of cytotoxic T-lymphocytes [107]. Moreover, the significance of the HL tumour microenvironment has been shown by the observation that an increased number of CD68-positive tumour-associated macrophages has been correlated with both a reduced PFS and also an increased relapse risk post-autograft [108]. Furthermore, the PD-1 ligand genes are situated on chromosome 9p24.1, and copy number gains in this location are seen commonly in the nodular sclerosing subtype of HL [109]. The therapeutic efficacy of monoclonal anti-PD-1 antibodies has been demonstrated in relapsed or refractory Hodgkin Lymphoma [56].

5.2.2 Diffuse Large B Cell Lymphoma

Diffuse Large B Cell Lymphoma (DLBCL) is B cell neoplasm of large B lymphoid cells [76]. It can present as either *de novo* disease or it can be secondary to transformation from a pre-existing

indolent lymphoma (eg Follicular Lymphoma). It is one of the most common forms of lymphoma, representing approximately 30% of all Non-Hodgkin lymphoma diagnoses. Typically affecting the elderly population, the median age of presentation is 64 years [110]. On immunophenotype analysis, DLBCL expresses CD19, CD20, CD22, CD79a and the majority of cases express BCL6. There may also be expression of CD10 and a small minority of cases may express CD5. Characteristically classified as a high-grade, aggressive lymphoma, the proliferation index on immunohistochemistry detection is usually high. The International Prognostic Index (IPI) score (comprising age, Ann Arbor stage, serum LDH level, performance status and number of extranodal sites of disease) is used as a predictor of clinical outcome [111, 112]. The majority of patients with DLBCL are cured with first-line chemotherapy including Rituximab although those with a high IPI at presentation have a worse overall survival [113].

The advances in gene expression profiling have shown that there are different subtypes of DLBCL depending on their cell of origin which are classified as either Germinal Centre (GC)-type DLBCL or Activated B-cell (ABC) DLBCL [114, 115]. The activated B-cell subtype has been associated with a worse prognosis [116, 117].

5.2.3 Follicular Lymphoma

Follicular Lymphoma (FL) is a neoplasm of germinal centre (follicle centre) mature B cells. It is the most common form of indolent NHL and constitutes approximately 20% of all lymphomas [76]. It typically presents with lymphadenopathy but splenomegaly and bone marrow involvement is also common. The median age of presentation is 59 [110] although there is a recognised variant which presents in childhood. It is characteristically considered to have an indolent clinical course, although it is incurable in the majority of cases and frequent relapses are common. FL may transform to a more aggressive subtype of lymphoma over time. The annual risk of high grade transformation is 3% [118, 119] and is associated with a worse clinical outcome [119].

On immunophenotype analysis, Follicular Lymphoma expresses surface immunoglobin (Sig+), BCL2, BCL6, CD10 and B-cell associated proteins CD19, CD20, CD22, CD79a. It does not express

CD5 or CD43. Follicular lymphoma is assigned a histological grade at diagnosis which is dependent upon the number of centroblasts visible per high powered field. Grades 1-2 are considered low grade whereas Grade 3 is further subdivided into A or B, depending on whether there are solid sheets of centroblasts present [76]. The histological classification is important as, typically, Grade 3b FL is clinically treated as an aggressive lymphoma.

In the majority of cases, FL is characterised by the t(14;18)(q32;q21) translocation which generates a BCL2-IGH fusion gene. This results in Bcl2 overexpression and resistance to apoptosis. This translocation is present in approximately 90% of all cases of grade 1-2 FL [120]. The FL International Prognostic Index (FLIPI) score is used as a risk stratification tool and consists of age, Ann Arbor stage, Haemoglobin level, number of nodal areas and serum lactate dehydrogenase level [121, 122].

The presence of T regulatory cells in the FL tumour microenvironment has been studied by numerous research groups but there is a discrepancy in the conclusions drawn, with high levels being associated with improved survival [123] but conversely, in other studies high levels are associated with the absence of B symptoms and low risk FLIPI scores [124]. Interestingly, the presence of CD57+ T cells has been associated with a significantly higher frequency of adverse clinical features [124]. The pattern of distribution of Tregs cells has also been shown to be important with a follicular pattern of Tregs associated with inferior survival and with risk of transformation [125].

5.2.4 Mantle Cell Lymphoma

Mantle Cell Lymphoma (MCL) is a mature B cell neoplasm and an uncommon subtype of Non-Hodgkin's Lymphoma, representing between 3-10% of NHL diagnoses [76, 126, 127]. Although it often presents clinically with widespread lymphadenopathy, extranodal disease is frequently present and may affect sites including the gastrointestinal tract. Commonly, the peripheral blood is involved and may be detected by flow cytometry [76]. The median age of presentation is 68 years of age and the disease has a male predominance [126]. The Mantle Cell International Prognostic Index (MIPI) is used as a risk stratification score consisting of age,

performance status, lactate dehydrogenase (LDH) and leukocyte count with high-risk groups having a median survival of only 29 months [128].

MCL is characterised by the presence of the t(11;14)(q13;q32) translocation between IGH@ and cyclin D1 (*CCND1*) genes. This leads to the overexpression of Cyclin D1, a protein which is not normally expressed in B lymphocytes. Cyclin D1 acts to regulate cyclin-dependent kinases (namely CDK4 and CDK6) by binding to them and causing cell cycle dysfunction and also acts to regulate cell proliferation [127].

On immunophenotype analysis, Mantle Cell Lymphoma is positive for CD20, CD5, FMC-7, Bcl-2 and CD43, whilst it is negative for CD10 and BCL-6. Almost all cases express Cyclin D1 by immunohistochemistry although there are recognised cases of Cyclin D1 negative MCL which may express Cyclin D2 or D3 [76, 129]. The overexpression of the transcription factor SOX11 (which is normally absent in B lymphocytes) in the majority of conventional Mantle Cell Lymphomas has led to the postulation that it has a role in the pathogenesis of the disease by promoting tumour angiogenesis [130]. Conversely, negative or low expression of SOX11 is seen in indolent forms of the disease [131].

In the past, the median overall survival of MCL was reported as 30 – 43 months [128, 132, 133] but with the advent of new therapeutic strategies focussing on delivering intensive frontline chemotherapy, followed by consolidation with high dose therapy and autologous haematopoietic stem cell transplantation, the median overall survival has improved. The NORDIC lymphoma group has recently reported their 15-year follow-up data using this strategy which has resulted in a median survival of 12.7 years with median progression free survival of 8.5 years [134]. Similarly to CLL, Ibrutinib (a Bruton's Tyrosine Kinase [BTK] inhibitor which causes the dysregulation of the B-cell receptor signaling pathways) has shown efficacy in the treatment of relapsed or refractory MCL [135].

5.2.5 Anaplastic Large Cell Lymphoma – ALK+ and ALK-

Anaplastic large cell lymphoma (ALCL) is a T cell neoplasm of large lymphoid cells. In adults, it is an uncommon malignancy, constituting approximately 3% of non-Hodgkin lymphomas [136].

It is more common in younger patients where it represents up to 10-20% of childhood lymphomas [137]. The majority of patients with ALCL present with advanced stage disease and extranodal sites of disease are common.

The diagnosis is further subdivided into those patients who have the presence of a chromosomal translocation involving the ALK (anaplastic lymphoma kinase) gene and different fusion partners. This disease entity is referred to as ALCL ALK positive (+). The most common translocation is between the ALK gene and the nucleophosmin (NPM) gene: t(2;5)(p23;q35) which generates a NPM-ALK chimeric fusion protein. The majority of ALK+ALCL (75-85%) have the t(2;5)/*NPM-ALK* translocation present [76].

ALK negative (ALK-) ALCL, characterised by the absence of an ALK chromosomal translocation, is considered to be a separate clinico-pathological entity from ALK+ ALCL. Typically, it has an older median age of presentation, a more aggressive disease course and a worse prognosis than ALK+ ALCL [138]. Whereas childhood ALCL is more commonly ALK positive, adult ALCL is frequently ALK negative [139]. The median age of presentation of ALK+ ALCL is 30 years, whereas it is 55 years for ALK- ALCL [140].

On analysis of immunophenotype, Anaplastic Large Cell Lymphoma is positive for CD30 and the ALCL ALK+ subtype is positive for ALK immunohistochemical staining. The tumour typically expresses T cell antigens, eg CD2, CD5 and CD4 but may be negative for CD3 and Bcl2. There are reported cases which may not express any T cell antigens and this is termed a “null phenotype” [76, 141].

5.3 Aims

The aims of the immunohistochemistry staining of the human lymphoma-infiltrated lymph node biopsies were as follows:

1. To detect whether CD4+ CTLs were present in human lymphomas (as they have not been previously described in these malignancies).

2. To characterise their prevalence with respect to other components of the CD4+ compartment.

3. To establish whether they are more prevalent in specific subtypes of lymphoma compared with the reactive LN subgroup.

5.4 Triple-Colour Immunohistochemistry (IHC) staining of human lymph node biopsies infiltrated with lymphoma for CD4, Granzyme B and FoxP3 to detect the presence of cytotoxic CD4+ T lymphocytes

5.4.1 Comparison with reactive lymph nodes

In collaboration with Prof. Teresa Marafioti's laboratory, triple immunohistochemical staining was performed on the cut slides from formalin-fixed paraffin-embedded (FFPE) biopsies for CD4, FoxP3 and Granzyme B**.** In the majority of cases, the chromogen-antibody combination was CD4 (brown), FoxP3 (red), Granzyme B (blue). In a minority of cases, a green chromogen was used to identify FoxP3, with CD4 (brown) and Granzyme B (red). Human tonsillar biopsies, previously stored as FFPE blocks, were obtained from the Department of Histopathology's archive and used as positive controls. The initial optimisation of chromogens and antibody dilutions were performed on human tonsils. During the staining process, it was determined that 1 biopsy from the MCL group and 1 biopsy from the CHL group had insufficient high quality tissue present and so these groups had only 5 biopsies included in the final data analysis.

As a control group, six lymph node biopsies with the diagnosis of "reactive lymph node" were also obtained from the Department of Histopathology archive by the same method. These biopsies were not infiltrated by a malignancy and were used as a normal control to compare with the lymphoma biopsies.

5.4.2 Counting and Analysis Technique

Each of the triple stained biopsy slides were image-scanned using a Hamamatsu NanoZoomer digital slide scanner. Five layers, each of 300nm depth, were scanned at x40 resolution and

saved as NanoZoomer Digital Pathology Image files for later analysis. Scanning was performed as soon as possible after triple-staining was performed to minimise the time for any chromogen degradation. The slide images were visualized using NDP.view2 (NanoZoomer Digital Pathology) software.

Five areas at x40 magnification were identified from the tumour area of each biopsy diagnostic of disease (Figure 5-1). For the control "reactive" lymph node biopsies, five areas at x40 magnification were chosen at random. Using Image J software, where a grid was superimposed on each area, all of the stained cells in these five areas were manually counted and allocated to one of 7 different combination groups (Table 15):

Cell Type	IHC Staining Positive For:	IHC Staining Negative For:
1	CD4	FoxP3, Granzyme B
2	FoxP3	CD4, Granzyme B
3	Granzyme B	CD4, FoxP3
4	CD4, FoxP3	Granzyme B
5	CD4, Granzyme B	FoxP3
6	FoxP3, Granzyme B	CD4
7	CD4, FoxP3, Granzyme B	Nil

Table 15: The different cell type combinations identifiable by triple immunohistochemical staining for CD4, Granzyme B and FoxP3.

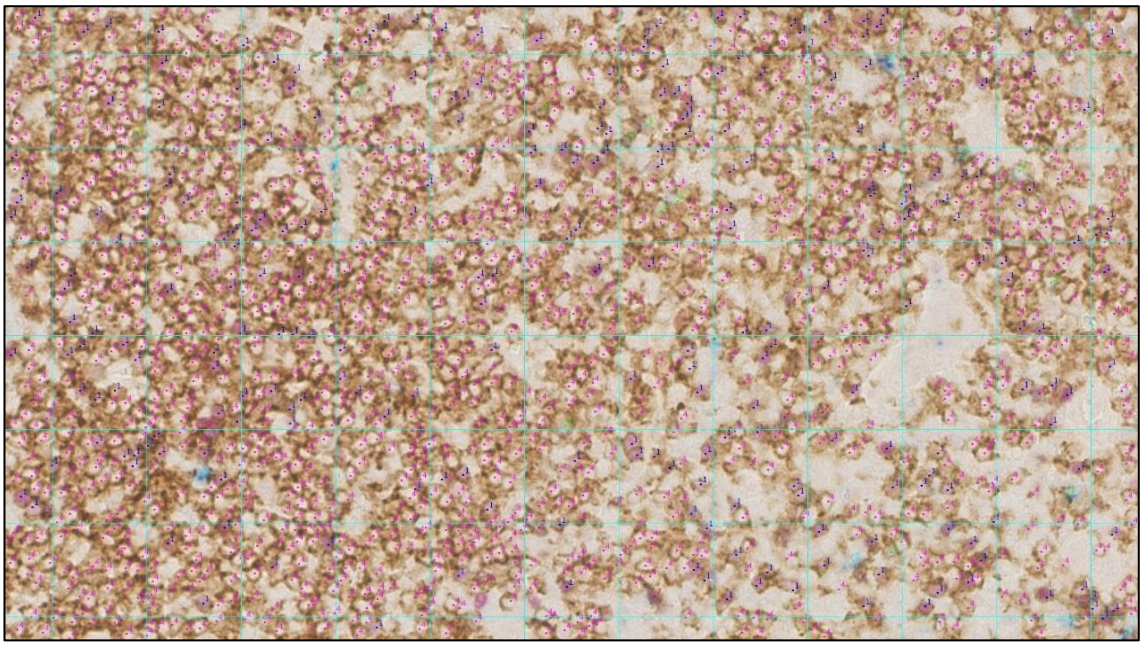

Figure 5-1: A lymph node biopsy infiltrated with Mantle Cell Lymphoma (x40 magnification). The biopsy has been triple IHC stained for CD4 (brown), FoxP3 (red) and Granzyme B (blue). Using ImageJ software, a grid has been superimposed upon the image and each cell has been counted and marked with a corresponding number depending upon the cell type that it represents. The number of each cell counted is recorded in the ImageJ programme and collated for data analysis.

5.4.3 Identification of Tumour Regions

The triple-stained biopsy slides were reviewed with Prof Teresa Marafioti, Consultant Histopathologist, to determine the area of tumour infiltration on each biopsy. The tumour area was identified by comparing the triple-stained biopsy slide with both the original diagnostic Haematoxylin and Eosin (H+E) slide and the original diagnostic single-stained IHC slides obtained from the same biopsy block which were positive for tumour-specific markers (eg Cyclin D1 for MCL; CD30 for CHL)**.** The area, once marked upon an image of the single-tumour marker stained slide, was superimposed upon the triple-stained biopsy slide (Figure 5-1; Figure 5-2)**.**

A.

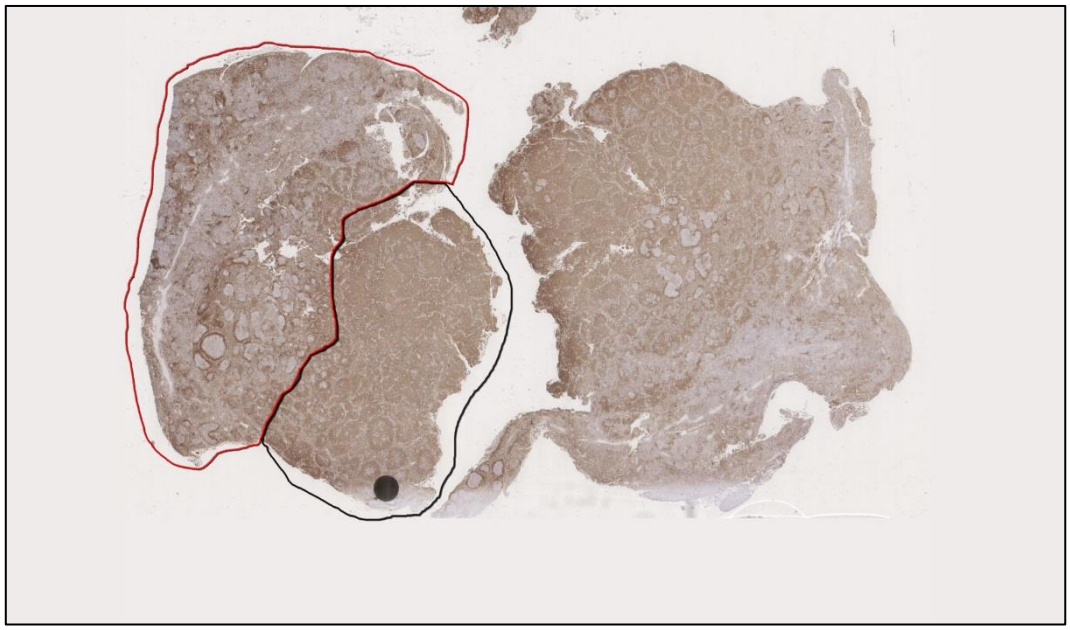

B.

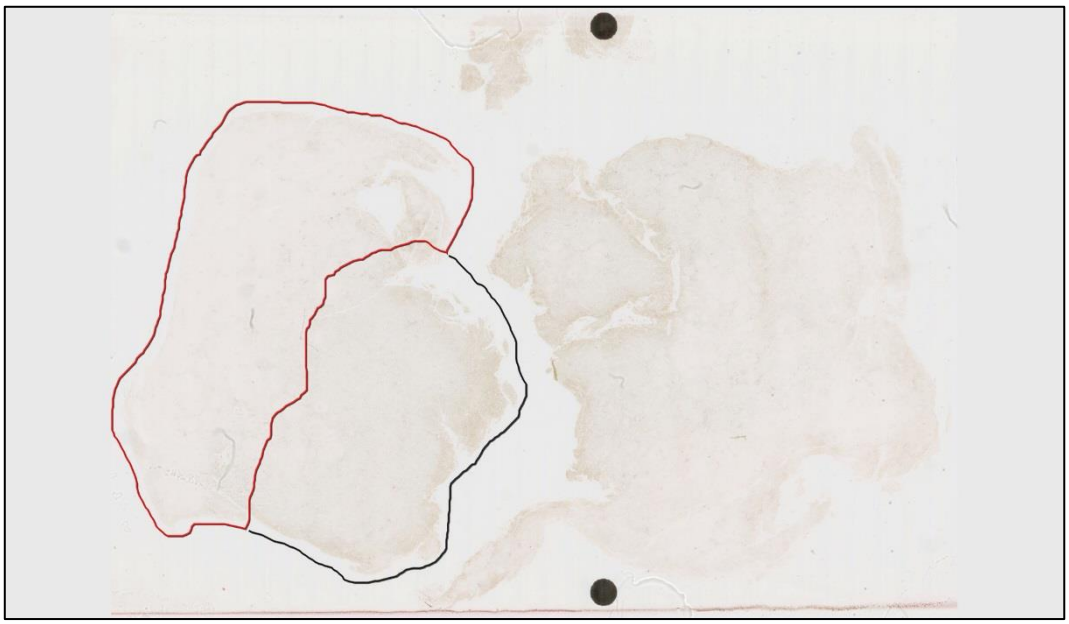

Figure 5-2: (A + B) Two tissue sections from the same lymph node biopsy infiltrated with Follicular Lymphoma showing the demarcation of tumour and normal lymph node areas. Figure 4.2a shows an immunohistochemistry staining for BCL-2 (brown), a tumour marker for Follicular Lymphoma. The area marked with a red line indicates the area of the lymph node which has not been infiltrated by lymphoma ('normal' tissue) and the area marked in black represents the area infiltrated with lymphoma and showing a positive stain for BCL-2. Figure 4.2b shows a tissue section from the same biopsy with the red and black areas transposed onto the section. This section has been stained by triple immunohistochemistry for CD4 (brown), FoxP3 (green) and Granzyme B (red). The transposed red and black areas allow for the tumour area to be identified on the triple-stained slide.

Case	Histological Diagnosis	Age at time of biopsy (Years)	Sex	Immunophenotype	Proliferative index (Ki67)	CMV serological status (IgG)
1	Mantle Cell Lymphoma	57	M	CD20, CD79a, CD5, Cyclin D1.	50%	Unknown
2	Mantle Cell Lymphoma	66	M	CD19, CD20, CD5, Cyclin D1.	Not specified	Positive
3	Mantle Cell Lymphoma	64	M	CD19, CD20, CD5, Cyclin D1.	5-10%	Positive
4	Mantle Cell Lymphoma	60	M	CD20, CD5, CD79a, Cyclin D1.	30%	Negative
5	Mantle Cell Lymphoma	57	M	CD20, CD5, CD79a, Cyclin D1.	20%	Positive
6	Diffuse Large B Cell Lymphoma (Non-GC)	75	F	CD20, BCL-6, MUM1 weak positive.	40-50%	Positive
7	Diffuse Large B Cell Lymphoma (Non-GC)	56	M	CD20, BCL-6, MUM1,	70%	Negative
8	Diffuse Large B Cell Lymphoma (Non-GC)	63	M	CD20, BCL-6, MUM1.	60%	Unknown
9	Diffuse Large B Cell Lymphoma (GC)	45	M	CD20, BCL-6 patchy	60%	Positive
10	Diffuse Large B Cell Lymphoma (GC)	35	F	CD20, BCL-6, MUM1.	80-90%	Positive
11	Diffuse Large B Cell Lymphoma (GC)	86	F	CD20, BCL-6, MUM1.	50-60%	Positive

12	Follicular Lymphoma (Grade 3a)	39	M	CD20, BCL2, BCL6.	Not specified	Positive
13	Follicular Lymphoma (Grade 1-2)	71	F	CD20, CD10, BCL-6.	Not specified	Positive
14	Follicular Lymphoma (Grade 1)	79	M	CD20, BCL-2, BCL-6, CD10.	5-10%	Unknown
15	Follicular Lymphoma (Grade 3a)	66	F	CD20, CD10, BCL-6, BCL-2.	Not specified	Positive
16	Follicular Lymphoma (Grade 1-2)	57	F	CD20, CD10, BCL-6, BCL-2.	10%	Unknown
17	Follicular Lymphoma (Grade 1-2/3a)	56	M	CD20, BCL-2, CD10, BCL-6.	>50%	Positive
18	Classical Hodgkin Lymphoma	45	F	CD30, PAX5 weakly positive.	Not specified	Unknown
19	Classical Hodgkin Lymphoma	52	F	CD30, BCL-6, BCL-2, MUM1, weak CD15.	Not specified	Unknown
20	Classical Hodgkin Lymphoma	57	F	CD30, CD15, PAX5 weak positive.	Not specified	Unknown
21	Classical Hodgkin Lymphoma	13	M	CD30, PAX5 weak positive, MUM1.	Not specified	Negative
22	Classical Hodgkin Lymphoma	10	M	CD30, CD15, PAX5,	Not specified	Negative
23	ALK+ Anaplastic Large Cell Lymphoma	33	F	CD7, CD30, ALK.	Not specified	Positive
24	ALK+ Large B Cell Lymphoma	37	M	Not specified.	Not specified	Unknown

25	ALK- Anaplastic Large Cell Lymphoma	31	F	CD30, Perforin, CD4.	Not specified	Positive
26	ALK- Peripheral T Cell Lymphoma	54	M	CD3, CD5, CD2, CD4, CD7 patchy, ICOS, PD-1, perforin and GZB.	80%	Negative

Table 16: Lymphoma: Patient Characteristics. The patient characteristics of the human lymph node biopsies infiltrated with lymphoma. F = Female, M = Male, GC = Germinal Centre, ALK = anaplastic lymphoma kinase, CMV = Cytomegalovirus.

Case	Histological Diagnosis	Age at time of biopsy (Years)	Sex	Clinical indication for biopsy	CMV serological status (IgG)
1	Reactive lymphadenopathy	65	F	Cervical Lymphadenopathy	Unknown
2	Reactive lymphadenopathy	11	M	Cervical Lymphadenopathy	Unknown
3	Reactive lymphadenopathy	45	F	Inguinal lymphadenopathy	Unknown
4	Reactive lymphadenopathy	69	F	Weight loss and Lymphadenopathy	Unknown
5	Reactive lymphadenopathy	35	M	Lymphadenopathy	Negative
6	Reactive lymphadenopathy	32	M	Cervical Lymphadenopathy	Positive

Table 17: Reactive Lymph Node Patient Characteristics. The patient characteristics of lymph node biopsies with the histological diagnosis of reactive lymphadenopathy. F = Female, M = Male, CMV = Cytomegalovirus.

5.4.4 Patient Characteristics

The characteristics of the patients whose lymph node biopsies were examined are shown in Table 16. The median age of the patients was 56.5 years (range 10 – 86 years). There were 11 females and 15 males. The cytomegalovirus serological status was unknown in 8 cases, CMV IgG positive in 13 patients and CMV IgG negative in 5 patients. The formal histological diagnostic reports were reviewed to obtain the immunophenotype of each tumour biopsy. The proliferation index was low in those patients with Mantle Cell Lymphoma and high in those patients with DLBCL, as expected. Both Germinal-centre and non-germinal centre subtypes of DLBCL were included in the study.

The patient characteristics of the reactive lymph node biopsies are shown in Table 17. The cytomegalovirus serological status was unknown in 4 cases, CMV IgG negative in 1 case and CMV IgG positive in 1 case. The median age was 40 years (range: 11-69 years). There were 3 females and 3 males. None of the patients were infiltrated with a malignancy and none had a known active systemic

viral infection. A selection of images of the triple-stained reactive lymph node biopsies are shown in Figure 5-9, Mantle Cell Lymphoma biopsies are shown in Figure 5-10 andFigure 5-11, Diffuse Large B Cell Lymphoma biopsies are shown in Figure 5-12Figure 5-13Figure 5-14Figure 5-15, Follicular lymphoma biopsies are shown in Figure 5-16,Figure 5-17Figure 5-19, Classical Hodgkin Lymphoma biopsies are shown in Figures Figure 5-18Figure 5-20Figure 5-21, an ALK negative PTCL biopsy is shown in Figure 5-23, an ALK+ ALCL in shown in Figure 5-22 and an ALK – ALCL biopsy is shown in Figure 5-24.

5.4.5 Results: CD4+ populations

(1) CD4+Granzyme B+ (FoxP3 negative) population

The CD4+GZB+ population reflects the typical phenotype of cytotoxic CD4+ cells. The cells are present in all of the human lymphoma subtypes (Figure 5-3d) albeit at low levels. There is no significant increase in the absolute number of CD4+GZB+ cells between the different lymphoma subtypes and the reactive LNs. There is a trend towards an increase in absolute number of CD4+GZB+ cells in MCL and CHL, compared with the reactive LNs, although this does not reach statistical significance.

When considering the composition of the CD4+ compartment, there is a significant increase in the percentage of CD4+GZB+ cells, out of the total CD4+ population, in MCL ($P = 0.0259$) and DLBCL ($P = 0.0300$) when compared with the reactive LNs (Figure 5-5b), although this percentage is not more than 10% of the total CD4+ population. When considering all stained cells on the biopsy slides, the CD4+GZB+ population is relatively low at <8% with no significance difference between the different disease subgroups (Figure 5-4d).

The percentage of CD4+GZB+ cells of the total CD4+ population was not significantly different between those patients who were CMV seropositive or CMV seronegative (Figure 5-7A) although it should be noted that the CMV serostatus was unknown in 12 biopsies. There was also no correlation between the percentage of CD4+GZB+ cells of the total CD4+ population and the age of the patients [Figure 5-8B; R=0.1275 (95% CI: -0.2 – 0.43)].

(2) CD4+FOXP3+ (Granzyme B negative) population

The CD4+FOXP3+ population reflects the T regulatory (Tregs) cells present in the lymph node biopsies. There is no statistically significant difference in the absolute number of Tregs in the different lymphoma subgroups compared with the reactive LNs (Figure 4.3e). There was a trend for a decrease in Tregs in DLBCL but this was not significant**.** There was also no statistically significant difference in the percentage of Tregs in any of the lymphoma subgroups compared with the reactive LNs as a percentage of either the total stained cells (Figure 5-4e) or the CD4+ population (Figure 5-5c).

(3) CD4+ (Granzyme B negative, FOXP3 negative) population

The CD4+ population (single stain positive) reflects those CD4+ cells that are negative for FOXP3 (therefore not Tregs) and those that are negative for GZB (therefore not known as cytotoxic). There is a significant decrease in the absolute number of CD4+ cells in the DLBCL group compared with the reactive LNs (P = 0.0128)(Figure 5-3a). The majority of the total CD4+ population are single positive stained for CD4+ (approx. 80%) (Figure 5-4Figure 5-5a). There is no significant difference between the disease subgroups in the percentage of the total CD4+ population comprised of CD4+ (FOXP3-GZB-) cells (Figure 5-5a).

(4) CD4+Granzyme B+ FOXP3+ population

Tregs have occasionally been described as expressing Granzyme B [72]**.** The absolute number of triple positive cells was low in all subgroups with no statistically significant difference between the disease groups (Figure 5-3g). The percentage of triple stained cells was low both as a percentage of all stained cells (Figure 5-4g) and as a percentage of the total CD4+ population (approx. <1%) (Figure 5-5d). Therefore, the majority of Tregs in these lymph node biopsies were Granzyme B negative.

5.4.6 Results: Granzyme B+ populations

Granzyme B is expressed by cytotoxic CD4 cells (as described above) but also by other cytotoxic lymphocytes, namely NK, NKT cells and CD8+ cells. Therefore, the Granzyme B positive cells (which are CD4 negative) in this investigation could represent these cells and, with only a triple stain, we are unable to distinguish between NK, NKT and CD8 lymphocytes.

(1) Granzyme B+ (CD4 negative FOXP3 negative) population

There is no significant difference in the absolute number of GZB+ cells between the different disease subtypes (Figure 5-3c). As a percentage of total stained cells (including those that will be CD4+) there was a trend towards an increase in GZB+ cells in DLBCL and ALK+ tumours although this was not statistically significant.

(2) Granzyme B+ FOXP3+ (CD4 negative) population

The overall absolute numbers of these cells was low (<30) with no significant difference between the subgroups and the reactive LNs (Figure 5-3f). This was also shown in the percentage of all total stained cells, where they comprised a very small percentage of all stained cells (approx. <1%) (Figure 5-4f). This population is likely to be an artefact of staining as FOXP3 expression is closely associated with CD4 expression**.**

5.4.7 Results: FOXP3+ (CD4- Granzyme B-) population

This population was low in both absolute numbers (Figure 5-3b) and percentage of all stained cells (Figure 5-4b). Its significance in the cell populations are unknown as, mentioned above, FoxP3 is usually associated with CD4 expressing cells. Damage caused to the cells by the storing and sectioning process may have led to these cells lacking expression of CD4. Their low

absolute numbers suggest that they do not play a predominant role in the composition of the tumour microenvironment.

5.4.8 Ratios of CD4+ Effectors to Treg cells

The ratio of absolute numbers of CD4+ effector cells to T regulatory cells in the lymphoma and reactive lymph node biopsies is shown in Figure 5-6a. There is no significant difference in the CD4+effector to T reg ratio between the lymphoma subtypes and the reactive lymph node biopsies. The ratio is approximately below 10:1 across the different lymph node biopsies examined.

5.4.9 Ratio of Tregs to CD4+GZB+ cells

The ratio of absolute numbers of T regulatory cells to CD4+ CTLs in the lymphoma and reactive lymph node biopsies is shown in Figure 5-6b. There was a statistically significant decrease in the Treg: CD4+GZB+ ratio in the DLBCL biopsies when compared with the reactive lymph node biopsies ($P = 0.0321$).

5.4.10 Summary of lymphoma immunohistochemistry results

In summary, the IHC staining confirmed that CD4+ CTLs are present in all studied human lymphoma subtypes, although at a low percentage, comprising of <10% of the total CD4 population. This percentage is lower in the reactive LNs where they comprise <2% of the CD4+ population. However, the percentage of CD4+CTLs are significantly increased in both MCL and DLBCL lymphoma subtypes as a percentage of the CD4+ population. There is a significant decrease in the absolute number of single-positive CD4+ cells in DLBCL when compared to reactive LNs. This significant difference does not remain, however, when examining the CD4+ cells as a percentage of all stained cells, or as a percentage of the CD4+ population. This perhaps signifies the amount of tumour infiltrate in the DLBCL biopsies which results in a lower absolute number of stained cells and which is reflective of a low number of CD4+ cells present in the biopsies.

A.

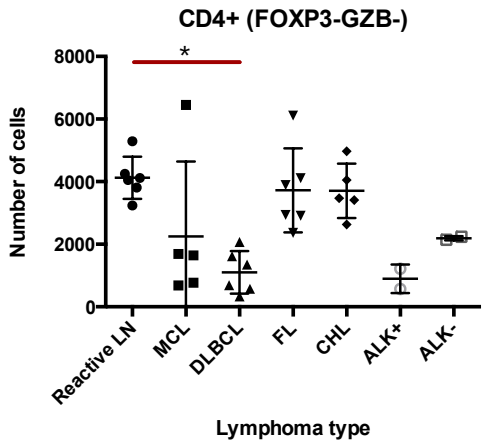
CD4+ (FOXP3-GZB-)
*
8000
6000
4000
2000
0
Number of cells
Reactive LN
MCL
DLBCL
FL
CHL
ALK+
ALK-
Lymphoma type

B.

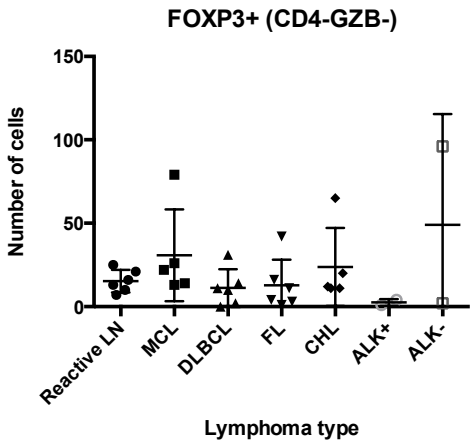
FOXP3+ (CD4-GZB-)
150
100
50
0
Number of cells
Reactive LN
MCL
DLBCL
FL
CHL
ALK+
ALK-
Lymphoma type

C.

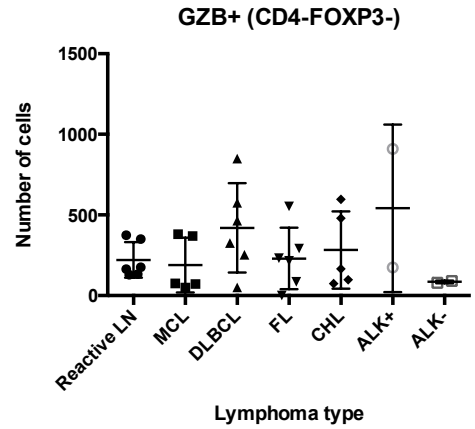
GZB+ (CD4-FOXP3-)
1500
1000
500
0
Number of cells
Reactive LN
MCL
DLBCL
FL
CHL
ALK+
ALK-
Lymphoma type

D.

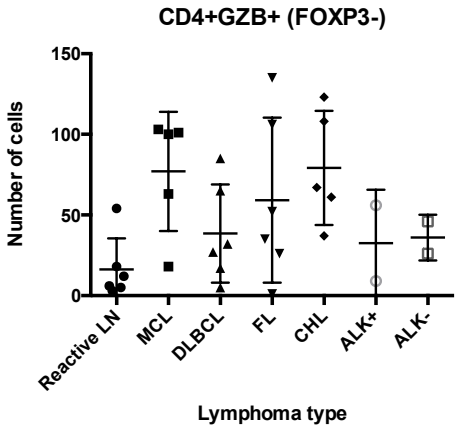
CD4+GZB+ (FOXP3-)
150
100
50
0
Number of cells
Reactive LN
MCL
DLBCL
FL
CHL
ALK+
ALK-
Lymphoma type

E.

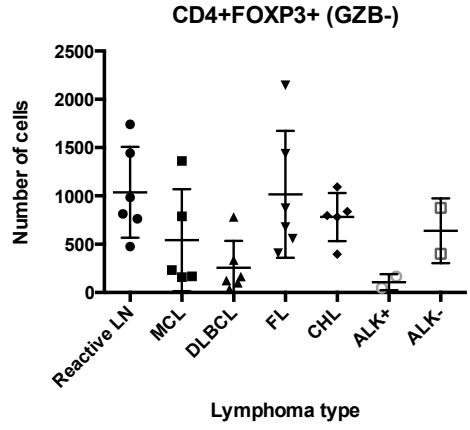
CD4+FOXP3+ (GZB-)
2500
2000
1500
1000
500
0
Number of cells
Reactive LN
MCL
DLBCL
FL
CHL
ALK+
ALK-
Lymphoma type

F.

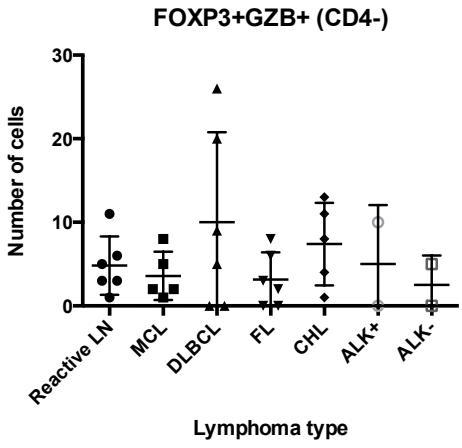
FOXP3+GZB+ (CD4-)
30
20
10
0
Number of cells
Reactive LN
MCL
DLBCL
FL
CHL
ALK+
ALK-
Lymphoma type

G.

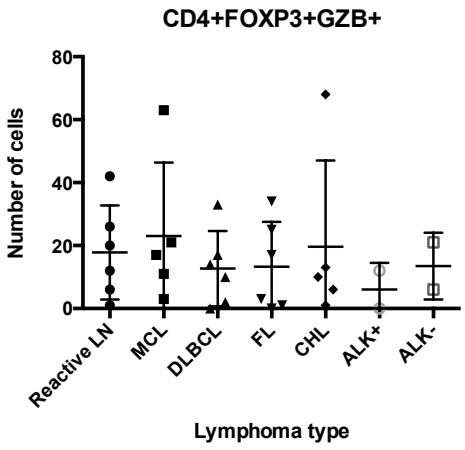

Key: LN = Lymph node, MCL = Mantle cell lymphoma, DLBCL = Diffuse large B cell lymphoma, FL = Follicular lymphoma, CHL = Classical Hodgkin Lymphoma, ALK = Anaplastic Lymphoma Kinase, GZB = Granzyme B.

Figure 5-3: (A-G) The absolute numbers of stained cells in the human lymph node biopsies which have been triple IHC stained for Granzyme B, CD4 and FOXP3. Figures 5.3a-g show the results for each positive staining outcome: Figures 5.3a-c show those cells that are positive for single markers (CD4+, FOXP3+, GZB+). Figure 5.3d-f show those cells that are positive for double markers (CD4+GZB+, CD4+FOXP3+, FOXP3+GZB+) and Figure 5.3g shows the triple positive cells (CD4+GZB+FOXP3+). Figure 5.3a shows that there is a significant decrease in the number of CD4+ (FOXP3-GZB-) cells in the DLBCL lymph nodes when compared to the reactive LNs. Figures 5.3b and 5.3c show that there is no significant difference in the absolute number of cells positive for GZB or FOXP3 only. Figure 5.3d confirms the presence of CD4+GZB+ cells in both reactive LNs and lymphoma infiltrated lymph nodes which has not previously been described. There is a trend towards an increase in the absolute number of CD4+GZB+ cells in MCL and CHL when compared to the reactive LNs but this does not reach statistical significance. Figure 5.3e shows a decrease in the absolute number of CD4+FOXP3+ cells in DLBCL and ALK+ biopsies when compared with the reactive LNs but this does not reach statistical significance. There are low absolute numbers of FOXP3+GZB+ cells (Figure 5.3f) and of triple-positive cells (Figure 5.3g) with no significant difference between the different lymph node groups.

A.

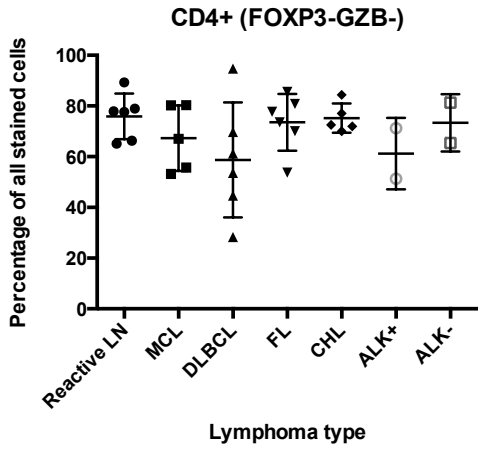
CD4+ (FOXP3-GZB-)
Percentage of all stained cells
100
80
60
40
20
0
Reactive LN
MCL
DLBCL
FL
CHL
ALK+
ALK-
Lymphoma type

B.

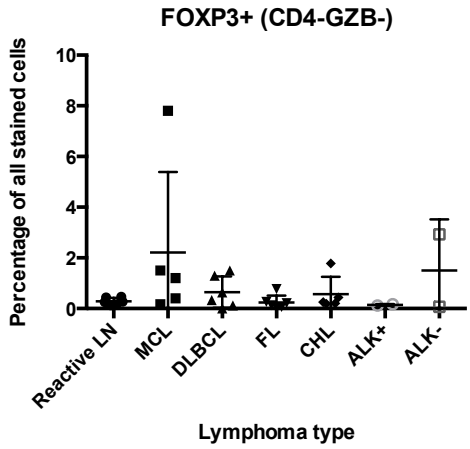
FOXP3+ (CD4-GZB-)
Percentage of all stained cells
10
8
6
4
2
0
Reactive LN
MCL
DLBCL
FL
CHL
ALK+
ALK-
Lymphoma type

C.

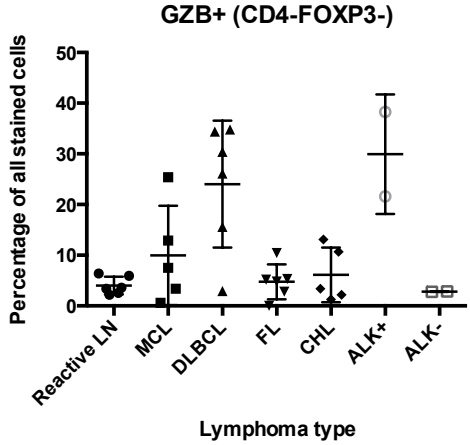
GZB+ (CD4-FOXP3-)
Percentage of all stained cells
50
40
30
20
10
0
Reactive LN
MCL
DLBCL
FL
CHL
ALK+
ALK-
Lymphoma type

D.

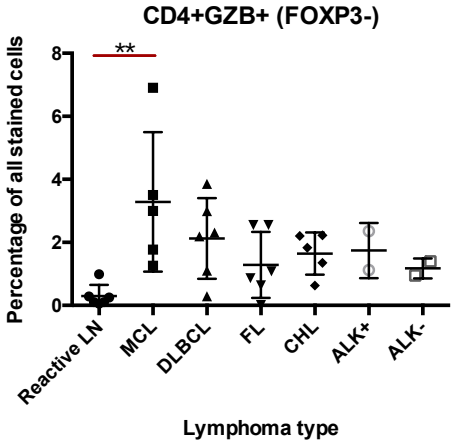
CD4+GZB+ (FOXP3-)
**
Percentage of all stained cells
8
6
4
2
0
Reactive LN
MCL
DLBCL
FL
CHL
ALK+
ALK-
Lymphoma type

E.

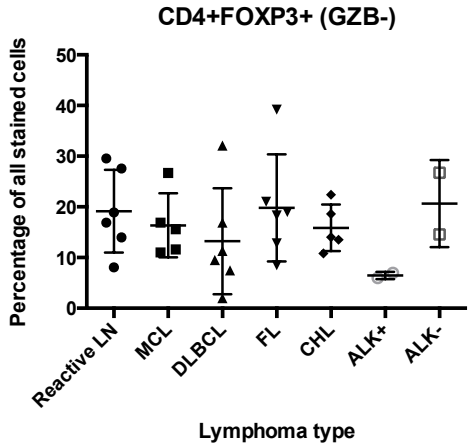
CD4+FOXP3+ (GZB-)
Percentage of all stained cells
50
40
30
20
10
0
Reactive LN
MCL
DLBCL
FL
CHL
ALK+
ALK-
Lymphoma type

F.

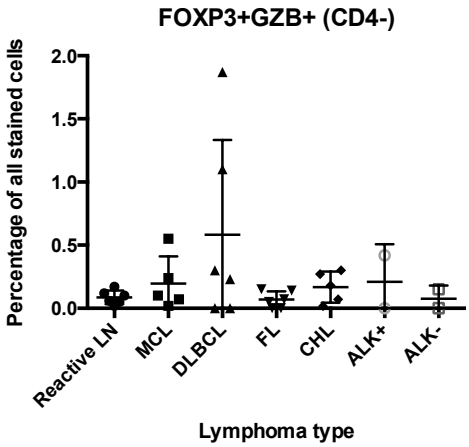
FOXP3+GZB+ (CD4-)
Percentage of all stained cells
2.0
1.5
1.0
0.5
0.0
Reactive LN
MCL
DLBCL
FL
CHL
ALK+
ALK-
Lymphoma type

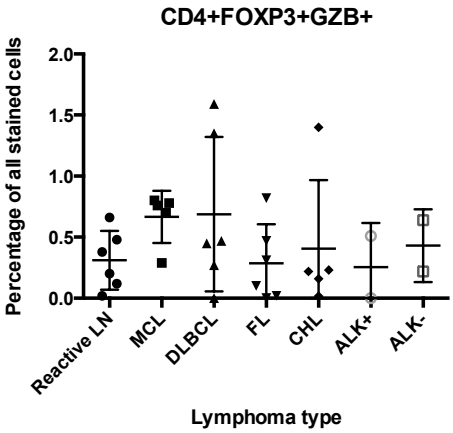

Key: LN = Lymph node, MCL = Mantle cell lymphoma, DLBCL = Diffuse large B cell lymphoma, FL = Follicular lymphoma, CHL = Classical Hodgkin Lymphoma, ALK = Anaplastic Lymphoma Kinase, GZB = Granzyme B.

Figure 5-4: (A-G) The percentage numbers of each cell type out of the total stained cells in the human lymph node biopsies following triple IHC staining for Granzyme B, CD4 and FOXP3. Figures 5.4a-g show the results for each positive staining outcome: Figures 5.4a-c show those cells that are positive for single markers (CD4+, FOXP3+, GZB+). Figure 5.4d-f show those cells that are positive for double markers (CD4+GZB+, CD4+FOXP3+, FOXP3+GZB+) and Figure 5.4g shows the triple positive cells (CD4+FOXP3+GZB+). Figure 5.4a demonstrates that the percentage of single stained CD4+ cells out of the total stained cells was consistently high (approx. 60-80%) but no significant difference in the percentage of CD4 single positive cells was seen between the different disease subtypes. Figure 5.4c shows a trend of increased percentage of single positive GZB+ cells in DLBCL and ALK+ lymphomas but this did not reach statistical significance. There was a significantly higher percentage of CD4+GZB+ cells in MCL when compared with reactive LNs (P=0.0099)(Figure 5.4d). The percentage of FOXP3+ (Figure 5.4b), FOXP3+GZB+ (Figure 5.4f) and CD4+FOXP3+GZB+ cells (Figure 5.4g) was consistently low with no statistical significant difference between the disease groups. There was no statistically significant difference in the percentage of CD4+FOXP3+ cells between the groups (Figure 5.4e).

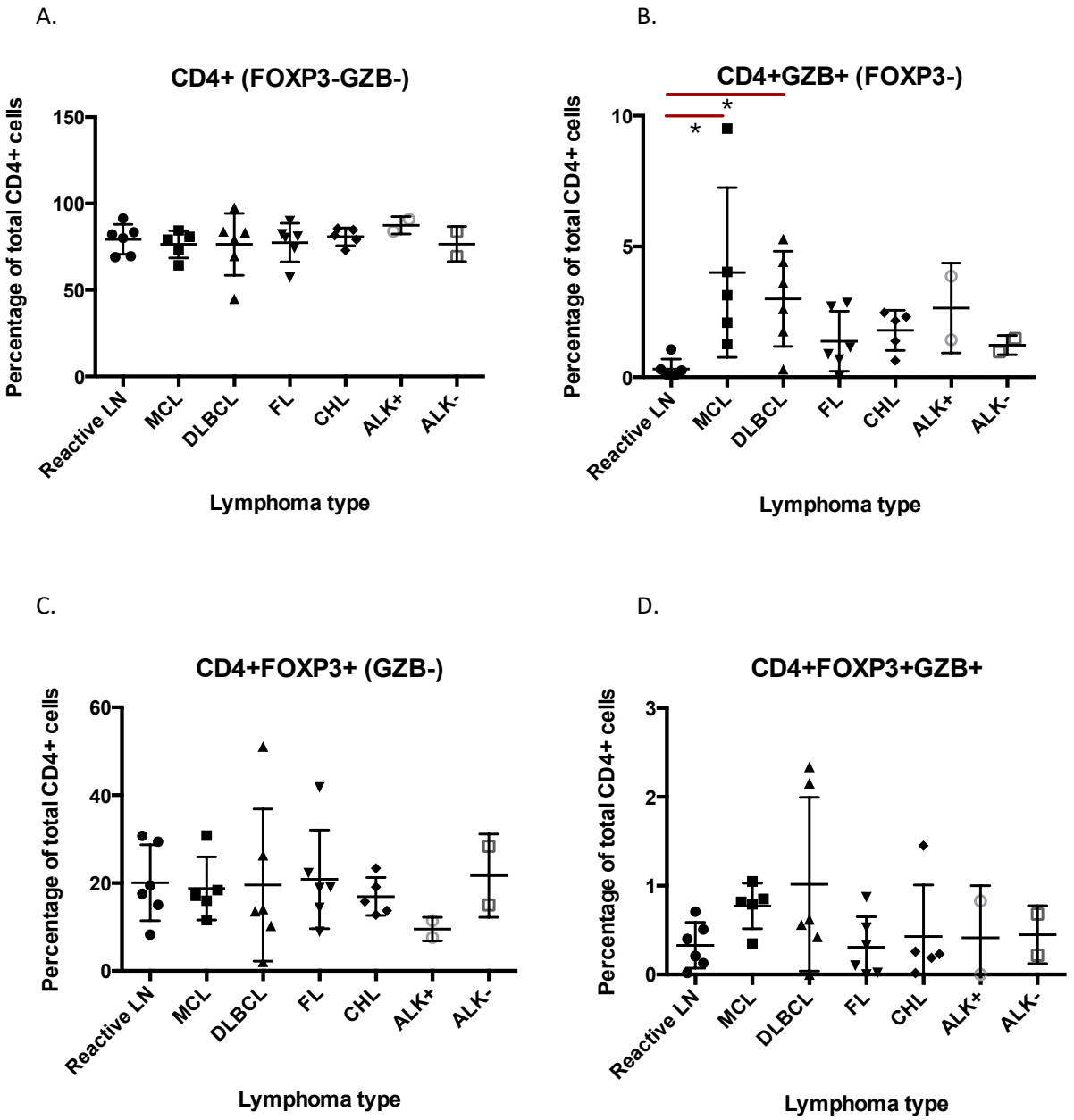

Figure 5-5: (A-D) The percentage of stained cells out of the total CD4+ cells in the human lymph node biopsies following triple IHC staining for Granzyme B, CD4 and FoxP3. Figures 5.5a-d show the results for each positive staining outcome: Figures 5.5a shows the percentage of cells that are positive for CD4+ only (GZB- FOXP3-). Figures 5.5b-c show the percentage of cells that are positive for double markers (CD4+GZB+ or CD4+FOXP3+) and Figure 5.5d shows the percentage of triple positive cells (CD4+FOXP3+GZB+). The majority of the cells in the CD4+ T cell compartments are single stained CD4+ cells (GZB-FOXP3-) (Figure 5.5a). There is no significant difference between different lymphoma subtypes. There is a statistically significant increase in the percentage of CD4+GZB+ cells in MCL and DLBCL when compared with the reactive LNs (Figure 5.5b). There is no statistically significant difference in the percentage of CD4+FOXP3+ cells between the different disease groups (Figure 5.5c). The percentage of triple-positive cells is low and there is no significant difference demonstrated between the difference lymphoma subgroups (Figure 5.5d).

Key: LN = Lymph node, MCL = Mantle cell lymphoma, DLBCL = Diffuse large B cell lymphoma, FL = Follicular lymphoma, CHL = Classical Hodgkin Lymphoma, CLL = Chronic Lymphocytic Leukaemia, ALK = Anaplastic Lymphoma Kinase, GZB = Granzyme B.

A.

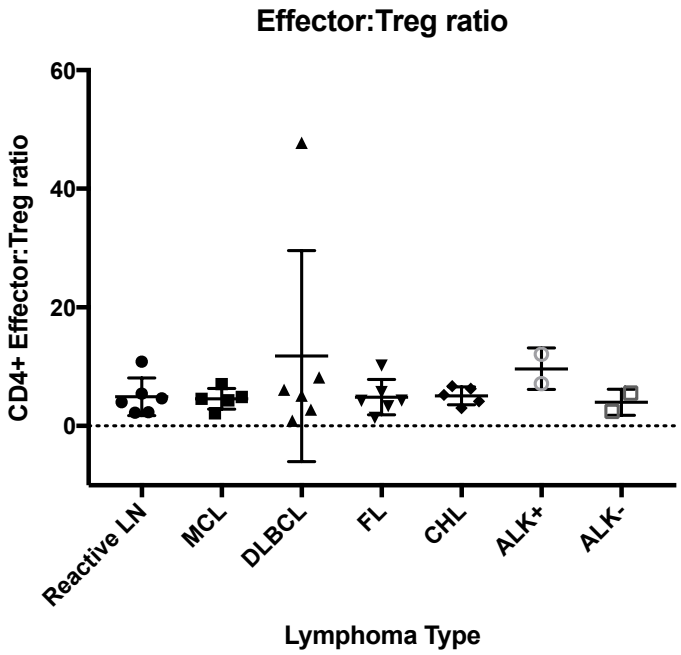

B.

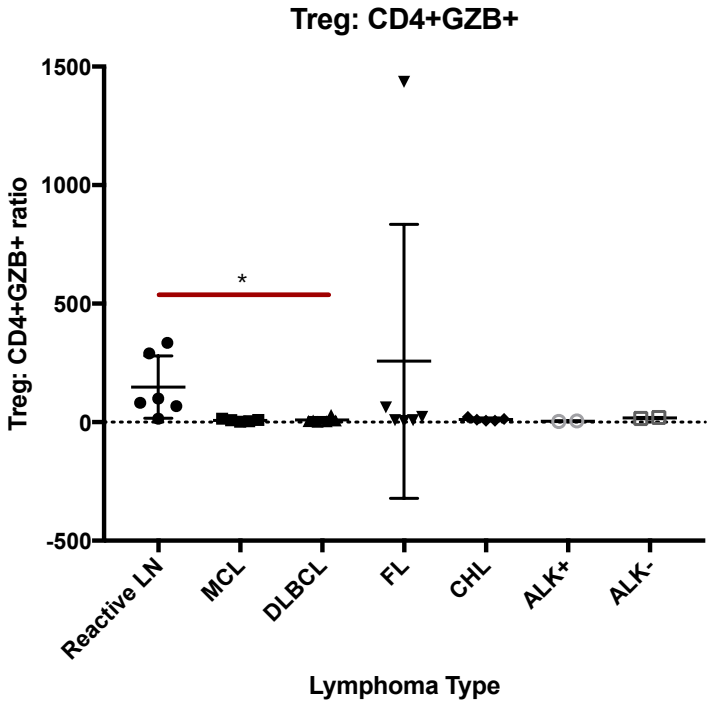

Figure 5-6: The ratio of CD4+effector cells to Tregs (A) and the ratio of Tregs to CD4+GZB+ cells (B) in the lymphoma and reactive lymph node biopsies. There is no significant difference in the ratio of CD4+effector cells to Tregs between the lymphoma subtypes and reactive lymph nodes. There is a significant decrease in the Treg:CD4+GZB+ ratio in the DLBCL lymph nodes when compared to the reactive lymph node biopsies (P = 0.0321).

Key: LN = Lymph node, MCL = Mantle cell lymphoma, DLBCL = Diffuse large B cell lymphoma, FL = Follicular lymphoma, CHL = Classical Hodgkin Lymphoma, CLL = Chronic Lymphocytic Leukaemia, ALK = Anaplastic Lymphoma Kinase, GZB = Granzyme B.

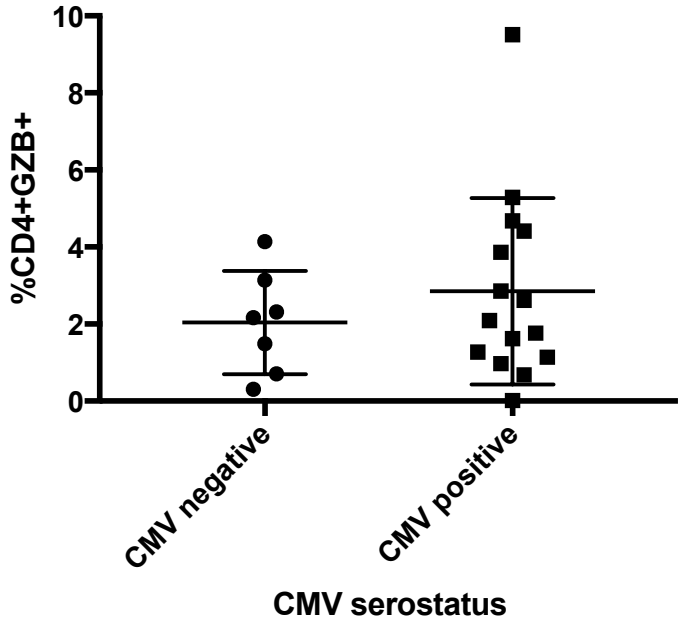

Figure 5-7: The percentage of CD4+GZB+ cells of the total CD4+ population in the patients who are known to be CMV seropositive and seronegative.

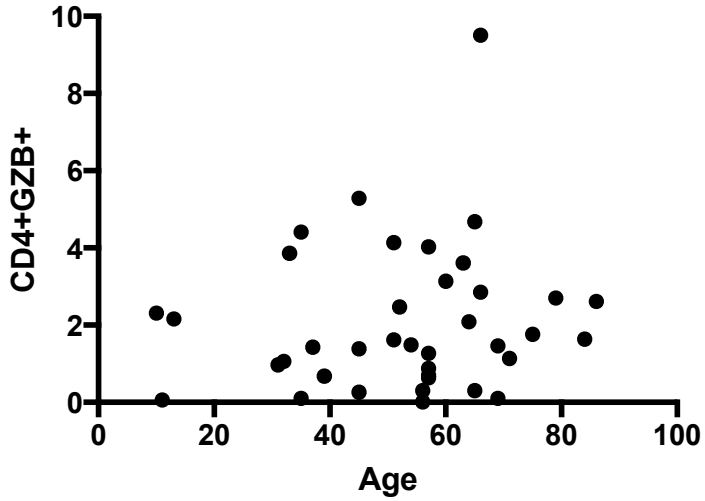

Figure 5-8: The percentage of CD4+GZB+ cells of the total CD4+ population and the age of the patients.

CD4 = Brown
FoxP3 = Red
Granzyme B = Blue

A.

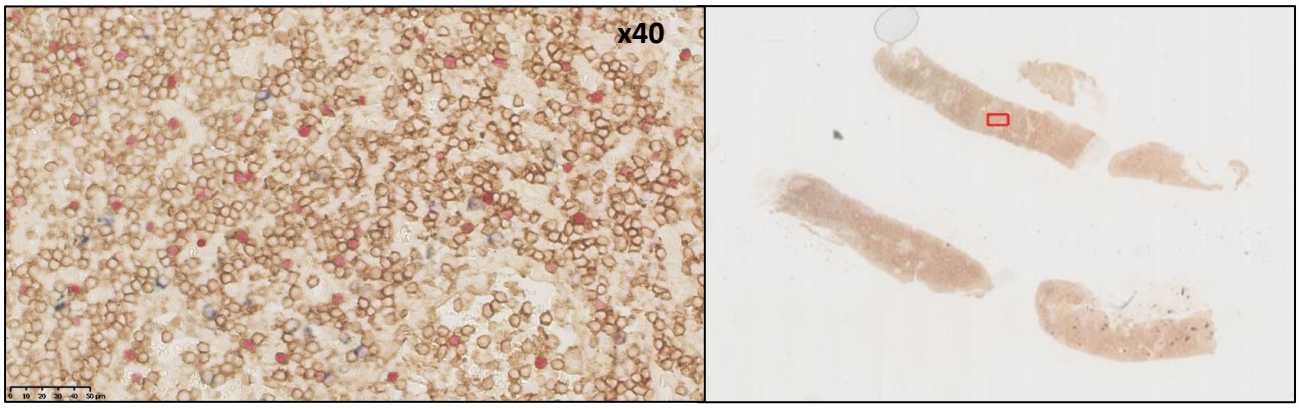

B.

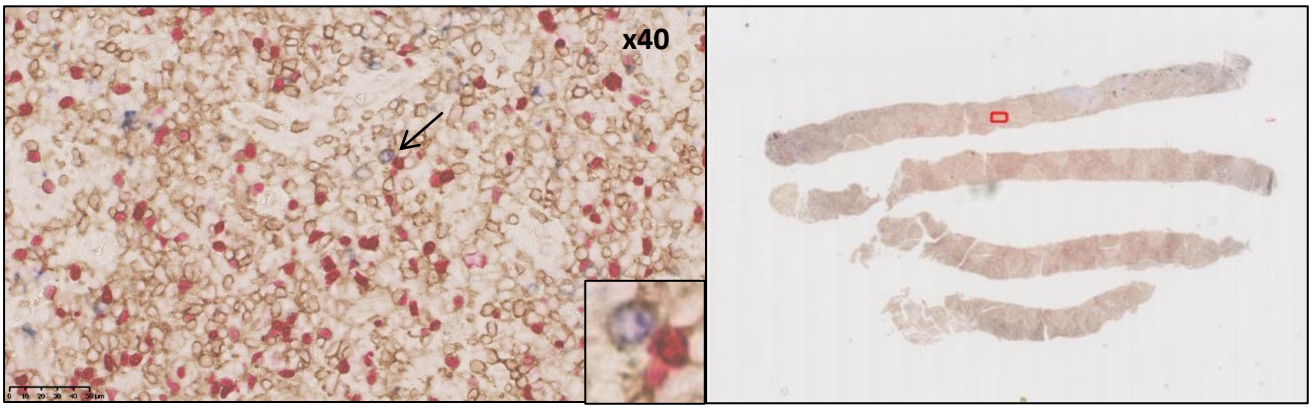

Figure 5-9: (A+B) Two examples of lymph node core biopsies which have the histological diagnosis of a “reactive” lymph node. These lymph node biopsies have been stained using triple-colour immunohistochemistry for CD4 (brown), FoxP3 (red) and Granzyme B (blue). The image on the left is a x40 magnification field of the lymph node biopsy. This x40 magnification field corresponds to the red box located in the image of the lymph node core biopsy in the image on the right. In Figure 5.9B, the arrow corresponds to the site of the magnified image in the box in the right-hand corner. This shows a CD4+GZB+ (Brown and Blue) cell.

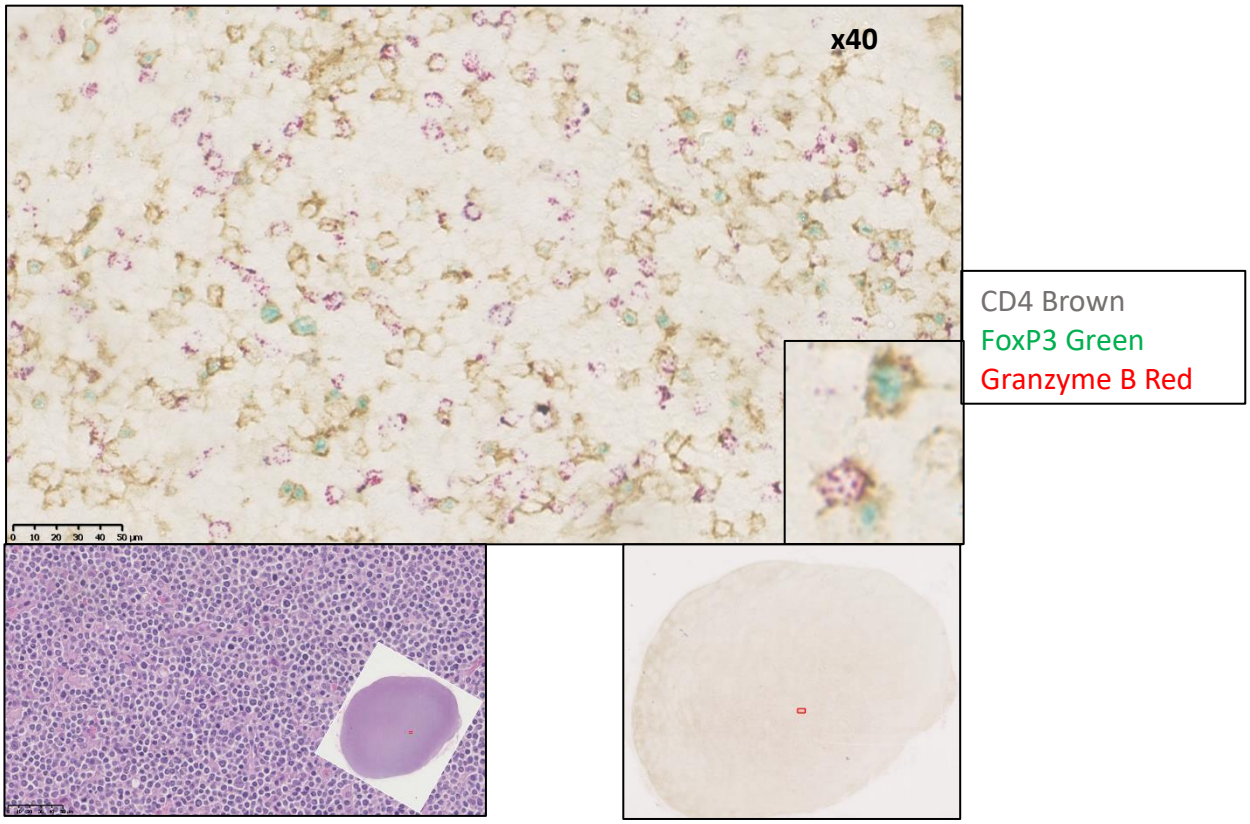

Figure 5-10: A lymph node biopsy infiltrated with Mantle Cell Lymphoma. The biopsy has been stained using triple IHC for CD4 (brown), FoxP3 (green) and Granzyme B (red) and is shown in the main image (at x40 magnification) The smaller box shows a triple positive cell (CD4+FOXP3+GZB+) and a CD4+GZB+ cell. The bottom left box shows the Haematoxylin and Eosin (H+E) stained slide. The bottom right box shows the location of the x40 magnification image on the lymph node biopsy and is signified by a red box.

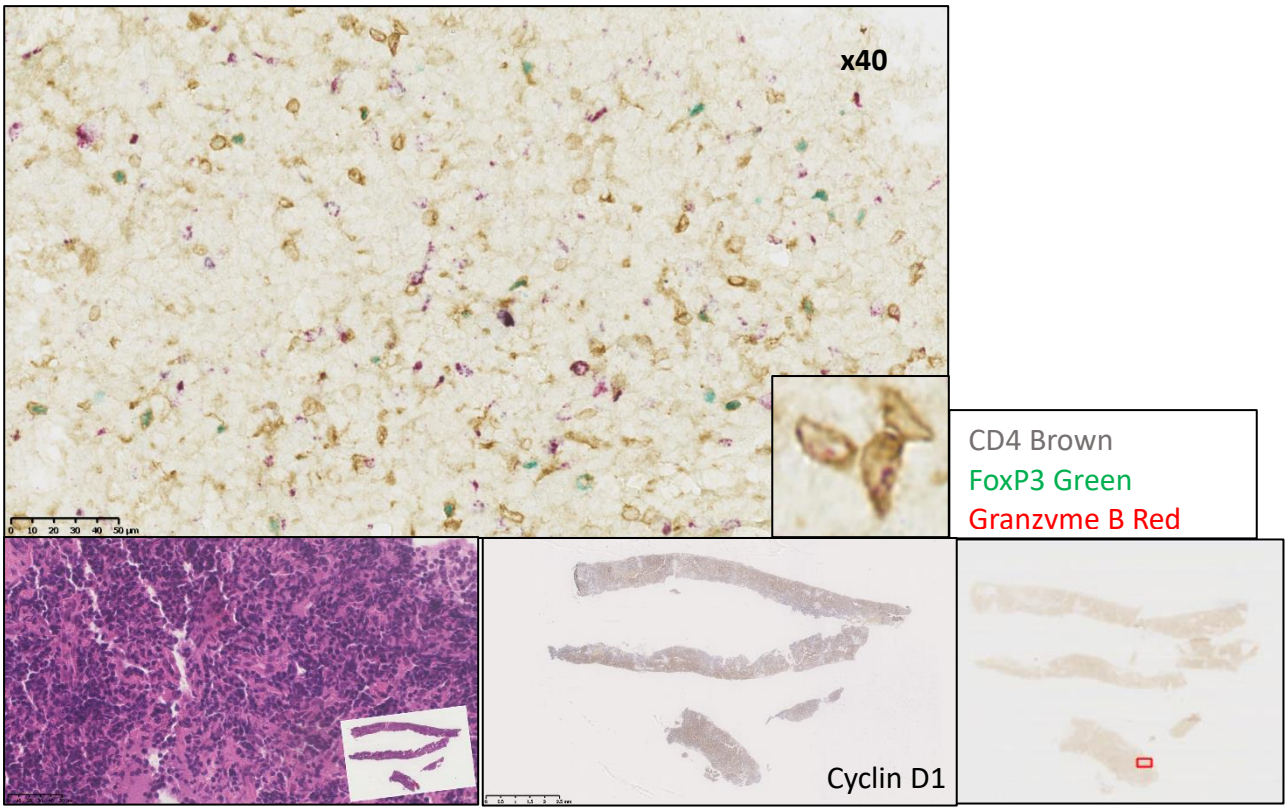

Figure 5-11: A lymph node biopsy infiltrated with Mantle Cell Lymphoma. The biopsy has been stained using triple IHC for CD4 (brown), FoxP3 (green) and Granzyme B (red) and is shown in the main image (x40 magnification). The smaller box shows three CD4+GZB+ cells. The top right image shows the location of the x40 magnification image on the lymph node biopsy and is signified by a red box. The bottom left image shows the Haematoxylin and Eosin (H+E) stained slide. The bottom middle image shows the areas of the biopsy stained positive for Cyclin D1 (brown). The bottom right image shows the areas of the biopsy that are stained positive for CD5 (brown).

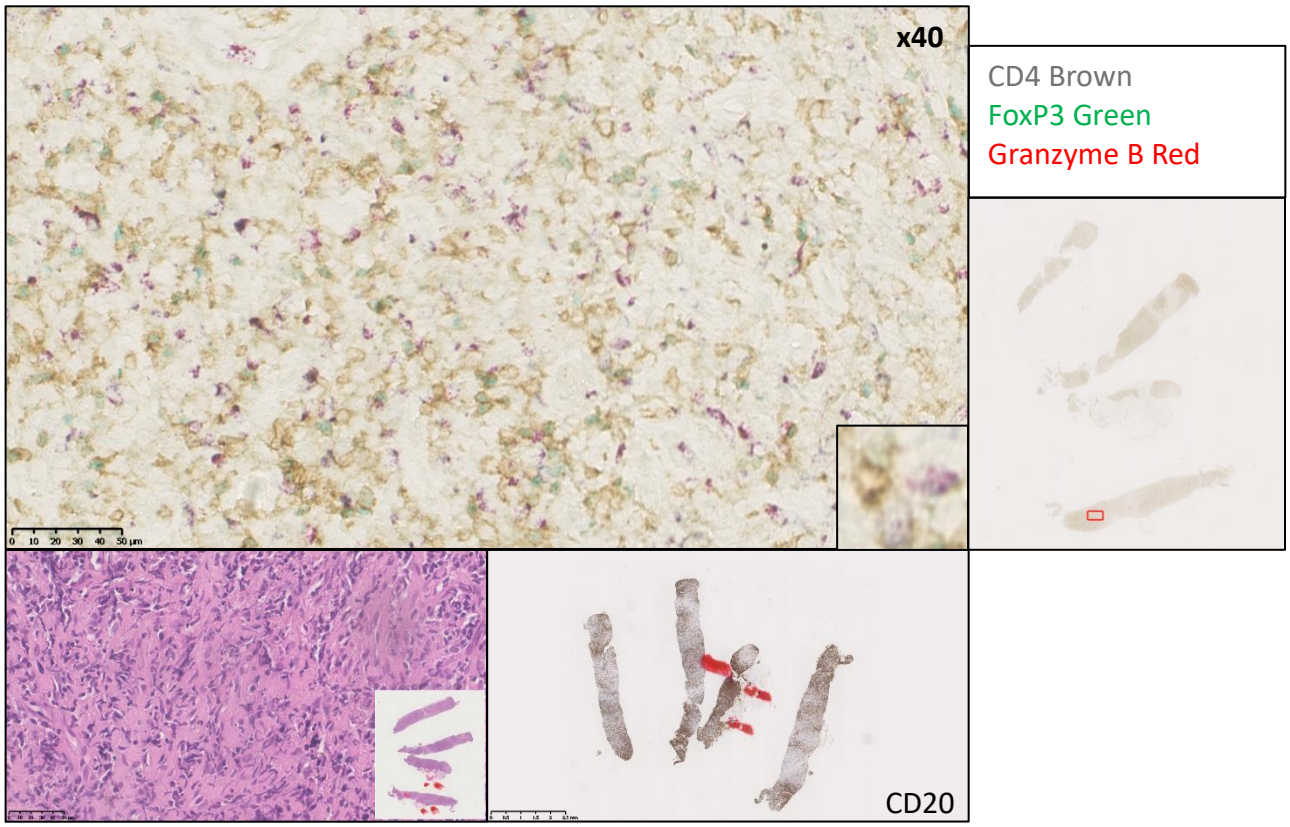

Figure 5-13: A lymph node biopsy infiltrated with Diffuse Large B Cell Lymphoma (DLBCL). The biopsy has been stained using triple IHC for CD4 (brown), FoxP3 (green) and Granzyme B (red) and is shown in the main image (x40 magnification). The smaller box shows a CD4+GZB+ cell. The top right image shows the location of the x40 magnification image on the lymph node biopsy and is signified by a red box. The bottom left image shows the Haematoxylin and Eosin (H+E) stained slide. The bottom right image shows the areas of the biopsy stained positive for CD20 (brown).

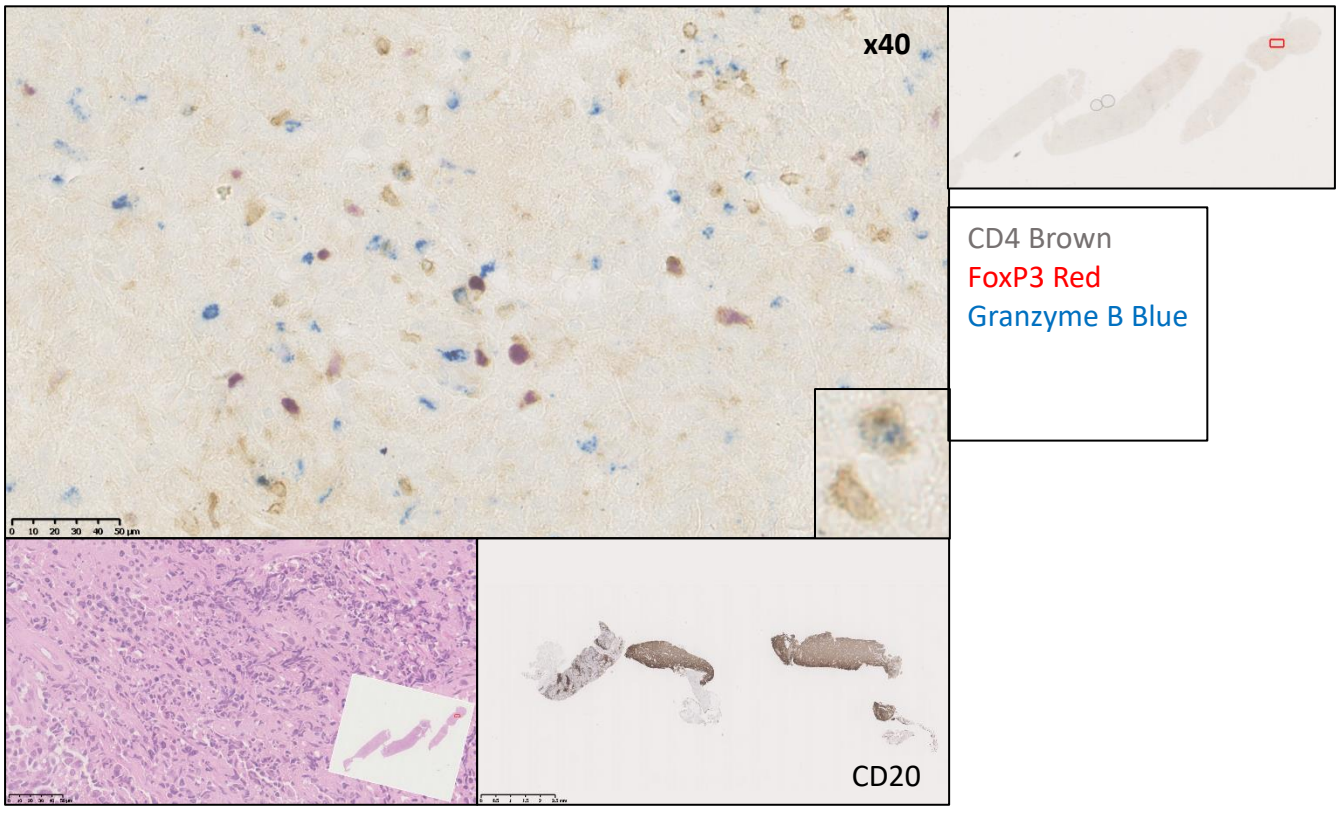

Figure 5-12: A lymph node biopsy infiltrated with Diffuse Large B Cell Lymphoma (DLBCL). The biopsy has been stained using triple IHC for CD4 (brown), FoxP3 (red) and Granzyme B (blue) and is shown in the main image (x40 magnification). The smaller box shows a CD4+GZB+ cell and a CD4+ cell. The top right image shows the location of the x40 magnification image on the lymph node biopsy and is signified by a red box. The bottom left image shows the Haematoxylin and Eosin (H+E) stained slide. The bottom right image shows the areas of the biopsy stained positive for CD20 (brown).

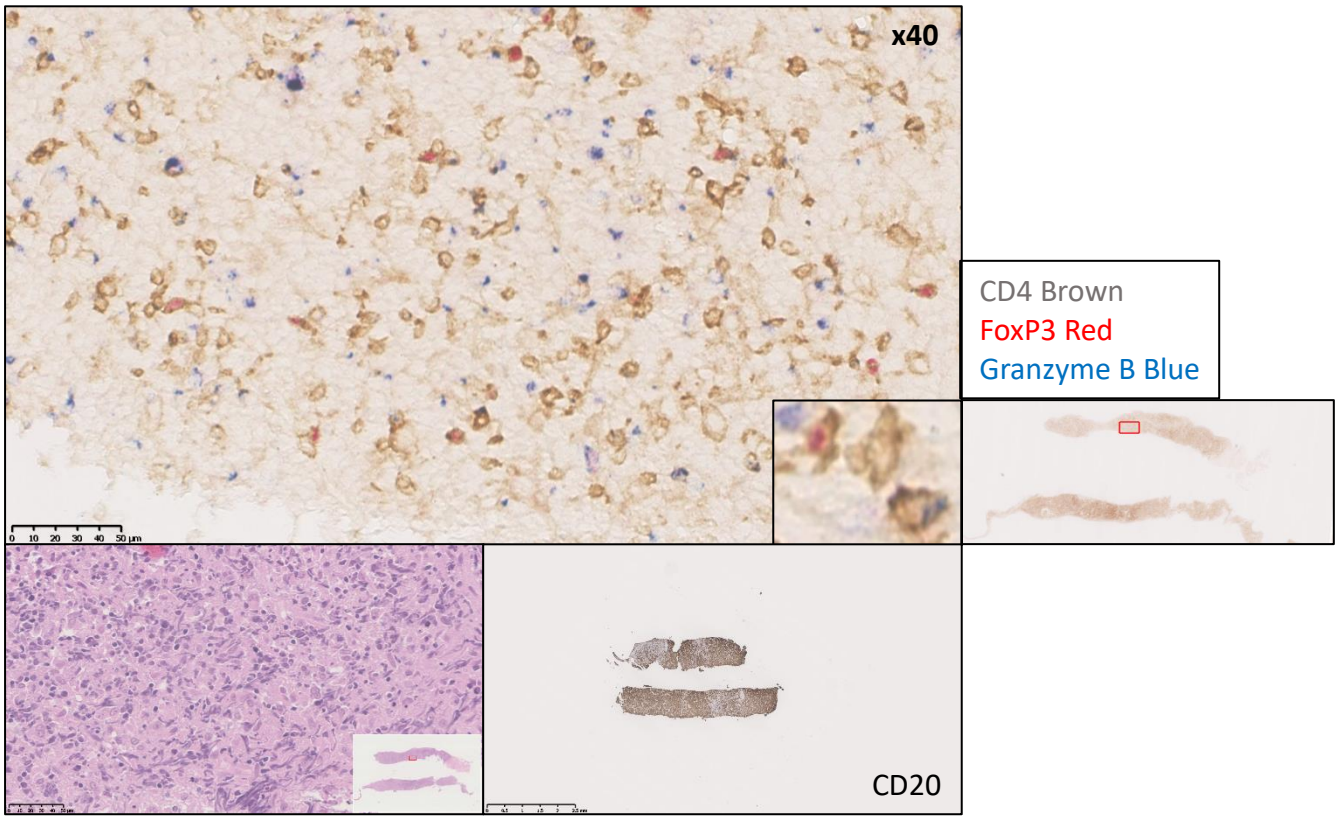

Figure 5-15: A lymph node biopsy infiltrated with Diffuse Large B Cell Lymphoma (DLBCL). The biopsy has been stained using triple IHC for CD4 (brown), FoxP3 (red) and Granzyme B (blue) and is shown in the main image (x40 magnification) The smaller box shows a CD4+GZB+ cell, a CD4+ cell, a GZB+ cell and a CD4+FOXP3+ cell. The top right image shows the location of the x40 magnification image on the lymph node biopsy and is signified by a red box. The bottom left image shows the Haematoxylin and Eosin (H+E) stained slide. The bottom right image shows the areas of the biopsy stained positive for CD20 (brown).

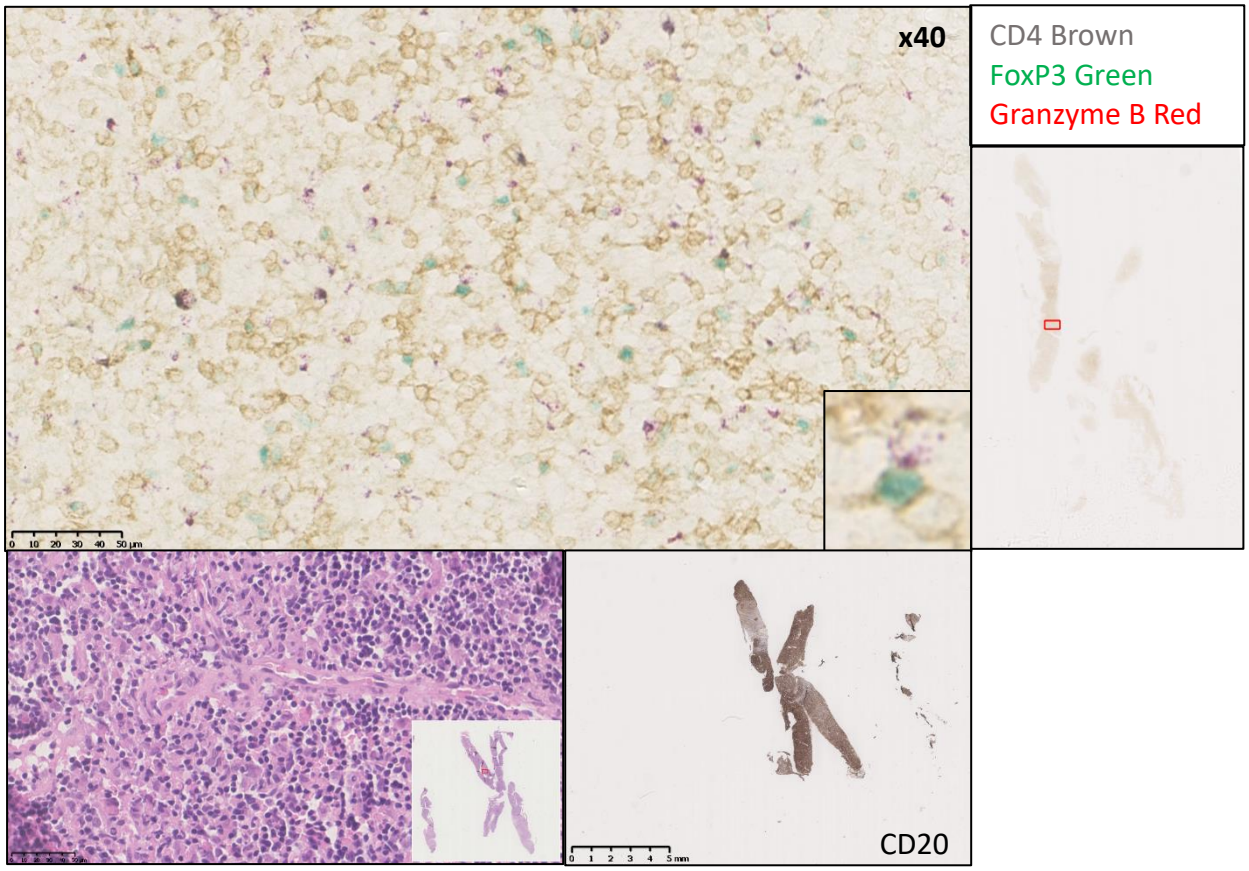

Figure 5-14: A lymph node biopsy infiltrated with Diffuse Large B Cell Lymphoma (DLBCL). The biopsy has been stained using triple IHC for CD4 (brown), FoxP3 (green) and Granzyme B (red) and is shown in the main image (x40 magnification). The smaller box shows a CD4+GZB+ cell, a CD4+ cell and a CD4+FOXP3+ cell. The top right image shows the location of the x40 magnification image on the lymph node biopsy and is signified by a red box. The bottom left image shows the Haematoxylin and Eosin (H+E) stained slide. The bottom right image shows the areas of the biopsy stained positive for CD20 (brown).

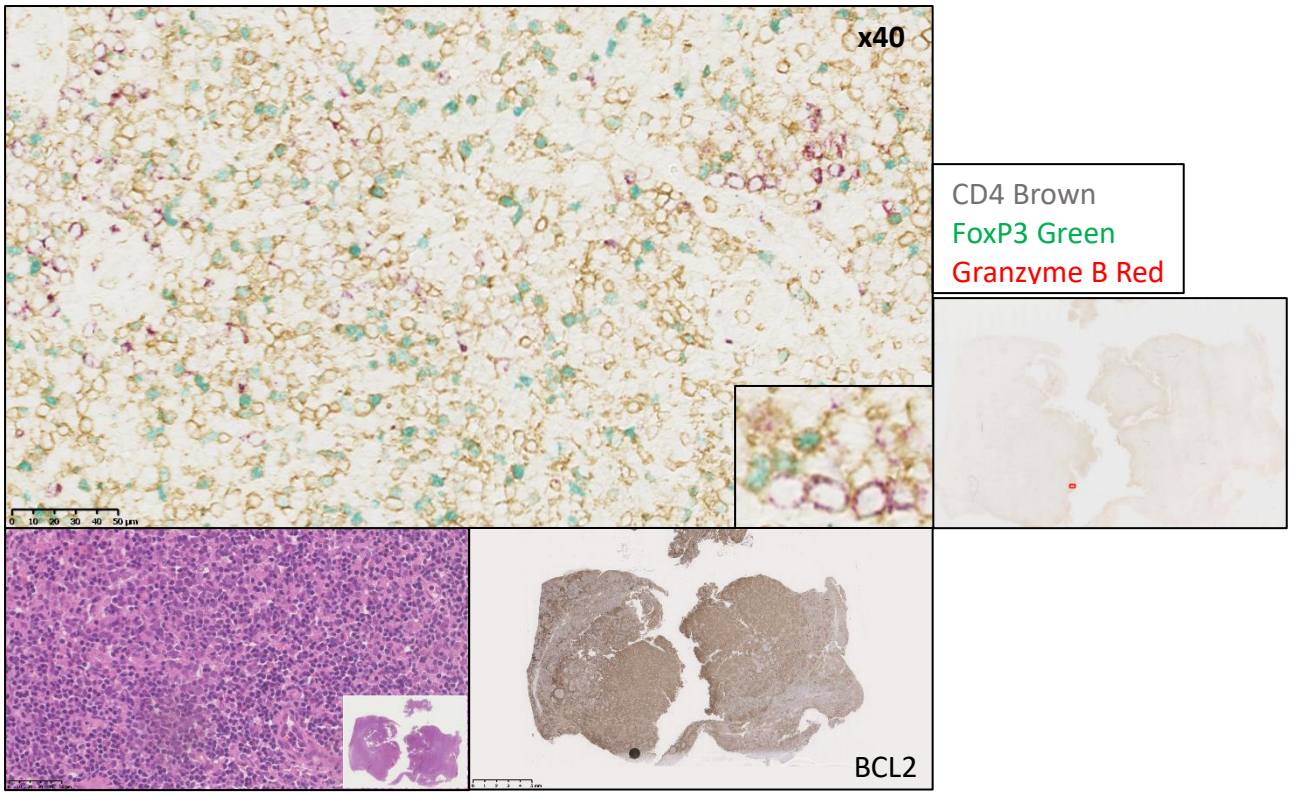

Figure 5-17: A lymph node biopsy infiltrated with Follicular Lymphoma (FL). The biopsy has been stained using triple IHC for CD4 (brown), FoxP3 (green) and Granzyme B (red) and is shown in the main image (x40 magnification). The top right image shows the location of the x40 magnification image on the lymph node biopsy and is signified by a red box. The bottom left image shows the Haematoxylin and Eosin (H+E) stained slide. The bottom right image shows the areas of the biopsy stained positive for BCL2 (brown).

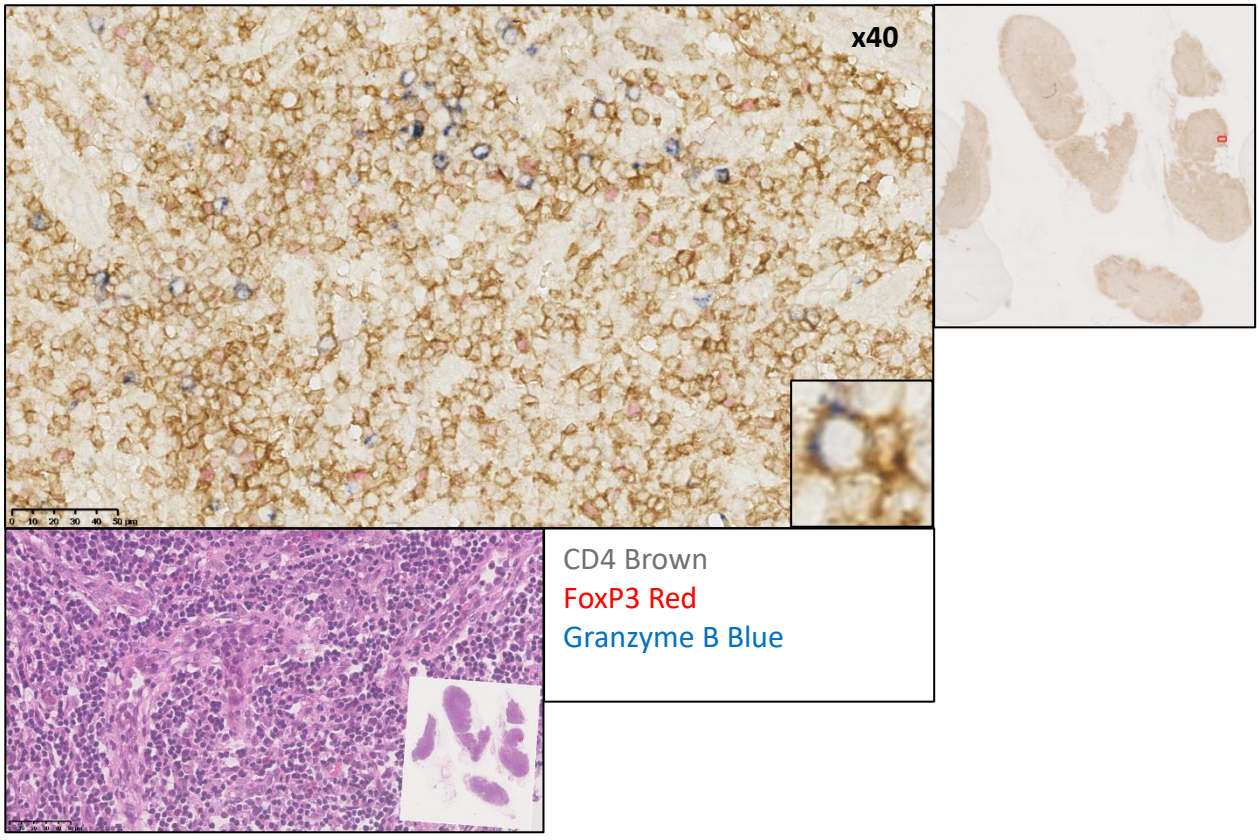

Figure 5-16: A lymph node biopsy infiltrated with Follicular Lymphoma (FL). The biopsy has been stained using triple IHC for CD4 (brown), FoxP3 (red) and Granzyme B (blue) and is shown in the main image (x40 magnification). The top right image shows the location of the x40 magnification image on the lymph node biopsy and is signified by a red box. The bottom left image shows the Haematoxylin and Eosin (H+E) stained slide.

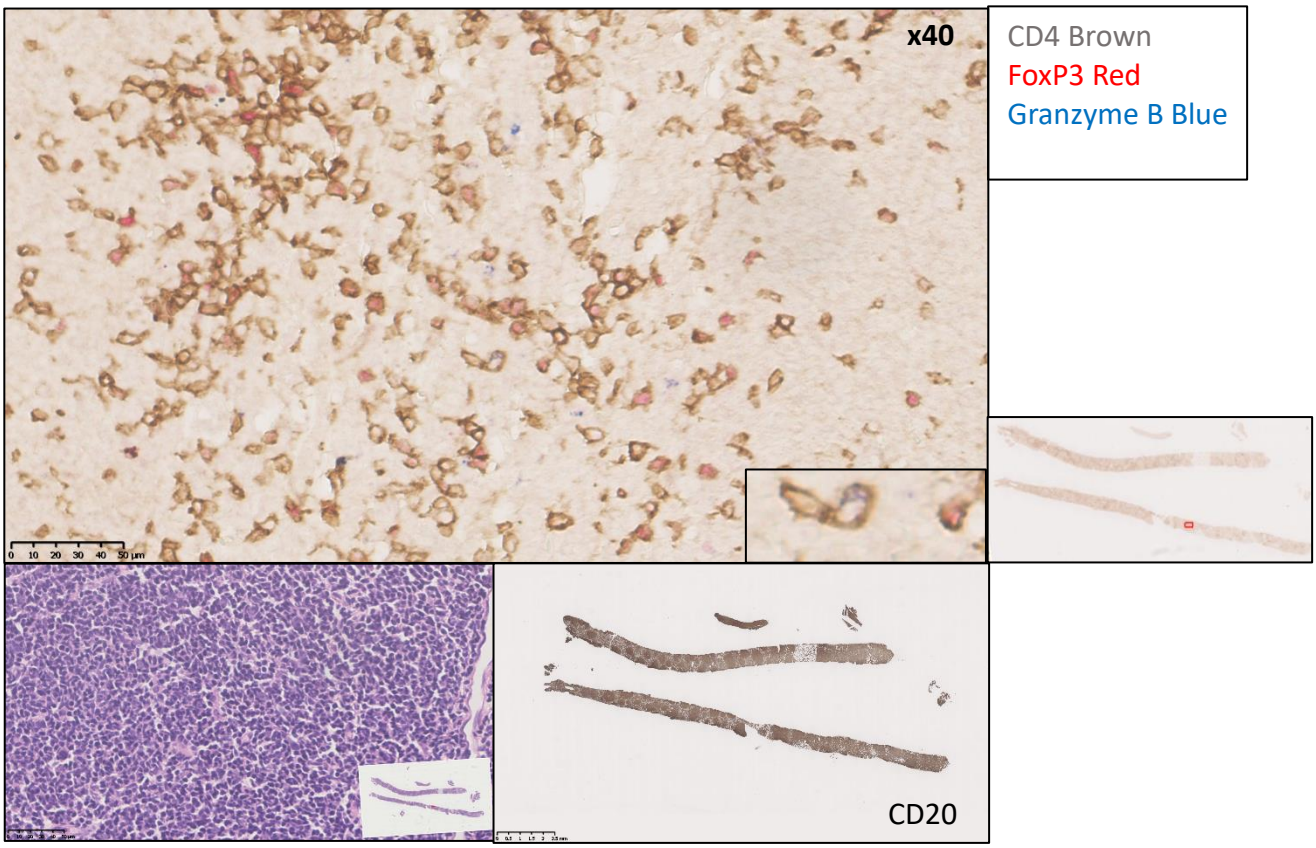

Figure 5-19: A lymph node biopsy infiltrated with Follicular Lymphoma (FL). The biopsy has been stained using triple IHC for CD4 (brown), FoxP3 (red) and Granzyme B (blue) and is shown in the main image (x40 magnification). The top right image shows the location of the x40 magnification image on the lymph node biopsy and is signified by a red box. The bottom left image shows the Haematoxylin and Eosin (H+E) stained slide. The bottom right image shows the areas of the biopsy stained positive for CD20 (brown).

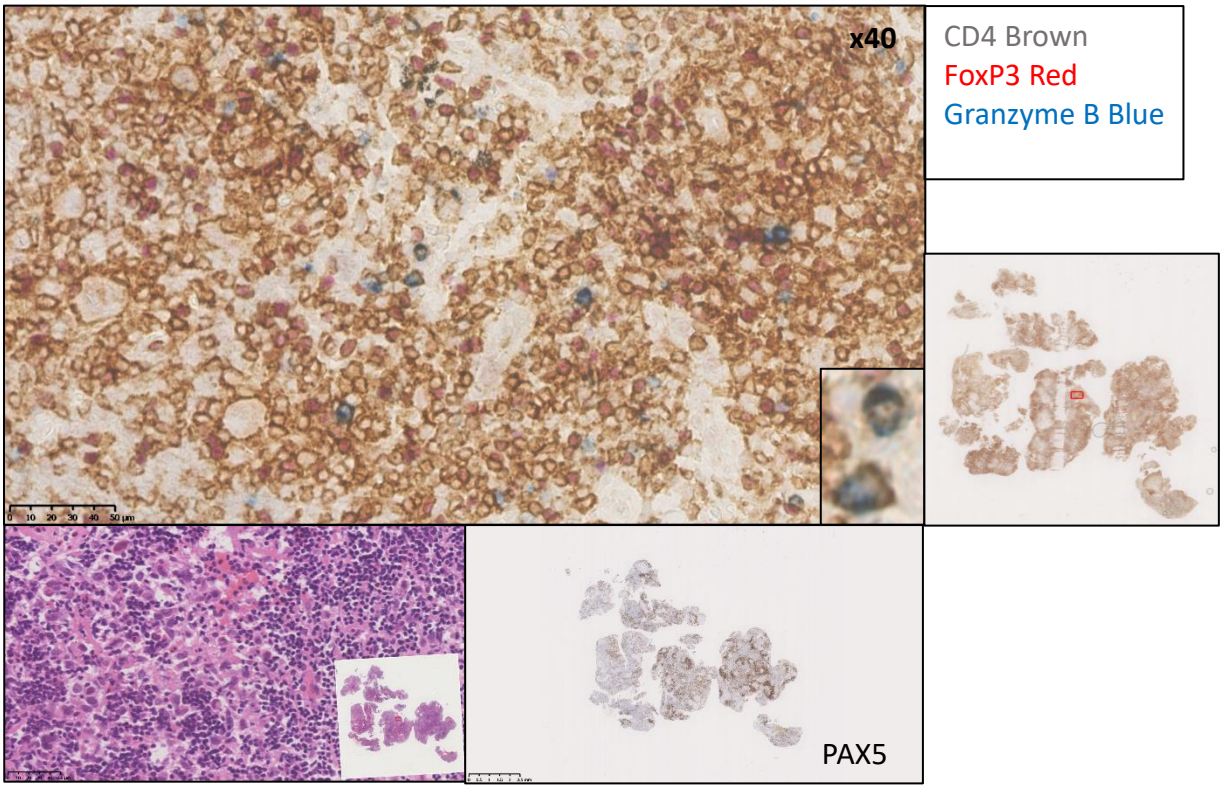

Figure 5-18: A lymph node biopsy infiltrated with Classical Hodgkin Lymphoma (CHL). The biopsy has been stained using triple IHC for CD4 (brown), FoxP3 (red) and Granzyme B (blue) and is shown in the main image (x40 magnification). The top right image shows the location of the x40 magnification image on the lymph node biopsy and is signified by a red box. The bottom left image shows the Haematoxylin and Eosin (H+E) stained slide. The bottom right image shows the areas of the biopsy stained positive for PAX5 (brown).

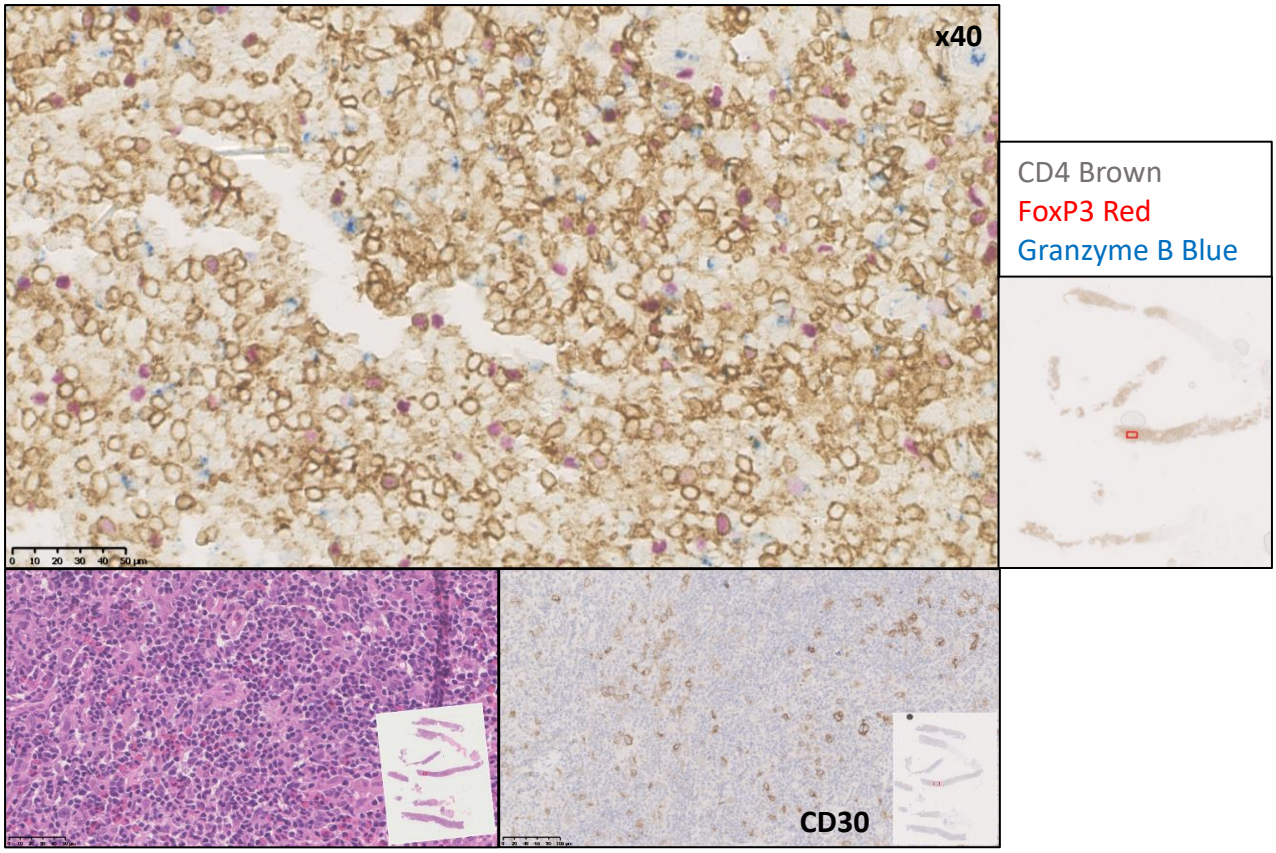

Figure 5-21: A lymph node biopsy infiltrated with Classical Hodgkin Lymphoma (CHL). The biopsy has been stained using triple IHC for CD4 (brown), FoxP3 (red) and Granzyme B (blue) and is shown in the main image (x40 magnification). The top right image shows the location of the x40 magnification image on the lymph node biopsy and is signified by a red box. The bottom left image shows the Haematoxylin and Eosin (H+E) stained slide. The bottom right image shows the areas of the biopsy stained positive for CD30 (brown).

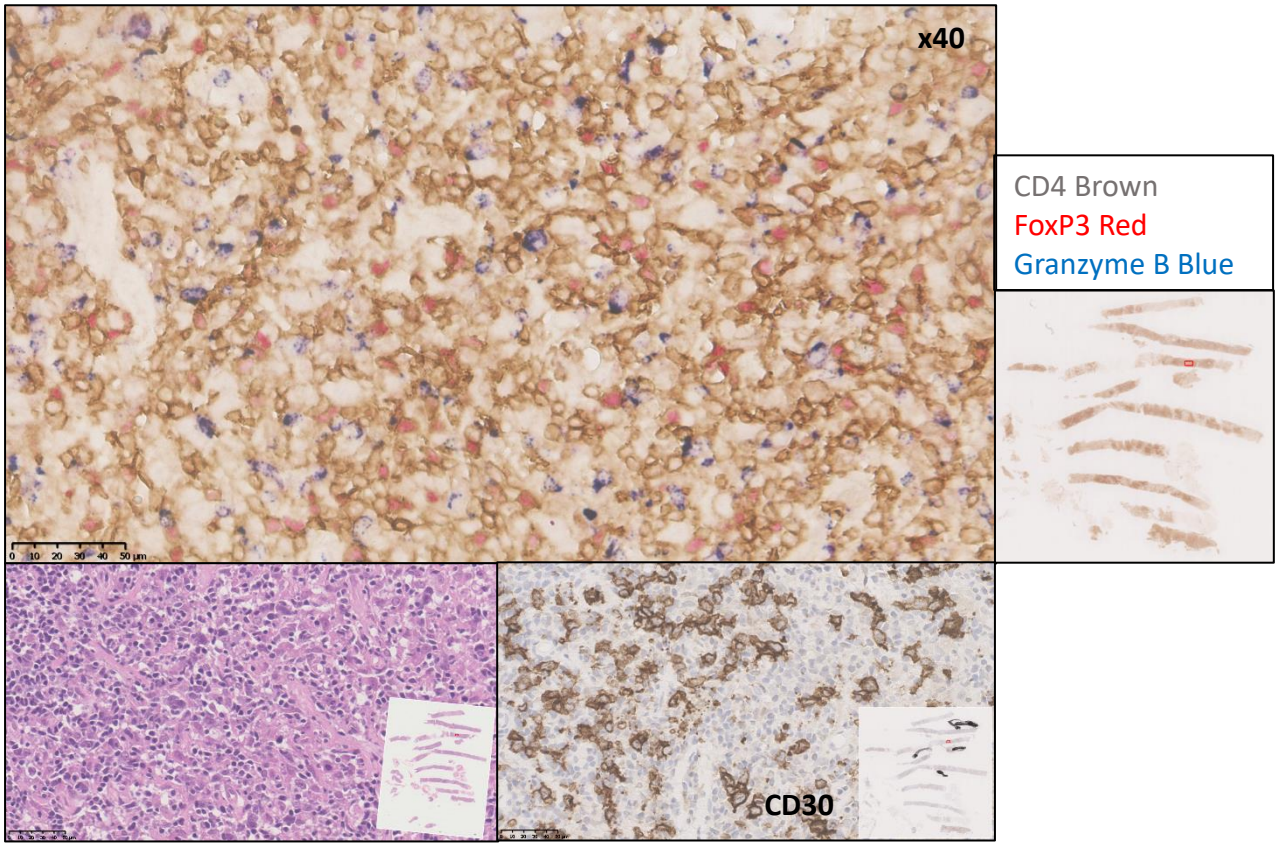

Figure 5-20: A lymph node biopsy infiltrated with Classical Hodgkin Lymphoma (CHL). The biopsy has been stained using triple IHC for CD4 (brown), FoxP3 (red) and Granzyme B (blue) and is shown in the main image (x40 magnification). The top right image shows the location of the x40 magnification image on the lymph node biopsy and is signified by a red box. The bottom left image shows the Haematoxylin and Eosin (H+E) stained slide. The bottom right image shows the areas of the biopsy stained positive for CD30 (brown).

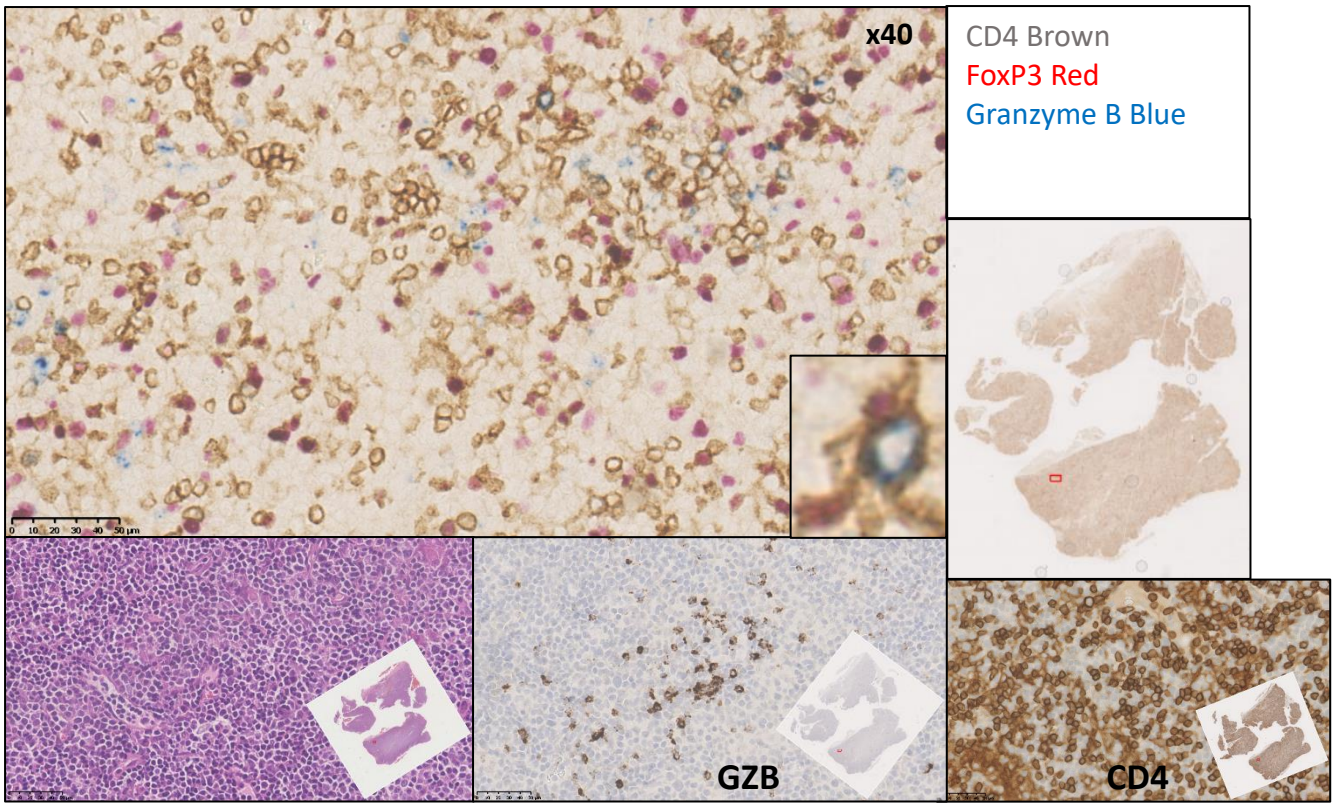

Figure 5-23: A lymph node biopsy infiltrated with ALK- PTCL. The biopsy has been stained using triple IHC for CD4 (brown), FoxP3 (red) and Granzyme B (blue) and is shown in the main image (x40 magnification). The top right image shows the location of the x40 magnification image on the lymph node biopsy and is signified by a red box. The bottom left image shows the Haematoxylin and Eosin (H+E) stained slide. The bottom middle and bottom right images shows the areas of the biopsy stained positive for GZB and CD4 (brown).

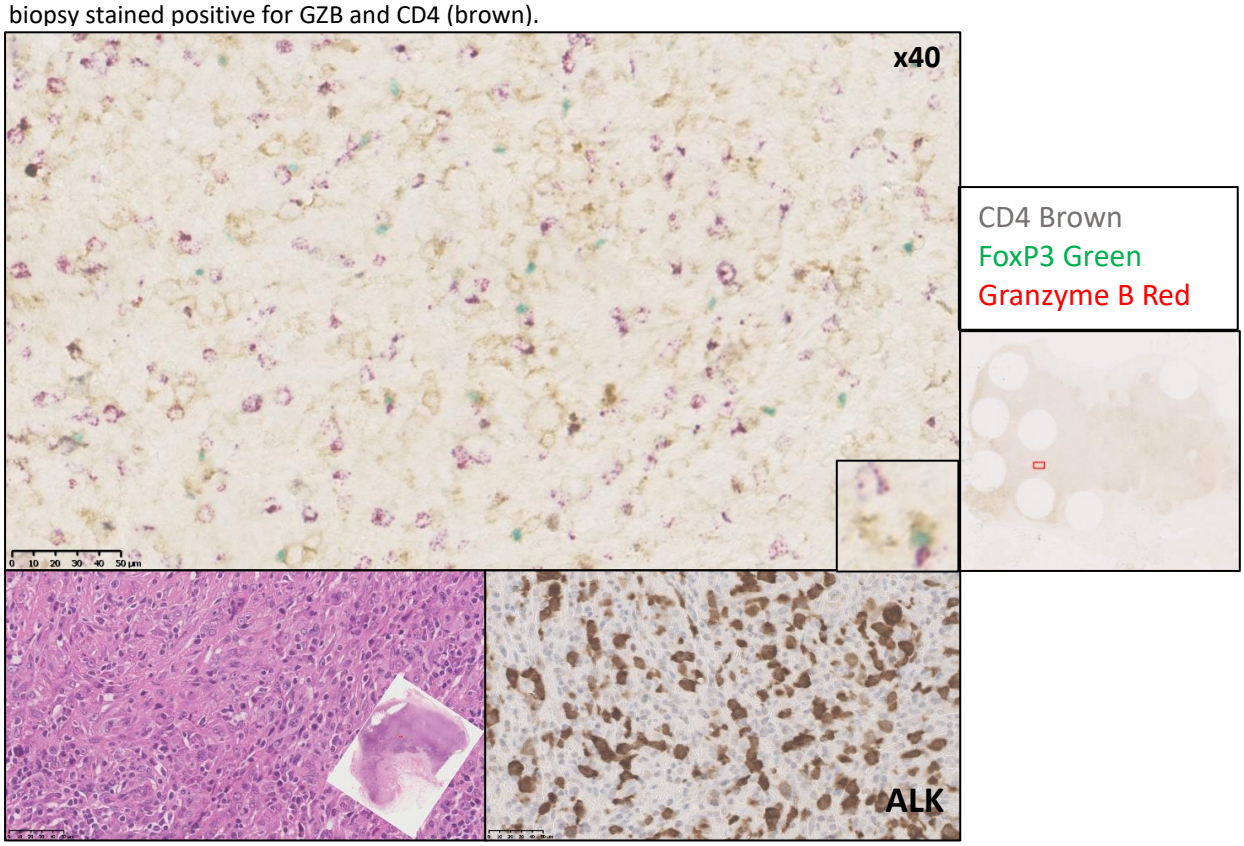

Figure 5-22: A lymph node biopsy infiltrated with ALK+ ALCL. The biopsy has been stained using triple IHC for CD4 (brown), FoxP3 (red) and Granzyme B (blue) and is shown in the main image (x40 magnification). The top right image shows the location of the x40 magnification image on the lymph node biopsy and is signified by a red box. The bottom left image shows the Haematoxylin and Eosin (H+E) stained slide. The bottom right image shows the areas of the biopsy stained positive for ALK (brown).

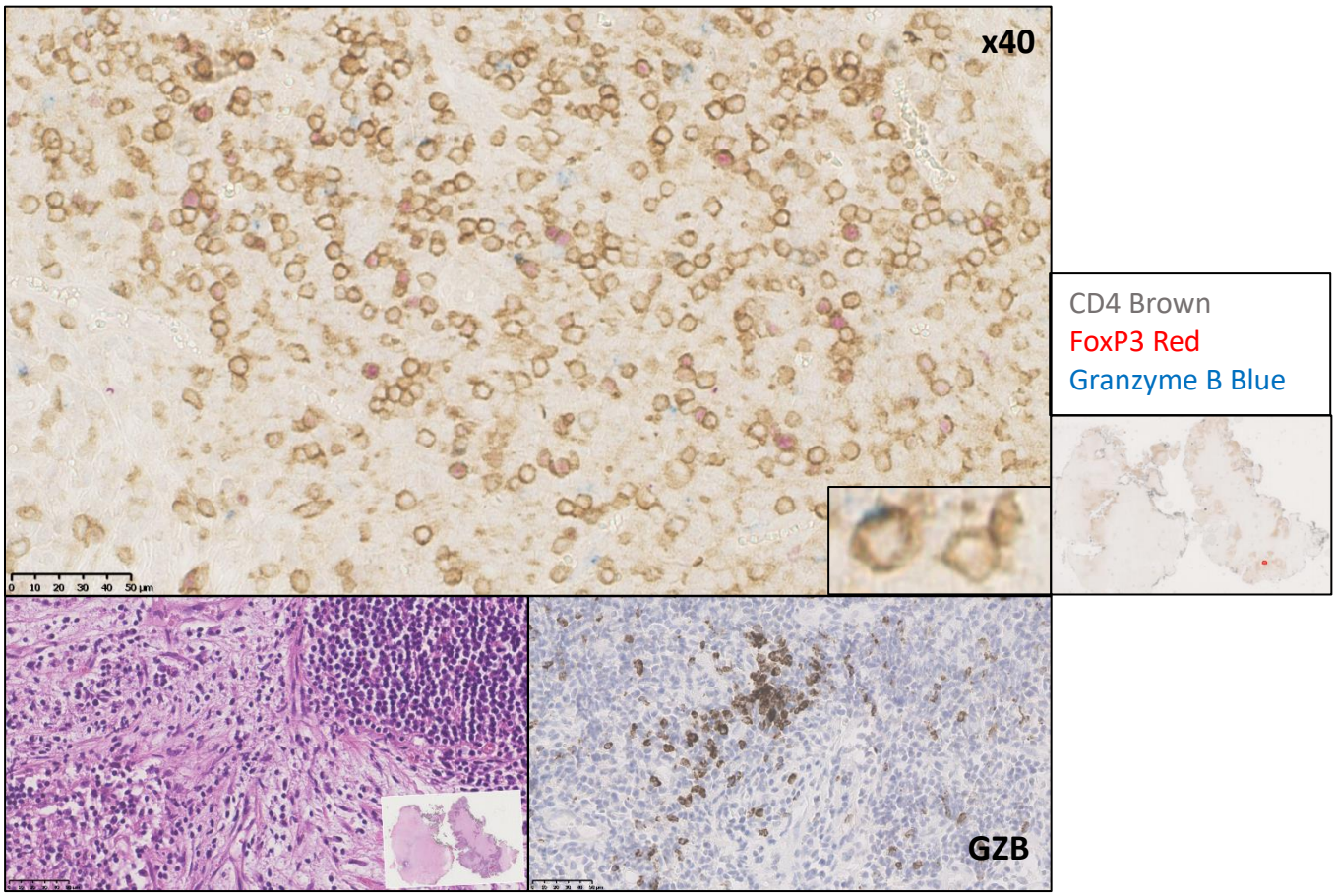

Figure 5-24: A lymph node biopsy infiltrated with ALK- ALCL. The biopsy has been stained using triple IHC for CD4 (brown), FoxP3 (red) and Granzyme B (blue) and is shown in the main image (x40 magnification). The top right image shows the location of the x40 magnification image on the lymph node biopsy and is signified by a red box. The bottom left image shows the Haematoxylin and Eosin (H+E) stained slide. The bottom right image shows the areas of the biopsy stained positive for GZB (brown).

5.5 Flow cytometry to identify the presence and phenotype of cytotoxic CD4+ T lymphocytes in the bone marrow aspirates of patients with Multiple Myeloma

Multiple myeloma is a plasma cell neoplasm which represents 10-15% of haematological malignancies [142, 143]. Malignant plasma cells secrete a monoclonal immunoglobulin, known as a paraprotein, which may be detected in the blood or urine in the majority of cases. Multiple myeloma is typically diagnosed in older adults and the median age of presentation is 69 years of age [144]. Prior to a diagnosis of multiple myeloma, pre-malignant states may have been present, including MGUS (monoclonal gammopathy of undetermined significance).

Multiple myeloma often presents with end-organ damage, affecting the kidneys, producing bone lesions including lytic lesions, anaemia and hypercalcaemia. There is often an associated decrease in the presence of polyclonal immunoglobulins which is termed immune paresis and contributes to the condition's immune dysfunction with an associated increased susceptibility to infections. The analysis of the immunophenotype of malignant plasma cells shows that they are positive for CD79a, CD138, CD38 and VS38c but are usually negative for CD19 and they lack surface Ig expression [76]. There may be aberrant expression of CD56.

At the time of diagnosis of Multiple Myeloma, due to the nature of disease and the usual absence of lymphadenopathy, lymph node biopsies were not available for analysis. In collaboration with Prof. Kwee Yong's laboratory, bone marrow aspirates had been obtained from patients with Multiple Myeloma at diagnosis and before the initiation of therapy. These bone marrow aspirates were analysed by flow cytometry to assess for the presence and characterisation of cytotoxic CD4+ cells.

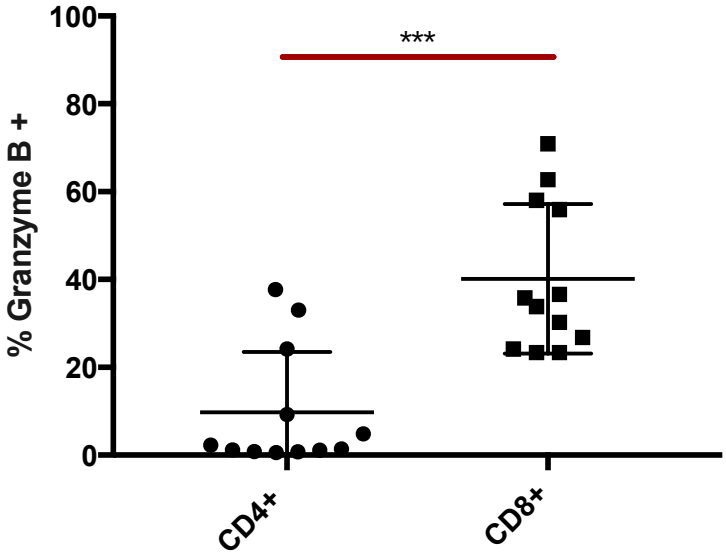

Figure 5-25: The percentage of Granzyme B expression in the CD4+ and CD8+ cells in the bone marrow aspirates of 12 patients with newly diagnosed multiple myeloma. There is a significant increase in the percentage of Granzyme B expression in CD8+ cells when compared to CD4+ cells (P=0.0005).

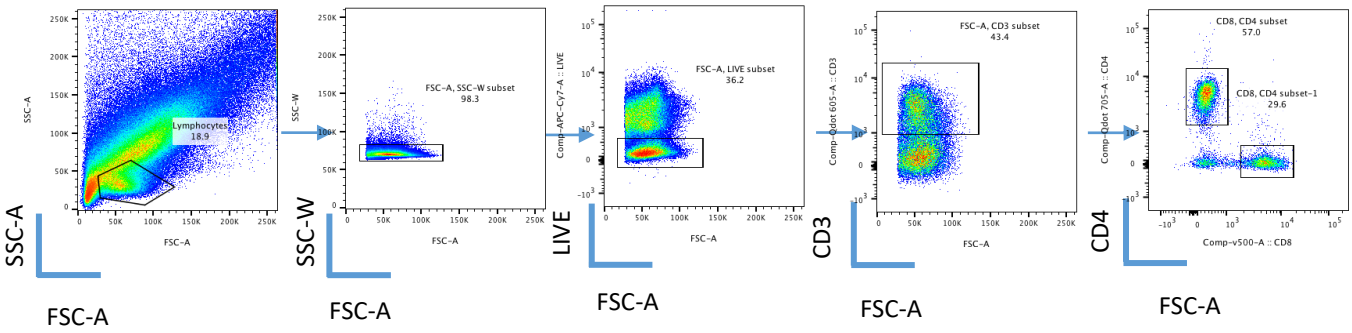

Figure 5-26: The gating strategy used to analyse the CD4+ and CD8+ cells from the bone marrow aspirates of patients with newly diagnosed multiple myeloma by flow cytometry.

A.

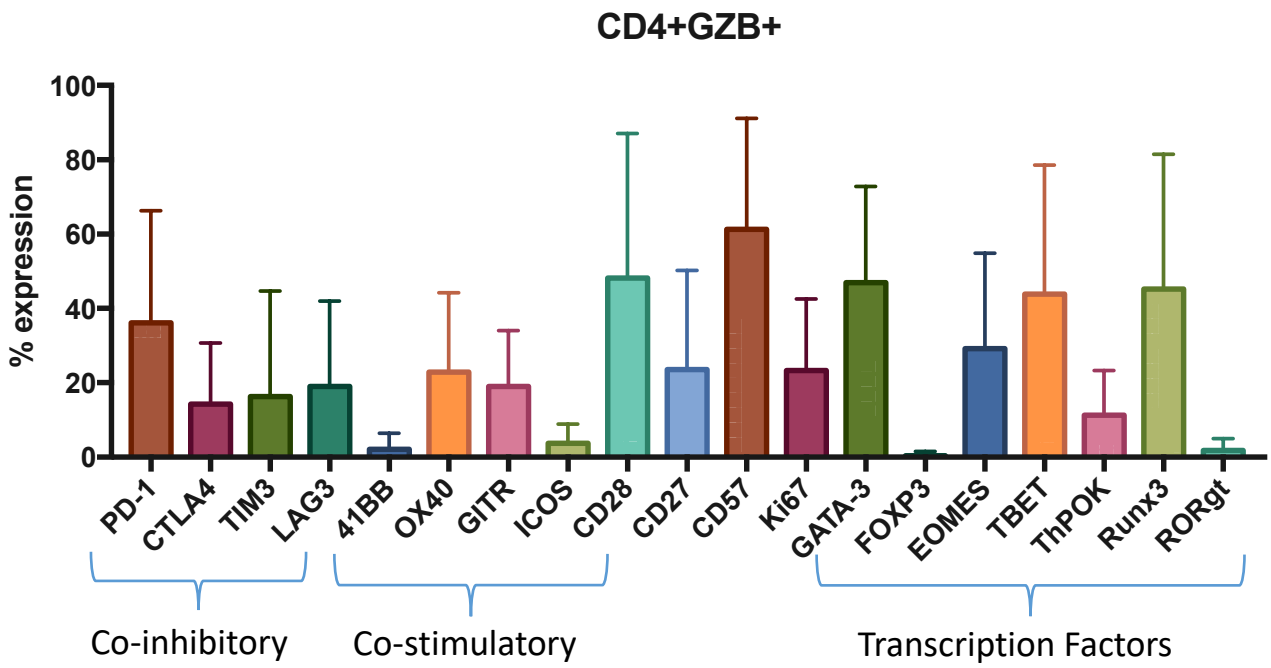

B.

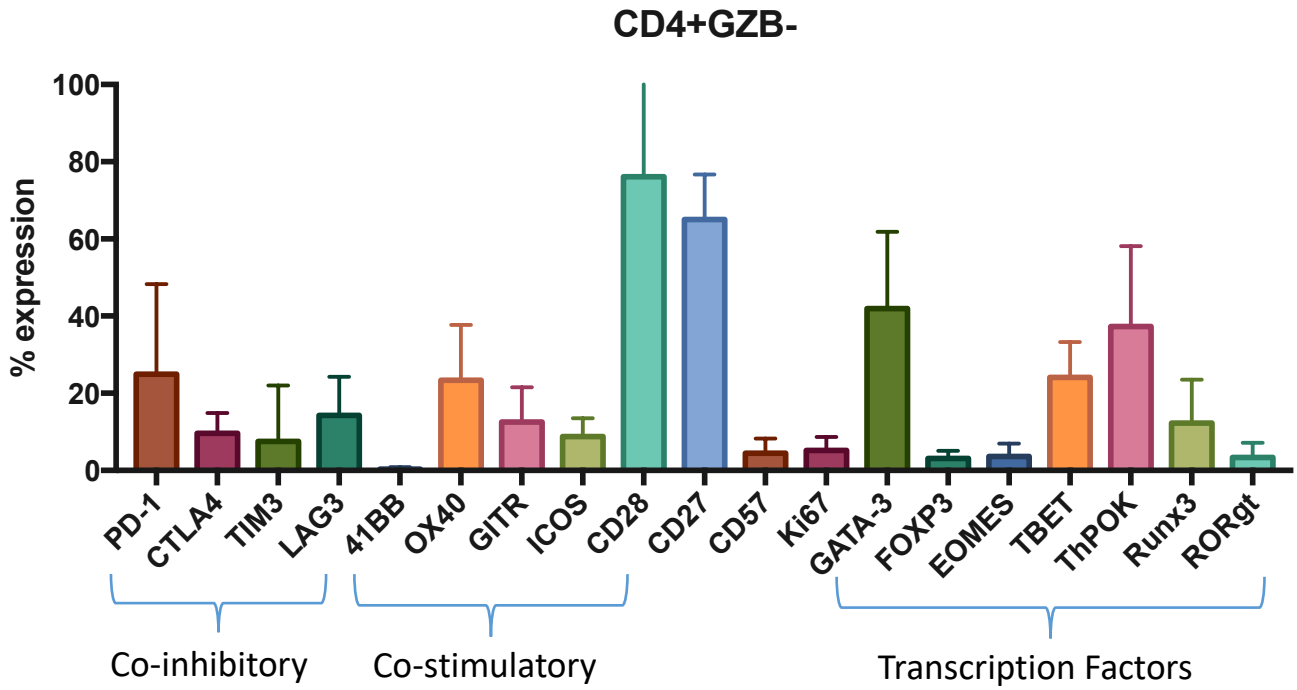

Figure 5-27: The phenotype of CD4+ cells in the bone marrow aspirates of 12 patients with newly diagnosed multiple myeloma. The percentage expression of co-inhibitory receptors, co-stimulatory receptors and transcription factors was assessed. Figure 5.27A shows the phenotype of CD4+Granzyme B+ cells and Figure 5.27B shows the phenotype of CD4+ Granzyme B- cells.

A.

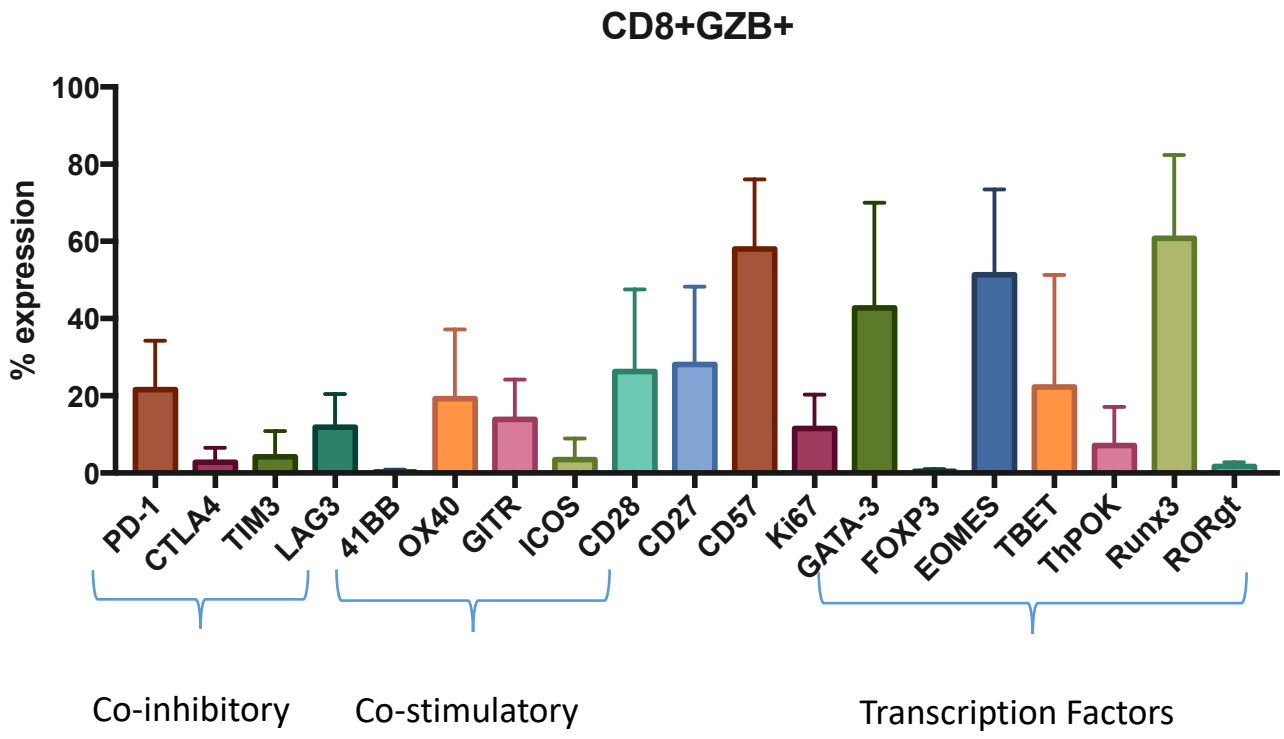

B.

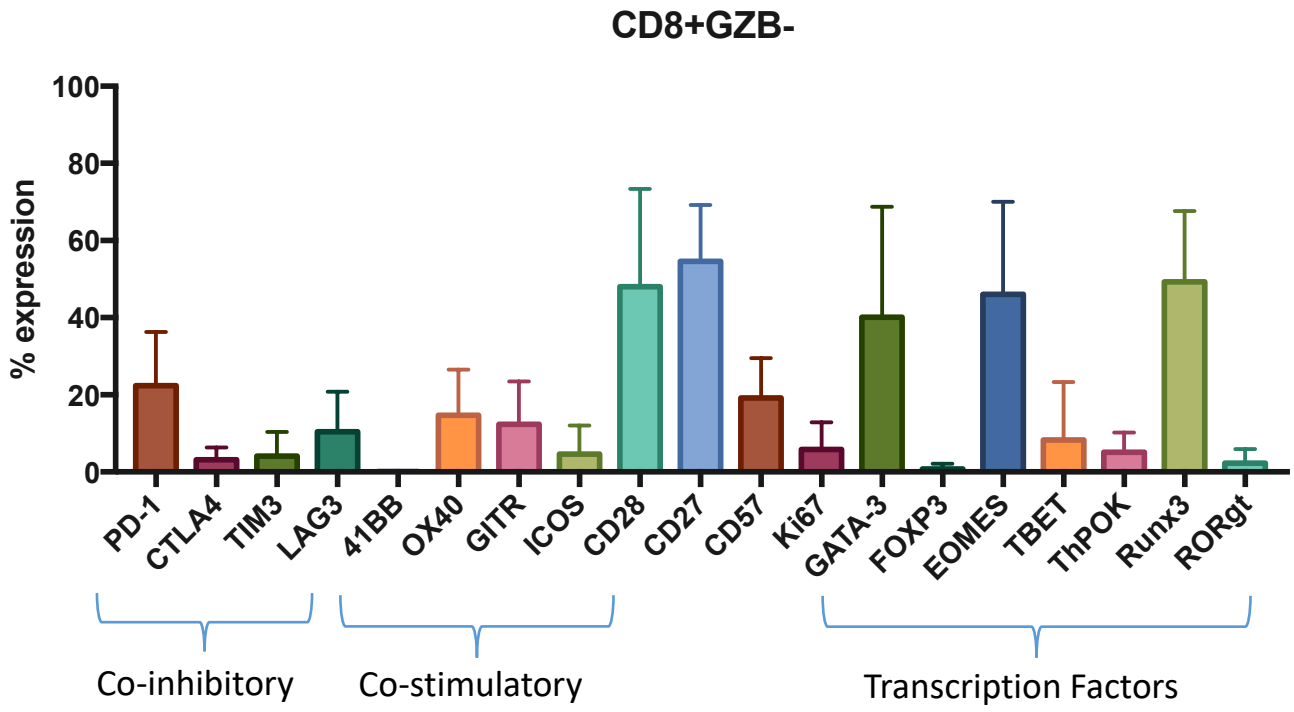

Figure 5-28: The phenotype of CD8+ cells in the bone marrow aspirates of 12 patients with newly diagnosed multiple myeloma. The percentage expression of co-inhibitory receptors, co-stimulatory receptors and transcription factors was assessed. Figure 5.28A shows the phenotype of CD8+Granzyme B+ cells and Figure 5.28B shows the phenotype of CD8+ Granzyme B- cells.

5.5.1 Patient Characteristics

Bone marrow aspirates from 12 patients with newly diagnosed Multiple Myeloma were stained with fluorophore-conjugated antibodies for flow cytometry analysis to detect and characterise cytotoxic CD4+ cells in the samples. The patient characteristics are shown in Table 18. The median age was 59 years (range: 37 – 71 years). The majority of patients were male (8/12) and the median paraprotein level was 28.45g/L (range: 2-68g/L). The median lymphocyte count at presentation was 2.07 x 10^9/L (range: 1.21-10.6 x 10^9/L) and the median percentage of plasma cells in the bone marrow trephine biopsy was % (range: 10-90%). The CMV status of the patients was not available.

Case	Age (Years)	Sex (F/M)	Lymphocyte Count (x 10^9/L)	Paraprotein (g/L)	Percentage of plasma cells in the bone marrow trephine biopsy (%)
1	54	F	2.4	31	80
2	53	M	2.2	3.9+0.1	75
3	69	M	10.6*	68	90
4	55	F	2.06	45.9	Not done
5	69	M	2.35	5	25-30%
6	67	M	1.86	50	60
7	55	F	2.3	2	15
8	37	M	1.9	38.5	Not done
9	60	M	2.08	17	10-15%
10	59	M	1.21	25.9	30
11	71	F	1.29	2 bands: 10 and TFTQ	50
12	59	M	1.99	51	70-80%

Table 18: The patient characteristics of the Multiple Myeloma bone marrow aspirate samples. All samples were taken from patients with a new diagnosis of Multiple Myeloma and prior to the initiation of chemotherapy. F = Female, M = Male, TFTQ = Too faint to quantify, *circulating plasma cells present.

5.5.2 Phenotype of CD4+ Granzyme B+ T lymphocytes

The median percentage of CD4+GZB+ cells was 1.875% (range: 0.62% - 37.73%). As in the CLL samples, there was a significant increase in the percentage of CD8+GZB+ cells when compared with CD4+GZB+ cells (P = 0.0005) (Figure 5-25). The CD4+GZB+ cells expressed CD57 but had low levels of expression of CD27 and Ki67 (Figure 5-7A). The cells were negative for expression of ICOS and 41BB and only had low levels of expression of the co-inhibitory receptors CTLA-4, TIM-3 and LAG-3. PD-1 had variable levels of expression with the median level of 31.7% (range 0-100%). Regarding transcription factors, approximately half of the CD4+GZB+ cells expressed TBET, GATA-3 and RUNX3. The cells did not express FOXP3.

5.5.3 Phenotype of CD4+ Granzyme B- T lymphocytes

The CD4+GZB- subset included T regulatory cells as well as Granzyme B negative CD4+ effector cells. In contrast to the CD4+GZB+ subset, these cells had high levels of CD28 and CD27 expression whereas they did not express CD57 (Figure 5-7B). Their proliferation index (Ki67) was low. There was also a lower level of PD-1 expression than in the CD4+GZB+ subset (median level of 15.7% expression). The cells also did not express EOMES and had a higher level of ThPOK expression. Runx3 expression was lower than the CD4+GZB+ cells. The majority of the CD4+GZB- cells did not express the co-inhibitory receptors CTLA-4, TIM3 and LAG3, and the co-stimulatory receptors 41BB, OX40, GITR and ICOS.

5.5.4 Phenotype of CD8+ Granzyme B+ T lymphocytes

The median percentage of CD8+GZB+ T lymphocytes was 34.8% (range 23.3 – 70.9%) (Figure 5-25). The majority of cells expressed CD57 but did not express CD27 or CD28 (Figure 5-28A). The majority of cells did not express the co-inhibitory receptors PD-1, CTLA-4, TIM3 or LAG3. The majority of cells also did not express the co-stimulatory receptors 41BB, OX40, GITR or ICOS. The CD8+GZB+ cells had a low proliferation index as measured by Ki67. Regarding the transcription factors, the cells did not express FOXP3, TBET, ThPOK or RORgt. There were higher levels of expression for EOMES, GATA-3 and Runx3.

5.5.5 Phenotype of CD8+ Granzyme B- T lymphocytes

The majority of the CD8+GZB- population expressed CD28 and CD27, in contrast to the CD8+GZB+ cells (Figure 5-28B). The majority of CD8+GZB- cells did not express the co-inhibitory receptors PD-1, CTLA-4, TIM3 or LAG3. The majority of cells also did not express the co-stimulatory receptors 41BB, OX40, GITR or ICOS. Unlike the CD8+GZB+ cells, the majority of CD8+GZB- cells did not express CD57. Similarly to the CD8+GZB+ cells, the CD8+GZB- cells did not express FOXP3, TBET, ThPOK or RORgt but the majority of cells did express EOMES, GATA-3 and Runx3.

5.5.6 Comparison of CD4+ Granzyme B+ cells with CD8+ Granzyme B + cells

Although there was a significantly higher percentage of CD8+GZB+ than CD4+GZB+ cells (Figure 5-25), there were many similarities in their phenotype. Both groups of cells expressed CD57+ but did not express CD27 and CD28, unlike their Granzyme B negative counterparts. There was a higher level of EOMES expression in the CD8+GZB+ cells than the CD4+GZB+ cells whereas there was a higher level of Tbet expression in the CD4+GZB+ cells. The majority of cells in both subgroups did not express the co-inhibitory and co-stimulatory receptors studied although there was a higher median level of cells expressing PD-1 in the CD4+GZB+ cells than in the CD8+GZB+ cells.

5.5.7 Summary of Multiple Myeloma analysis

These results show for the first time the presence of CD4+CTLs in the bone marrow aspirate samples of patients with newly diagnosed Multiple Myeloma. The phenotype of these cells appear to have more in common with CD8+Granzyme B+ cells, which are also cytotoxic, than with the CD4+ cells that do not express Granzyme B. Although we are unable to directly compare the CLL results from Chapter 3 with the myeloma results in view of the different primary sample material (peripheral blood versus bone marrow aspirates) the phenotype of CD57 expression without CD27 and CD28 expression is similar between the two diseases. Furthermore, the phenotypic similarities between the CD4+GZB+ and CD8+GZB+ cells , as opposed to the Granzyme B negative subtypes, is consistent between the two diseases. Further assessment of CD4+GZB+ cells in multiple myeloma should be made in a larger group of patients and correlated with bone marrow trephine biopsy results.

5-29A. CD4+s

Control PBMCs

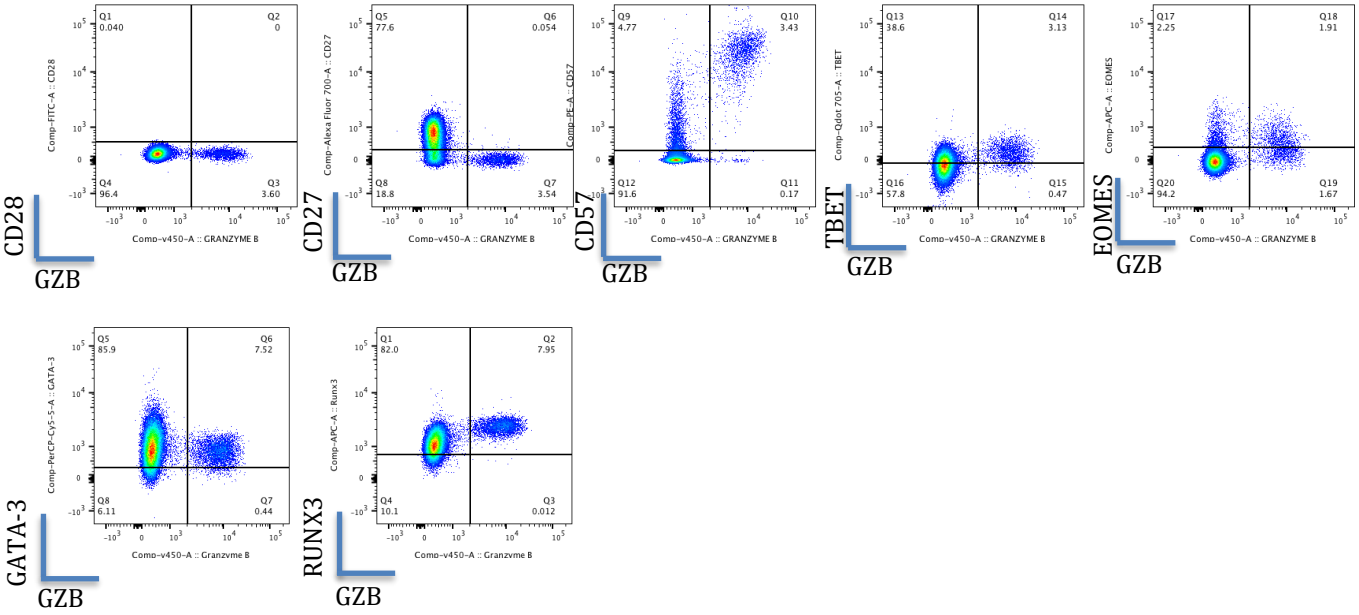

Multiple Myeloma BMA

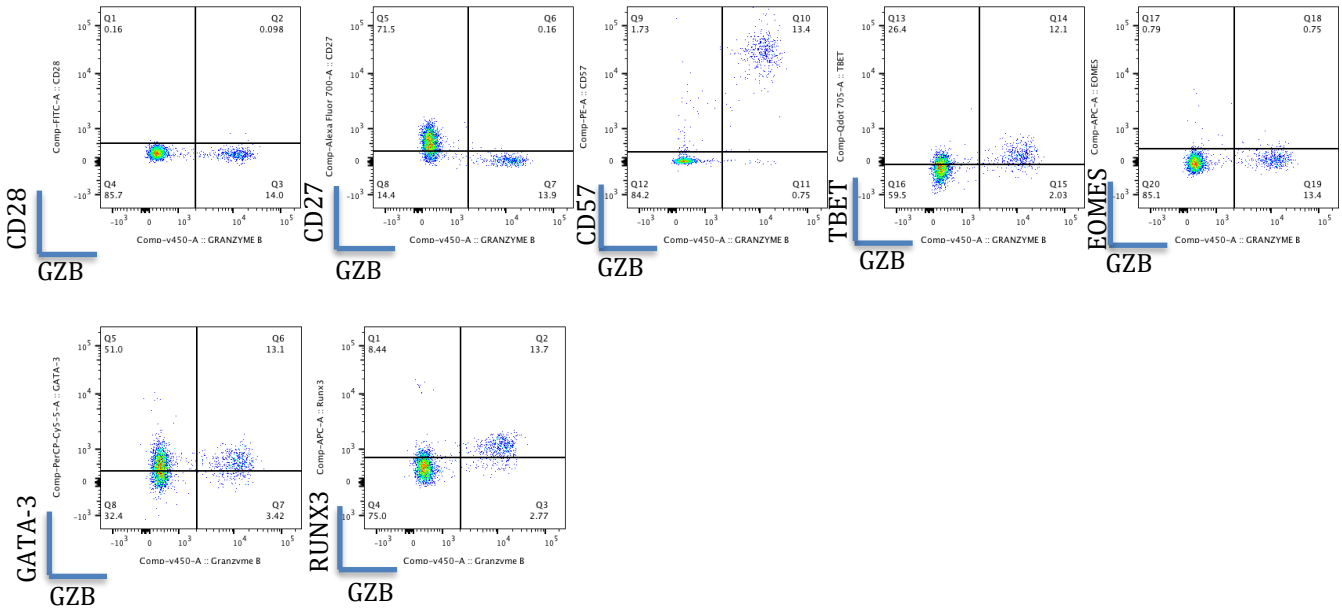

Figure 5-29: Examples of dot plot flow cytometry data from the bone marrow aspirates (BMA) of patients with newly diagnosed myeloma and a healthy control's peripheral blood mononuclear cells. Figure 5.29A shows CD3+CD4+ cells whereas Figure 5.29B shows CD3+CD8+ cells.

5-29B. CD8+s

Control PBMCs

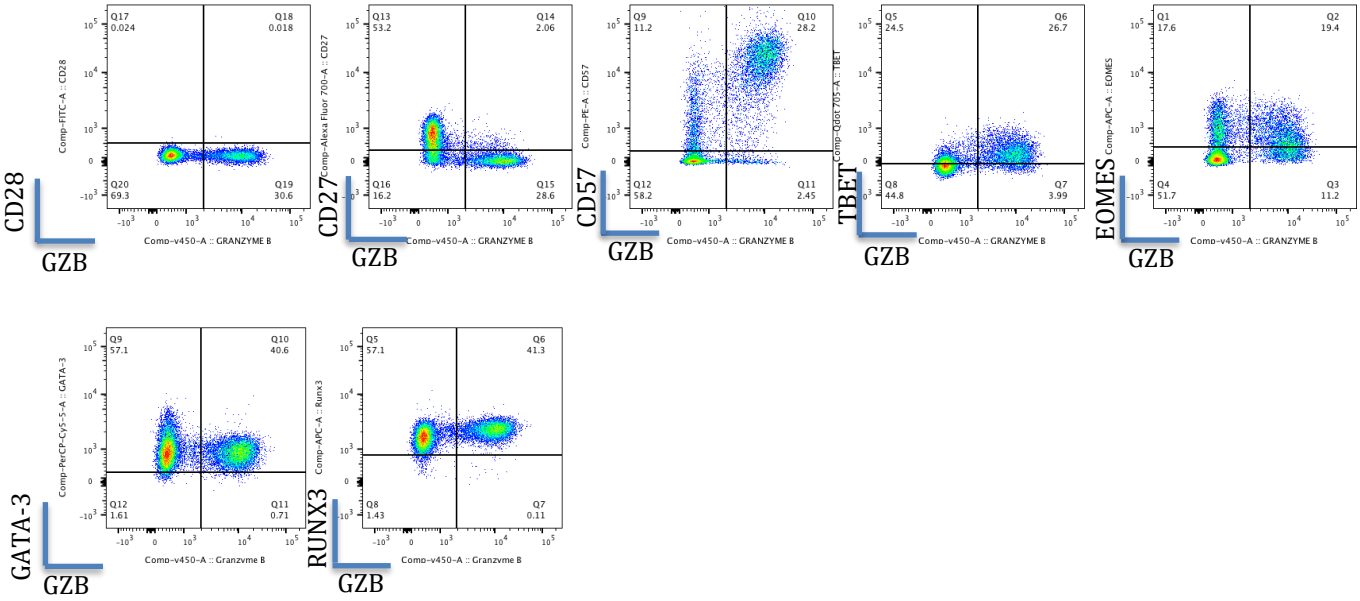

Multiple Myeloma BMA

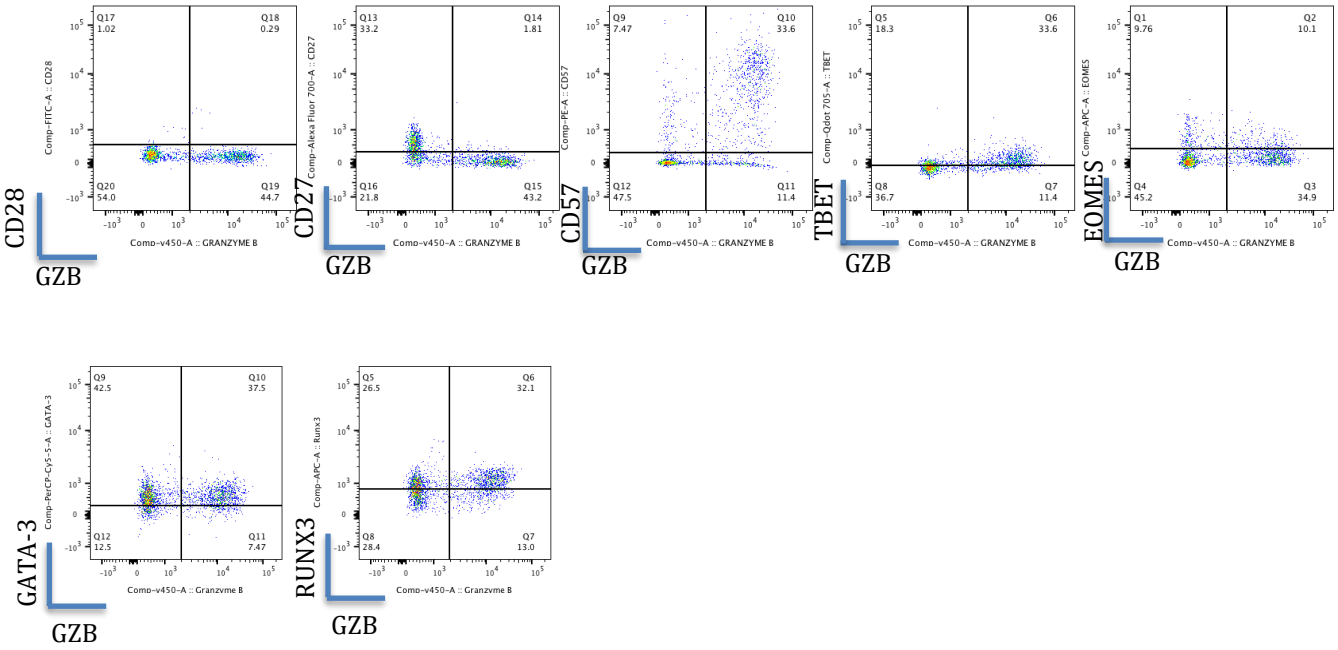

Chapter 6 Chromatin Immunoprecipitation sequencing for low cell numbers: optimisation of technique

6.1 Introduction

The previous chapters have been focused mainly on the phenotypic characteristics of the cytotoxic CD4+ T lymphocytes and their presence in the peripheral blood and tumour microenvironment of haematological malignancies. To further investigate the characteristics of CD4+ CTLs and to understand the regulation of their cytotoxic function, we decided to perform epigenetic profiling of this subset of cells. Epigenetic profiling examines the protein-DNA interactions within cells and allows for the identification of super-enhancers that are active in a specific cellular subset. The detection of these active super-enhancers can further help to identify the genes which are responsible for the particular characteristics of a subset of cells.

Understanding the epigenetic determinants of cytotoxic CD4+ T cell function and identifying the regulatory elements and genes that distinguish them from other CD4+ T cell lineages could potentially enable us to target, harness and amplify their cytotoxic function in the therapeutic setting.

Traditionally, epigenetic profiling by ChIP (Chromatin Immunoprecipitation) sequencing has been performed on relatively large numbers of cells and the protocols are usually designed for use with 10^7 – 10^8 cells. This has limited its use in the epigenetic profiling of rare immune cellular subsets. The number of CD4+ CD57+ cells in the peripheral blood samples of CLL patients is less than 10^6 and often as low as 10^5 (from the samples of 20mls of whole blood after electronically cell-sorting) which has restricted the application of ChIP protocols to this cellular subgroup. There have been, however, recent advances in the optimisation of ChIP protocols for small cell numbers. For example, Seumois *et al* [145] performed an epigenomic analysis of Th2 memory cells in patients with asthma using a protocol optimised to be applied to 10^5 cells.

Our aim was to optimise a ChIP protocol for use with low cell numbers, based upon the Seumois *et al* paper [145], which would then enable us to proceed to perform ChIP sequencing of the CD4+ CTLs and identify the epigenetic determinants of their cytotoxic function.

6.2 The principle of Chromatin Immunoprecipitation (ChIP)

Chromatin Immunoprecipitation (ChIP) is a technique used to enrich an area of chromatin that encompasses a specific antigen by using immunoprecipitation of protein-DNA complexes which are bound to antibodies. ChIP sequencing refers to the combination of the technique of Chromatin Immunoprecipitation with next generation sequencing which allows for the enrichment of DNA sequences that are bound to a certain protein. ChIP enables the examination of the interaction of proteins with DNA sequences which allows for the identification of the binding sites of these DNA-associated proteins.

Chromatin is comprised of DNA and histone proteins which together form the nucleosome. The associated histone proteins serve to regulate the chromatin functions which include the repair of DNA and the regulation of gene expression. Modifications in the histone proteins, for example by methylation or acetylation, can affect the binding of transcription factors to specific DNA regions.

The ChIP technique is a complex, multi-step process and each step needs to be optimised to ensure the accurate success of the method. Briefly, the process involves the cells undergoing a reversible cross-linking process where the aim is to bind the DNA to its proteins to preserve the DNA-protein interaction. The cells can then be frozen and thawed at a later date for analysis. Next, sonication is used to shear the chromatin into fragments, aiming for a size of 200 – 1000bp. Immunoprecipitation of the DNA-protein complexes is performed by the addition of antibodies to the chosen antigen region of interest, for example, a protein or protein modification. Following immunoprecipitation, the DNA-protein complexes' cross-links are reversed and qPCR is performed using primers specific for relevant promoters.

As mentioned above, the previous major limitations of the technique included the need for large numbers of cells (in the region of 10^7 – 10^8 cells) as a starting material and also the length of time for the procedure, which often took many days.

6.3 Aims

The aims of this chapter were:

1. To optimise the chromatin immunoprecipitation (ChIP) techniques for small cells numbers (eg 1 x 10^6 and 1 x 10^5 cells), in particular the optimum sonication settings required for DNA fragment generation.

2. The optimization of the ChIP technique would then allow for ChIP-seq by next generation sequencing to identify the epigenetic determinants of cytotoxic CD4+ T cell function and the regulatory elements and genes that distinguish them from other CD4+ cell lineages.

Cell sorting strategy

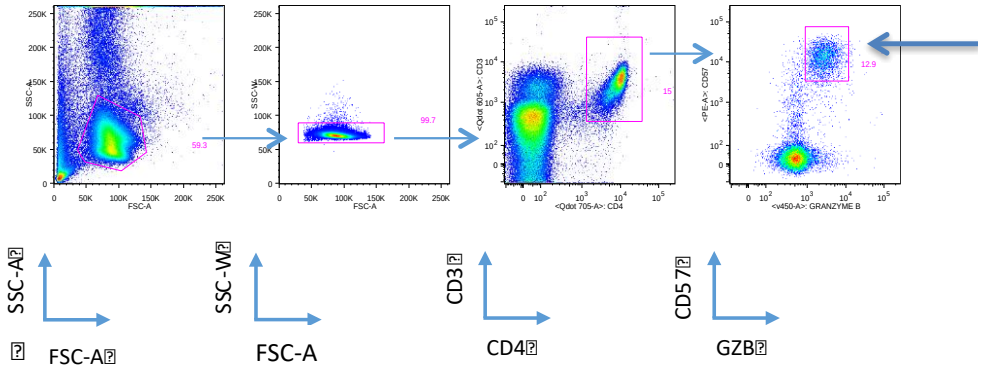

Figure 6-1: The cell sorting strategy for identifying CD4+CD57+ cells which are Granzyme B positive from the peripheral blood of patients with CLL.

A. Pre-selection

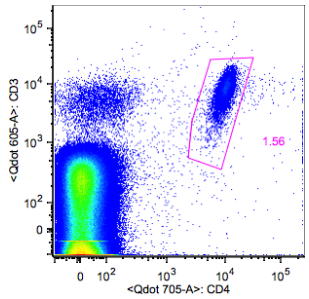

B. Post-selection

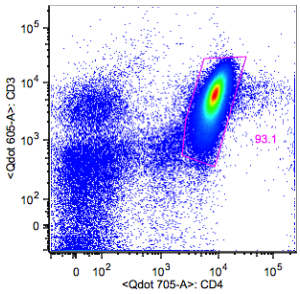

Figure 6-2: The negative selection for CD3+CD4+ cells from the peripheral blood of healthy donors. Figure 6-2A shows the cells pre-selection and Figure 6-2B shows the cells post-selection with enrichment of the CD3+CD4+ cells.

6.4 Samples used for ChIP optimisation

The optimisation experiments were performed on total CD4+ cells which were isolated from the blood of healthy donors. Eighty millilitres (80mls) of whole blood was obtained from healthy donors by venesection and peripheral blood mononuclear cells (PBMCs) were isolated from the whole blood. The PBMCs were then labelled and CD4+ cells were negatively selected using magnetic Miltenyi beads kits. The isolated CD4+ cells were tested for purity using a small sample which were stained for flow cytometry analysis (Figure 6.2).

The CD4+ cells were then counted and separated into aliquots of different cell amounts (1 x 10^5 and 1 x 10^6 cells) for cross-linking.

6.5 Cross-Linking Protocol

The purpose of cross-linking is to reversibly bind the DNA to its protein to preserve this interaction for later epigenomic profiling. Traditionally, this is performed by the use of Formaldehyde. In essence, 11% formaldehyde was added to the negatively selected CD4+ cells and these cells were left at room temperature for 20 minutes. The cross-linking reaction was then stopped by the addition of 2.5M glycine and the cells were washed twice with PBS (phosphate-buffered saline). The aliquots were then “flash-frozen” in liquid nitrogen and transferred to the -80^{o}C freezer for storage. The timing of cross-linking needs to be optimised because if the samples are cross-linked excessively, the result is a decrease in the quantity of protein that is linked to the DNA. Conversely, if the cross-linking is too brief, the protein-DNA binding may not be adequate to preserve the DNA-protein association which is essential for epigenomic analysis.

6.6 Sonication efficiency

The purpose of sonication in ChIP experiments is to use ultrasound waves to shear the chromatin into small fragments (typically of 200bp – 1000bp) and enables the chromatin to become soluble. This is an essential step in the protocol because if the samples are under-sonicated, the resultant relatively large fragments could increase the risk of non-specific binding. Over-sonication should also be avoided as this would result in small fragments which could increase the risk of protein disruption and may reduce the chance of primer detection in the PCR experiments. The machine used for the sonication experiments was the Bioruptor Pico sonication system (Diagenode) which enabled up to 6 samples to be concurrently sonicated, thereby reducing experimental variation. The aim of the initial experiments was to assess the appropriate sonication settings to ensure adequate chromatin shearing for low cell numbers. Samples of 1×10^5 and 1×10^6 CD4+ cells were used in the experiments.

6.6.1 Agarose gel electrophoresis to assess sonication quality

To assess sonication efficiency, the CD4+ cells which had previously been cross-linked and frozen were thawed, lysed and sonicated (at different sonication settings). The cross-links were then reversed, using proteinase K, and the DNA was isolated. The DNA concentration was assessed using the Nanodrop machine and then the sonication efficiency was assessed by agarose gel electrophoresis. The full protocol is detailed in Chapter 2. A summary flow-chart of the experiment is shown in Figure 6.3.

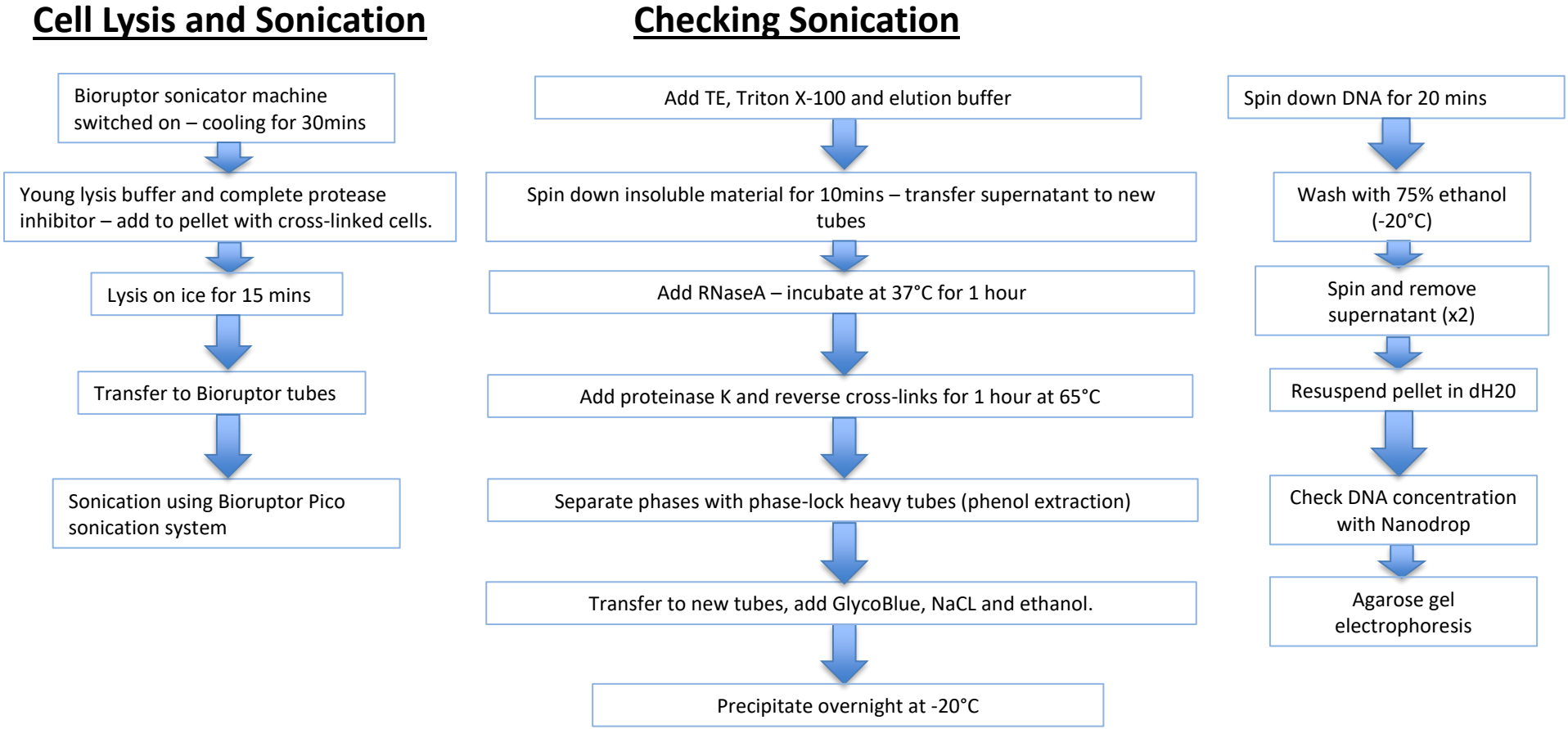

Figure 6-3: A summary flow-chart of the protocol for checking sonication efficiency.

An initial experiment was performed to check the sonication efficiency using 2 different lysis buffers – Young's lysis buffer 3 and an alternative lysis buffer (used by Seumois et al [145]). The experiment was performed using 1 x 10^6 CD4+ cells. The cells had been sonicated for different numbers of cycles but with the same on/off settings for each cycle – on for 25 seconds and off for 30 seconds. The cycle lengths tested were 7, 12 and 20 cycles for both buffers. One extra sample was sonicated for 4 cycles with the Young's lysis buffer. The results are shown in Figure 6.4 and 6.5. Figure 6.4 shows that there is variability in the DNA concentration obtained with the ranges of 50 – 200 ng/ul demonstrated. Figure 6.5 shows the most sonication exhibited for 12 and 20 cycles of sonication for both buffers. The 4 and 7 cycle samples which used the Young's lysis buffer 3 were under-sonicated. Therefore, it was concluded that the optimum sonication settings were likely to be between 7 and 12 cycles.

The next experiments were performed to further elicit the optimum number of sonication cycles for different numbers of cells as a starting material. Using three different cell numbers (1 x 10^6, 1 x 10^5 and 5 x 10^4 cells), duplicate runs of either 9 or 10 cycles of sonication were performed (Figure 6.6A). The DNA quantification was variable between 40ng/ul -140 ng/ul (Figure 6.6B). Figure 6.6A shows that the gel results were of insufficient quality to determine sonication efficiency. The experiment was repeated using 1 x 10^6, 5 x 10^5 and 5 x 10^4 cells at 8, 9, 10 and 11 cycles of sonication (Figures 6.7A-D). These results show, however, that the samples were not sonicated adequately, as indicated by the band at the top of the gel for each sample.

To elicit the cause of the inadequate sonication of the samples, an experiment was performed to compare the Bioruptor Pico machine, which had been used, with a second Bioruptor sonication machine.

A simple experiment was performed with 1 x 10^6 cells to compare the two different machines. The “on” time was increased to 30 seconds and the “off” time was kept at 30 seconds. The cycle numbers that were tested were 7, 12 and 20. In this experiment, it is shown that the original Bioruptor Pico machine achieved better sonication of the samples than the second machine (Figure 6.8A). This showed that the original Bioruptor Pico machine was functioning and a repeat test was performed to confirm these finding (Figure 6.8B). This did not, however, explain the variability in sonication quality between the tests.

6.7 Agilent Bioanalyser to assess sonication quality

One possible cause for the variation in the ability to assess sonication efficiency may have been that agarose gel electrophoresis was not the most sensitive technique for the sonication of low cell numbers. We decided to check the sonication efficiency by using high-sensitivity DNA chips with the Agilent Bioanalyser machine. Figure 6.9 shows the results of an experiment examining different sonication cycles (7, 12, 20, 28 and 36 cycles) for 1 x10^6 and 1 x 10^5 CD4+ cells. The samples were diluted to 450pg/ul, as per the standard Jenner lab protocol, and one sample was undiluted as a comparison (Sample 11, 1 x 10^6 cells, 12 cycles). The electrophoresis showed that the samples that had been diluted to 450pg/ul did not record a tracing of sonicated DNA, whereas the undiluted sample showed a peak which reflected a sample that was too concentrated for analysis. This led to the conclusion that diluting the samples to 450pg/ul was making the samples too dilute for adequate analysis of sonication efficiency.

6-4.

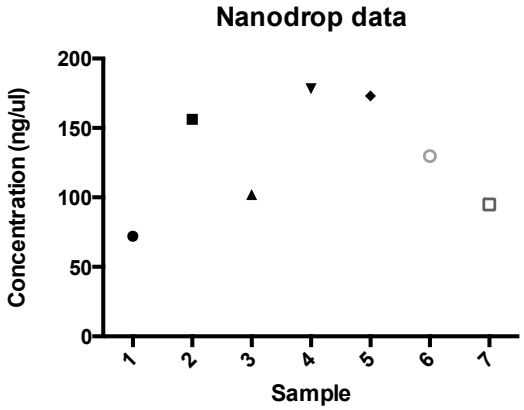

Figure 6-4: The DNA concentration, as assessed by the Nanodrop machine, for samples 1-7 which had been exposed to different sonication settings (each sample contained 1 x 106 cells).

6-5.

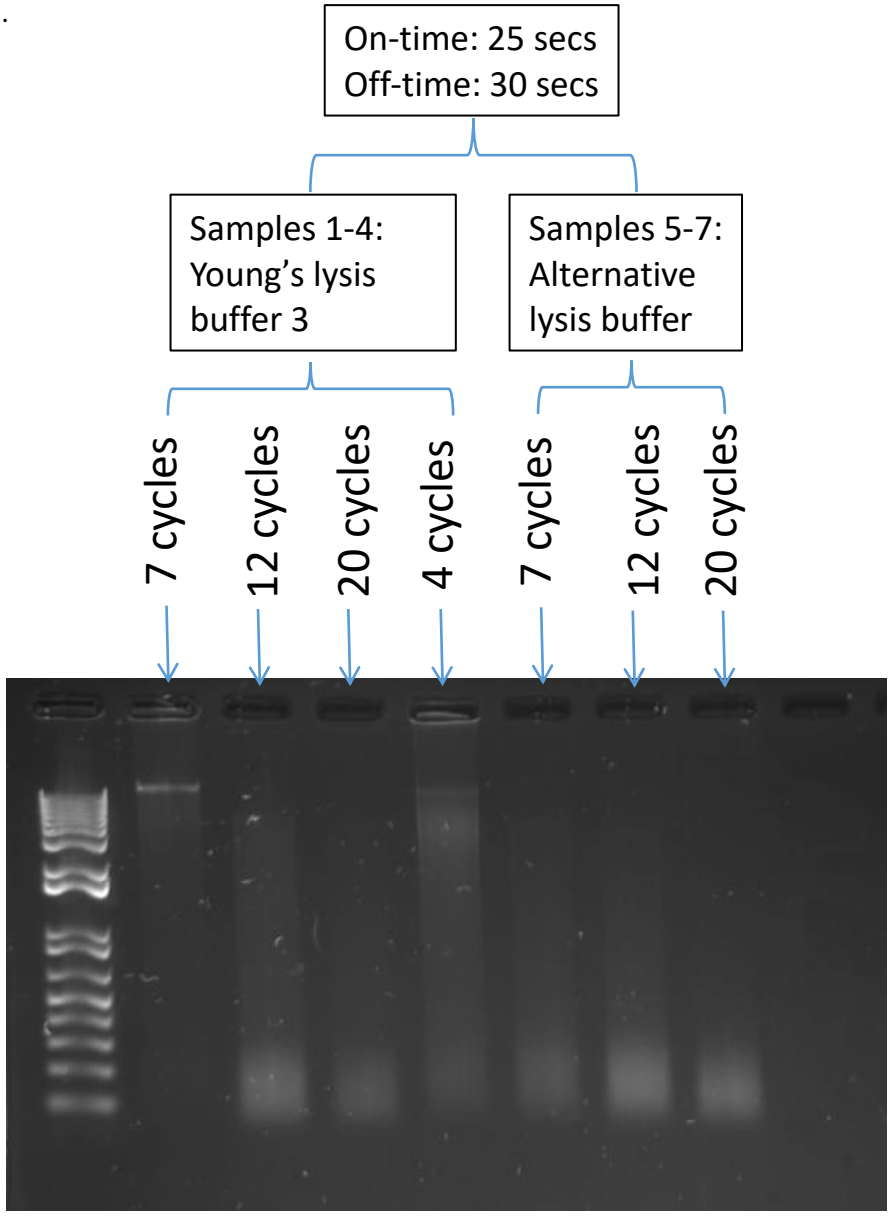

Figure 6-5: The agarose gel of the same 7 samples (listed from 1-7 from left to right on the gel).

A.

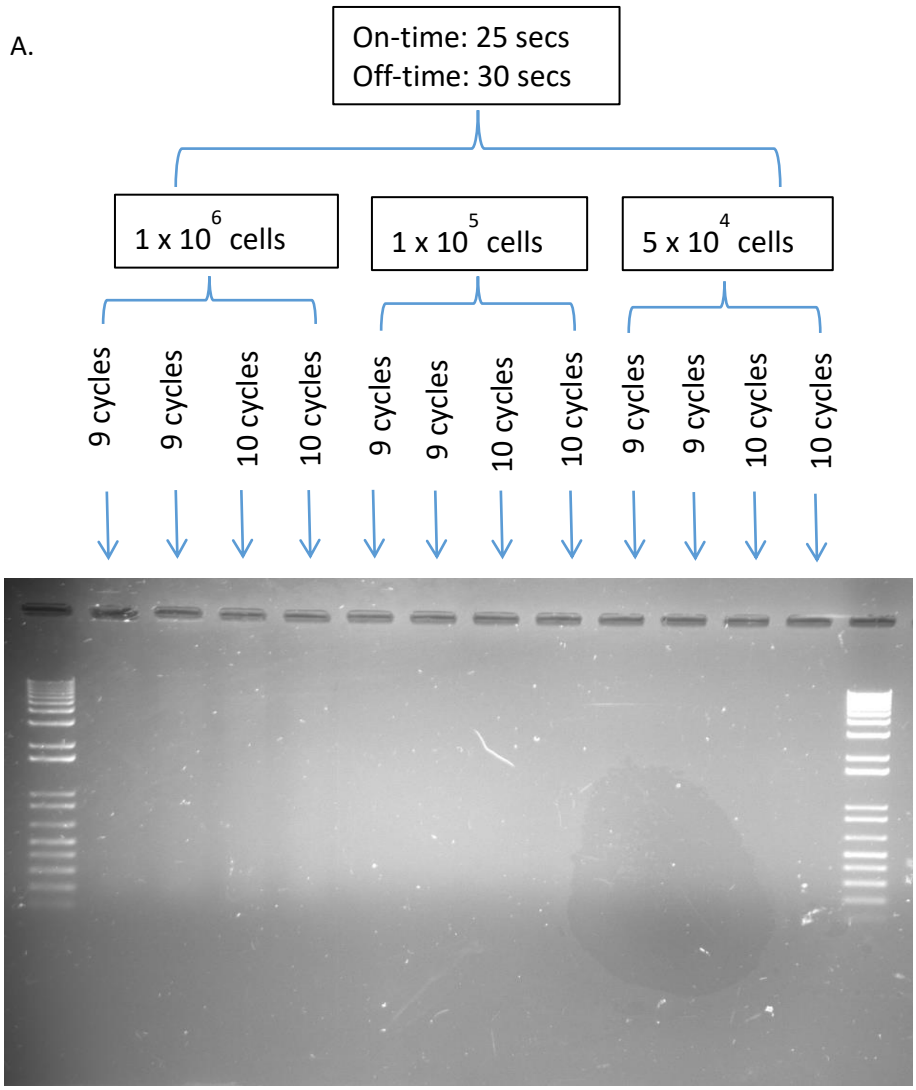

B.

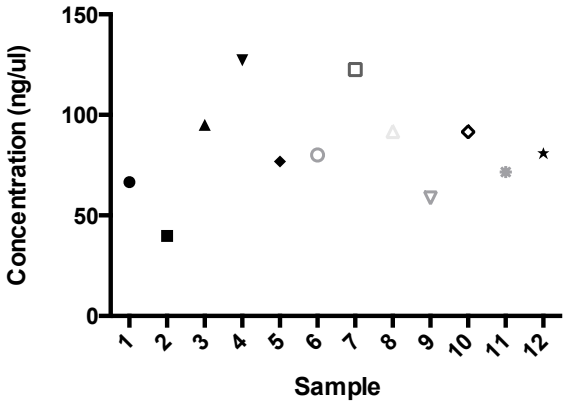

Figure 6-6: (A+B) Different sonication setting with different starting quantities of CD4+ T cells. Figure A shows the agarose gel electrophoresis for different sonication setting with different starting quantities of CD4+ T cells. Figure 4B shows the DNA concentration for each of the same 12 samples as assessed by the Nanodrop machine.

A.

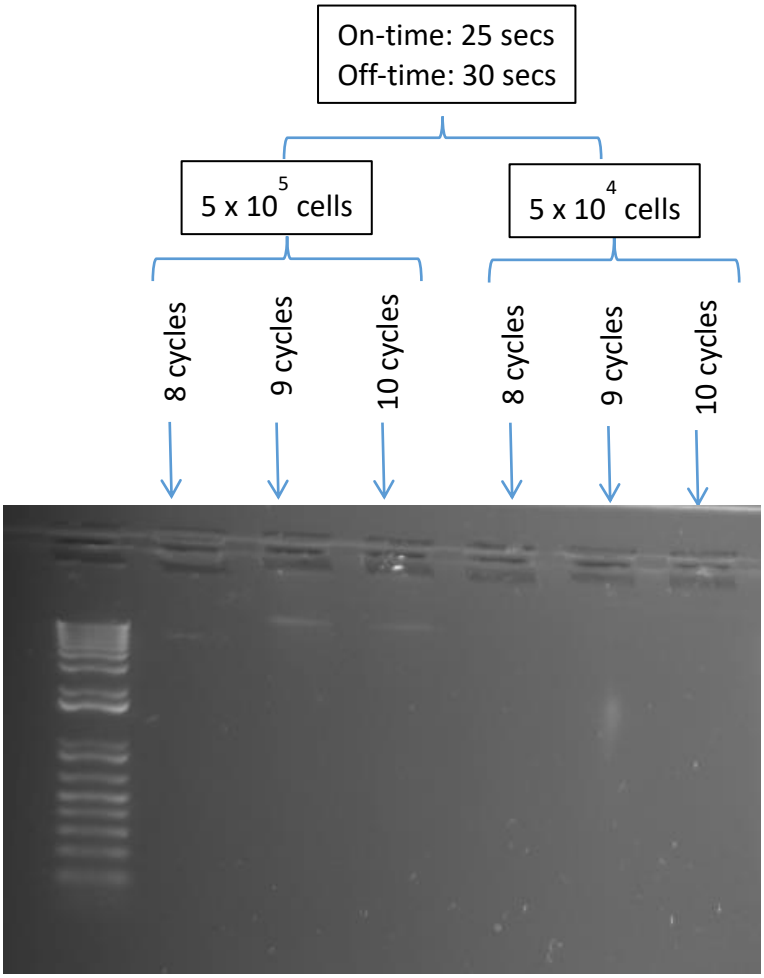

B.

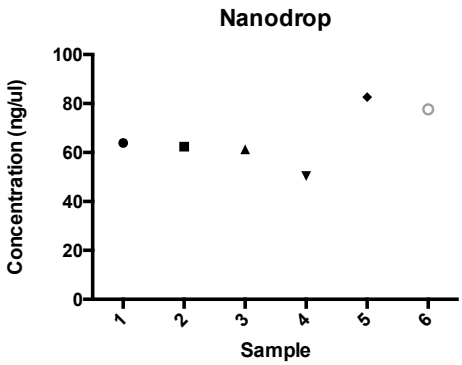

C.

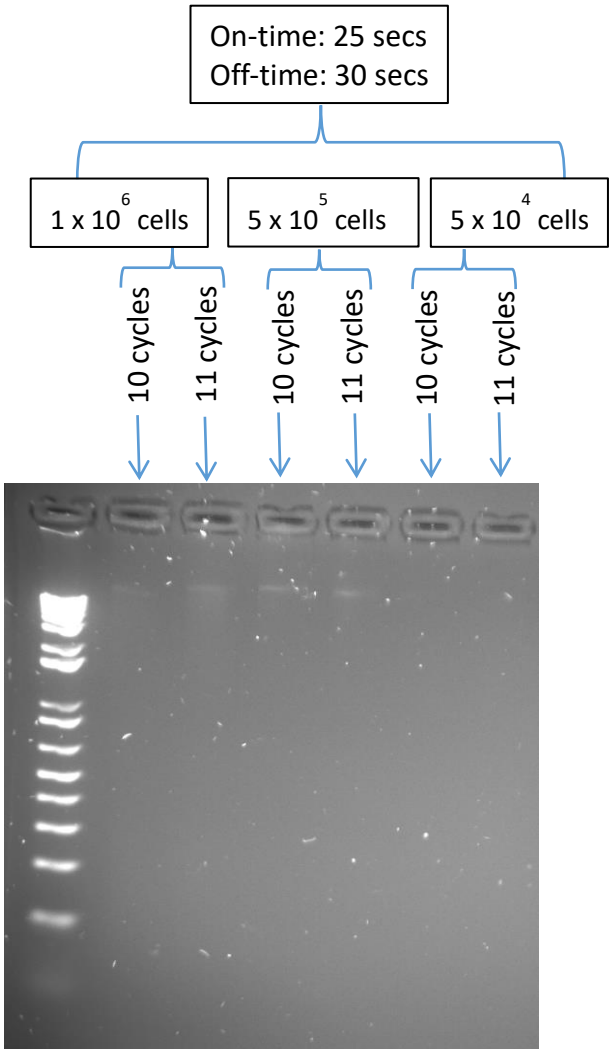

D.

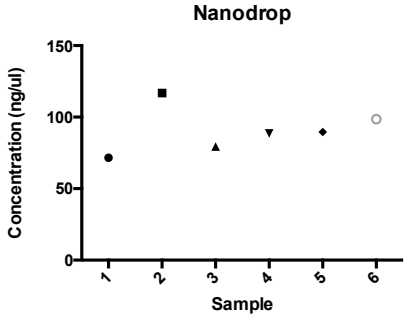

Figure 6-7: (A-D) The testing of different sonication setting with different cell numbers. Figure B and D show the DNA concentration as quantified using the Nanodrop machine.

A.

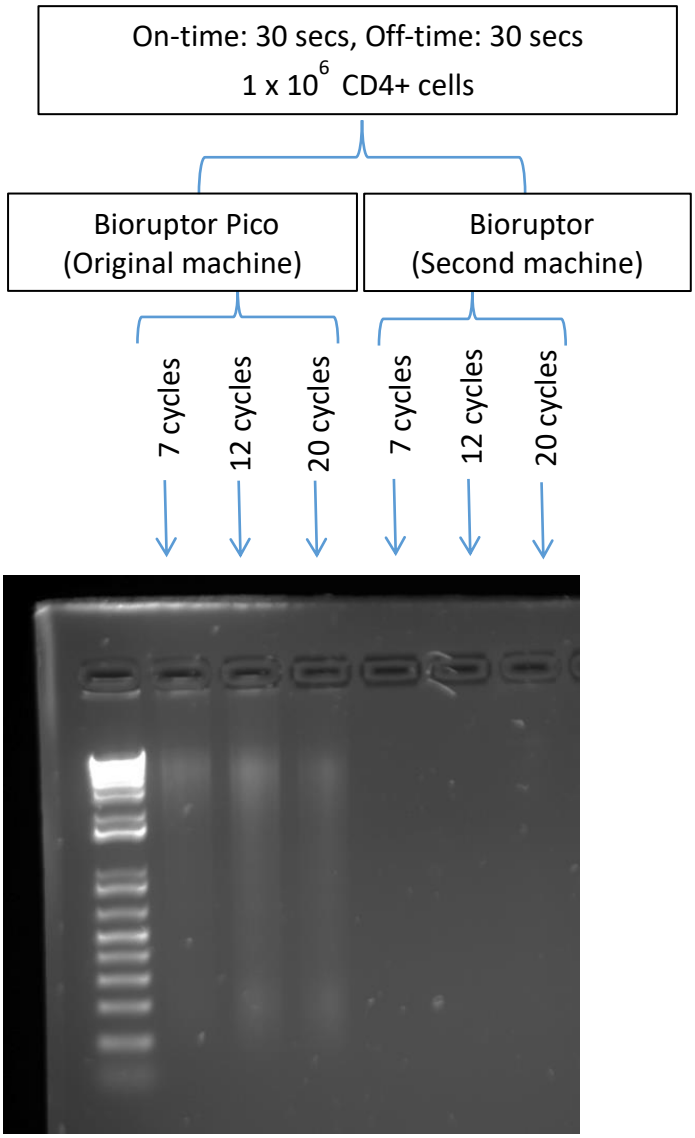

B.

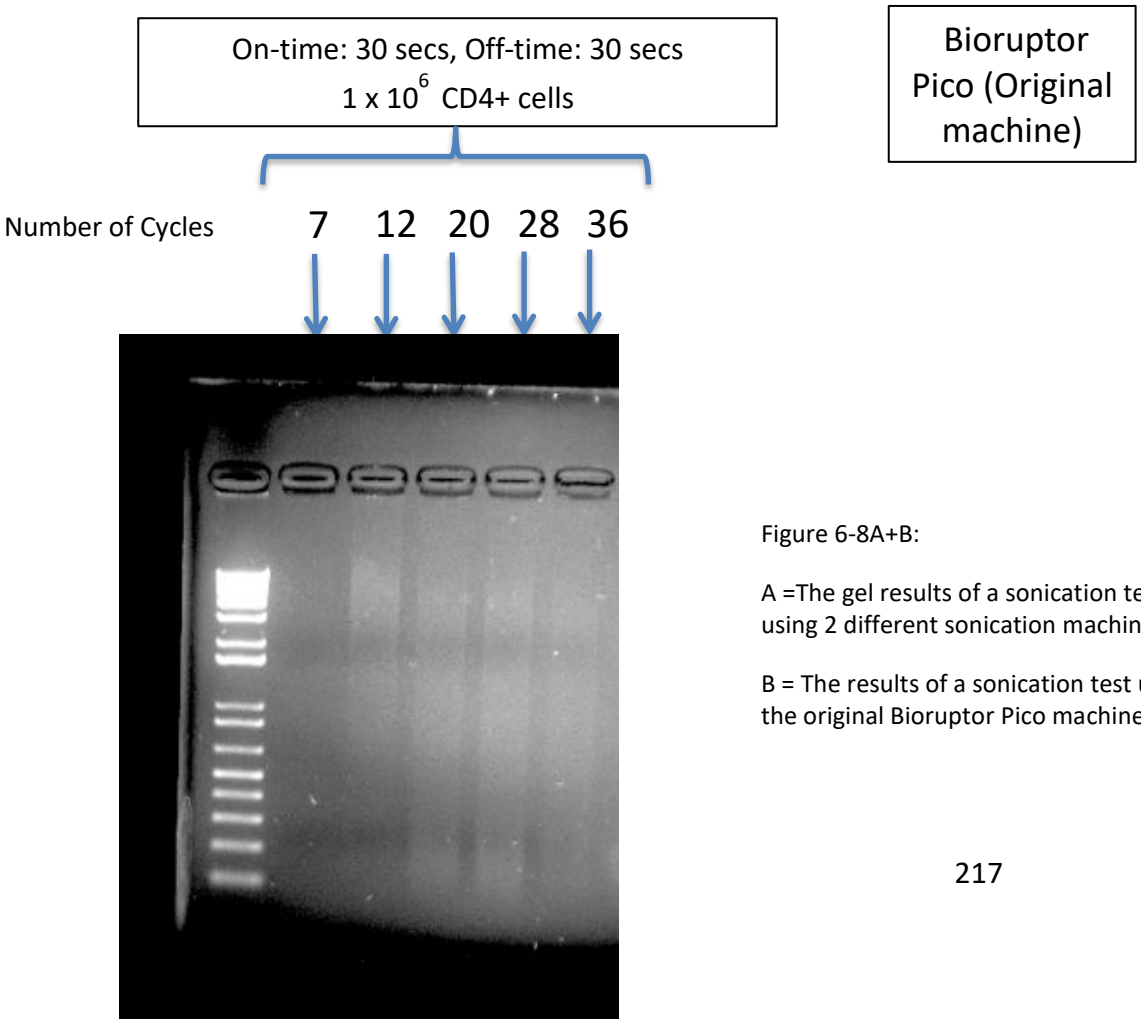

Figure 6-8A+B:

A =The gel results of a sonication test using 2 different sonication machines.

B = The results of a sonication test using the original Bioruptor Pico machine.

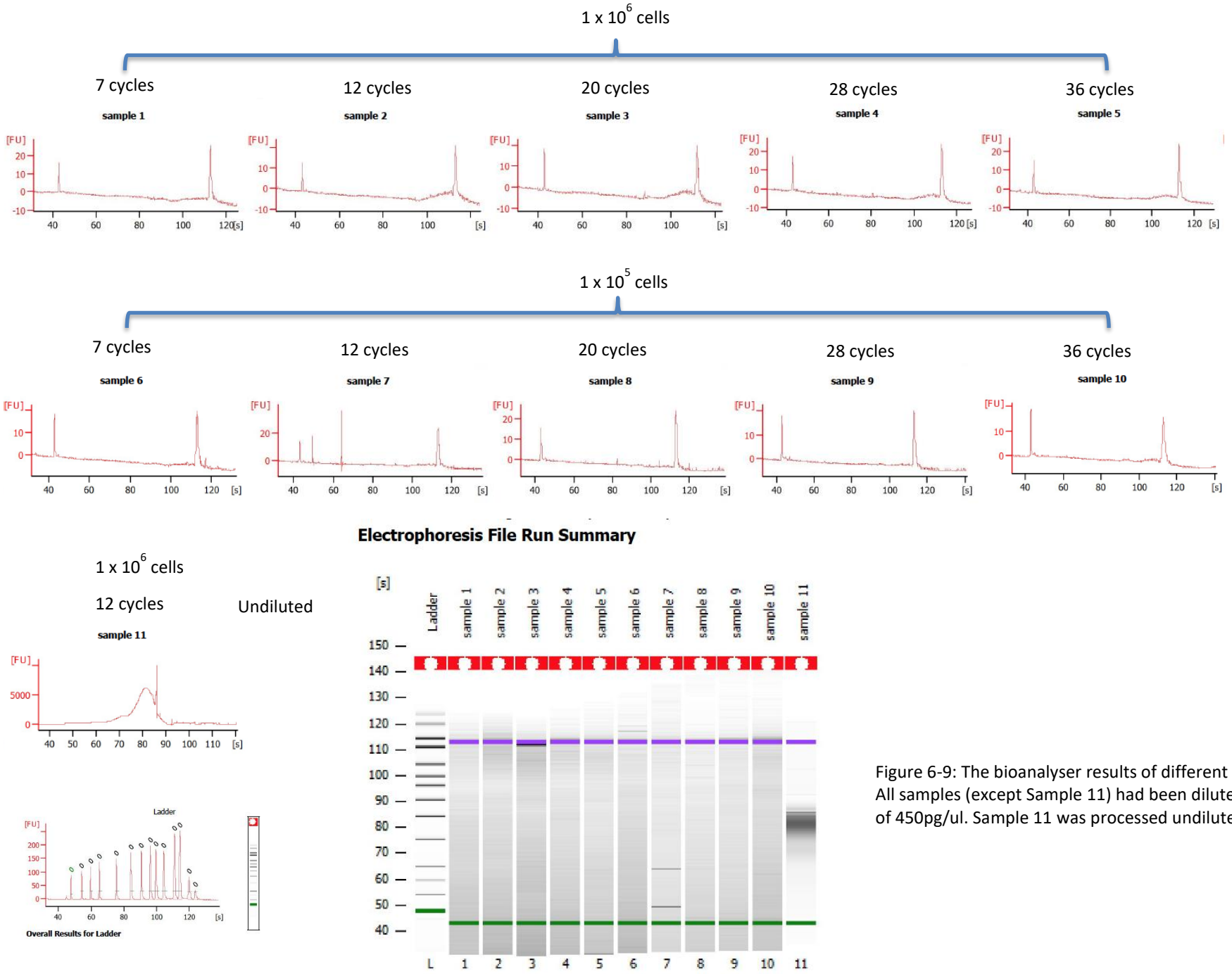

Figure 6-9: The bioanalyser results of different sonication settings. All samples (except Sample 11) had been diluted to a concentration of 450pg/ul. Sample 11 was processed undiluted.

A.

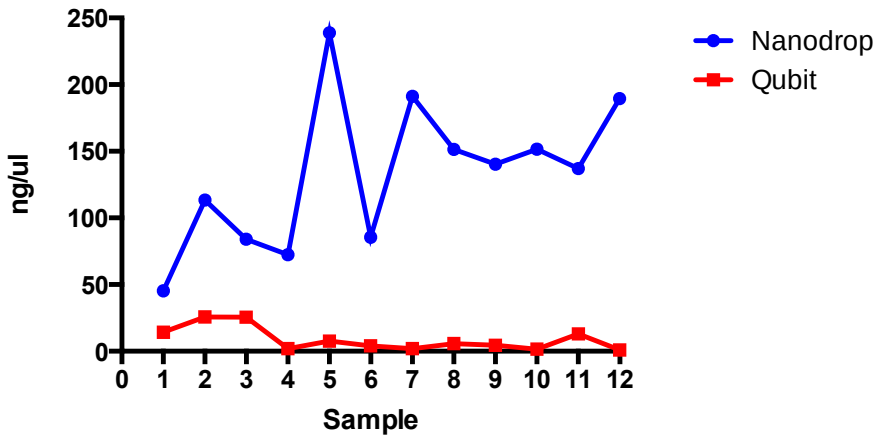

B.

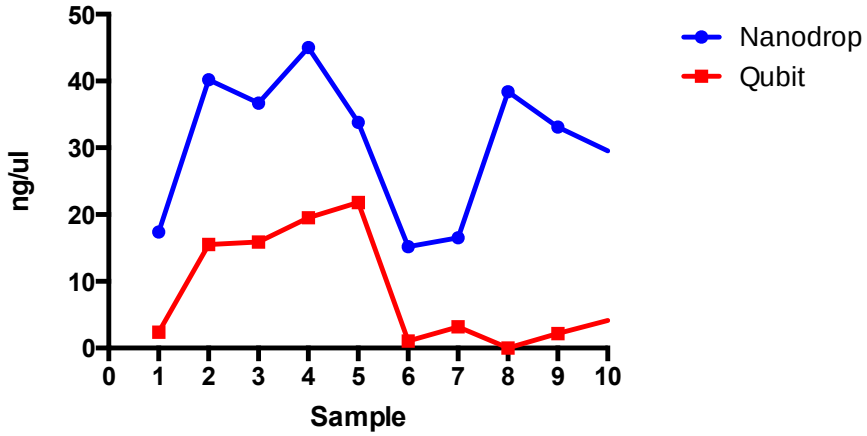

Figure 6-10: The comparison of DNA quantification by using the Nanodrop and Qubit machines on the same samples.

6.8 Quantification of DNA – Nanodrop versus Qubit quantification

Before proceeding to experiments testing different dilutions of the samples, we decided to investigate whether the Nanodrop machine was the best machine for DNA quantification from the samples of small cell numbers. The Nanodrop is a spectrophotometer that measures the quantity of light of a particular wavelength. The detection limit of DNA is reported as 2ng/ul up to 15,000ng/ul. The Qubit machine is a fluorometer that reports a detection range of 0.5ng/ml – 5ug/ml. Therefore, we performed an experiment to compare the quantification levels from two different experiments on both the Nanodrop and Qubit machines. Both experiments demonstrated that the Nanodrop overestimated the DNA quantification when compared with the Qubit machines (Figures 6.10A+B). Therefore, we decided to use the Qubit machine for DNA quantification for the remainder of the experiments performed in this chapter.

6.9 The optimum sample dilution for detection of sonicated DNA using the Agilent Bioanalyser machine.

An experiment was performed to test different dilutions of samples to elicit the optimum sample dilution for sonication assessment using the Bioanalyser machine. Using samples of 1 x 10^5 and 1 x 10^6 cells, dilutions of 500pg/ul, 1500pg/ul and 4000pg/ul were examined. These were compared with a positive control in the form of Input samples (1 x 10^8 Th1 cell line cells from the Jenner lab) which had been diluted at the same concentratios. The negative controls for the Bioanalyser machine contained no DNA sample (Figure 6.11). This experiment demonstrates that a sample dilution of 4000pg/ul is the optimum dilution for assessment of sonication (as demonstrated by the clear peak in sonication fragments at approx. 200bp).

A range of sonication cycles were then tested using 1 x 10^5 and 1 x 10^6 cells at 7, 12, 20, 28 and 36 cycles, with samples diluted to 4000pg/ul following DNA quantification with the Qubit fluorometer and analysed using the Agilent Bioanalyser machine. The results are shown in Figure 6.12. There were some samples which were analysed in the undiluted state as their Qubit measurements showed that their quantification was not high enough to obtain a concentration of 4000pg/ul. This showed that the most efficient sonication settings appeared to be 20, 28 and 36 cycles (Figure 6.12).

6.10 Adaptation of the cross-linking protocol to enhance sonication efficiency

To further enhance the sonication efficiency, we referred back to the Seumois *et al* paper's protocol [145]. The Jenner lab protocol had advised cross-linking with 11% formaldehyde for 20 minutes. The Seumois *et al* protocol, however, had only cross-linked for 10 minutes. As discussed above, the optimisation of cross-linking timing was important to ensure preservation of the DNA-protein interactions without disrupting the protein configuration. Therefore, we performed experiments on CD4+ cells which had been negatively selected from the PBMCs of healthy donors and then cross-linked with 11% formaldehyde for only 10 minutes. The experiments showed that cross-linking for only 10mins improved the sonication efficiency for the 1 x 10^6 cells for less cycles. Therefore, in this condition, 7 and 12 cycles appeared to sonicate most efficiency and 20, 28 and 36 cycles appear to oversonicate the samples (Figure 6.13). With this experiment, the samples were processed with the Bioanlayser twice in view of the lack of detection of sonicated DNA with the 1 x 10^5 cells samples. The repeat Bioanalyser analysis (Figure 6.14) replicated the same results for the 1 x 10^6 cell samples but the traces remained poor for the 1 x 10^5 cells although sonicated DNA appeared to be present in all the samples.

6.11 Comparison of DNA purification techniques

The Jenner lab protocol had recommended phenol-chloroform DNA purification using Qiagen MaXtract High Density tubes. The Seumois *et al* paper, however, had used "DNA Clean and Concentrator" columns (Zymo research) for DNA purification. The benefits of using the DNA Clean and Concentrator columns was the lack of use of phenol-chloroform, which has well-documented toxicities, the need for a fume cupboard and a shorter time of processing (2 minutes only). An experiment, using CD4+ cells which had been cross-linked for 10 minutes, was performed to compare the Phenol-Chloroform DNA purification technique with the Zymo DNA Clean and Concentrator columns. Using 1 x 10^6 cells, the samples underwent sonication with 20, 28 and 36 cycles and had been either purified using Phenol-chloroform or the Zymo columns. As is shown in Figure 6.15 there was no apparent difference in the sonication efficiency of the Phenol-chloroform purification method when compared to the Zymo columns.

6.12 ChIP optimisation with qPCR results.

A summary flow chart of the ChIP protocol is shown in Figure 6.16. Briefly, the antibody was bound to Protein G magnetic beads for 6-8 hours. The cross-linked cells underwent cell lysis and sonication. Sonication efficiency was tested on 10% of the sample using the Agilent Bioanalyser High Sensitivity DNA chip, as shown in the experiments above. The sonicated samples underwent chromatin immunoprecipitation with the addition of the antibody-bead complex to the sonicated cell lysate overnight. Next, the DNA was eluted and the cross-links were reversed. The DNA was purified using the Zymo DNA Clean and Concentrator tubes and the DNA was quantified using the Qubit fluorometer. The samples then underwent qPCR testing to assess for relative enrichment.

In our experiment, the initial ChIP experiment was performed using an antibody to H3K27ac (Abcam). This is a histone H3 modification resulting in acetylation at the 27^{th} lysine residue. It has been identified as an important mark for the identification of enhancers [146]. The CD4+ T cells, which had been negatively selected from the PBMCs of healthy donors, were stimulated using PMA and Ionomycin to ensure that IFNg was produced by the cells prior to the cells' use in the ChIP protocol. Flow cytometry was performed to ensure that the cells were producing IFNg (see Figure 6.17). Therefore, for qPCR analysis to look for relative enrichment at different sonication setting, IFNG TSS (Transcription Start Site) primer was used and ACTB UP primers were used as a negative control.

Ideally, the IFN TSS should be relatively enriched at a ratio of at least 5:1 when compared with the negative control. On the basis of the previous sonication experiments, 1×10^5 cells were sonicated at 7, 12 and 20 cycles. The 1×10^6 cell samples were sonicated at 20 cycles, 28 cycles and 36 cycles. With the 1×10^5 cells samples, although the IFNg had more relative enrichment, this was not at a ratio of 5:1. The 20 cycles sample had the largest relative enrichment but this was only at a ratio of approximately 2:1. With respect to the 1×10^6 cells, there was no apparent enrichment between the ACTB UP and IFNG TSS readings.

In view of the lack of enrichment, it was decided to run the qPCR experiment again but without the dilution of input samples prior to the run. The results of the run are shown in Figure 6.18 and this shows that there is no difference in the relative enrichment between the ACTB UP and IFNG TSS results.

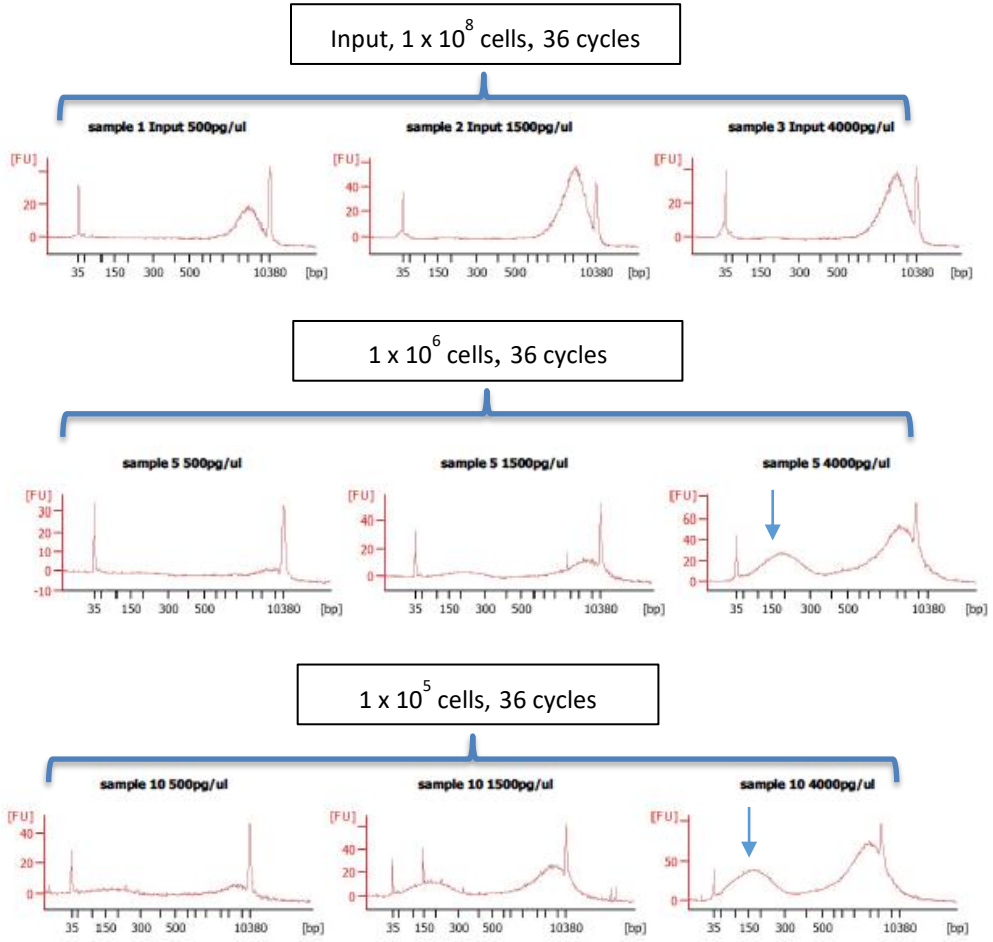

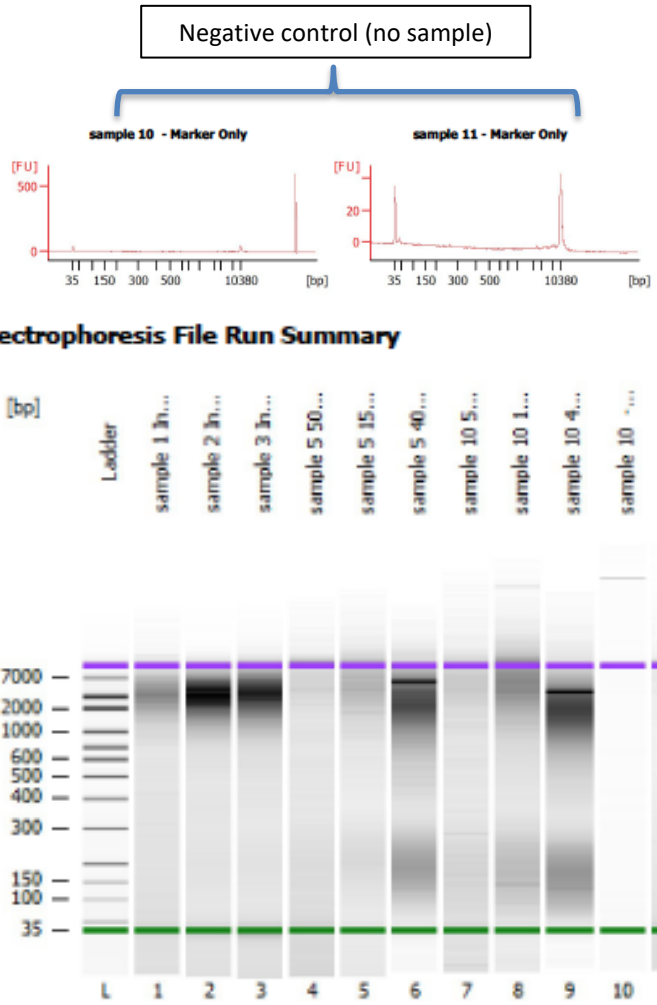

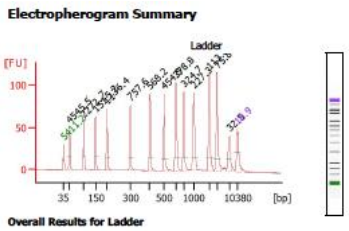

Figure 6-11: The comparison of different sample dilutions for 1 x 10^5 and 1 x 10^6 cells. The input samples were used as a positive control and the negative control consisted of runs containing the marker only and no sample. The arrows show the sonicated DNA peaks at approximately 200bp.

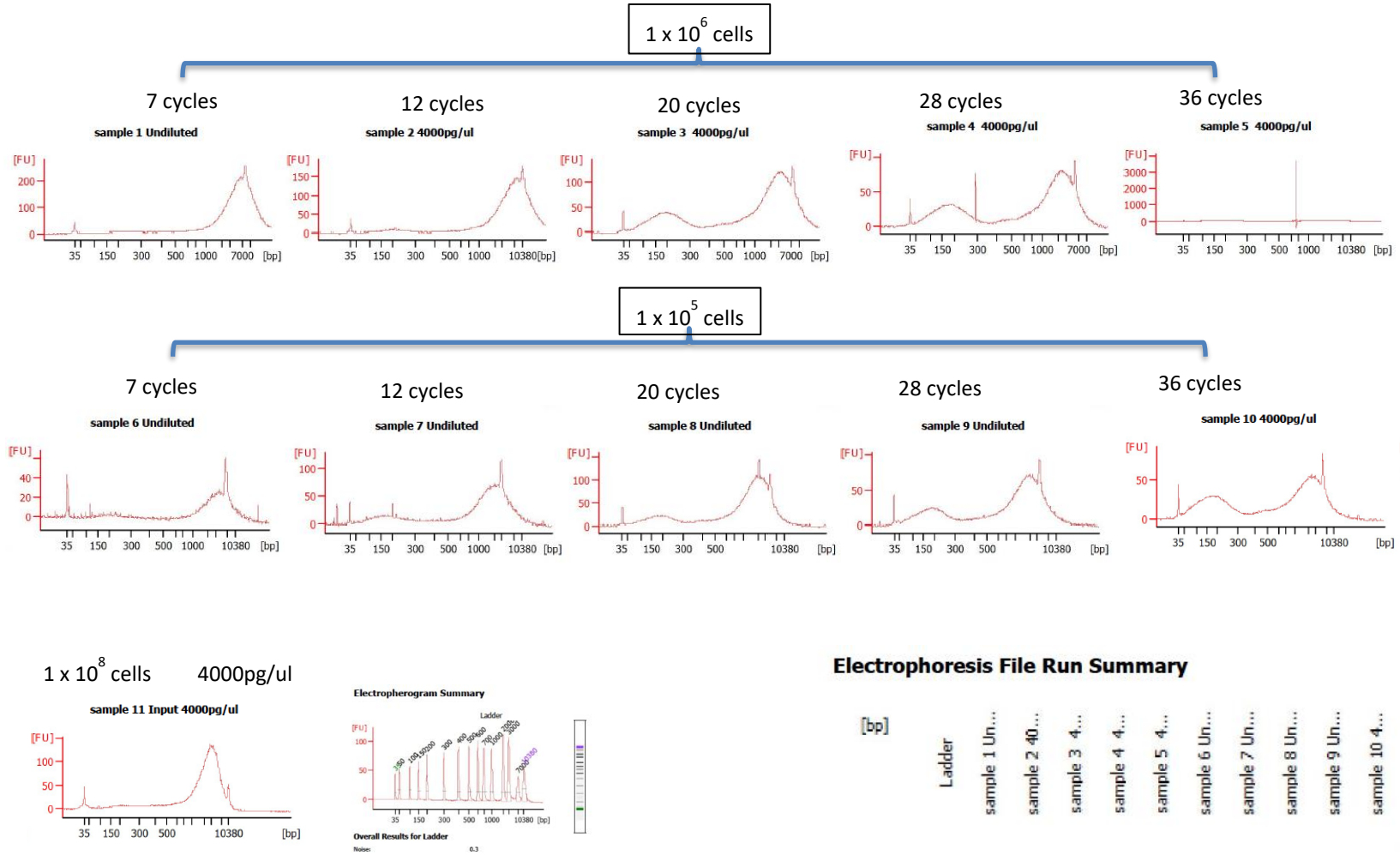

Figure 6-12: The comparison of different sonication settings for 1 x 10^5 and 1 x 10^6 cells.

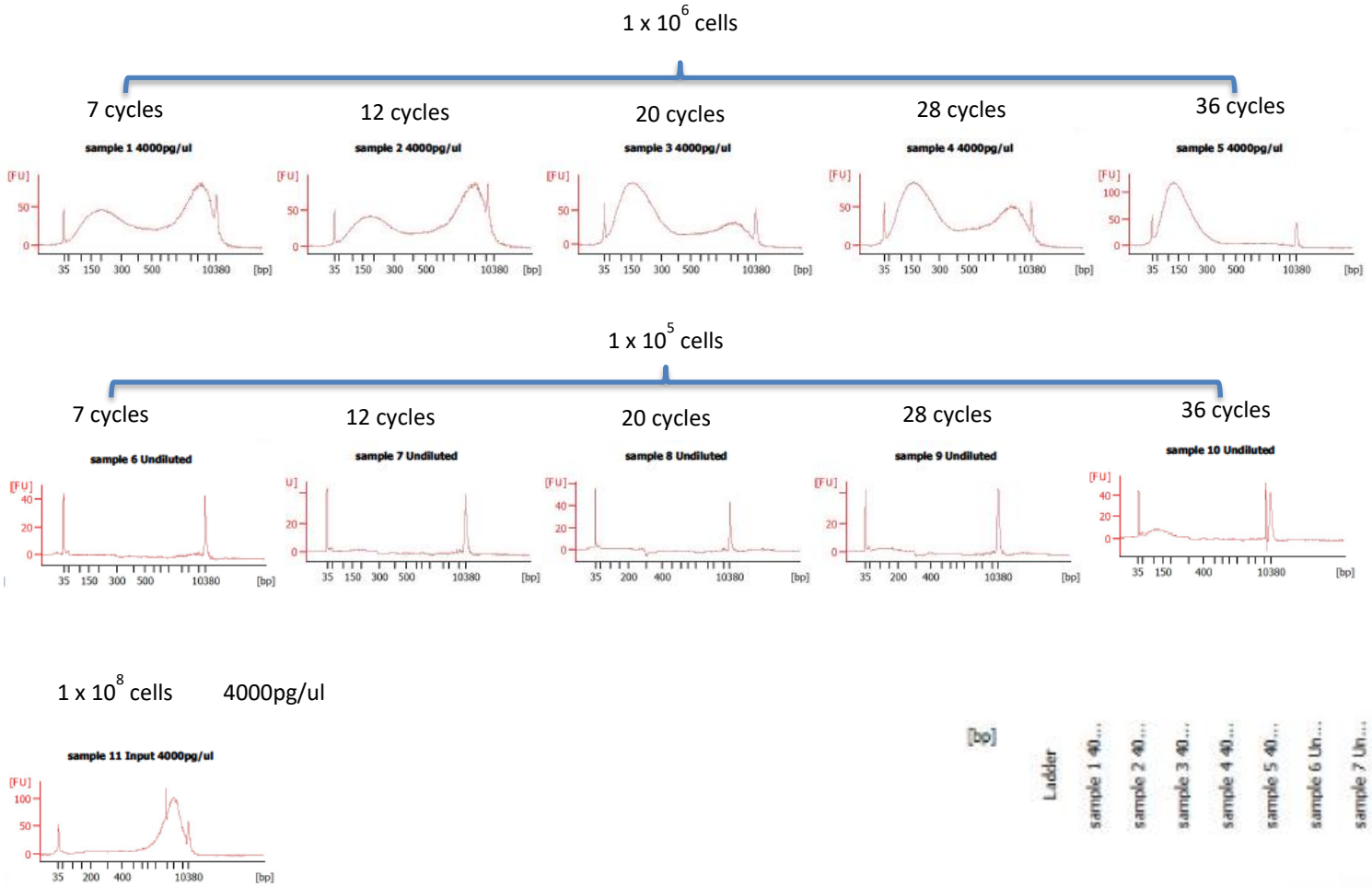

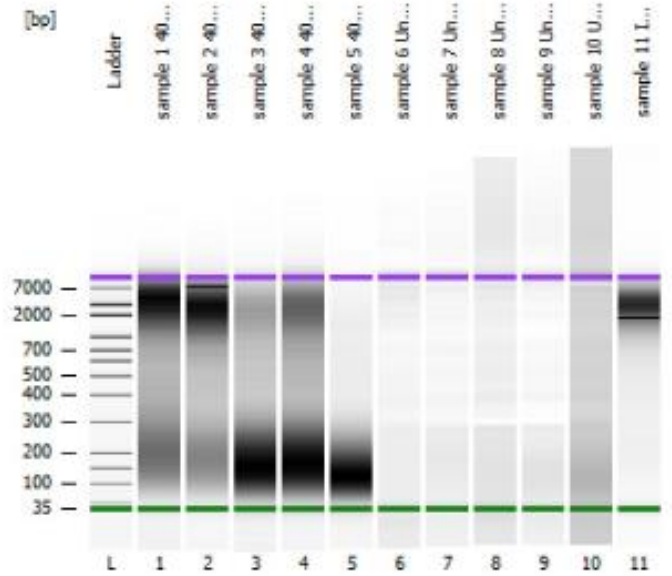

Figure 6-13: The comparison of different sonication settings for 1 x 10^5 and 1 x 10^6 cells using cells that have been cross-linked for 10 minutes only.

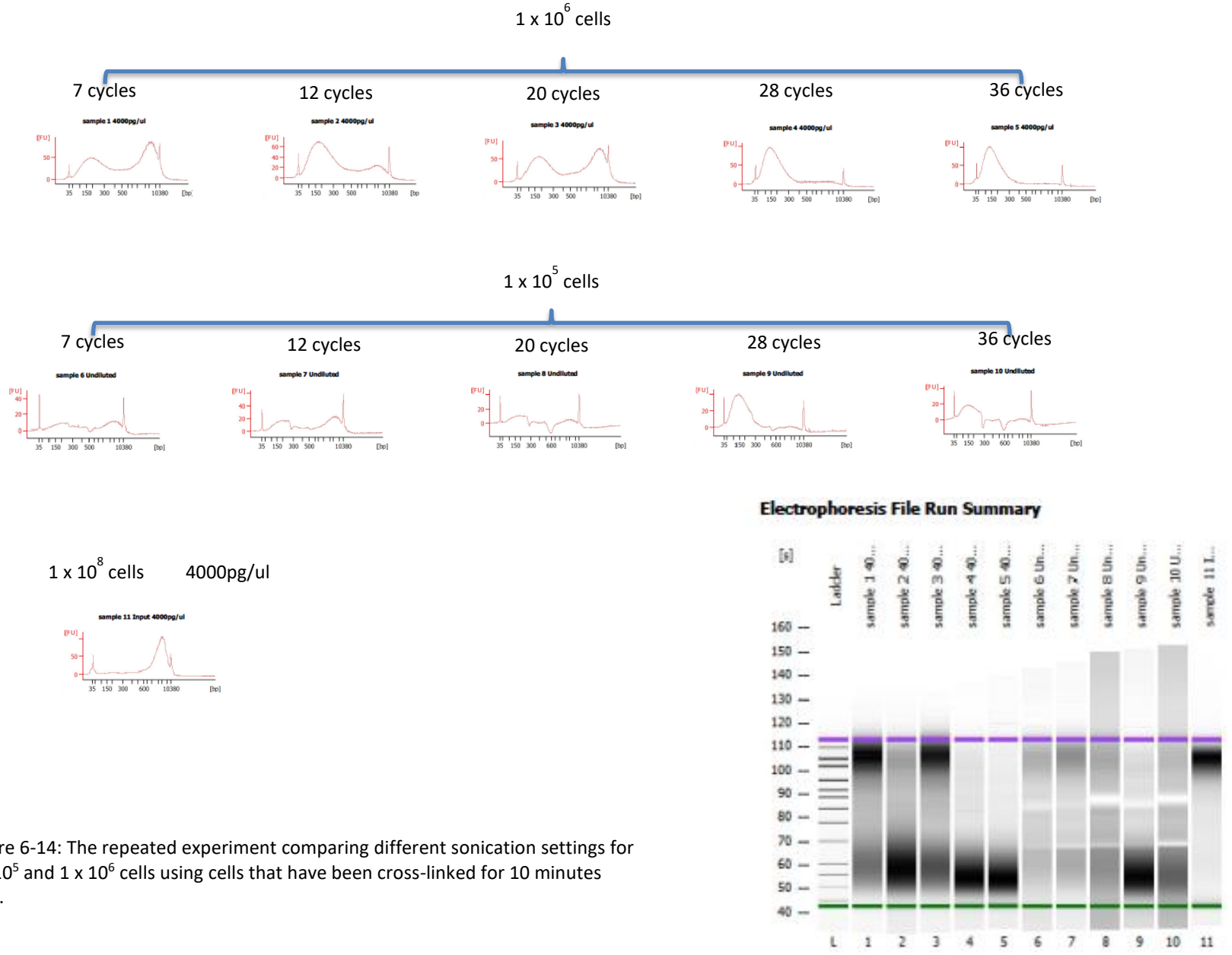

Figure 6-14: The repeated experiment comparing different sonication settings for 1 x 10^5 and 1 x 10^6 cells using cells that have been cross-linked for 10 minutes only.

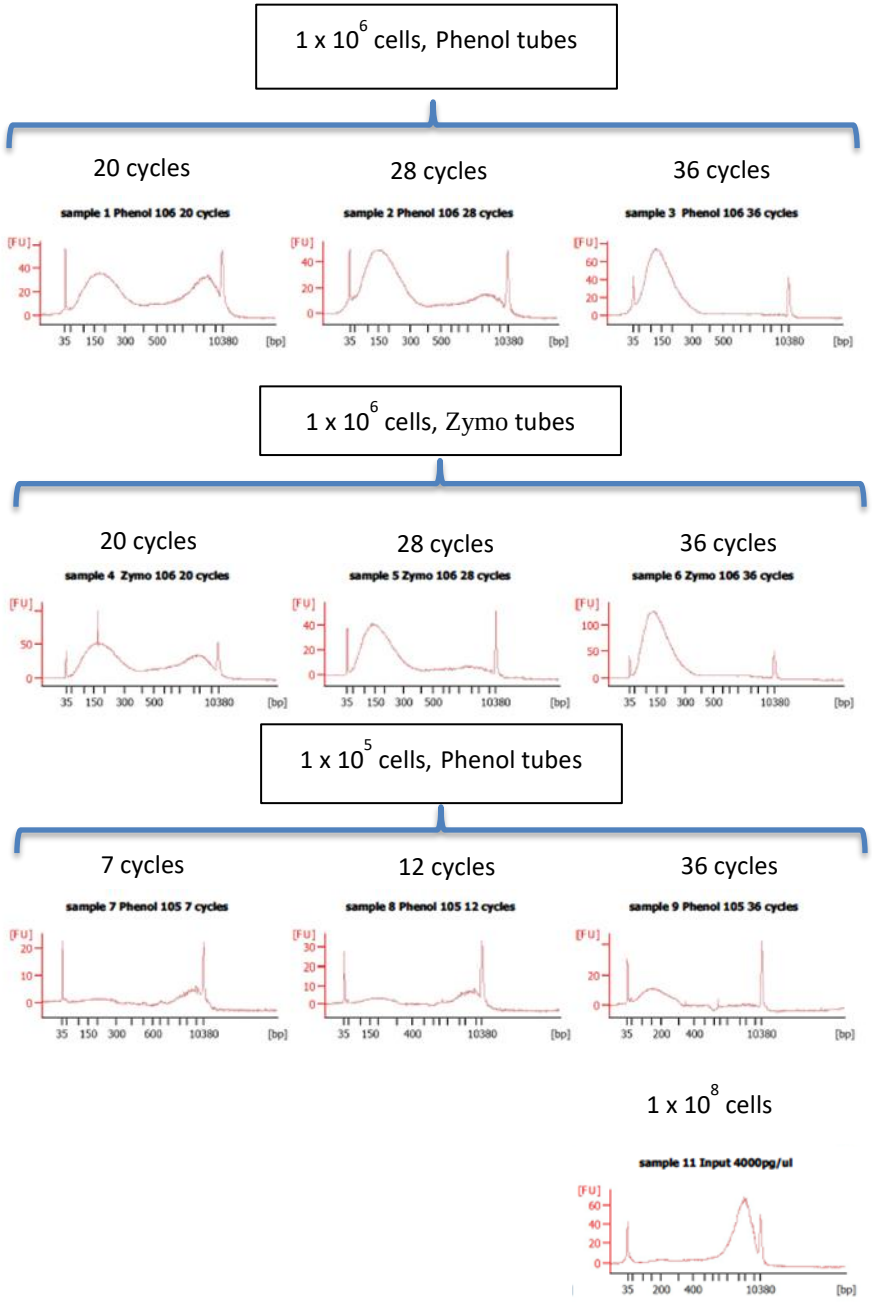

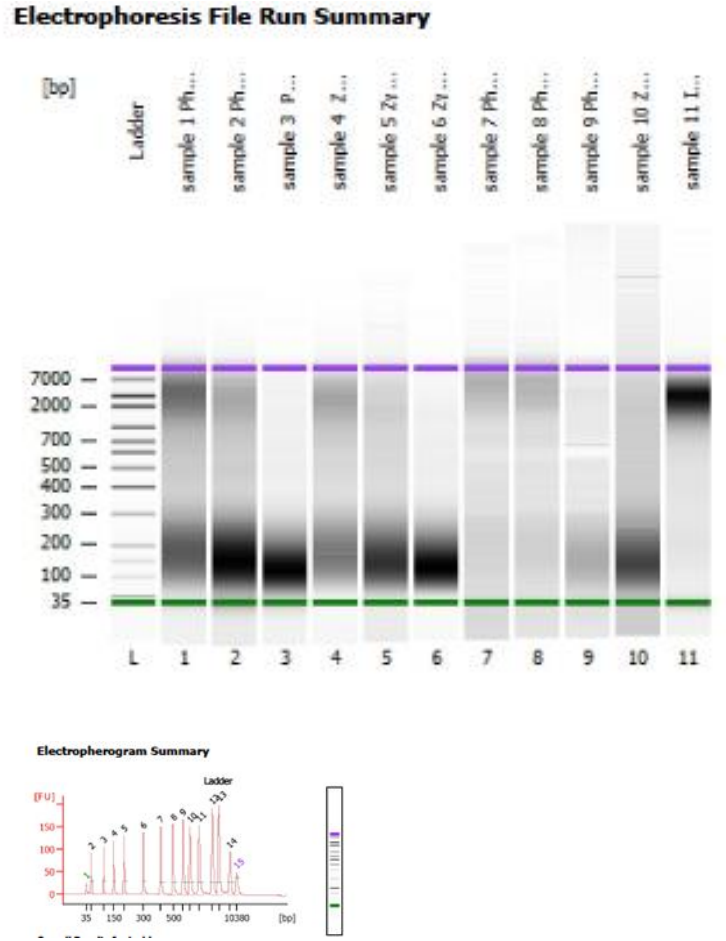

Figure 6-15: The comparison of different sonication settings for 1 x 10^5 and 1 x 10^6 cells using Phenol and Zymo DNA Clean and Concentrator tubes for DNA purification.

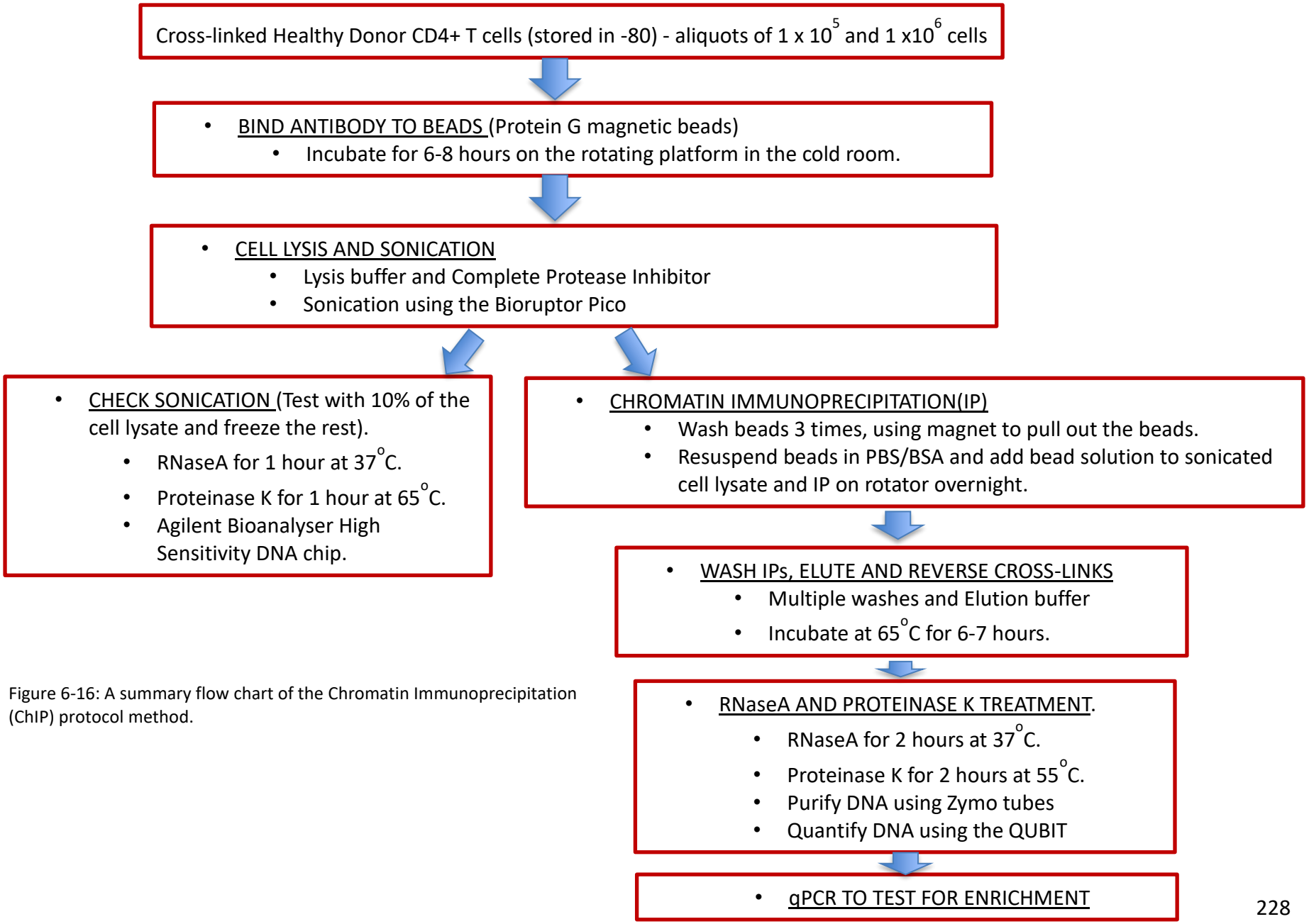

Figure 6-16: A summary flow chart of the Chromatin Immunoprecipitation (ChIP) protocol method.

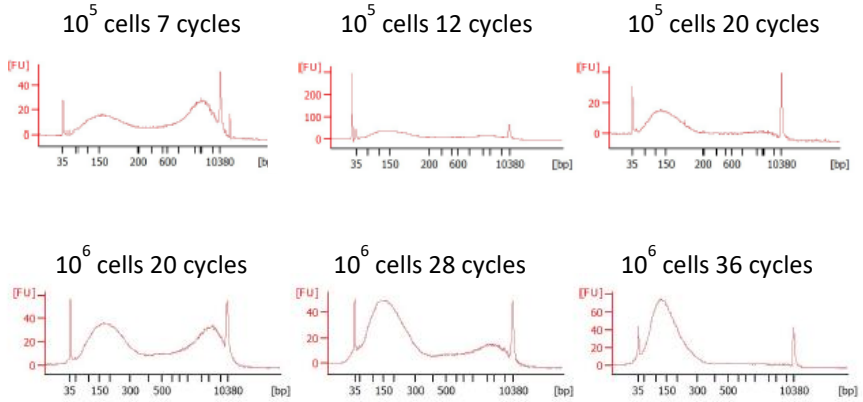

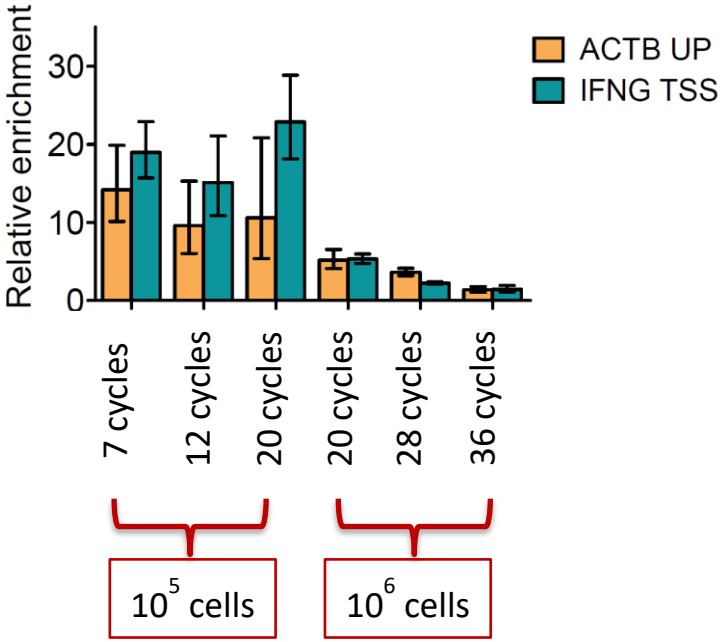

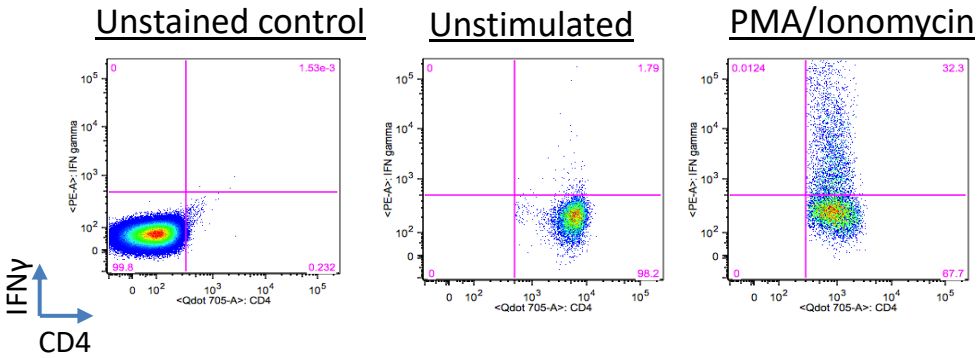

Figure 6-17: Healthy donor CD4+ T cells were selected and stimulated using PMA and Ionomycin. The flow cytometry plots show that these cells produce IFNγ (unstained and unstimulated controls are also shown). The cells were sonicated at different settings and underwent Chromatin Immunoprecipitation (ChIP). qPCR was performed to check for relative enrichment of IFN TSS (with ACTB UP used as a negative control) at the difference sonication settings.

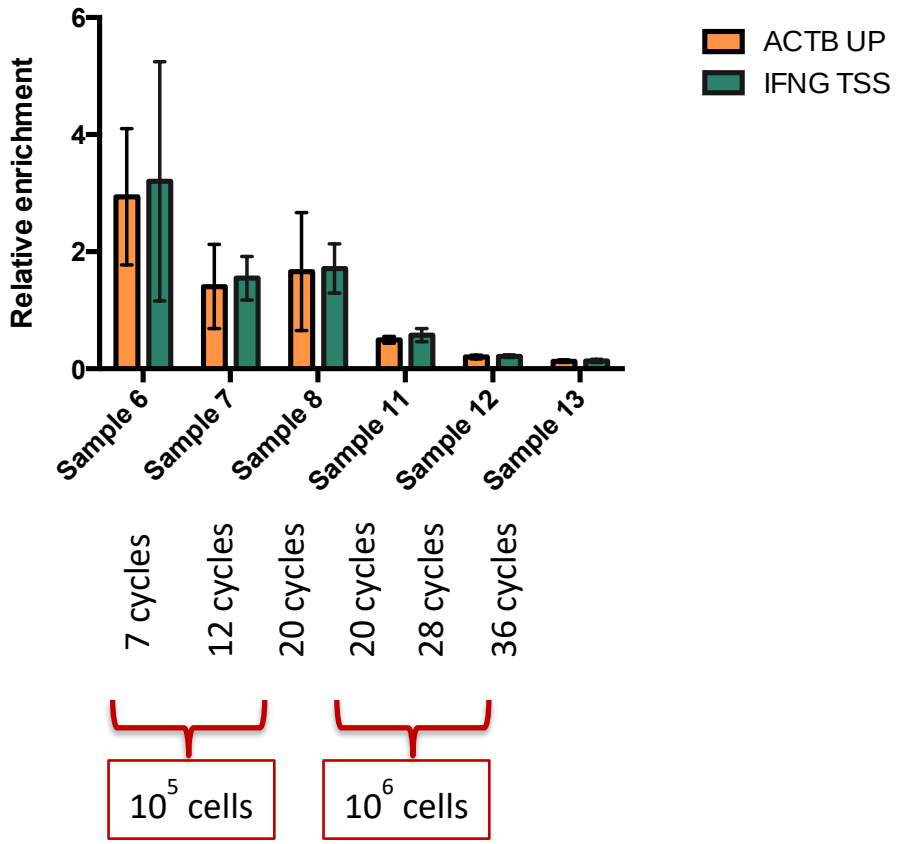

Figure 6-18: Healthy donor CD4+ T cells were sonicated at different settings and underwent Chromatin Immunoprecipitation (ChIP). qPCR was performed to check for relative enrichment of IFN TSS (with ACTB UP used as a negative control) at the difference sonication settings.

6.13 Discussion

The experiments detailed above highlight the difficulties in optimising a technique, to ensure consistent replication of results, for both sonication efficiency checks and chromatin immunoprecipitation on samples that contain small cells numbers, specifically samples of 1 x 10^6 and 1 x 10^5 CD4+ cells. It became apparent after the initial experiments that assessing sonication efficiency by using agarose gel electrophoresis was not specific enough. Although the 1 x 10^6 cell samples were visualised on occasion, it was inappropriate to assess sonication efficiency on the smaller numbers of 1 x 10^5 cells. The use of the Agilent Bioanalyser machine with the high-specificity DNA chips enabled visualisation of the sonication fragments in more detail. Furthermore, the quantification of DNA using the Nanodrop machine appeared to overestimate the amount of DNA present in the sample. This may also have resulted in the difficulties in visualising the sonicated DNA fragments. The Qubit fluorometer quantification was consistently reporting values which were less that the Nanodrop quantification for all duplicate samples analysed. Therefore, the Qubit fluorometer should be used for DNA quantification from CD4+ cell samples containing 1 x 10^6 or fewer cells. The experiments also show that the optimum sample dilution for the assessment of sonication efficiency, when using the Agilent Bioanalysis and high-specificity DNA chip, is 4000pg/ul provided that the DNA is quantified using the Qubit fluorometer.

The Phenol-Chloroform DNA purification techniques have a number of disadvantages when compared with the Zymo DNA Clean and Concentrator columns. Phenol is known to have corrosive effects on the mucous membranes, skin and eyes and should only be used for experiments performed in a fume cupboard. Chloroform can also cause eye irritation and CNS depression. The DNA Clean and Concentrator columns do not have these toxic risks associated with them. The method is also quicker than the Phenol-Chloroform purification technique and, according to the experiment performed above, does not result in a difference in sonication efficiency. Therefore, the DNA Clean and Concentrator should be considered as a reasonable alternative to the Phenol-Chloroform DNA purification technique.

The use of qPCR to assess for relative enrichment of H3K27ac showed that we were unable to demonstrate a difference between the negative control and the positive control. The question as to whether IFNG TSS was the best primer to use should be addressed. The starting material used in the experiments was negatively selected CD4+ cells from healthy donors. This sample would contain naïve CD4+ cells, as well as CD4+ cells which had differentiated into different CD4+ subsets. This would include cells that will not produce IFNg on stimulation with PMA and Ionomycin. Therefore, unlike a Th1 CD4+ cell line, which would be expected to produce higher levels of IFNg on activation, a polyclonal CD4+ group would not all be expected to produce IFNg on stimulation. Indeed, in our experiments, using flow cytometry, approximately 32% of CD4+ cells expressed IFNg. This may have affected the ability of the qPCR to detect adequate levels of relative enrichment. Therefore, one approach in the future may be to optimise the technique using a standard cell line first (a source of homogenous cells) before applying the technique to human samples.

Chapter 7 Discussion

The principle aim of this project was to characterise CD4+CTLs and to identify their presence in human cancer, particularly haematological malignancies. We have shown that they are present in the tumour microenvironment of CLL, Multiple Myeloma and both Hodgkin and Non-Hodgkin Lymphomas, which has not been previously described. The most extensive investigation was performed on the peripheral blood from patients with untreated CLL. The presence of CD4+GZB+ cells was identified in the lymph nodes (and significantly increased when compared to reactive lymph nodes) and bone marrow trephine biopsies of patients with CLL which are the principle tumour microenvironments in this disease.

The tumour microenvironment in CLL provides signals to assist the survival of the malignant B-CLL cells. Whilst circulating B-CLL have a low proliferation index, the bone marrow and lymphoid organs are the major sites of proliferation of the malignant CD5+ B-CLL cells [147]. Anti-apoptotic signalling in the tumour environment has been shown to promote the proliferation of the B-CLL cells. *In vitro* culture of B-CLL cells has demonstrated that, when cultured with stromal cells, the level of apoptosis of these cells is reduced, in comparison with *in vitro* culture of the B-CLL cells alone, suggesting that the stromal cells are providing anti-apoptotic signals to the B-CLL cells [148]. Bone marrow stromal cells in CLL utilise the anti-apoptotic Bcl-2 family of proteins to promote survival of the B-CLL cells [149]. B-CLL tumour proliferation is highest in the lymph nodes, than in the bone marrow and blood, and B-cell receptor and NF-KB activation is also higher in the lymph node [150]. The significant increase in CD4+GZB+ cells in the CLL bone marrow trephine biopsies that has been demonstrated in this project, when compared with the CLL lymph node biopsies, may be an indication that the CD4+ CTLs are acting to suppress the B-CLL proliferation in the bone marrow. Alternatively, the high tumour proliferation in the lymph node may act to suppress the expansion of CD4+CTLs. Acquisition of CD4+CTLs from the bone marrow aspirates of patients with CLL and *in vitro* functional assays to examine their interaction with B-CLL cells and stromal cells may help to answer this question.

The immunohistochemistry studies performed in this project have established the presence of cytotoxic CD4+ in the lymph nodes of a selection of mature B cell lymphomas, as well as confirming their presence in the lymph nodes of CLL patients. The initial hypothesis that they would be present has been confirmed, although the significant increase in the percentage of CD4+GZB+ cells out of the total CD4+ population in MCL and DLBCL was not expected. We initially hypothesised that the percentage of CD4+GZB+ cells would be increased in CLL, mirroring the results in the peripheral blood, and Classical Hodgkin Lymphoma (CHL), a disease which is renowned for its unique tumour microenvironment where only 1% of the tumour mass is comprised of malignant cells whilst the remaining population consists of an infiltration of reactive cells. Furthermore, CHL is often associated with EBV infection, a virus that in turn has been associated with a higher level of cytotoxic CD4+ cells. With respect to CHL, however, no increase in CD4+GZB+ cells was seen when compared with the reactive lymph node biopsies. This may have been reflective of the small number biopsies included in our survey or indicate that the inflammatory infiltrate seen in CHL does not include an excess of CD4+CTLs.

It is perhaps surprising that the CLL lymph nodes did not have a higher percentage of cytotoxic CD4+ considering the peripheral blood results. However, it should be noted that the number of biopsies in each subgroup was small, and also the patient population undergoing lymph node biopsies (where disease transformation can be excluded) may be different from early stage, untreated CLL patients who have been diagnosed through peripheral blood flow cytometry only. A further limitation of our study was the partial availability of CMV serological status of the lymph node biopsy patients as those patients who were CMV seropositive may have been expected to have a higher percentage of CD4+GZB+.

The CD4:CD8 ratio in lymph node biopsies of patient with MCL have recently been shown to be correlated independently with overall survival: a high CD4:CD8 ratio is associated with longer survival [151]. The total CD4+ T cell levels were noted to be higher in more indolent forms of the disease and CD4+ levels fell as the disease became more aggressive. It would be interesting to investigate whether this expanded CD4+ population was composed of an increased level of CD4+GZB+ cells, as it was in the patients in the aforementioned HCC study [8], and as the data from our research would suggest. The significant increase in CD4+GZB+ cells seen in the MCL lymph nodes when compared to reactive lymph nodes is interesting as there are similarities between CLL and MCL

immunophenotypically. Both conditions are mature B cell neoplasms which aberrantly express CD5. Mantle cell lymphoma is considered to follow a more aggressive clinical course than the majority of patients diagnosed with CLL and it also expresses Cyclin D1 in the majority of cases, which CLL does not express [152]. That both of these conditions have a significantly increased percentage of CD4+GZB+ cells suggests that, in these two diseases, there may be common interactions with their tumour microenvironment.

Naïve CD4+ T cells differentiate into distinct effector or regulatory cell subsets following activation including Th1, Th2, Th17, Tfh and Treg subsets. At present, it is unclear as to whether cytotoxic CD4+ T cells comprise a separate subset to the ones previously described, but the subset that it most closely resembles is T helper 1 (Th1). This subset is characterised by the production of the cytokine interferon γ, and their role in orchestrating the immune response against viral and intracellular bacterial infections. The T-box transcription factor, T-bet, is most closely associated with the differentiation to this subset. Our expanded CD4+CD57+ cells from the peripheral blood of patients with CLL showed the ability to secrete Interferon gamma, following a period of cell culture, as shown in the EliSPOT experiments. Other research groups have shown that the Class I-restricted T cell-associated molecule (CRTAM) is expressed upon activation in a small subset of CD4+ cells which express Granzyme B, Perforin and EOMES, secrete Interferon gamma and also display cytotoxic functions after culture [153]. It is interesting, however, that the CD4+GZB+ cells isolated from the bone marrow aspirates from patients with Multiple Myeloma in our study showed that the majority expressed GATA-3, a transcription factor associated with the Th2 phenotype. These data serve to support the theory that, although closely aligned to the Th1 phenotype, CD4+CTLs appear to be a distinct lineage in their own right.

Furthermore, both Eomes and T-bet transcription factors have been implicated in the development of cytotoxicity in CD8+ T cells [154] and therefore the expression of both of these in the cytotoxic CD4+ cells from the patients with CLL allude to a common link with CD8+ cytotoxic function. Previously, Appay *et al* [155] examined by a basic gene microarray analysis CD4+ and CD8+ cells at five different stages of differentiation from healthy controls and showed that, at the late stage of differentiation, defined as CD27-CD28-CCR7-, both CD4+ and CD8+ cells had upregulated the Granzyme B gene (when compared to early stages of differentiation) and that their transcriptional profiles were similar. The striking similarities in phenotype between the CD4+GZB+ cells and CD8+GZB+ cells in the peripheral blood of patients with CLL suggest that these two subtypes may be more closely related than originally appreciated. The similarities may be related to their cytotoxic

function or may be related to a common reactivity towards a specific antigen. The possibility that these cells are CMV-reactive has been raised previously [88] and the increased percentage in the peripheral circulation of CD4+GZB+ cells in those patients who are CMV seropositive would serve to support this hypothesis. The association of the CMV status and cytotoxic CD4+ level does not, however, explain the median percentage of CD4+GZB+ cells in CMV negative patients being 3.06% (range: 0.60 – 18.8%), above the normal range in healthy individuals. Therefore, we performed a comparison of the phenotype of CD4+GZB+ cells in CMV seronegative and CMV seropositive patients with CLL by using CyTOF® (mass cytometry) which allowed us to compare an extended phenotype analysis of these two patient groups. The CyTOF data showed that the CD4+GZB+ cells shared many phenotypic similarities with the CD8+GZB+ cells, specifically their expression of CD57 and lack of expression of CD27 and CD28. This was in contrast to the CD4+GZB- cells which did not express CD57.

The concept as to whether the CD4+GZB+ cells are "exhausted" following chronic antigen stimulation has not been supported by our data. Exhausted T cells are defined by their ability to gradually lose effector functions and upregulate multiple co-inhibitory receptors [156]. This exhausted state can be reversed with the use of checkpoint inhibitors against PD-1 or CTLA-4 [157] [67]. Our data shows that these cells were able to proliferate and secrete cytokines including Interferon Gamma. The cells also expressed PD-1 but did not express other co-inhibitory receptors such as LAG3 or TIM3.

The observation that the majority of CD4+GZB+ cells express CD57 allowed for us to devise a cell sorting strategy to electronically sort these cells using a FACS Aria machine as we are unable to sort using Granzyme B expression due to its intracellular location. We have demonstrated that we were able to successfully isolate and expand these cells *in vitro*. Further optimisation of the expansion and culture techniques are required in view of the secretion of Interferon gamma without antigenic stimulation despite the cells being rested for 7 days.

The optimisation of the ChIP sequencing analysis (in collaboration with Dr Richard Jenner's laboratory) of the CD4+CD57+ cytotoxic cells in comparison with CD4+CD57- and CD8+CD57+ cells from the peripheral blood of patients with CLL would enable epigenetic analysis to be undertaken to help to define the transcription factors and regulatory elements, including super-enhancers, which are essential for cytotoxic CD4+ cell differentiation. The comparison cell subsets would further enable us to establish whether their transcriptional profile is similar to the CD8+CD57+ cells or whether they are more closely related to the non-cytotoxic subgroup (CD4+CD57-). Furthermore,

the transcriptional profile will allow the research to focus on cellular pathways to study and inhibit in functional models using the M64 cytotoxic CD4+ *in vitro* assay.

7.1 Limitations of the study

There were a number of study limitations encountered during the project. The first limitation was the small numbers of CD4+CTLs that were obtained from the CLL peripheral blood samples. The initial CLL project outline had limited the volume of blood obtained from the CLL patients to 20 mls. This resulted in only small absolute numbers of CD4+CTLs being available for isolation from these samples. In turn, this limited our ability to both perform standard ChIP sequencing protocols on these cells and also limited the availability of the cells for functional assays. As an attempt to circumvent this issue, we were able to electronically cell-sort the CD4+CTLs, using CD57 as an extracellular marker of the cytotoxic phenotype, and then perform a rapid expansion protocol on the cells to increase the cell numbers. This protocol, however, involved the use of high concentrations of IL-2 (6000 units/ml) during the expansion process and, as other research have shown, IL-2 is able to increase the expression of Granzyme B *in vitro* in T cells ([90]). Different cell expansion techniques that do not require the use of high concentrations of IL-2 may be required. There is also the possibility that expansion may result in a change in the genomic profile of the cells and to directly analyse their transcriptional profile without expansion would be preferable, particularly due to the reports of the acquisition of cytotoxic phenotype after prolonged cell culture.

The next limitation encountered was the analysis of the triple-colour immunohistochemistry biopsy slides, which had to be performed manually. Manual counting of cells has historically been the method of analysis of stained slides but the method is time-consuming and is not able to exclude the potential for reporter bias. An attempt to address this issue was made by the investigator who counted the cells being unaware of the subtype of lymphoma samples being analysed. The recruitment of two different researchers to separately analyse the stained slides may also help to limit the potential counting bias. There are automated machines available to perform cell counting analysis particularly for immunofluorescent markers although the availability is more limited for immunohistochemical staining. Furthermore, the majority of these automated systems have been optimised for single stained slides and not triple stained slides. With respect to the antigens examined in this study, nuclear and surface staining would be able to be automatically counted but

the cytoplasmic vesicles of Granzyme B would be more difficult to automatically count and would require optimisation of the technique to ensure counting accuracy.

7.2 Future studies

This project examined the presence of the CD4+ CTLs in haematological malignancies by flow cytometry, on the peripheral blood of patients with CLL or the bone marrow aspirates of patients with Multiple Myeloma, and triple-colour immunohistochemistry of Lymphoma lymph node biopsies. Now that we have identified their presence in the tumour microenvironment, it would be valuable to examine their phenotype in the lymphoma tumour microenvironment. Obtaining fresh lymph node biopsy samples would enable the extraction and isolation of tumour-infiltrating lymphocytes which could be interrogated by flow cytometry. This would also enable *in vitro* assays to be performed to assess their functional abilities. As diagnostic lymph node biopsies are moving towards core biopsies, the amount of tissue obtained from fresh lymph node biopsies may be small, resulting in the isolation of a small number of cells only. An alternative would be to obtain fine needle aspirates from the enlarged lymph nodes from patients before treatment. Other researchers have performed FNAs on patients with CLL and obtained a median cell yield obtained was 4.1 $x10^6$ (range $1–13×10^6$) cells [158].

The issue of whether the CD4+ CTLs have anti-viral or anti-tumour functions in the context of a malignancy has not been resolved during this project. The percentage of CD4+CTLs was significantly increased in the peripheral blood of patients with CLL who were CMV seropositive when compared with CLL patients who were seronegative which would seem to support an antiviral function. The CD4+CTL population, however, was increased in the CMV seronegative CLL population when compared with the normal controls. Performing further experiments on the peripheral blood of healthy donors who are CMV seropositive or seronegative, but who do not have CLL, may further enable us to examine whether the phenotype of these cells is uniform, regardless of whether a malignancy is present, which may suggest a purely antiviral function.

Furthermore, CLL is known to be a disease associated with immunodeficiency, including hypogammaglobulinaemia, T cell dysfunction (both in cytokine profiling and proliferative abilities) and clinically manifesting as a susceptibility to infections. Therefore, future work could investigate

the presence of cytotoxic CD4+ cells in a malignancy, also associated with a known virus, but not known to be associated with a functional immunodeficiency. Peripheral blood and tumour samples from patients with oropharyngeal squamous cell carcinoma, which is frequently associated with human papillomavirus (HPV) infection [159], could be examined to identify whether the CD4+CTLs are present and if they are phenotypically similar to the cells seen in CLL and Multiple Myeloma.

The importance of genomic profiling of CD4+CTLs in understanding the determinants of their cytotoxic function highlights the need for further experiments to be undertaken to attempt to optimise the CHIP sequencing protocol for small cell numbers. There are recent techniques that have been described that could be used for the genomic profiling of CD4+ CTLs. One of these techniques is an assay for transposase-accessible chromatin using sequencing ("ATAC-seq") which captures open chromatin sites and has been optimised for the use with between 500 – 50,000 cells [160]. Furthermore, Nano-Chip sequencing protocols to perform whole-genome chromatin profiling using 10,000 cells [161] and Micro-ChIP assays using 1000 cells have been described [162].

The examination of peripheral blood samples from patients with CLL who have progressive or transforming disease could give an insight into the characteristics of CD4+CTLs as the disease state changes. The peripheral blood samples examined in this project were from patients with stable disease who did not require treatment. If a disease is progressing, and if the CD4+CTLs had an anti-tumour effect, then it may be hypothesised that these cells would expand in number to attempt to suppress the tumour cells.

7.3 Conclusions

In conclusion, we have shown for the first time that CD4+ CTLS are present in the tumour microenvironment of haematological malignancies, specifically CLL, NHL, HL and multiple myeloma. They express a phenotypic profile which is similar to other cytotoxic cells, namely CD8+ CLTs and NK cells, specifically which the increased expression of CD57, Perforin, Granzyme A and the transcription factor EOMES. Although we have identified an association of increased percentage of CD4+ CTLs in the blood of patients with CLL who are CMV seropositive, we also have identified significantly increased levels in some individuals who are CMV seronegative. CD4+CTLs share some features with a Th1 helper cell lineage, particularly with respect to Tbet expression and the production of Interferon gamma, but they have also been shown to express GATA.3, which is usually

associated with Th2, indicating that they may represent their own class of CD4+ cells. Further studies are required to examine their genomic profile and the determinants of their cytotoxic function.

Chapter 8 References

1. Fleischer, B., *Acquisition of specific cytotoxic activity by human T4+ T lymphocytes in culture.* Nature, 1984. **308**: p. 365-367.
2. Jellison, E., S. Kim, and R. Welsh, *Cutting Edge: MHC Class II-Restricted Killing In Vivo during Viral Infection.* The Journal of Immunology, 2005. **174**: p. 614-618.
3. Appay, V., et al., *Characterization of CD4(+) CTLs ex vivo.* J Immunol, 2002. **168**(11): p. 5954-8.
4. Lowin, B., et al., *Cytolytic T-cell cytotoxicity is mediated through perforin and Fas lytic pathways.* Nature, 1994. **370**(6491): p. 650-2.
5. Nikiforow, S., et al., *Cytolytic CD4(+)-T-cell clones reactive to EBNA1 inhibit Epstein-Barr virus-induced B-cell proliferation.* J Virol, 2003. **77**(22): p. 12088-104.
6. Porakishvili, N., et al., *Cytotoxic CD4+ T cells in patients with B cell chronic lymphocytic leukemia kill via a perforin-mediated pathway* Haematologica, 2004. **89**: p. 435-443.
7. Casazza, J., et al., *Acquisition of direct antiviral effector functions by CMV-specific CD4+ T lymphocytes with cellular maturation.* The Journal of Experimental Medicine, 2006. **203**(13): p. 2865-2877.
8. Fu, J., et al., *Impairment of CD4+ Cytotoxic T Cells Predicts Poor Survival and High Recurrence Rates in Patients with Hepatocellular Carcinoma.* Hepatology, 2013. **58**: p. 139-149.
9. Sun, Q., R. Burton, and K. Lucas, *Cytokine production and cytolytic mechanism of CD4+ cytotoxic T lymphocytes in ex vivo expanded therapeutic Epstein-Barr virus-specific T-cell cultures.* Blood, 2002. **99**(9): p. 3302-3309.
10. Martorelli, D., et al., *Role of CD4+ cytotoxic T lymphocytes in the control of viral diseases and cancer.* Int Rev Immunol, 2010. **29**(4): p. 371-402.
11. Namekawa, T., et al., *Functional subsets of CD4 T cells in rheumatoid synovitis.* Arthritis Rheum, 1998. **41**(12): p. 2108-16.
12. Xanthou, G., et al., *CD4 cytotoxic and dendritic cells in the immunopathologic lesion of Sjogren's syndrome.* Clin Exp Immunol, 1999. **118**(1): p. 154-63.

13. Duftner, C., et al., *Prevalence, clinical relevance and characterization of circulating cytotoxic CD4+CD28- T cells in ankylosing spondylitis.* Arthritis Res Ther, 2003. **5**(5): p. R292-300.
14. Giaretta, F., et al., *Different regulatory and cytotoxic CD4+ T lymphocyte profiles in renal transplants with antibody-mediated chronic rejection or long-term good graft function.* Transpl Immunol, 2013. **28**(1): p. 48-56.
15. Faber, L.M., et al., *Generation of CD4+ cytotoxic T-lymphocyte clones from a patient with severe graft-versus-host disease after allogeneic bone marrow transplantation: implications for graft-versus-leukemia reactivity.* Blood, 1995. **86**(7): p. 2821-8.
16. Quezada, S., et al., *Tumor-reactive CD4+ T cells develop cytotoxic activity and eradicate large established melanoma after transfer into lymphopenic hosts.* Journal of Experimental Medicine, 2010. **207**(3): p. 637-650.
17. Zhang, L.J., et al., *Detection of human cytomegalovirus DNA, RNA, and antibody in normal donor blood.* J Infect Dis, 1995. **171**(4): p. 1002-6.
18. Bate, S.L., S.C. Dollard, and M.J. Cannon, *Cytomegalovirus seroprevalence in the United States: the national health and nutrition examination surveys, 1988-2004.* Clin Infect Dis, 2010. **50**(11): p. 1439-47.
19. Staras, S.A., et al., *Seroprevalence of cytomegalovirus infection in the United States, 1988-1994.* Clin Infect Dis, 2006. **43**(9): p. 1143-51.
20. Peggs, K.S., *Adoptive T cell immunotherapy for cytomegalovirus.* Expert Opin Biol Ther, 2009. **9**(6): p. 725-36.
21. Hanley, P.J. and C.M. Bollard, *Controlling cytomegalovirus: helping the immune system take the lead.* Viruses, 2014. **6**(6): p. 2242-58.
22. Reusser, P., et al., *Cytotoxic T-lymphocyte response to cytomegalovirus after human allogeneic bone marrow transplantation: pattern of recovery and correlation with cytomegalovirus infection and disease.* Blood, 1991. **78**(5): p. 1373-80.
23. Erard, V., et al., *Reduced Mortality of Cytomegalovirus Pneumonia After Hematopoietic Cell Transplantation Due to Antiviral Therapy and Changes in Transplantation Practices.* Clin Infect Dis, 2015. **61**(1): p. 31-9.

24. van Leeuwen, E.M., et al., *Emergence of a CD4+CD28- granzyme B+, cytomegalovirus-specific T cell subset after recovery of primary cytomegalovirus infection.* J Immunol, 2004. **173**(3): p. 1834-41.
25. van Leeuwen, E.M., et al., *Strong selection of virus-specific cytotoxic CD4+ T-cell clones during primary human cytomegalovirus infection.* Blood, 2006. **108**(9): p. 3121-7.
26. Rickinson, A.B., et al., *Cellular immune controls over Epstein-Barr virus infection: new lessons from the clinic and the laboratory.* Trends Immunol, 2014. **35**(4): p. 159-69.
27. Styczynski, J., et al., *Outcome of treatment of Epstein-Barr virus-related post-transplant lymphoproliferative disorder in hematopoietic stem cell recipients: a comprehensive review of reported cases.* Transpl Infect Dis, 2009. **11**(5): p. 383-92.
28. Carpenter, B., et al., *Incidence and dynamics of Epstein-Barr virus reactivation after alemtuzumab-based conditioning for allogeneic hematopoietic stem-cell transplantation.* Transplantation, 2010. **90**(5): p. 564-70.
29. Sun, Q., et al., *CD4(+) Epstein-Barr virus-specific cytotoxic T-lymphocytes from human umbilical cord blood.* Cell Immunol, 1999. **195**(2): p. 81-8.
30. Maartens, G., C. Celum, and S.R. Lewin, *HIV infection: epidemiology, pathogenesis, treatment, and prevention.* Lancet, 2014. **384**(9939): p. 258-71.
31. Curiel, T.J., et al., *CD4+ human immunodeficiency virus type 1 (HIV-1) envelope-specific cytotoxic T lymphocytes derived from the peripheral blood cells of an HIV-1-infected individual.* AIDS Res Hum Retroviruses, 1993. **9**(1): p. 61-8.
32. Ehret, R., et al., *Human immunodeficiency virus glycoprotein-specific CD4+ cytotoxic T lymphocytes are involved in two types of cytotoxicity: antigen-specific and cell-cell fusion-related cell lysis.* AIDS Res Hum Retroviruses, 1997. **13**(12): p. 1017-21.
33. Miskovsky, E.P., et al., *Studies of the mechanism of cytolysis by HIV-1-specific CD4+ human CTL clones induced by candidate AIDS vaccines.* J Immunol, 1994. **153**(6): p. 2787-99.
34. Heinkelein, M., S. Sopper, and C. Jassoy, *Contact of human immunodeficiency virus type 1-infected and uninfected CD4+ T lymphocytes is highly cytolytic for both cells.* J Virol, 1995. **69**(11): p. 6925-31.

35. Johnson, S., et al., *Cooperativity of HIV-Specific Cytolytic CD4 T Cells and CD8 T Cells in Control of HIV Viremia.* J Virol, 2015. **89**(15): p. 7494-505.
36. Masson, D. and J. Tschopp, *A family of serine esterases in lytic granules of cytolytic T lymphocytes.* Cell, 1987. **49**(5): p. 679-85.
37. Stepp, S.E., et al., *Perforin gene defects in familial hemophagocytic lymphohistiocytosis.* Science, 1999. **286**(5446): p. 1957-9.
38. Martinvalet, D., et al., *Granzyme A cleaves a mitochondrial complex I protein to initiate caspase-independent cell death.* Cell, 2008. **133**(4): p. 681-92.
39. Mullbacher, A., et al., *Granzyme A is critical for recovery of mice from infection with the natural cytopathic viral pathogen, ectromelia.* Proc Natl Acad Sci U S A, 1996. **93**(12): p. 5783-7.
40. Pereira, R.A., M.M. Simon, and A. Simmons, *Granzyme A, a noncytolytic component of CD8(+) cell granules, restricts the spread of herpes simplex virus in the peripheral nervous systems of experimentally infected mice.* J Virol, 2000. **74**(2): p. 1029-32.
41. Heusel, J.W., et al., *Cytotoxic lymphocytes require granzyme B for the rapid induction of DNA fragmentation and apoptosis in allogeneic target cells.* Cell, 1994. **76**(6): p. 977-87.
42. Shresta, S., et al., *Natural killer and lymphokine-activated killer cells require granzyme B for the rapid induction of apoptosis in susceptible target cells.* Proc Natl Acad Sci U S A, 1995. **92**(12): p. 5679-83.
43. Andrade, F., et al., *Granzyme H destroys the function of critical adenoviral proteins required for viral DNA replication and granzyme B inhibition.* Embo j, 2007. **26**(8): p. 2148-57.
44. Hua, G., et al., *Ignition of p53 bomb sensitizes tumor cells to granzyme K-mediated cytolysis.* J Immunol, 2009. **182**(4): p. 2152-9.
45. Pao, L.I., et al., *Functional analysis of granzyme M and its role in immunity to infection.* J Immunol, 2005. **175**(5): p. 3235-43.
46. Peggs, K.S., S.A. Quezada, and J.P. Allison, *Cancer immunotherapy: co-stimulatory agonists and co-inhibitory antagonists.* Clin Exp Immunol, 2009. **157**(1): p. 9-19.
47. Waterhouse, P., et al., *Lymphoproliferative disorders with early lethality in mice deficient in Ctla-4.* Science, 1995. **270**(5238): p. 985-8.

48. Tivol, E.A., et al., *Loss of CTLA-4 leads to massive lymphoproliferation and fatal multiorgan tissue destruction, revealing a critical negative regulatory role of CTLA-4.* Immunity, 1995. **3**(5): p. 541-7.
49. Leach, D.R., M.F. Krummel, and J.P. Allison, *Enhancement of antitumor immunity by CTLA-4 blockade.* Science, 1996. **271**(5256): p. 1734-6.
50. Peggs, K.S., et al., *Blockade of CTLA-4 on both effector and regulatory T cell compartments contributes to the antitumor activity of anti-CTLA-4 antibodies.* J Exp Med, 2009. **206**(8): p. 1717-25.
51. Simpson, T.R., et al., *Fc-dependent depletion of tumor-infiltrating regulatory T cells co-defines the efficacy of anti-CTLA-4 therapy against melanoma.* J Exp Med, 2013. **210**(9): p. 1695-710.
52. Nishimura, H., et al., *Development of lupus-like autoimmune diseases by disruption of the PD-1 gene encoding an ITIM motif-carrying immunoreceptor.* Immunity, 1999. **11**(2): p. 141-51.
53. Nishimura, H., et al., *Autoimmune dilated cardiomyopathy in PD-1 receptor-deficient mice.* Science, 2001. **291**(5502): p. 319-22.
54. Dong, H., et al., *Tumor-associated B7-H1 promotes T-cell apoptosis: a potential mechanism of immune evasion.* Nat Med, 2002. **8**(8): p. 793-800.
55. Iwai, Y., et al., *Involvement of PD-L1 on tumor cells in the escape from host immune system and tumor immunotherapy by PD-L1 blockade.* Proc Natl Acad Sci U S A, 2002. **99**(19): p. 12293-7.
56. Ansell, S.M., et al., *PD-1 blockade with nivolumab in relapsed or refractory Hodgkin's lymphoma.* N Engl J Med, 2015. **372**(4): p. 311-9.
57. Dong, C., et al., *ICOS co-stimulatory receptor is essential for T-cell activation and function.* Nature, 2001. **409**(6816): p. 97-101.
58. Wong, S.C., et al., *Impaired germinal center formation and recall T-cell-dependent immune responses in mice lacking the costimulatory ligand B7-H2.* Blood, 2003. **102**(4): p. 1381-8.
59. Hutloff, A., et al., *ICOS is an inducible T-cell co-stimulator structurally and functionally related to CD28.* Nature, 1999. **397**(6716): p. 263-6.
60. Tan, J.T., et al., *4-1BB costimulation is required for protective anti-viral immunity after peptide vaccination.* J Immunol, 2000. **164**(5): p. 2320-5.

61. DeBenedette, M.A., et al., *Analysis of 4-1BB ligand (4-1BBL)-deficient mice and of mice lacking both 4-1BBL and CD28 reveals a role for 4-1BBL in skin allograft rejection and in the cytotoxic T cell response to influenza virus.* J Immunol, 1999. **163**(9): p. 4833-41.
62. Croft, M., *The role of TNF superfamily members in T-cell function and diseases.* Nat Rev Immunol, 2009. **9**(4): p. 271-85.
63. Stephens, G.L., et al., *Engagement of glucocorticoid-induced TNFR family-related receptor on effector T cells by its ligand mediates resistance to suppression by CD4+CD25+ T cells.* J Immunol, 2004. **173**(8): p. 5008-20.
64. Schaer, D.A., J.T. Murphy, and J.D. Wolchok, *Modulation of GITR for cancer immunotherapy.* Curr Opin Immunol, 2012. **24**(2): p. 217-24.
65. Schaer, D.A., et al., *GITR pathway activation abrogates tumor immune suppression through loss of regulatory T cell lineage stability.* Cancer Immunol Res, 2013. **1**(5): p. 320-31.
66. Workman, C.J., et al., *Lymphocyte activation gene-3 (CD223) regulates the size of the expanding T cell population following antigen activation in vivo.* J Immunol, 2004. **172**(9): p. 5450-5.
67. Nguyen, L.T. and P.S. Ohashi, *Clinical blockade of PD1 and LAG3--potential mechanisms of action.* Nat Rev Immunol, 2015. **15**(1): p. 45-56.
68. Sabatos, C.A., et al., *Interaction of Tim-3 and Tim-3 ligand regulates T helper type 1 responses and induction of peripheral tolerance.* Nat Immunol, 2003. **4**(11): p. 1102-10.
69. Ngiow, S.F., M.W. Teng, and M.J. Smyth, *Prospects for TIM3-Targeted Antitumor Immunotherapy.* Cancer Res, 2011. **71**(21): p. 6567-71.
70. Anderson, A.C., et al., *Promotion of tissue inflammation by the immune receptor Tim-3 expressed on innate immune cells.* Science, 2007. **318**(5853): p. 1141-3.
71. Porakishvili, N., et al., *Expansion of CD4+ T cells with a cytotoxic phenotype in patients with B-chronic lymphocytic leukaemia (B-CLL).* Clinical and Experimental Immunology, 2001. **126**: p. 29-36.
72. Cao, X., et al., *Granzyme B and perforin are important for regulatory T cell-mediated suppression of tumor clearance.* Immunity, 2007. **27**(4): p. 635-46.

73. Marafioti, T., et al., *The inducible T-cell co-stimulator molecule is expressed on subsets of T cells and is a new marker of lymphomas of T follicular helper cell-derivation.* Haematologica, 2010. **95**(3): p. 432-9.
74. Binet, J.L., et al., *A clinical staging system for chronic lymphocytic leukemia: prognostic significance.* Cancer, 1977. **40**(2): p. 855-64.
75. Leipold, M.D., E.W. Newell, and H.T. Maecker, *Multiparameter Phenotyping of Human PBMCs Using Mass Cytometry.* Methods Mol Biol, 2015. **1343**: p. 81-95.
76. Swerdlow SH, et al., *WHO Classification of Tumors of the Haematopietic and Lymphoid Tissues.* 2008, Lyon, France: IARC.
77. Goldin, L.R., et al., *Familial risk of lymphoproliferative tumors in families of patients with chronic lymphocytic leukemia: results from the Swedish Family-Cancer Database.* Blood, 2004. **104**(6): p. 1850-4.
78. Rai, K.R., et al., *Clinical staging of chronic lymphocytic leukemia.* Blood, 1975. **46**(2): p. 219-34.
79. Binet, J.L., et al., *A new prognostic classification of chronic lymphocytic leukemia derived from a multivariate survival analysis.* Cancer, 1981. **48**(1): p. 198-206.
80. Yee, K.W., S.M. O'Brien, and F.J. Giles, *Richter's syndrome: biology and therapy.* Cancer J, 2005. **11**(3): p. 161-74.
81. Brown, J.R., M.J. Hallek, and J.M. Pagel, *Chemoimmunotherapy Versus Targeted Treatment in Chronic Lymphocytic Leukemia: When, How Long, How Much, and in Which Combination?* Am Soc Clin Oncol Educ Book, 2016. **35**: p. e387-98.
82. Niemann, C.U., et al., *Disruption of in vivo Chronic Lymphocytic Leukemia Tumor-Microenvironment Interactions by Ibrutinib--Findings from an Investigator-Initiated Phase II Study.* Clin Cancer Res, 2016. **22**(7): p. 1572-82.
83. Ramsay, A.G., et al., *Chronic lymphocytic leukemia T cells show impaired immunological synapse formation that can be reversed with an immunomodulating drug.* J Clin Invest, 2008. **118**(7): p. 2427-37.
84. Riches, J.C., et al., *T cells from CLL patients exhibit features of T-cell exhaustion but retain capacity for cytokine production.* Blood, 2013. **121**(9): p. 1612-21.
85. Porakishvili, N., et al., *Expansion of CD4+ T cells with a cytotoxic phenotype in patients with B-chronic lymphocytic leukaemia (B-CLL).* Clin Exp Immunol, 2001. **126**(1): p. 29-36.

86. Focosi, D., et al., *CD57+ T lymphocytes and functional immune deficiency.* J Leukoc Biol, 2010. **87**(1): p. 107-16.
87. Munk Pedersen, I. and J. Reed, *Microenvironmental interactions and survival of CLL B-cells.* Leuk Lymphoma, 2004. **45**(12): p. 2365-72.
88. Walton, J., et al., *Patients with B cell chronic lymphocytic leukaemia have an expanded population of CD4+ perforin expressing T cells enriched for human cytomegalovirus specificity and an effector-memory phenotype.* British Journal of Haematology, 2009. **148**: p. 274-284.
89. Wherry, E.J., *T cell exhaustion.* Nat Immunol, 2011. **12**(6): p. 492-9.
90. Janas, M.L., et al., *IL-2 regulates perforin and granzyme gene expression in CD8+ T cells independently of its effects on survival and proliferation.* J Immunol, 2005. **175**(12): p. 8003-10.
91. Walton, J.A., et al., *Patients with B cell chronic lymphocytic leukaemia have an expanded population of CD4 perforin expressing T cells enriched for human cytomegalovirus specificity and an effector-memory phenotype.* Br J Haematol, 2010. **148**(2): p. 274-84.
92. te Raa, G.D., et al., *CMV-specific CD8+ T-cell function is not impaired in chronic lymphocytic leukemia.* Blood, 2014. **123**(5): p. 717-24.
93. Riches, J.C. and J.G. Gribben, *Hanging tough: CMV-specific CD8+ T cells in CLL.* Blood, 2014. **123**(5): p. 608-9.
94. Pourgheysari, B., et al., *The number of cytomegalovirus-specific CD4+ T cells is markedly expanded in patients with B-cell chronic lymphocytic leukemia and determines the total CD4+ T-cell repertoire.* Blood, 2010. **116**(16): p. 2968-74.
95. Parry, H.M., et al., *Cytomegalovirus infection does not impact on survival or time to first treatment in patients with chronic lymphocytic leukemia.* Am J Hematol, 2016. **91**(8): p. 776-81.
96. Johansson, U., et al., *Guidelines on the use of multicolour flow cytometry in the diagnosis of haematological neoplasms. British Committee for Standards in Haematology.* Br J Haematol, 2014. **165**(4): p. 455-88.
97. Cheng, Y. and E.W. Newell, *Deep Profiling Human T Cell Heterogeneity by Mass Cytometry.* Adv Immunol, 2016. **131**: p. 101-34.
98. Leong, M.L. and E.W. Newell, *Multiplexed Peptide-MHC Tetramer Staining with Mass Cytometry.* Methods Mol Biol, 2015. **1346**: p. 115-31.

99. Newell, E.W., et al., *Cytometry by time-of-flight shows combinatorial cytokine expression and virus-specific cell niches within a continuum of CD8+ T cell phenotypes.* Immunity, 2012. **36**(1): p. 142-52.
100. Palma, M., et al., *T cells in chronic lymphocytic leukemia display dysregulated expression of immune checkpoints and activation markers.* Haematologica, 2016.
101. Imai, T., et al., *Identification and molecular characterization of fractalkine receptor CX3CR1, which mediates both leukocyte migration and adhesion.* Cell, 1997. **91**(4): p. 521-30.
102. Fergusson, J.R., et al., *CD161 defines a transcriptional and functional phenotype across distinct human T cell lineages.* Cell Rep, 2014. **9**(3): p. 1075-88.
103. Hodgkin, *On some Morbid Appearances of the Absorbent Glands and Spleen.* Med Chir Trans, 1832. **17**: p. 68-114.
104. Howlader N, N.A., Krapcho M, Garshell J, Miller D, Altekruse SF, Kosary CL, Yu M, Ruhl J, Tatalovich Z,Mariotto A, Lewis DR, Chen HS, Feuer EJ, Cronin KA (eds). *SEER Cancer Statistics Review, 1975-2011.* National Cancer Institute. Bethesda, MD,. **http://seer.cancer.gov/csr/1975_2011/(** based on November 2013 SEER data submission, posted to the SEER web site, April 2014.).
105. Heslop, H.E., et al., *Long-term outcome of EBV-specific T-cell infusions to prevent or treat EBV-related lymphoproliferative disease in transplant recipients.* Blood, 2010. **115**(5): p. 925-35.
106. Bollard, C.M., et al., *Sustained complete responses in patients with lymphoma receiving autologous cytotoxic T lymphocytes targeting Epstein-Barr virus latent membrane proteins.* J Clin Oncol, 2014. **32**(8): p. 798-808.
107. Steidl, C., J.M. Connors, and R.D. Gascoyne, *Molecular pathogenesis of Hodgkin's lymphoma: increasing evidence of the importance of the microenvironment.* J Clin Oncol, 2011. **29**(14): p. 1812-26.
108. Steidl, C., et al., *Tumor-associated macrophages and survival in classic Hodgkin's lymphoma.* N Engl J Med, 2010. **362**(10): p. 875-85.
109. Peggs, K.S., *Recent advances in antibody-based therapies for Hodgkin Lymphoma.* Br J Haematol, 2015.
110. Armitage, J.O. and D.D. Weisenburger, *New approach to classifying non-Hodgkin's lymphomas: clinical features of the major histologic subtypes. Non-Hodgkin's Lymphoma Classification Project.* J Clin Oncol, 1998. **16**(8): p. 2780-95.

111. Sehn, L.H., et al., *The revised International Prognostic Index (R-IPI) is a better predictor of outcome than the standard IPI for patients with diffuse large B-cell lymphoma treated with R-CHOP.* Blood, 2007. **109**(5): p. 1857-61.
112. *A predictive model for aggressive non-Hodgkin's lymphoma. The International Non-Hodgkin's Lymphoma Prognostic Factors Project.* N Engl J Med, 1993. **329**(14): p. 987-94.
113. Chaganti, S., et al., *Guidelines for the management of diffuse large B-cell lymphoma.* British Journal of Haematology, 2016. **174**(1): p. 43-56.
114. Alizadeh, A.A., et al., *Distinct types of diffuse large B-cell lymphoma identified by gene expression profiling.* Nature, 2000. **403**(6769): p. 503-11.
115. Rosenwald, A., et al., *The use of molecular profiling to predict survival after chemotherapy for diffuse large-B-cell lymphoma.* N Engl J Med, 2002. **346**(25): p. 1937-47.
116. Lenz, G., et al., *Stromal gene signatures in large-B-cell lymphomas.* N Engl J Med, 2008. **359**(22): p. 2313-23.
117. Staudt, L.M., *Molecular diagnosis of the hematologic cancers.* N Engl J Med, 2003. **348**(18): p. 1777-85.
118. Al-Tourah, A.J., et al., *Population-based analysis of incidence and outcome of transformed non-Hodgkin's lymphoma.* J Clin Oncol, 2008. **26**(32): p. 5165-9.
119. Montoto, S., et al., *Risk and clinical implications of transformation of follicular lymphoma to diffuse large B-cell lymphoma.* J Clin Oncol, 2007. **25**(17): p. 2426-33.
120. Horsman, D.E., et al., *Comparison of cytogenetic analysis, southern analysis, and polymerase chain reaction for the detection of t(14; 18) in follicular lymphoma.* Am J Clin Pathol, 1995. **103**(4): p. 472-8.
121. Solal-Celigny, P., et al., *Follicular lymphoma international prognostic index.* Blood, 2004. **104**(5): p. 1258-65.
122. Relander, T., et al., *Prognostic factors in follicular lymphoma.* J Clin Oncol, 2010. **28**(17): p. 2902-13.
123. Carreras, J., et al., *High numbers of tumor-infiltrating FOXP3-positive regulatory T cells are associated with improved overall survival in follicular lymphoma.* Blood, 2006. **108**(9): p. 2957-64.

124. Alvaro, T., et al., *Immunohistochemical patterns of reactive microenvironment are associated with clinicobiologic behavior in follicular lymphoma patients.* J Clin Oncol, 2006. **24**(34): p. 5350-7.
125. Farinha, P., et al., *The architectural pattern of FOXP3-positive T cells in follicular lymphoma is an independent predictor of survival and histologic transformation.* Blood, 2010. **115**(2): p. 289-95.
126. Zhou, Y., et al., *Incidence trends of mantle cell lymphoma in the United States between 1992 and 2004.* Cancer, 2008. **113**(4): p. 791-8.
127. Cheah, C.Y., J.F. Seymour, and M.L. Wang, *Mantle Cell Lymphoma.* J Clin Oncol, 2016. **34**(11): p. 1256-69.
128. Hoster, E., et al., *A new prognostic index (MIPI) for patients with advanced-stage mantle cell lymphoma.* Blood, 2008. **111**(2): p. 558-65.
129. Mozos, A., et al., *SOX11 expression is highly specific for mantle cell lymphoma and identifies the cyclin D1-negative subtype.* Haematologica, 2009. **94**(11): p. 1555-62.
130. Palomero, J., et al., *SOX11 promotes tumor angiogenesis through transcriptional regulation of PDGFA in mantle cell lymphoma.* Blood, 2014. **124**(14): p. 2235-47.
131. Royo, C., et al., *Non-nodal type of mantle cell lymphoma is a specific biological and clinical subgroup of the disease.* Leukemia, 2012. **26**(8): p. 1895-8.
132. Andersen, N.S., et al., *A Danish population-based analysis of 105 mantle cell lymphoma patients: incidences, clinical features, response, survival and prognostic factors.* Eur J Cancer, 2002. **38**(3): p. 401-8.
133. Velders, G.A., et al., *Mantle-cell lymphoma: a population-based clinical study.* J Clin Oncol, 1996. **14**(4): p. 1269-74.
134. Eskelund, C.W., et al., *15-year follow-up of the Second Nordic Mantle Cell Lymphoma trial (MCL2): prolonged remissions without survival plateau.* Br J Haematol, 2016. **175**(3): p. 410-418.
135. Wang, M.L., et al., *Targeting BTK with ibrutinib in relapsed or refractory mantle-cell lymphoma.* N Engl J Med, 2013. **369**(6): p. 507-16.
136. *A clinical evaluation of the International Lymphoma Study Group classification of non-Hodgkin's lymphoma. The Non-Hodgkin's Lymphoma Classification Project.* Blood, 1997. **89**(11): p. 3909-18.

137. Mora, J., et al., *Large cell non-Hodgkin lymphoma of childhood: Analysis of 78 consecutive patients enrolled in 2 consecutive protocols at the Memorial Sloan-Kettering Cancer Center.* Cancer, 2000. **88**(1): p. 186-97.
138. Eyre, T.A., et al., *Anaplastic lymphoma kinase-positive anaplastic large cell lymphoma: current and future perspectives in adult and paediatric disease.* Eur J Haematol, 2014. **93**(6): p. 455-68.
139. Turner, S.D., et al., *Anaplastic large cell lymphoma in paediatric and young adult patients.* Br J Haematol, 2016. **173**(4): p. 560-72.
140. Sibon, D., et al., *Long-term outcome of adults with systemic anaplastic large-cell lymphoma treated within the Groupe d'Etude des Lymphomes de l'Adulte trials.* J Clin Oncol, 2012. **30**(32): p. 3939-46.
141. Hapgood, G. and K.J. Savage, *The biology and management of systemic anaplastic large cell lymphoma.* Blood, 2015. **126**(1): p. 17-25.
142. Kyle, R.A. and S.V. Rajkumar, *Multiple myeloma.* Blood, 2008. **111**(6): p. 2962-72.
143. Moreau, P., M. Attal, and T. Facon, *Frontline therapy of multiple myeloma.* Blood, 2015. **125**(20): p. 3076-84.
144. Howlader, N., et al., *SEER Cancer Statistics Review, 1975-2013,*. National Cancer Institute. Bethesda, MD.
145. Seumois, G., et al., *Epigenomic analysis of primary human T cells reveals enhancers associated with TH2 memory cell differentiation and asthma susceptibility.* Nat Immunol, 2014. **15**(8): p. 777-88.
146. Creyghton, M.P., et al., *Histone H3K27ac separates active from poised enhancers and predicts developmental state.* Proc Natl Acad Sci U S A, 2010. **107**(50): p. 21931-6.
147. Ramsay, A.D. and M. Rodriguez-Justo, *Chronic lymphocytic leukaemia--the role of the microenvironment pathogenesis and therapy.* Br J Haematol, 2013. **162**(1): p. 15-24.
148. Lagneaux, L., et al., *Chronic lymphocytic leukemic B cells but not normal B cells are rescued from apoptosis by contact with normal bone marrow stromal cells.* Blood, 1998. **91**(7): p. 2387-96.
149. Patel, V., et al., *Impact of bone marrow stromal cells on Bcl-2 family members in chronic lymphocytic leukemia.* Leuk Lymphoma, 2014. **55**(4): p. 899-910.

150. Herishanu, Y., et al., *The lymph node microenvironment promotes B-cell receptor signaling, NF-kappaB activation, and tumor proliferation in chronic lymphocytic leukemia.* Blood, 2011. **117**(2): p. 563-74.
151. Nygren, L., et al., *T-Cell Levels Are Prognostic in Mantle Cell Lymphoma.* Clinical Cancer Research, 2014. **20**(23): p. 6096-6104.
152. Hoeller, S., et al., *Composite mantle cell lymphoma and chronic lymphocytic leukemia/small lymphocytic lymphoma: a clinicopathologic and molecular study.* Hum Pathol, 2013. **44**(1): p. 110-21.
153. Takeuchi, A., et al., *CRTAM determines the CD4+ cytotoxic T lymphocyte lineage.* J Exp Med, 2016. **213**(1): p. 123-38.
154. Cruz-Guilloty, F., et al., *Runx3 and T-box proteins cooperate to establish the transcriptional program of effector CTLs.* The Journal of Experimental Medicine, 2009. **206**(1): p. 51-59.
155. Appay, V., et al., *Sensitive Gene Expression Profiling of Human T Cell Subsets Reveals Parallel Post-Thymic Differentiation for CD4+ and CD8+ Lineages.* The Journal of Immunology, 2007. **179**: p. 7406-7414.
156. Wherry, E.J. and M. Kurachi, *Molecular and cellular insights into T cell exhaustion.* Nat Rev Immunol, 2015. **15**(8): p. 486-99.
157. Barber, D.L., et al., *Restoring function in exhausted CD8 T cells during chronic viral infection.* Nature, 2006. **439**(7077): p. 682-7.
158. Yallop, D., et al., *Direct Evidence for a Chronic Antigen Driven T Cell Response In CLL Lymph Nodes*, in *Blood*. 2010.
159. Guo, T., D.W. Eisele, and C. Fakhry, *The potential impact of prophylactic human papillomavirus vaccination on oropharyngeal cancer.* Cancer, 2016. **122**(15): p. 2313-23.
160. Buenrostro, J.D., et al., *Transposition of native chromatin for fast and sensitive epigenomic profiling of open chromatin, DNA-binding proteins and nucleosome position.* Nat Methods, 2013. **10**(12): p. 1213-8.
161. Adli, M. and B.E. Bernstein, *Whole-genome chromatin profiling from limited numbers of cells using nano-ChIP-seq.* Nat Protoc, 2011. **6**(10): p. 1656-68.
162. Dahl, J.A. and P. Collas, *A rapid micro chromatin immunoprecipitation assay (microChIP).* Nat Protoc, 2008. **3**(6): p. 1032-45.